

# UNIVERSITÀ DEGLI STUDI DI MILANO

Facoltà di Scienze Agrarie e Alimentari

Dipartimento di Scienze per gli Alimenti, la Nutrizione e l'Ambiente



Scuola di Dottorato in

Innovazione Tecnologica per le Scienze Agro-Alimentari e Ambientali

**Ciclo XXVI**

## MICROBIAL FOOD FERMENTATIONS: INNOVATIVE APPROACH USING INFRARED SPECTROSCOPY

*Settore disciplinare: AGR 15*

Thesis of

Silvia GRASSI

R09271

Supervisor: Prof.ssa Ernestina CASIRAGHI

Cosupervisor: Prof. Roberto FOSCHINO,

PhD Coordinator: Prof. Roberto PRETOLANI

Anno Accademico 2012-2013



*There is no comparison between that which is lost by  
not succeeding and that which is lost by not trying.*

Francis Bacon





## Table of contents

<b>PREFACE</b>	7
<b>RIASSUNTO</b>	10
<b>1. FOOD FERMENTATION AND PROCESS ANALYTICAL TECHNOLOGY</b>	
1.1 Historical background	15
1.2 Fermentation process control	18
1.3 References	20
<b>2. SPECTROSCOPY</b>	
2.1 Spectroscopy: Theory	25
2.1.1 The electromagnetic radiation	25
2.1.2 Molecular energy	28
2.1.3 Principles of infrared spectroscopy	32
2.2 Near Infrared Spectroscopy (NIR)	34
2.2.1 Spectra interpretation	34
2.2.2 Instrumentation	37
2.2.3 Sample interface and measurement modes	39
2.3 Mid infrared spectroscopy (MIR)	42
2.3.1 Spectra interpretation	42
2.3.2 Instrumentation	44
2.3.3 Sample interface and measurement modes	45
2.4 References	46
<b>3. CHEMOMETRICS</b>	
3.1 Spectral pre-treatment	49
3.2 Principal Component Analysis	51
3.3 Multivariate Curve Resolution	53
3.3.1 MCR-ALS	54
3.4 Multivariate Regressions	57
3.4.1 Partial Least Squares regression	57
3.4.2 Locally weighted regression	58
3.5 References	59

## 4. FOOD FERMENTATION MONITORING: EXAMPLES

4.1	OVERVIEW OF MILK LACTIC ACID FERMENTATION MONITORING	
	Paper I: Monitoring of lactic acid fermentation process using FT-NIR spectroscopy	69
	Paper II: Modelling milk lactic acid fermentation using Multivariate Curve Resolution-Alternating Least Square (MCR-ALS)	91
	Paper III: Applicazione di tecniche spettroscopiche IR al monitoraggio della produzione di lattici fermentati	111
4.2	WINE MALOLACTIC BIOTRANSFORMATION MONITORING	
	Paper IV: Near infrared and mid infrared spectroscopy in oenology: determination of main components involved in malolactic transformation	121
	Paper V: Near and Mid Infrared Spectroscopy to detect malolactic biotransformation of <i>Oenococcus oeni</i> in a wine-model	131
4.3	BEER FERMENTATION MONITORING	
	Paper VI: Beer fermentation: monitoring of process parameters by FT-NIR and Multivariate data analysis	149
	Paper VII: Assessment of the sugars and ethanol development in beer fermentation with FT-IR and multivariate curve resolution models	169
4.4	OVERVIEW OF DOUGH FERMENTATION FOR PANETTONE PRODUCTION	
4.4.1	State-of-the-art	187
4.4.2	Material and Methods	188
4.4.3	Preliminary results	189
4.4.4	References	196

## 5. CONCLUSIONS

General conclusions	199
---------------------	-----

## APPENDIX: Contributions to national and international congresses

# PREFACE

Interest in food quality and production has increased in recent decades, mainly due to changes in consumer habits and behaviour, and the development and increase in the industrialisation of food chains. The growing demand for quality and safety in food production obviously calls for high standards for quality and process control, which in turn requires appropriate analytical tools for the analysis of food.

In particular, many unit operations in industrial food processes are related to microbial fermentation, namely milk coagulation in dairy, dough in bakery, as well as must fermentation in wine and beer productions.

Fermentation is one of the earliest methods adopted to obtain value-added food products with an extended shelf life. Humans applied fermentation to make products such as wine, mead, cheese and beer long before the biochemical process behind was understood. Even now the biochemistry of fermentations commonly applied in food processes has many aspects which have not been fully investigated yet.

Briefly, fermentation is any metabolic process in which an organism converts a carbohydrate, such as starch or sugar, into an alcohol and/or organic acids entailing modifications in the final product.

The transition to industrial productions entailed a standardisation of the fermentation processes and the obtained products. Currently, the main objective is to develop instruments able to be implemented in the process in order to closely monitor the products of interest and to detect in real time the smallest changes bringing to a more effective process control and management.

In this contest, spectroscopy revealed to be an interesting analytical method to monitor food fermentations processes. Spectroscopy is a secondary analytical method which consists in recording the absorption changes due to the interaction of electromagnetic radiation with the matter. The basic principle is that every chemical compound absorbs, transmits or reflects light (electromagnetic radiation) over a certain range of wavelengths. The information recorded can, thus, be used to measure the amount of a known chemical substance if correlated to a reference analysis. Spectroscopy reveals to be one of the most useful methods for quantitative analysis in various fields such as chemistry, physics, biochemistry, material and chemical engineering and clinical applications. Indeed, any application that deals with chemical substances or materials can use this technique. Moreover, the improved instrumentation for performing in-line and on-line analyses at industrial level has rose in the last decades giving the opportunity to obtained real-time information about the progression of any process and allowed its implementation as strategy to monitor complex systems as food production.

The food monitoring with spectroscopic devices has become possible thanks to Chemometrics (i.e. multivariate data analysis). Chemometrics has widely demonstrated to be the perfect partner to spectroscopy to deal with the complex chemical/physical systems that food matrix conforms. Chemometrics is able to extract relevant information from redundant and noisy spectra. In the last years the combination of spectroscopic analysis and Chemometrics was applied crosswise in food processes for qualitative and quantitative modelling in industrial applications. In particular, for the determination of compositional parameters affecting quality and safety of fermented food products such as wine, beer, yoghurt, vinegar and bakery products. Nevertheless, concerning complex biotransformations spectroscopy and Chemometrics are emerging techniques in food fermentation monitoring.

The purpose of this PhD Thesis is the demonstration of the feasibility in the combination of spectroscopy and Chemometrics as an innovative working procedure for real time monitoring of food fermentation processes.

The thesis consists of three main chapters integrated with eight papers, which are published or submitted in scientific journals.

Chapter 1 Chapters 2 and 3 present an introduction to the main fermentations and their control from an historical prospective, the employed analytical techniques (Near infrared and Mid Infrared spectroscopy) and to Chemometrics, respectively. Chapter 4 presents the experiments carried out on various fermentation food processes. In this section seven papers represent examples of applications of different spectroscopic methods in strong combination with Chemometrics to food fermentation processes as yogurt fermentation (Paper I, II and Paper III), wine malolactic transformation (Paper IV and V) and beer (Paper VI and VII). In addition to the mentioned papers a brief state of the art and some preliminary results are reported regarding sourdough leaving process monitoring.

The two basic Chemometrics tools, principal component analysis (PCA) and partial least squares (PLS) regression were mainly applied to the spectroscopic data collected from the fermentation processes in order to evaluate the results and focus on the relevant information and to correlate the spectral features with different relevant physical and/or chemical parameters such as the concentration of the main chemical species involved in the biotransformation. In particular, the principal components (PCs) scores obtained by monitoring wine and yoghurt fermentations were modelled as function of time to find out kinetic parameters, as maximum acceleration and deceleration of the transformation, important for the process control (PAPER I and V). The spectroscopic data obtained during yoghurt and beer fermentation monitoring were also investigated with multivariate curve resolution- alternating least squares (MCR-ALS), proving to be able to resolve multi-component mixtures into a simpler model (PAPER II and VII).

The main conclusive remarks on the presented studies are given in Chapter 5 (CONCLUSIONS AND PERSPECTIVE), including a discussion of challenges and future perspectives for further application of spectral monitoring and chemometrics in fermented food processes.

# RIASSUNTO

L'interesse per la qualità del cibo e la produzione è aumentata negli ultimi decenni, soprattutto a causa dei cambiamenti delle abitudini dei comportamenti dei consumatori, nonché lo sviluppo e il progresso dato dalla industrializzazione della catena alimentare. La crescente domanda di qualità e sicurezza nella produzione alimentare richiede ovviamente elevati standard di qualità e di processo, che a loro volta necessitano di adeguati strumenti analitici per l'analisi delle materie prime, dei prodotti finiti e degli intermedi di processo.

In particolare, molte operazioni unitarie dei processi alimentari industriali sono legati alla fermentazione microbica, ad esempio la coagulazione del latte nella produzione di prodotti lattiero-caseari, impasti acidi per pani e dolci tradizionali, così come mosto in fermentazione per la produzione di vino e birra.

La fermentazione è uno dei primi metodi adottati dagli essere umani per ottenere prodotti alimentari a valore aggiunto con una shelf-life prolungata. I processi di fermentazione sono stati utilizzati dagli esseri umani fin dall'antichità per l'ottenimento di prodotti come il vino, l'idromiele, i formaggi e la birra. Tutto questo molto prima che il processo biochimico fosse noto. Tuttoggi la biochimica delle fermentazioni comunemente applicate in processi alimentari ha molti aspetti che non sono stati ancora completamente indagati.

Brevemente, quando parliamo di fermentazione intendiamo qualunque processo metabolico in cui un organismo converte un carboidrato, quale amido o zucchero, in un alcool e/o in acidi organici che comportano modifiche nel prodotto finale.

Il passaggio alla produzione industriale ha comportato una standardizzazione dei processi di fermentazione e dei relativi prodotti ottenuti. Attualmente, l'obiettivo principale è quello di sviluppare strumenti in grado di essere implementati nel processo produttivo al fine di monitorare attentamente i prodotti di interesse e di rilevare in tempo reale i più piccoli cambiamenti. Ciò comporta l'ottenimento di gestione e controllo di processo più efficaci.

In questo contesto, la spettroscopia ad infrarosso si è rivelata essere un metodo analitico interessante per monitorare i processi di fermentazione degli alimenti. La spettroscopia è un metodo analitico secondario che consiste nel registrare variazioni di assorbimento dovuti all'interazione della radiazione elettromagnetica con la materia. Il principio di base è che ogni composto chimico assorbe, trasmette o riflette la luce (radiazione elettromagnetica) in un determinato intervallo di lunghezze d'onda. Le informazioni registrate possono, pertanto, essere utilizzate per misurare la quantità di una sostanza chimica nota se correlata ad una analisi di riferimento. Negli anni passati i metodi spettroscopici si sono dimostrati uno dei metodi più utili per l'analisi quantitativa in vari campi come la chimica, la fisica, la biochimica, la scienza dei

materiali e l'ingegneria chimica, nonché le applicazioni cliniche. Infatti, qualsiasi applicazione che si occupa di sostanze chimiche o materiali può avvalersi di questa tecnica. Inoltre, la strumentazione e la gestione dei dati ottenuti è notevolmente migliorata negli ultimi decenni permettendo l'implementazione in line e on-line delle analisi in campo industriale, dando la possibilità di ottenere informazioni in tempo reale circa l'avanzamento dei processi e ha permesso la sua attuazione come strategia per monitorare sistemi complessi come quelli relativi alla produzione alimentare.

Inoltre, un efficace monitoraggio dei prodotti alimentari con dispositivi spettroscopici è diventato possibile grazie all'utilizzo della chemiometria (cioè l'analisi multivariata dei dati). Le tecniche chemiometriche hanno dimostrato di poter estrarre informazioni rilevanti da spettri ridondanti e rumorosi, quali derivanti dall'analisi di processi alimentari. Negli ultimi anni la combinazione dell'analisi spettroscopica e della chemiometria è stata applicata trasversalmente in processi alimentari per la modellazione qualitativa e quantitativa da sistemi complessi come gli alimenti monitorati a livello industriale. In particolare, per la determinazione dei parametri compositivi che influenzano la qualità e la sicurezza dei prodotti alimentari fermentati come vino, birra, yogurt, aceto e prodotti da forno. Tuttavia, per quanto riguarda l'utilizzo della spettroscopia e della chemiometria per il monitoraggio del processo di biotrasformazione esse sono ancora poco investigate e per questo risultano tecniche emergenti nel monitoraggio della fermentazione degli alimenti.

Lo scopo di questa tesi di dottorato è quello di dimostrare la fattibilità dell'applicazione di diverse tecniche spettroscopiche, in combinazione con tecniche chemiometriche, per il monitoraggio in tempo reale dei processi fermentativi in produzioni alimentari.

La tesi si compone di tre capitoli principali integrati con otto documenti, che sono stati pubblicati e presentati in riviste scientifiche.

I capitoli 1, 2 e 3 presentano un'introduzione alle principali fermentazioni ed il loro controllo da una prospettiva storica, le tecniche analitiche impiegate (vicino e medio infrarosso) e le tecniche chemiometriche applicate, rispettivamente. Il capitolo 4 presenta le sperimentazioni svolte in vari processi di fermentazione alimentare. In questa sezione sette articoli presentano esempi di applicazioni di diversi metodi spettroscopici in forte combinazione con tecniche chemiometriche a processi di fermentazione. In particolare per la fermentazione di yogurt (PAPER I, II e III), della trasformazione malolattica in vino (PAPER IV e V) e fermentazione del mosto a birra (PAPER VI e VII). Oltre agli articoli scientifici riportati, un breve stato dell'arte e alcuni risultati preliminari sono riportati per quanto riguarda il monitoraggio del processo di impasti acidi.

I due strumenti chemiometrici principalmente utilizzati sono stati l'analisi delle componenti principali (PCA) e la regressione con il metodo partial least squares (PLS). Essi sono stati applicati ai dati spettroscopici raccolti dai processi di fermentazione al

fine di valutare preliminarmente i risultati ed estrarne le informazioni rilevanti e per correlare le caratteristiche spettrali con i differenti parametri fisici e/o chimici raccolti come la concentrazione delle principali specie chimiche coinvolte nella biotrasformazione. In particolare, gli score delle componenti principali (PC) ottenuti monitorando vino e yogurt sono stati modellati in funzione del tempo di fermentazione per determinarne i parametri cinetici, vale a dire la massima accelerazione e decelerazione della trasformazione, fondamentali per il controllo di processo (PAPER I e V). I dati spettroscopici ottenuti durante il monitoraggio della fermentazione di yogurt e birra sono stati studiati con il metodo multivariate curve resolution.alternating least square (MCR-ALS), che si è dimostrato di essere in grado di risolvere miscele a più componenti in un modello più semplice (PAPER II e VII).

Le principali osservazioni conclusive sugli studi presentati sono riportati nel capitolo 5 (CONCLUSIONS and PERSPECTIVES), compresa una discussione sulle prospettive future.



# **1. Food fermentation and process analytical technology**



## 1.1. Historical background

Anthropologists hypothesize that the outliving and evolution of human being is closely related with fermented food.

The main advantages of food fermentations are (1) development of a diversity of flavours, aromas, and textures in food substrates; (2) preservation of substantial amounts of food through lactic acid, alcohol, acetic acid, and alkaline fermentations; (3) biological enrichment of food substrates with protein, essential amino acids, and vitamins; (4) elimination of antinutrients; (5) a decrease in cooking time and fuel requirement (Steinkraus, 1996).

In simplistic words, fermentation is any metabolic process in which an organism converts a carbohydrate, such as starch or a sugar, into an alcohol or acids entailing modifications in the final product.

A wide number of food products have been fermented in the history and are nowadays implemented in food industries. Manufacturing processes are really different from one to the other due to the high variety of food groups, ingredients added and starter cultures inoculated.

In this chapter a brief historical background of representative fermented food group is presented.

### *Alcoholic beverages*

Alcoholic fermentations are among the most ancient fermentation documented.

Wine and beer produced in ancient time were completely different from those we use to consume today. They were particularly nutritive and rich in energy due to the presence of the yeast in the final product and high amount of vitamins B (Steinkraus, 2004). Among them, the kefir beer from prehistoric times (Steinkraus, 1996), the Chicha produced in Inca times (Escobar et al., 1977), the ancient version of rice sake in Japan (Yoshizawa and Ishikawa, 1979), the Bouza-beer from ancient Egypt (Teramoto et al., 2001) and Pulque produced by fermenting Agave in ancient Mexico (Steinkraus, 1996) are the most know fermentations. The biotransformations characterising the final products were driven by yeast as *Saccharomyces cerevisiae*, *Endomycopsis fibuliger*, bacteria as *Zymomonas mobilis* and molds as *Aspergillus* sp. and *Rhizopus* sp.



**Figure 1.** Detail of a painting showing the wine making process in the ancient Egypt, walls of Nakhte's tomb, Thebes, ca. 1400 BC

### *Acetic acid product: vinegar*

Vinegar is a by-product of alcoholic beverages and its discovery was almost certainly accidental. An old document from Babylon (5,000 BC) documents the production of vinegar by fermenting the fruit of date palms.

Romans made vinegar also from grape and figs. Actually, the origin of the word comes from the Latin term *vinum* meaning wine and *acer* meaning sour. The use of vinegar as ancient condiment and pickling agent comes from the fermentation of alcoholic beverage in presence of oxygen (Cabezudo et al., 1981) by *Acetobacter* sp., the main responsible of the conversion of ethanol into acetic acid.

In 1864 Pasteur discovered that vinegar was produced by the action of microorganisms '*Mycoderma aceti*' on the wine and from that discovery the production became a controlled large scale process (Cabezudo et al., 1981).

### *Milk lactic acid fermentation*

The exact origin of fermented milk is difficult to establish. There are evidences of its production in Mesopotamia by Sumerians and Babylonians, in Egypt and in Asia (Tamine, 2007). Probably fermented milk products were consumed since humans started milking cows, sheep and goats. In case of the milk was not immediately consumed and, therefore, it was stored in containers made of stomachs of animals (Steinkraus, 1996) where the milk became sour due to its natural content of lactic acid bacteria (LAB). From this accidental discovery, it comes the origin of fermented milk, among which yoghurt is the most spread in the world. The homeland of yoghurt has been accepted as Balkan Peninsula and before the '50s its commercialisation out of the Middle East region was limited. The increase in yoghurt acceptability was mainly related to product innovation especially the enrichment with fruits and sweeteners (Tamine, 2007).

## 1. Food fermentation and process analytical technology

Another class of products deriving from the accidental fermentation of milk in animal stomachs and intestines is the cheese. Indeed, the storage in such container for longer times allowed the whey separation from the curded milk and became a primitive cheese due to the activity of lactic microorganism and the rennet present in the bowel. Nowadays the number of species involved in milk lactic acid fermentation is huge and from this a lot of varieties of final products produced. Mainly they are named as LAB and can be grouped in mesophilic and thermophilic. Among the mesophilic LAB coming from north and east Europe *Lactococcus lactis*, *Leuconostoc mesenteroides*, *Lactobacillus casei* and *paracasei*. Representative of the thermophilic bacteria (south and east Europe) is worth to mention the mixed starter culture use for yoghurt production, i.e. *Streptococcus thermophilus* and *Lactobacillus bulgaricus*.

### *Fermented meat products*

Meat products have been fermented worldwide for centuries. The first proof of sausage and ham production in Europe date to Roman Empire, in Diocletian time (Lücke & Hechelmann, 1987). At that time there was already the distinction among highly cured, smoked, lightly salted and dried hams. Sausages were invented as a means for using leftovers of meat and entrails, they were prepared with blood, fat and meat scrap from pork and beef.

Chinese raw cured hams are claimed to be the first ones. Famous traditional Chinese hams are Jingha and Yunan (Zeuthen, 2007).

There are also famous Chinese type of sausages made from goat and lamb meat with onion, bean sauce, ginger and pepper (Leistner, 1995).

Despite the different origin the final products obtained, such as ham and sausages, are very similar. Most of the fermented sausages are smoked, whereas in the Mediterranean area they are air dried. Other type of fermented sausages developed as a consequence of advanced meat processing techniques (Lücke & Hechelmann, 1987).

The natural fermentation of sausages is a complex microbial process, LAB and coagulase-negative cocci are the main representatives. LAB are usually present in high hygienic quality raw meat at low numbers but they rapidly dominate causing a pH reduction, and production of acetic acid, ethanol, acetoin, pyruvic acid and carbon dioxide contributing to the typical flavour (Rantsiou and Cocolin, 2008). The cocci participate in the development and stability of red colour through nitrate reductase activity and different aromatic substances.

### *Fermented vegetables*

Vegetable were mainly fermented to consume products also out of their season, especially to have a vegetable source during the winter. Korean traditional *kimchi* is one of the most famous fermented vegetable groups in the East. Actually is not defying

## 1. Food fermentation and process analytical technology

a single product but different formulation composed of Chinese cabbage, radish and other vegetables. The common practice is a first step of salting (brining) to direct the fermentation process.

Nowadays, in the global market only cabbage (*sauerkraut* and Korean *kimchi*), cucumbers (pickles), olives and peppers are of real economic importance. LAB responsible for the fermentation of vegetables belongs to the genera *Streptococcus*, *Leuconostoc*, *Pediococcus* and *Lactobacillus* (Fleming and McFeeters, 1981).

### *Fermented cereal foods: dough*

Cereals are a good media for microbial fermentations due to their high content of carbohydrates, minerals, vitamins and sterols needed by microorganisms. Beer is one of the most famous cereal fermented product. Its historical origins have been discussed previously in the alcoholic beverage section. Some details of dough and sourdough obtained from cereal fermentation are presented herein.

Bread fermentation is a 5000-year-old process. It is characterised by the renewal of previously risen dough, also called the starter dough. The manufacture of beer and bread has been really close since the beginning of their handcraft production. In ancient Egypt the starter dough was activated by collecting the foam that rose to the surface of brewing mash tubs. The mentioned method was taken up again in the seventeenth century (Poitrenaud et al., 2004). The awareness of the role of yeast in the leavening process was discovered only between 1857 and 1863 by Louis Pasteur; whereas right now baker's yeast (*Saccharomices cerevisiae*) is the most microorganisms produced.

In particular the starter dough used by Egyptian was probably a sourdough (Wood, 1996). It means that the “mother” was composed of LAB and yeast naturally present in the flour. The mutualistic combination of them is the main responsible of the leavening capacity due to their production of CO<sub>2</sub>. Yeast from beer or wine production could also be added to the dough to increase the leavening capacity as described before (Solvejg Hansen, 2004). Nowadays different typical bread and traditional cakes are made by using sourdough, as it contributes to better flavor and texture and an extended the shelf-life.

## **1.2. Fermentation process control**

The main drawback of traditional production of fermented food is the inconsistency of the final products. This inconsistency usually leads to high production costs and a final quality which relies only on the experience of manufacturers.

Industrial fermentations during 20th century started to use selected starter cultures in wine, dairy, bread and meat production leading to a significant improvement in the

## 1. Food fermentation and process analytical technology

quality and safety of final products. In the past decades the starter characteristics (strains composition, vitality and technological properties, among others) have been one of the main parameters through which a food fermentation process has been controlled. Another important initial parameters to assess a correct start of the fermentation are the characteristics of the raw materials. Despite the precise assessment of the starting point the food industry still has to face different variation in the cycle of the fermentation time that might influence the quality of the final product. Therefore, large scale productions need quality assurance systems to guarantee the fulfilment of the required quality consistency of the final product. Indeed failures in the processes bring to huge economic losses. At present food companies are moving from this feed forward set up of the process to a statistical process control. Traditionally, the control is synonymous of monitoring product quality variables or some key process variables in a univariate way (Kourti, 2005). It means that a generic fermentation process is controlled by the fulfilment of each single variable (i.e. pH, CO<sub>2</sub> content, oxygen pressure, alcohol content and so on) into the specifications defined. It is important to consider that the variables to be monitored are huge number and highly correlated. This brings to a difficult management of a single control chart for each parameter. Moreover most of the analytical techniques used for evaluating parameters such as sugars, organic acids, and alcohol content are not applicable in the process but they required instrumentations of a laboratory leading to a time consuming and expensive control.

Process analytical technology (PAT) is being implemented in order to move the analytical instrumentations from the laboratory to the production site and, thereby, obtain rapid on-line and in-line analyses (Workman et al., 2005).

Historically, the term PAT, as stated by Workman et al. (2005), “has continued to evolve as a more appropriate term than process analytical chemistry (PAC) to describe the field of process analysis, as measurement technologies expanding to include many physical characterization tools. This term has existed since the turn of the century (ca. 1911) but is only now found in common usage.”

The main aim of PAT perfectly matches with the requirements of food fermentation industries. It was perfectly stated by Callis et al. (1987): “The goal of process analytical chemistry is to supply quantitative and qualitative information about a chemical process. Such information can be used not only to monitor and control a process, but also to optimize its efficient use of energy, time, and raw materials”.

The technological development has made PAT a multidisciplinary approach combining analytical chemistry, engineering and biology with multivariate data analysis. In particular, it allows model-predictive control. It means that it is possible to acquire real-time information from a sensor or combination of them and to continuously compare it with the optimal process trend. With such approach control actions can be

taken to correct the non-controlled conditions especially in batch processes, as fermentations, highly dependent on the process with time.

Among all the promising techniques that have been investigated for this purpose, the implementation of infrared spectroscopy has been used since 1930 in refining processes (e.g. Dow Chemical implemented Near Infrared probes in petrochemical PAT in 1970) (Bakeev, 2010). From its first application in the chemical industries infrared spectroscopy has been proved to offer detailed information in real-time on the on-going of several food processes (Woodcock et al., 2008; Karoui et al., 2010) and batch fermentations (Landgrebe et al., 2010). The use of infrared spectroscopy is presented in this thesis to perform the monitoring of different fermentation processes in order to answer the needs of food companies for the assessment of final product quality and production efficiency.

### 1.3 References

- Bakeev, K. A. (Ed.). (2010). *Process analytical technology: spectroscopic tools and implementation strategies for the chemical and pharmaceutical industries*. Wiley.
- Cabezudo, M.D., Herráiz, M., Llaguno C. and Martín, P. (1981). Some advances in alcoholic beverages and vinegar flavor research. In: *The Quality of Foods and Beverages* (pp. 225-240), George Charalambous and George Inglett. Academic Press.
- Callis, J. B., Illman, D. L. and Kowalski, B. R. (1987). Process analytical chemistry. *Analytical Chemistry*, 59:624A–635A.
- Escobar, A. (1977). The South American maize beverage chicha. Masters Degree Thesis. Cornell University, Ithaca, New York.
- Fleming, H. P., & McFeeters, R. F. (1981). Use of Microbial Cultures: Vegetable Products. *Food technology*, 35(1), 84-87.
- Karoui, R., Downey, G., & Blecker, C. (2010). Mid-Infrared Spectroscopy Coupled with Chemometrics: A Tool for the Analysis of Intact Food Systems and the Exploration of Their Molecular Structure– Quality Relationships– A Review. *Chemical reviews*, 110(10), 6144-6168.
- Kourti, T. (2005). Application of latent variable methods to process control and multivariate statistical process control in industry. *International Journal of adaptive control and signal processing*, 19(4), 213-246.
- Landgrebe, D., Haake, C., Höpfner, T., Beutel, S., Hitzmann, B., Scheper, T., & Reardon, K. F. (2010). On-line infrared spectroscopy for bioprocess monitoring. *Applied microbiology and biotechnology*, 88(1), 11-22.



## 1. Food fermentation and process analytical technology

- Leistner, L. (1995) Stable and safe fermented sausages world-wide. In: G Campbell-Platt, PE Cook. eds. *Fermented Meats*. London: Blackie Academic and Professional, pp.160–175.
- Lucke F. K. & Hechelmann. 1987. Starter cultures for dry sausages and raw ham. Composition and effect. *Fleischwirtsch*, 307–316.
- Poitrenaud, B., Hui, Y. H., Meunier-Goddik, L., Hansen, A. S., & Josephsen, J. (2004). Baker's yeast. In *Handbook of food and beverage fermentation technology*, 695-719. CRC Press.
- Rantsiou, K., & Cocolin, L. (2008). Fermented meat products. In *Molecular techniques in the microbial ecology of fermented foods* (pp. 91-118). Springer New York.
- Solveig Hansen, Å. Sourdough bread. In *Handbook of food and beverage fermentation technology* (2004) Hui, Y. H., Meunier-Goddik, L., Josephsen, J., Nip, W. K., & Stanfield, P. S. (Eds.). CRC Press.
- Steinkraus, K. H. (1996). *Handbook of Indigenous Fermented Foods*, Second Edition, Revised and Expanded. Taylor & Francis. Boca Raton, FL: CRC Press.
- Steinkraus, K.H. (2004). *Industrialization of Indigenous Fermented Foods*, Second Edition. Boca Raton, FL: CRC Press.
- Tamime, A. Y., & Robinson, R. K. (2007). *Tamime and Robinson's yoghurt: science and technology* (No. Ed. 3). Woodhead Publishing Ltd.
- Teramoto, Y., Yoshida, S., & Ueda, S. (2001). Characteristics of Egyptian boza and a fermentable yeast strain isolated from the wheat bread. *World Journal of Microbiology and Biotechnology*, 17(3), 241-243.
- Wood ED (1996). Back to the first sourdough, World sourdough from antiquity, Wood ED, ed., TenSpeed Press, California, Berkeley, pp 7–17.
- Woodcock, T., O'Donnell, C., & Downey, G. (2008). Review: Better quality food and beverages: the role of near infrared spectroscopy. *Journal of Near Infrared Spectroscopy*, 16, 1.
- Workman, J., Koch, Jr., M. & Veltkamp, D. (2005). Process analytical chemistry, *Analytical Chemistry*, 77:3789–3806.
- Yoshizawa, K. and Ishikawa, T. (1979). Industrialization of sake fermentation. In: *Industrialization of Indigenous Fermented Foods*. Editor: Steinkraus, K.H. Marcel Dekker Inc., New York. pp.127–168.
- Zeuthen, P. (2007). A historical prospective of meat fermentation. In *Handbook of fermented meat and poultry* (pp. 3-8). Blackwell Publishing. USA.

## 1. Food fermentation and process analytical technology

## **2. Spectroscopy**



## 2.1 Spectroscopy: theory

(Wilson et al., 1980; Miller, 2001; Stuart, 2004; Sandorfy et al., 2007)

Spectroscopy studies the interaction between electromagnetic radiation and matter. The electromagnetic radiation is the combination of electric and magnetic fields. Depending on the energy of the electromagnetic radiation, transition between different kinds of energy states are induced at atomic and/or molecular level.

In particular, it is used to indicate the separation, detection and recording of changes in energy (resonance peaks) affecting nuclei, atoms or whole molecules. These variations are due to the energy interaction between radiation and matter, specifically absorption or diffusion of electromagnetic radiation or particles.

The theoretical basis of the interaction between matter and radiation is the quantum nature of the transfer of energy from the radiation field to the material and vice versa. In fact, both matter and the electromagnetic field have a "dual nature", i.e. the ability to behave both as a wave and as a particle.

Electromagnetic radiation, among which the best known is the light, is nothing more than a form of energy transport of electromagnetic origin in space. According to the studies by James Clerk Maxwell, the first to postulate a set of equations that describe fully the electromagnetic phenomena, the movement of electric charges is capable of generating radiant energy waves in space. They are the result of the superposition of an electric field and a magnetic field orthogonal mutually coupled: each one is the source of the other and propagates with sinusoidal both in space and in time.

### 2.1.1 *The electromagnetic radiation*

The directions of oscillation in the space of the electric field and magnetic field, called polarization, are perpendicular to the propagation direction. In the space propagation, the electromagnetic wave follows common laws to all waves (electromagnetic, acoustic, physical) and has a wave nature.

The electromagnetic radiation is characterised by two properties: amplitude and periodicity. The periodicity can be described in term of its wavelength ( $\lambda$ ) or frequency ( $\nu$ ). Wavelength is the spatial period of the wave, the distance over which the wave's shape repeats, as reported in Figure 2.

The wavelength and the frequency of the electromagnetic radiation are related through the equation:

$$c = \lambda\nu \quad (1)$$

Where  $c$  is the velocity of the electromagnetic radiation in vacuum,  $\nu$  is the frequency which has reciprocal second ( $s^{-1}$ ) as unit, which is now referred as Hertz (Hertz= $s^{-1}$ ). Maxwell discovered that this propagation speed was constant for all the electromagnetic waves and in vacuum was approximately  $2.998 \times 10^{10}$  cm s $^{-1}$ , or the speed of light. Therefore, being  $c$  a constant, knowing the wavelength is possible to calculate the frequency and vice versa.

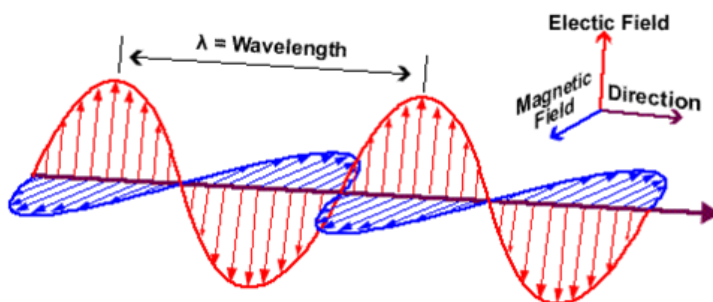


**Figure 2.** Electromagnetic radiation

The wavenumber, expressed in  $cm^{-1}$ , is another variable characterizing the radiation and is defined as the reciprocal of the wavelength. The unit of measurement,  $cm^{-1}$ , while not being given by the System International, is widely used in infrared (IR) and near infrared (NIR) spectroscopy.

The radiation, in addition to having a wave nature, reveals his corpuscular nature when it interacts with matter. That does not transmit to it a continuous quantity of energy, as is the case in classical physics, but sends "packets" of energy quantized. It can then be seen as a stream of particles called photons.

The theoretical basis of the interaction between radiation and energy states of matter is precisely this quantum nature with which the energy transfer occurs between the electromagnetic wave and the energy states of matter and vice versa. If we consider that the radiation is formed from many discrete energy called photons, and that the energy transmitted by a photon is proportional to the frequency of the electromagnetic wave, it can be traced back to the amount of energy that a photon of a certain wave transmits the matter by the Planck-Einstein relation:

$$E = h\nu = \frac{hc}{\lambda} = hc\nu \quad (2)$$

where  $E$  is the energy in Joules,  $h$  is the constant of Planck ( $6.62 \times 10^{-34}$  J s $^{-1}$ ) and  $\nu$  is the radiation frequency in Hertz. A radiation beam may have a 'intensity more or less strong depending on the amount of photons per unit time and unit area, but the quantum energy ( $E$ ) will always be the same for a given frequency of radiation.

Based on these parameters the whole electromagnetic spectrum is usually classified in regions by wavelength into electronic energy, radio, microwave, infrared, the visible region, ultraviolet, X-ray and gamma rays (Figure 3).

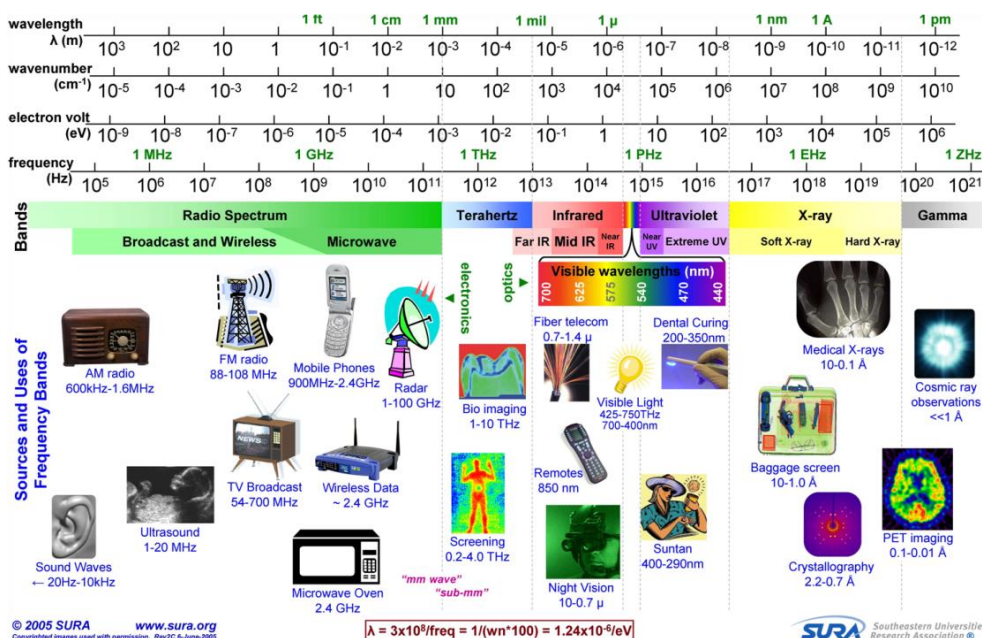


**Figure 3.** Chart of the electromagnetic spectrum illustrated with radiation sources and applications (reproduced from SURA, 2007).

The boundaries between regions are approximate and mainly based on the interaction between the radiation and the matter, as described in Table 1.

**Table 1.** List of different regions in the electromagnetic spectrum, the type of spectroscopy and the induced energy changes.

Region	Spectroscopy	Induced quantum change
Radiofrequency	Nuclear magnetic resonance and electron spin resonance	Changes of electronic spin Changes of nuclear spin
Microwave	Rotational	Molecular rotations
Infrared	Vibrational	Transition between the vibrational levels of molecules
Visible - Ultraviolet	Electronic	Outer electronic transitions
X-ray	X-ray	Inner electronic transitions
Gamma-ray	$\gamma$ -ray	Atomic nuclei excitation

The infrared region of the spectrum includes radiation with wavenumbers ranging from about 12,500 to 10  $\text{cm}^{-1}$  which correspond to wavelengths from 0.78 to 1000  $\mu\text{m}$ . It can be sub-divided into near infrared (12,500 to 4,000  $\text{cm}^{-1}$ ), mid infrared (4,000 to 400  $\text{cm}^{-1}$ ) and far infrared (400 to 10  $\text{cm}^{-1}$ ).

### 2.1.2 Molecular energy

Bohr (Bohr, 1914) based on the following postulates for the correct interpretation of the spectra of atoms and molecules:

1. The atomic systems exist in stable states without emitting electromagnetic energy,
2. The absorption or emission of electromagnetic energy takes place when an atomic system moves from one energy state to another,
3. The process of absorption or emission corresponds to a photon of radiant energy  $h\nu = E' - E''$ , where  $E' - E''$  is the energy difference between two states of an atomic system.

Thus, according to quantum physics, a molecule cannot rotate or vibrate freely with any value of energy, it is subject to what are called quantum-mate restrictions. Therefore, when the energy of a radiation matches a vibrating molecule, there is a net and measurable transfer of energy. It can be graphically represented as the energy change in the ordinate and wavelength in abscissa, i.e. one spectrum.

According to the third postulate of Bohr, the passage of energy from a photon in a molecule can take place only if the photon has a frequency, and therefore energy, equal to the one required from the molecule to pass from the equilibrium state to the excited. A molecule in space could have various form of energy, due to different kind of motion and intermolecular interaction. For instance, the molecule possesses translation energy due to the displacement of molecules in space as function of normal thermal motion of matter. When a photon of energy equal to the difference between the two configurations considered hits the molecule, an electron that is in the basic state has a certain probability to move to the upper level. The photon is absorbed by the molecule as well. After a certain time, few seconds, the electron returns to the ground state with the emission of the photon of energy equal to the energy jump between the two levels (Figure 4). Higher energy photons can bring the electron to a second level of excitation or next levels. It should be emphasized that not all transitions between the various levels are possible, but that, according to quantum mechanics, the possible transitions are only those that obey the selection rules, imposed essentially by the Exclusion Principle of Pauli which forbids the coexistence of more than two electrons on the same orbit. Photons at high energies in the ultraviolet can also rip the electron to the atom that is positively charged (ionized). In the area of the infrared, characterised by low energy, however, the photons are not able to excite the molecule, but may induce vibrational motions of the electrons. Even in this case, the energies associated with the various modes of vibration are quantized.



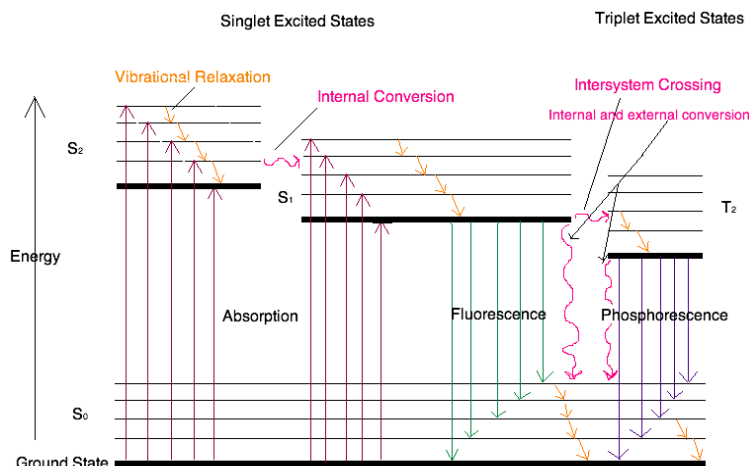


**Figure 4.** Jablonsky diagram (reproduced from <http://chemwiki.ucdavis.edu>)

Energy of the ground state and excited states are accompanied by the vibrational states. Electromagnetic radiations in the microwave area (even less energetic than the infrared area) are not able to induce vibrations but only the rotations of the molecule. So the effects of radiation on matter vary depending on the frequency of the radiation (and therefore the energy conveyed by it) and are represented in Figure 5.

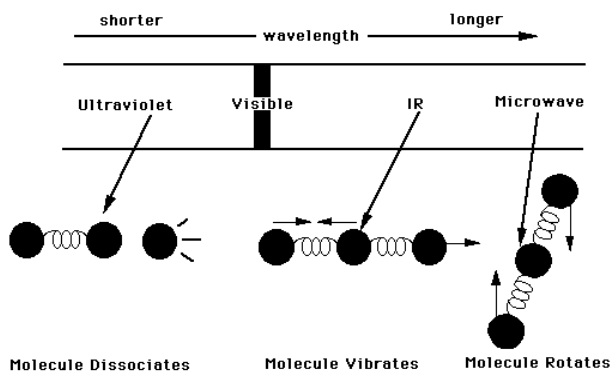


**Figure 5.** Molecular changes according to the different energy of the electromagnetic radiation. Examples with UV, visible, infrared and microwave.

The total energy of a molecule can be considered as the sum of the contributions of translational, electronic, rotational and vibrational energies as reported in equation 3:

$$E_{\text{total}} = E_{\text{trans}} + E_{\text{rot}} + E_{\text{vib}} + E_{\text{elec}} \quad (3)$$

In the atomic spectra the possible interactions are those relating to electrons in the valence shell. In the molecular spectra, though, for each electronic state, several

vibrational and rotational states are normally possible, and, as in the case of near infrared (NIR), also combinations of these and the presence of overtones. In NIR the energies involved are adapted to determine a change in the vibrational motion of the molecules and in particular of the links present in them.

Models to explain the vibrations are based on the concept of "harmonic oscillator" (Figure 6), a system in which two balls (the atoms) are attached by a bond (spring), and can be mathematically described by Hooke's Law (equation 4):

$$E = \frac{hc}{2\pi} = \sqrt{\frac{k}{\mu}} \quad (4)$$

Where  $k$  is the force constant of the bond between two atoms (two balls) and  $\mu$  is the reduced mass according to equation 5:

$$\mu = \frac{m_1 m_2}{m_1 + m_2} \quad (5)$$

In which  $m_1$  and  $m_2$  are the masses of the two atoms.

In the harmonic oscillator model (Figure 6) the potential energy of a vibrating system ( $V$ ) at any given time is assumed to be a quadratic function of the displacement of the atoms involved:

$$V = \frac{1}{2} k x^2 \quad (6)$$

where  $x$  is the displacement from the equilibrium position of the atoms and  $k$  the restoring force constant ( $5 \cdot 10^5$  dyne·cm<sup>-1</sup>).

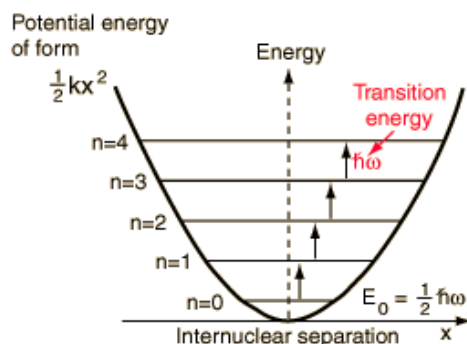


**Figure 6.** Scheme of the harmonic oscillator model, potential energy form vs. atomic displacement for diatomic molecule ( $m_1$  and  $m_2$ )

To determine the possible energy levels for a particular vibration a quantum theory model is needed, finding out that the vibrational levels are a set of discrete (quantized) energy levels, defined by the equation 7:

$$E_v = \left(v + \frac{1}{2}\right) h\nu \quad (7)$$

where  $E_v$  is the energy of the quantum level of the particular vibration,  $v$  is the vibrational quantum number,  $\nu$  is the fundamental frequency of the vibration.

This model represents a good approximation of only the symmetrical diatomic molecules. Although the harmonic model is often used to explain the vibrational spectroscopy, it does have limitations as it fails to describe the possible energy transitions that can occur in a molecule that has a large number of atoms, and especially not arranged symmetrically, i.e. in most of the organic molecules present in food.

Not all the vibrations of a particular molecular structure necessarily absorb infrared radiation, but only those vibrations that make vary the dipolar electric motion of the molecule (e.g. H<sub>2</sub>O). Indeed, the energy of a light photon (equation 2) must be equal to the energy of a vibrational transition, i.e. the energy difference between two vibrational states. In the case of a harmonic vibration (following equation 6 and 7) the energy difference is defined as in equation 8:

$$\Delta E = E_{v_2} - E_{v_1} = \Delta\nu h\nu \quad (8)$$

Where  $\Delta\nu$  is the change in the vibrational quantum number for the vibrational transition.

Due to the selective nature of light-molecule interaction imposed by quantum theory is possible to obtain relevant information in analytical spectroscopy.

### 2.1.3 Principles of infrared spectroscopy (Miller, 2001)

As said before, for a molecule to absorb infrared radiation it is necessary that the radiation has sufficient energy to induce vibrational transitions on the same molecule. The exact matching of radiation frequency with bond vibrational frequency is called resonance. Polyatomic molecules containing  $N$  atoms will have  $3N$  degrees of freedom. In linear molecules ( $3N-5$  degrees of freedom), 2 degrees are rotational and 3 are translational. In non-linear molecule ( $3N-6$  degrees of freedom), 3 of these degrees are rotational and 3 are translational; the remaining correspond to fundamental vibration. In the simple case of water molecule, a diatomic molecule, there are three degrees of

translation freedom, two degrees of rotational freedom and one degree of vibrational freedom.

The main types of bond vibrations are stretching and bending. An example of stretching and bending vibration of a molecule of water are shown in Figure 7.

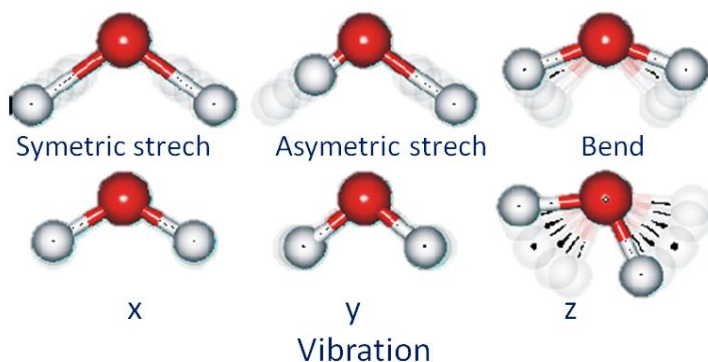


**Figure 7.** Stretching and bending vibration of a water molecule.

The stretching is the vibration of the bond along the plane, in consequence of which varies rhythmically the interatomic distance and it can be symmetrical (in-phase) or asymmetric (out-of-phase); bending vibrations are characterized by a variation of the angle between two atoms in the plane (scissoring and rocking) and out of plane (wagging and twisting).

The vibrational frequencies can be roughly related to the molecular properties through Hooke's Law, as described in the previous paragraph (2.1.2 Molecular energy). This approximation works well for diatomic molecules. Moreover, the resulting values do not differ much from the average values relating also to the stretching vibrations and bending for two atoms in a polyatomic molecule.

Since the values of the reduced mass of the groups -OH, -CH and -NH are rather similar, the spectral information is determined mainly by the value of  $k$ , which depends not only on the length and strength of the bond, but also from the surrounding environment, thus creating differences in energy absorption for each link that make specific and are used in the interpretation of a spectrum.

In reality, however, we analyze asymmetric diatomic molecules: this modifies their responses excitement caused by the incident radiation. The phenomena of mechanical anharmonicity, i.e. the loss of the equidistance between the different energy levels, and anharmonicity of electricity, i.e. the change of the equation of moment dipolar electric, leads the system far from ideal conditions (Figure 8). In particular, the anharmonicity leads to overtone bands, or anharmonic bands, whose frequency is not an integer multiple of the fundamental frequency with which oscillates the bond dipole of the molecule.

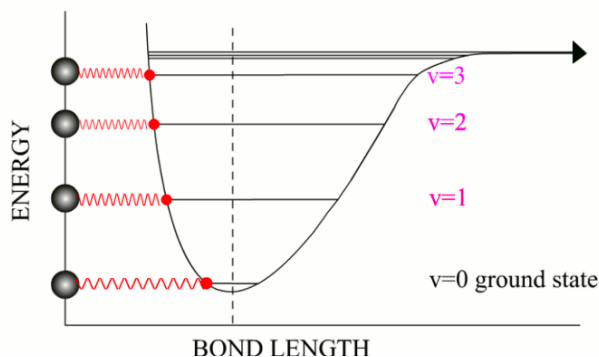


**Figure 8.** Vibrational bond anharmonicity and overtones

These phenomena are even more influential in a polyatomic molecule in which the reciprocal influences between atoms increase exponentially. The lack of harmonicity is even more evident in bonds involving hydrogen molecules, which have a very small mass. The results are vibrations with a greater amplitude and more intense absorption bands. These phenomena mainly influence the near-infrared spectrum.

In this prospective, infrared spectroscopy is applied for quantitative and qualitative analysis of materials regarding their tendency to absorb light in a certain area of the electromagnetic radiation. Near Infrared spectroscopy (NIR) is based on the absorption of radiation in the  $12,500 - 4,000 \text{ cm}^{-1}$  region, Mid Infrared (MIR) spectroscopy in the  $4,000-400 \text{ cm}^{-1}$  region.

The infrared spectrum of an organic compound provides a unique fingerprint that is easily distinguishable from the absorptions of all other compounds. Moreover, the high selectivity of the method often allows the quantitative determination of an analyte in a complex mixture without the need for preliminary separations.

## 2.2 Near Infrared (NIR) Spectroscopy

### 2.2.1 Spectra interpretation (Workman & Weyer, 2008)

The near infrared (NIR) spectrum is characterized by overtones and combinations of fundamental vibrations of molecules containing -CH, -OH, -NH groups; all groups present in food as constituent of fat, protein, sugar, and moisture.

A brief overview is given in this paragraph and summarized in Figure 9.

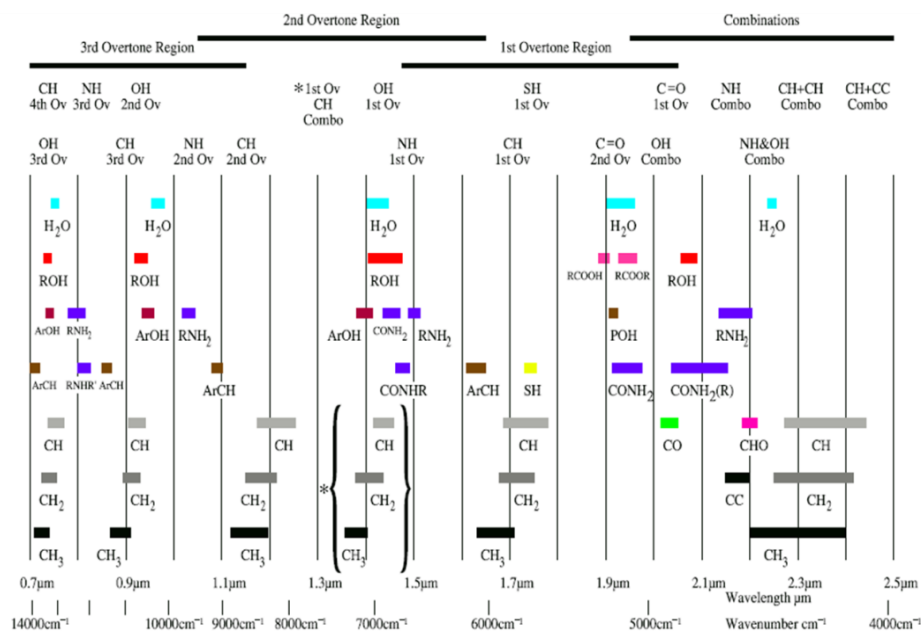


**Figure 9.** Schematic representation of overtone and combination bands absorptions in the NIR region.

### *Overtone and combination bands of the C -H*

The C-H bond is definitely the most important heteroatomic bond in organic molecules present in food and its fundamental overtone and combination bands can be found in the following spectral regions according to the kind of bond:

- Alkanes and Cycloalkans: 5,882-5,555  $\text{cm}^{-1}$  (first overtone), 8,696-8,264  $\text{cm}^{-1}$  (second overtone), 11,390–10,929  $\text{cm}^{-1}$  (third overtone); 6,666-7,690 and 4,545-4,500  $\text{cm}^{-1}$  (combination regions).
- Alkenes and alkynes: 6,100-6,200  $\text{cm}^{-1}$  (first overtone), 8,897-9,200  $\text{cm}^{-1}$  (second overtone), 12,500–10,776  $\text{cm}^{-1}$  (third overtone); 4,600-4,482 and 4,780-4,670  $\text{cm}^{-1}$  (combination regions).
- Aromatic compounds (benzene): around 6,000  $\text{cm}^{-1}$  (first overtone), 8,834  $\text{cm}^{-1}$  (second overtone), 11,442  $\text{cm}^{-1}$  (third overtone); 8,770  $\text{cm}^{-1}$  (combination of twice C-H stretch).

### *Overtone combination bands of the O- H*

The location of the bands due to the O-H bond, as all those that characterize a hydroxyl, dependent on the temperature and condition of the hydrogen bond. According to the compound containing the hydroxyl group is possible to assign the overtone and combination bands as follow:

- Alcohols: 6,240-6,850  $\text{cm}^{-1}$  (first overtone), 10,400  $\text{cm}^{-1}$  (second overtone of nonbonded O-H stretch), 13,500  $\text{cm}^{-1}$  (third overtone); 5,550-4,500  $\text{cm}^{-1}$  (combination of O-H stretching and bending).
- Phenols: 6,940-7,140  $\text{cm}^{-1}$  (first overtone), 10,000  $\text{cm}^{-1}$  (second overtone), 13,250  $\text{cm}^{-1}$  (third overtone); 4,760-5,210  $\text{cm}^{-1}$  (combination region).
- Carboxylic acids: around 6,920  $\text{cm}^{-1}$  (first overtone), 10,000  $\text{cm}^{-1}$  (second overtone of nonbonded carboxylic acid hydroxyl), 12,500  $\text{cm}^{-1}$  (third overtone); the main combination peak (O-H stretch combined with C=O stretch) is at 5,290  $\text{cm}^{-1}$ .
- Water (liquid): the main combination bands are present at 10,300 and 6,900  $\text{cm}^{-1}$  involving the symmetric and asymmetric stretch modes, although these two bands are generally referred to first and second overtones.

#### *Overtone and combination bands of the N- H*

Regarding the primary amines would expect a double band at about 6,553 and 6,730  $\text{cm}^{-1}$  due to a first overtone of stretching of the NH group and a band at about 9,700  $\text{cm}^{-1}$  for the second overtone, the third is a doublet at 12,400 and 12,840  $\text{cm}^{-1}$ . Primary amines show a combination region around 5,000  $\text{cm}^{-1}$ . Secondary amines have a single-band- first overtone around 6,530  $\text{cm}^{-1}$ . Secondary amines show a second set of combination bands around 12,380-12,000  $\text{cm}^{-1}$ . The aromatic amines show absorptions around 6,890 and 6,690  $\text{cm}^{-1}$ .

#### *Other important overtones and combination bands*

There are few other bands, apart from those that affect the bonds C-H, O-H or N-H, that may be considered important for the NIR spectra interpretation in food fermentation application.

The carbonyl group has an intense band at about 5,880  $\text{cm}^{-1}$  and therefore one should expect that also possesses one to five overtones at about 3,450, 5,130, 6,900, 8,620 and 10,300  $\text{cm}^{-1}$ . In addition to overtones, combination bands involving C=O stretching are present in the region 4,760-4,445  $\text{cm}^{-1}$  for aldehydes.

The first overtone of P-H stretching is appreciable at 5,288  $\text{cm}^{-1}$  and the POH group has a peak at 5,241  $\text{cm}^{-1}$ .

The thiol first overtone is present at 5,050  $\text{cm}^{-1}$  and its phosphorus group (PSH) shows a doublet at 5,080-5,000  $\text{cm}^{-1}$ .

The carbohydrates, consisting mostly of aliphatic cyclic groups with O-H residuals, have peculiar absorption related to these constitutional groups in the NIR region. The bands normally associated with starch and sugars as C-H and O-H bands are at 4,000  $\text{cm}^{-1}$  (C-H stretch and the combination of C-C and C-O-C stretch), 4,283-4,386  $\text{cm}^{-1}$  (combination of C-H stretch and CH<sub>2</sub> deformation), 4,762  $\text{cm}^{-1}$  (O-H bending and C-O stretch combination), 6,897  $\text{cm}^{-1}$  (2 $\nu$  of O-H) and a doublet at 9,911 and 10,288  $\text{cm}^{-1}$  (3 $\nu$  of O-H of saccharides).

The proteins instead show three main absorption bands, in the region of the combination of the NH group, in the region 10,277-9,800  $\text{cm}^{-1}$  (N-H first overtone), 6,667-6,536  $\text{cm}^{-1}$  (N-H second overtone), 4,878.4,853  $\text{cm}^{-1}$  (N-H stretching combination). Moreover in there region 4,613-4,587 is possible to distinguish N-H bend overtone and the combination of C=O stretch, N-H bending and C-N stretching.

### *Physical effects*

In addition to the information due to chemical constituents, it is possible to extract information concerning the physical properties of the sample analysed from the NIR spectra. Physical characteristic, such as particle size and shape or sample surface are reflected in scattering variation. Mainly what is observed in the spectra is a change in the baseline, and in co-linearity phenomena among the wavenumbers. For example, a multiplicative scattering effect (systematic baseline slope change between different spectra) can be observed when changing cuvette path while measuring a transparent solution in transmittance; or when measuring powders in diffusive reflectance. In other cases scattering effect can be additive light scattering (constant baseline drift between different spectra), i.e. for turbid aqueous solutions measured in visible transfection spectroscopy. The scattering effect is generally corrected from the spectra by applying different approaches, from very simple ones, like correction according to Beer-Lambert law or Kubelka-Munk theory or with multivariate techniques as multiplicative scatter correction (MSC) or standard normal variate (SNV) (Martens, Nielsen & Engelsen, 2003), which will be further introduced in Chapter 3.

In other cases the spectral information about physical changes can be useful for studying the system. This is the case presented in PAPERS I and II where changes in number and size of casein micelles during acid milk coagulation were modelled.

An example of a series of spectra collected during lactic acid fermentation monitoring (PAPER I, II and III) is reported in Figure 10. Is clear from Figure 10 how NIR spectra collected from a matrix in fermentation, in this case milk, are mainly characterized by water absorption at 6,900 and 5,555  $\text{cm}^{-1}$ , scattering effect, baseline drift.

From such kind of results is difficult to observe relevant information, is therefore necessary to pre-treat the data and to adopt multivariate data analysis strategies in order to highlight differences due to fermentation progress.



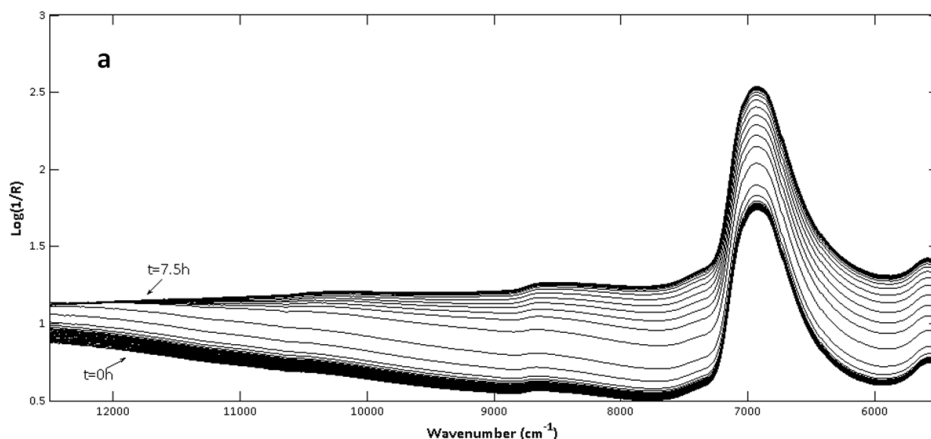


**Figure 10.** Series of spectra collected during a lactic acid fermentation trials from the experiments reported in PAPER I, II and III.

### 2.2.2 Instrumentation (McClure, 2001)

A generic spectrometer that emits in the infrared region is constituted by a group of basic elements: a radiation source, a wavelength selector, a system for the exposure of the sample to the radiation and a detector, according to the scheme shown in Figure 11 (McClure, 2001).

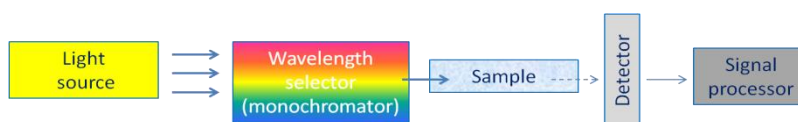


**Figure 11.** Schematic overview of basic components in spectroscopic instruments.

The radiation sources are mainly incandescent bulbs or light emitting diodes (LEDs). In many cases, normal tungsten lamps are used, being considered as a economic and helpful source of NIR radiation. Each source obviously has a specific range of emission wavelengths. For example, incandescent sources are effective for visible radiation and the NIR, the LEDs are limited to specific wavelengths according to the material used in their manufacture. Tungsten-halogen lamps with quartz envelopes are, by far, the most popular source of NIR energy.

Wavelength selectors are different in technology: diodes or filters, as photodiode arrays (PDA), diode array detector (DAD), laser diode (LD), fixed filters (FF), wedge interference filters (WIF), tilting filters (TF), liquid tuneable filters (LCTF), prism, grating, Fourier-transform NIR (FT-NIR).

Also among the detectors there are different ones to choose according to the kind of analysis to be performed. The most popular are: Silicon (photovoltaic) sensors, they range from 360 to 1000 nm, and PbS (lead sulphite) detectors are used for the 900-2600 nm region and indium gallium arsenide (InGaAs) detectors.

### *FT-NIR Instrument design*

This section presents in detail the Fourier-transform NIR spectrometer as in all the application presented the data have been collecting by this class of instruments. A diagram of such an instrument is shown in Figure 12.

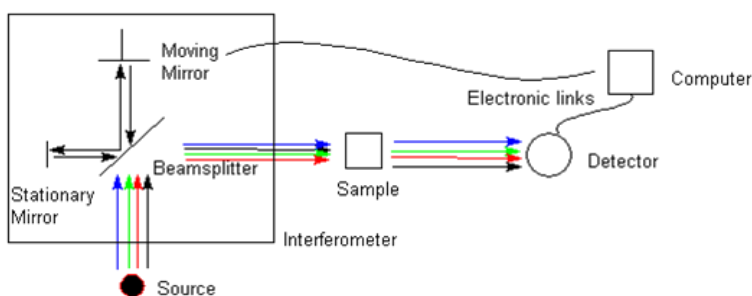


**Figure 12.** Instrumental setup of an FT-NIR instrument.

The core of a FT-NIR is the interferometer (square in Figure 12). The interferometer consist of a beam splitter, a fixed mirror and another mirror, which forms an angle of  $90^\circ$  with the first, moving back and forth precisely. In a standard Michelson interferometer (Figure 13 left), light from the source, after entering, is divided into two equal beams by a beamsplitter. One beam exceeds the splitter and one that is reflected. Both the radiation is then reflected by the mirrors to the splitter and pass through it. By changing the distance of the mirror from the splitter is caused a continuous change in the optical path difference between the two beams, thus create interference in the radiation. The intensity as a function of mirror displacement is called interferogram. The spectral information contained in an interferogram is then retrieved using a Fourier transformation.

Bruker and ABB instruments are not built with a Michelson configuration, but with double-pendulum interferometer (Figure 13 right). The advantage of an interferometer with cube corner mirrors (so called Rock Solid™ interferometer in Bruker instrument) is to minimise the problems due to mirror misalignment and thus to be more robust towards mechanical distortion. Moreover the position of mirrors in these systems is controlled using a Helium-Neon laser, which permit the performance of the internal calibration. The wavelength stability of the HeNe laser results in a high performance in term of wavelength accuracy and precision.

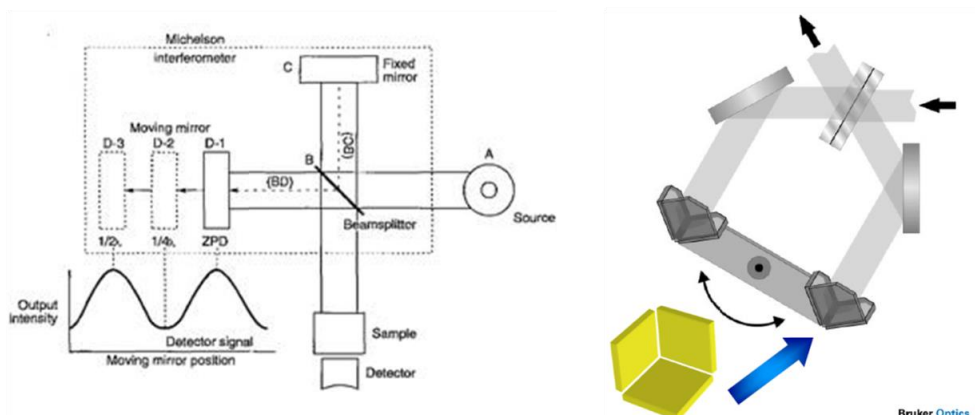


**Figure 13.** Schematic representation of interferometers. Left: a classical Michelson interferometer, right: Rock Solid™ interferometer contained in Bruker Optics instruments.

### 2.2.3 Sample interface and measurements modes

With the high throughput of FT spectrophotometers, it is possible to have different measurement channels and modules in one instrument. The multipurpose permits the analysis of different kind of samples (liquid, semi-solid, solid). There are three main types of optical measuring modes.

#### Sample interface

The standard approach is to measure the sample using **transmission** spectroscopy. The light from the source is directed to the sample with a focused or parallel beam. Some light is absorbed and the remaining energy is transmitted to the detector (Figure 14, left). Gasses and liquids are often sampled in transmission, but also reflecting and scattering samples could be measured.

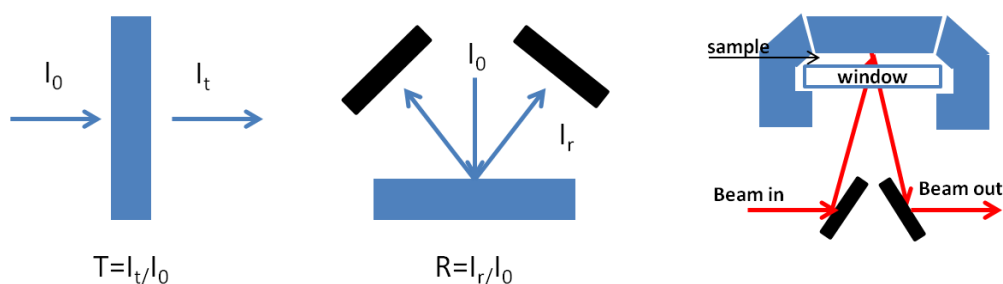


**Figure 14.** Principal of transmission, reflection and transfection.

The main sampling tools to be used in transmission spectroscopy are:

- Quartz cuvette with path length between 1 mm and 10 mm (used in Paper IV, VI, VII and VIII),
- Fiber optic probe for liquids in which the path length is defined by a fixed length at the probe head; according to the analysis different probe geometries could be used,
- Petri dishes use for samples with a consistency between solid and liquids from a point of view if their optical properties.

**Reflection** is used for solid surfaces, particles in powders, pellets or granulates. Reflection is generally referred to as diffusive reflection. In diffusive reflection spectroscopy, the incident light hits the sample surface and then is reflected with a different angle than the incident one. The light is generally collected at an angle between 5 and 85 degrees to the incident light (Figure 11, middle). There are different kinds of accessories to measure in diffusive reflection: integrating sphere, multiple fiber optic probes, rotating cups, etc. In situation in which the path of the container is too long or the kind of matrix does not allowed a simple measure in transmission, transfection measurement is an option. **Transfection** measures a combination of transmission and reflection. A mirror is placed in the light path, the light transmitted through the sample is reflected by the mirror at the same or almost the same angle as the incident beam and goes back to the detector (Figure 14, right). The detector can be a diffusive reflectance probe or an integrating sphere. This technique is useful for emulsions, gels and turbid liquids. In the applications presented transfection has been used for lactic acid fermentation monitoring (PAPER I, II and III). Paper V presents the use of diffusive transfection through the use of a fiber optic probe. Similar to regular transfection in diffusive transfection the light passes the sample twice but the diffusion of the light reflected, scattered or transmitted will pass through part of the sample. Numbers of probes are available in the market to apply this kind of measure directly on-line.

### *Sampling modes*

The timing of process measurement is fundamental for its control. Analysers can be referred to be off-line, at-line, on-line, in-line (Figure 15).

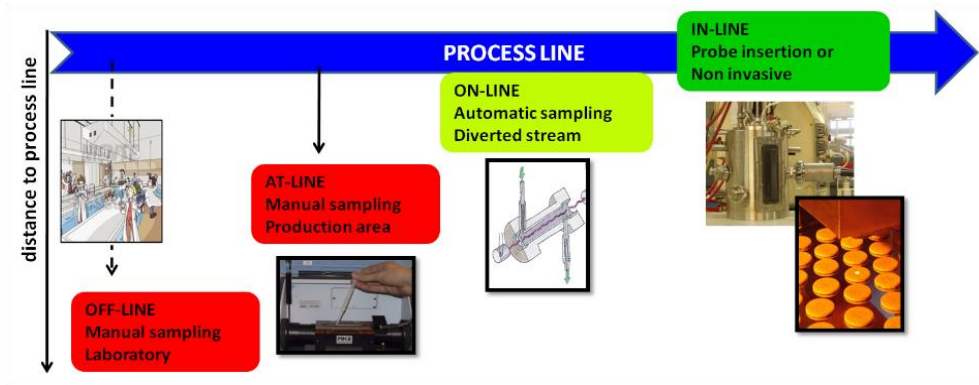


**Figure 15.** Places on the process line where spectroscopic instruments can be implemented.

- Off-line or laboratory analysis: samples are collected from the line and analysed in the laboratory, e.g. a Quality Control laboratory.
- At-line analysis: the instrument is placed close to the process line area but the sampling is done manually by an operator.
- On-line analysis: no operator is required as the analysis is made by automatic sampling in the process line: the product is deviated from the main line, analysed and reintroduced in the line. This could be necessary if the sample should be conditioned before analysis (removing bubbles, adjust in temperature).
- In-line analysis: in this case sensors are integrated into the production line.

## 2.3 Mid Infrared Spectroscopy (IR)

### 2.3.1 Spectra interpretation

Mid IR spectroscopy is based on the absorption in the range  $4,000 - 400 \text{ cm}^{-1}$  due to fundamental rotational molecular vibrations (banding and stretching). Contrary to NIR spectroscopy bands are less overlapped and the region  $1,500 - 1,000 \text{ cm}^{-1}$  defines a fingerprint characteristic of the sample under study. In general IR spectroscopy is often used to identify structures because functional groups give rise to characteristic bands both in terms of intensity and frequency (Figure 16).

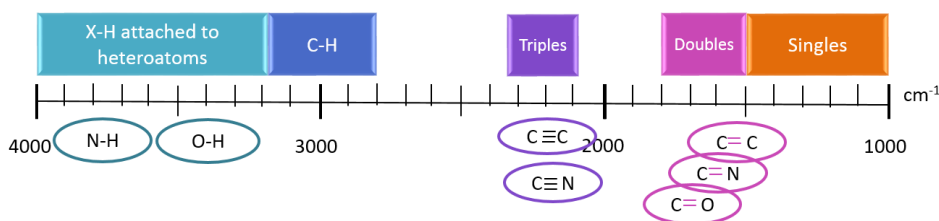


**Figure 16.** Schematic representation of vibration bands absorptions in the mid IR region.

The vibrational energy is directly related to the strength of bonds and the mass, thus permitting the identification of specific chemical entities. Table 2 reports examples of attribution of peaks to type of bonds.

The complexity of the matrix foodstuff and the combination of all the biochemical reactions occurring during fermentation enhances displacements of peaks due to the various compounds present in the matrix, which influence the absorbance of a bond. For this reason is more common to find the characterisation of typical peaks also according to the matrix under study. Therefore, there will often be a comprehensive study of the characteristic peaks founded for each different foodstuff in each paperwork reported in Chapter 4.

**Table 2.** Examples of absorption frequencies of functional groups in mid IR region.

<b>Bond</b>	<b>Type of bond</b>	<b>Absorption peak at <math>\text{cm}^{-1}</math></b>
<b>C-H</b>	Methyl and methylene	1470-1260 2870-2960
	C=CH <sub>2</sub>	900 3080-3020
	C=CH	990-900 3020
	Aromatic	900-690 3070
<b>C-C</b>	Aromatic	1660-1600 1580-1450
<b>C=O</b>		1775-1685
<b>O-H</b>	Alcohols, phenols	3670-3200
	Carboxylic acids	3560-3000
	Water	3700-3050
<b>N-H</b>	Primary Amines	1640-1560 3500-3400
	Secondary Amines	>3000
<b>C-O</b>	Primary Alcohols	1060-1040
	Secondary Alcohols	~1100
	Tertiary Alcohols	1200-1150
	Carboxylic acids	1300-1250
<b>C-N</b>	Aliphatic amines	1220-1020
	R-N-C	2110-2165
	R-N=C=S	1990-2140
<b>N-O</b>		1540-1380

By way of example Figure 17 reports the fingerprint region of spectra collected from different kind of sugars and ethanol typically present in wort fermenting to beer. This data are extracted from the results obtained in PAPERVII.

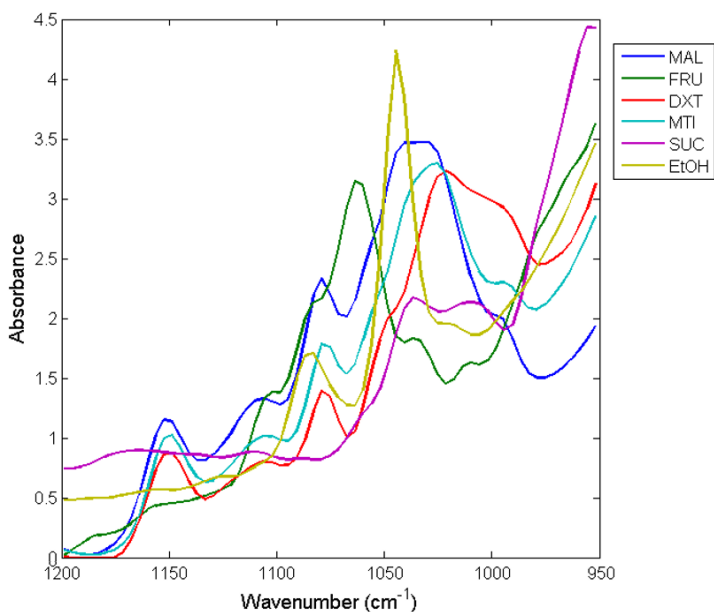


**Figure 17.** Example of spectral information in the IR fingerprint region ( $1,200\text{-}950\text{ cm}^{-1}$ ) of sugars (maltose, fructose, dextrin, maltotriose and sucrose) and ethanol present in beer in fermentation.

It is possible to notice that this region brings a lot of information, leading to a differentiation among some of the sugars, like fructose, sucrose and dextrin, and the ethanol. Anyway, the absorption peaks are overlapped, especially for maltose and maltotriose. Even in this region, characterised by specific absorption bands, the use of multivariate data analysis is necessary to have a more clear information from the spectral results.

### 2.3.2 Instrumentation

In the experiments monitored by mid IR spectroscopy (papers III, IV, V and VII) the instrument used was a FT-IR spectrometer. The details concerning the built-in technology have been already exposed in chapter 2.2. Briefly, the advantage of a FT-IR in respect with a FT-NIR is the higher sensitivity and speed in acquiring spectra. Moreover, progress has been done in the field of mid infrared region application in fitting a purge system to eliminate instability caused by the presence of air, i.e. interference of water (absorbing at  $3,657\text{ cm}^{-1}$  and  $1,595\text{ cm}^{-1}$ ) and carbon dioxide (absorbing at  $2,380\text{ cm}^{-1}$ ).



### 2.3.3 Sample interface and measurement modes

Sample presentation could be considered the most critical factor in the use of mid IR spectroscopy in food fermentation processes. Indeed it gives more detailed spectral information but its use is more limited if compare to the FT-NIR.

However in recent years advances in sample presentation technique have been done and different holders are on the market, especially for solid samples.

#### *Transmission windows and cells*

Transmission-based sample presentation techniques have been used for different kind of samples: from gases to liquids, from pastes to powders. As said before, measuring in transmission means that the IR beam of the spectrometer is passing through the sample and the transmitted IR intensity is measured. Owing to the high IR absorptivity of water, samples have to be very thin, usually only a few micrometres of optical path length. For analysing paste or viscous samples is, therefore, necessary to form smear or capillary films. Nowadays, transmission is mostly used for gas samples where is possible to use even cells with path from 1 to 20 cm.

Potassium bromide (KBr) pellets are used for the measurement of powders or granules. These preparations will not be reported in detailed as all the problems related to transmission windows have been solved by the implementation of attenuated total reflectance (ATR) cells.

#### *Attenuated total reflectance*

In this technique, the IR beam is guided in an IR transparent crystal by total reflection. Due to quantum mechanical properties of the IR light, the electromagnetic field may extend beyond the crystal surface for about one micron as a so-called evanescent field.

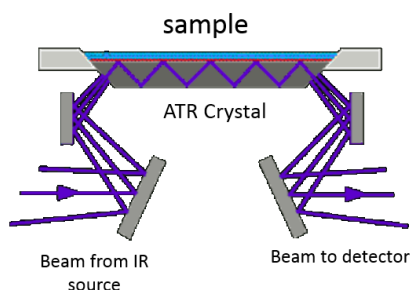


**Figure 18.** Scheme of an ATR cell.

As shown in Figure 18, the light from the source enters the ATR crystal and is reflected at the sample-element interface. Multiple reflections are generated due to the

angle of incidence of the accessory. At each point where reflection occurs, radiation penetrates the sample for a short distance and it decays logarithmically as a wave into the sample medium. Along the path the reflected energy is reduced by the part absorbed by the sample.

The material used to manufacture the internal reflectance element should have high refractive index, generally zinc selenide (ZnSe) or germanium (Ge) are the most employed.

An ATR cell has been used for yoghurt (PAPER III), wine (PAPER IV and V) and beer (PAPER VII) fermentation analysis. ATR revealed to be easy to use for liquid and viscous samples, with the only shrewdness of avoiding bubbles between the sample and the crystal.

### *Diffusive reflectance*

Diffusive reflectance modes can be adapted also for mid IR spectroscopy. It is generally used for products with textured surfaces which cannot be analysed by ATR and powders. In this case sample preparation is required and often means grinding to a fine powder and mixing with KBr.

## 2.4 References

- Bohr, H. (1914). A theorem concerning power series. *Proceedings of the London Mathematical Society*, 2(1), 1-5.
- Martens, H., Nielsen, J. P., & Engelsen, S. B. (2003). Light scattering and light absorbance separated by extended multiplicative signal correction. Application to near-infrared transmission analysis of powder mixtures. *Analytical Chemistry*, 75(3), 394-404.
- McClure, F. (2001). EAS Report. EAS-2001. *NIR news*, 12(6), 2-0.
- Miller, C. E. (2001). Chemical principles of near infrared technology. In *Near-infrared technology in the agricultural and food industries*, 2. American Association of Cereal Chemists. Minnesota, USA.
- Sandofy, C., Buchet, R., Lachenal, G. (2006) In: Ozaki, Y., McClure, W. F., & Christy, A. A. (Eds.). *Near-infrared spectroscopy in food science and technology*. Wiley.
- Stuart, B. H. (2004). *Infrared spectroscopy: fundamentals and applications*. Wiley. Chichester, UK.
- Wilson, E. B., Decius J.C., Cross P.C. (1980). *Molecular vibrations: the theory of infrared and Raman vibrational spectra*. Dover Publications Inc.
- Workman, J. & Weyer, I. (2008). *Practical Guide to Interpretive Near-Infrared Spectroscopy*, 332.

### **3. Chemometrics**



In the previous chapter it has been reported that the NIR e mid IR information is often characterized by overlapped bands, scattering effect, baseline drift and, as the others analytical techniques, is affected by the instrumental noise. Chemometrics is, therefore, the proper approach to explore and extract relevant information from spectral data, remove/correct/minimize the spectral artefact due to the experimental conditions and correlate the relevant information with the proper parameter to be controlled/measured. The general definition of Chemometrics is *the science of relating measurements made on chemical system or process to the state of the system via application of mathematical or statistical methods* (ICS, International Chemometrics Society). Chemometrics clusters several topics such as design of experiment, information extraction methods (modelling, classification and test of assumption) and techniques for studying and understanding chemical mechanisms.

In this chapter a general overview of the most common methods adopted in spectral data analysis are reported, with a particular detail to the less ordinary techniques which have been applied in this thesis.

### 3.1 Spectral pre-treatments

After the spectral data collection the first, and most important, step is to pre-process the data. The aim is to enhance the relevant information needed, and decrease the influence of unwanted side information contained in the spectra.

The most common pre-processing techniques used in infrared spectroscopy can be divided into two groups: scatter correction methods and spectral derivatives. The most representative for each category are presented below.

#### *Smoothing* (Gorry, 1990)

The purpose of smoothing correction is to minimise the noise present in the spectra. The smoothing method applied in the papers reported in this thesis is the one proposed by Savitzky and Golay (Savitzky & Golay, 1964), which is a moving window averaging method. An odd window size is selected, the data in the window are fitted by a polynomial (of different degree, generally second degree), and the central point of the window is replaced by the value of the polynomial. The choice of the size of the window is fundamental: large windows may eliminate important spectral information; while too small windows may not correct the noise present in the data.

#### *Scattering correction methods* (Rinnan *et al.*, 2009)

Scatter-corrective methods include Multiplicative Scatter Correction (MSC), Inverse MSC, Extended MSC, Extended Inverse MSC, de-trending, Standard Normal Variate (SNV) and normalisation. All the mentioned methods aim to reduce the spectral

variability related to the sample physical properties (scattering) and to adjust the baseline drift between samples.

The most commonly used techniques applied in this thesis are presented.

### MSC

Multiplicative Scatter correction is used as pre-processing method in NIR spectral data in order to remove artifacts and imperfections before data modeling.

MSC consists of two steps:

- The estimation of the correction coefficient (additive and multiplicative contribution):

$$\mathbf{X}_{org} = b_0 + b_{ref,1} \cdot \mathbf{X}_{ref} + \mathbf{e} \quad (9)$$

- The correction of the recorded spectrum:

$$\mathbf{X}_{corr} = \frac{\mathbf{X}_{org} - b_0}{b_{ref,1}} = \mathbf{X}_{ref} + \frac{\mathbf{e}}{b_{ref,1}} \quad (10)$$

Where  $\mathbf{X}_{org}$  is the spectra measured by the IR instrument,  $\mathbf{x}_{ref}$  is the reference spectrum used for pre-processing the entire dataset, generally the average spectrum of the calibration set, and  $\mathbf{e}$  is the un-modelled part of  $\mathbf{X}_{org}$ .  $b_0$  and  $b_{ref,1}$  are scalar parameters, calculated after a least square linear regression performed on the absorbance values of the sample spectrum versus those at the corresponding wavelength in the mean spectrum.  $b_0$  and  $b_{ref,1}$  represent the intercept and the slope of the linear equation, respectively.

MSC separates multiplicative and additive effects of the scatter in the spectra, minimizing spectral variation not related to the chemical composition of the sample.

### SNV

The basis of SNV is the same as for MSC, except that reference signal is not required. Thus the corrected spectrum ( $\mathbf{X}_{corr}$ ) is defined as:

$$\mathbf{X}_{corr} = \frac{\mathbf{X}_{org} - a_0}{a_1} \quad (11)$$

Where  $a_0$  is the average value of the sample spectrum to be corrected and  $a_1$  the standard deviation from the sample-spectrum. As no  $\mathbf{X}_{ref}$  is used the SNV normalisation is more effected by noisy spectra.

Dhanoa et al. (1994) have demonstrated that MSC and SNV are similar up to a simple rotation and offset correction. Nevertheless, an important consideration must be said.

While SNV does not change the shape of the spectra, MSC might slightly change the shape of the spectra being corrected. This is especially relevant when the spectrum chosen as reference is very different from the bulk of the spectra. This is the case of highly noisy spectra.

### *Spectral derivation*

Derivatives have the capability to remove additive and multiplicative effect and to enhance small spectral differences. In particular, the first derivative removes only additive effects (e.g. constant baseline drifts); whereas the second derivative removes also the presence of linear trends (multiplicative effects). Apart from this, both derivatives lead to an increased spectral resolution at the expense of a decrease of signal-to-noise ratio.

In the works presented in this thesis, Savitzky-Golay derivation was used. This method also includes a smoothing step. The method requires the optimization of three parameters:

- 1) The definition of a polynomial degree. Usually a second order polynomial degree is appropriate.
- 2) A window, i.e. the number of points used to calculate the polynomial. The optimization of this parameter is crucial, since large windows may eliminate important spectral information; while small windows may increase the noise of the data.
- 3) The derivative degree, depending which derivative wants to be performed.

In details to find the derivative at a centre point  $i$ : a polynomial is fitted in a symmetric window on the raw data, the parameters of the function fitted are calculated and the derivative is analytically found for that point.

## **3.2 Principal Component Analysis**

Principal component analysis, PCA, (Jackson, 1981) is a multivariate projection method which is used for general exploratory data analysis. It forms the basis of multivariate data analysis. It is applied for data compression, outliers' detection, pattern recognition and it is a powerful tool for data visualisation (Jolliffe, 1986). In addition, PCA provides an understanding of the relationships between all the variables (i.e. variables which contribute similar information to the model) and among variables and samples/observations.

Given a matrix of data ( $\mathbf{X}$ ) composed of  $m$  rows, representing observations, and  $n$  columns, standing for variables, PCA decomposes  $\mathbf{X}$  as sum of  $r$   $\mathbf{t}_i$  and  $\mathbf{p}_i$ :

$$\mathbf{X} = \mathbf{t}_1\mathbf{p}_1^T + \mathbf{t}_2\mathbf{p}_2^T + \mathbf{t}_r\mathbf{p}_r^T + \mathbf{E} = \mathbf{TP}^T + \mathbf{E} \quad (12)$$

Where  $\mathbf{T}$  stands for object scores and contains information about how the samples relate to each other,  $\mathbf{P}$  stands for variable loadings and unravel the magnitude (large or small correlation) and the manner (positive or negative correlation) in which the measured variables contribute to the scores, and  $\mathbf{E}$  for residuals, i.e. the unmodelled variation (Figure 19).

$$\mathbf{X} (M \times N) = \begin{bmatrix} | \\ | \\ | \end{bmatrix} \begin{bmatrix} \text{---} \\ \text{---} \\ \text{---} \end{bmatrix} + \begin{bmatrix} | \\ | \\ | \end{bmatrix} \begin{bmatrix} \text{---} \\ \text{---} \\ \text{---} \end{bmatrix} + \dots + \begin{bmatrix} | \\ | \\ | \end{bmatrix} \begin{bmatrix} \text{---} \\ \text{---} \\ \text{---} \end{bmatrix} + \mathbf{E} (M \times N)$$

$\mathbf{t}_1 \mathbf{p}_1^T \quad \mathbf{t}_2 \mathbf{p}_2^T \quad \mathbf{t}_a \mathbf{p}_a^T$

Figure 19. PCA decomposition of data matrix

Mathematically, PCA relies upon an eigenvector decomposition of the covariance or the correlation matrix of the process variables. For a given data matrix  $\mathbf{X}$  ( $M \times N$ ), where  $M$  are the observations/object and  $N$  the variables the covariance matrix is expressed as:

$$\mathbf{cov}(\mathbf{X}) = \frac{\mathbf{X}^T \mathbf{X}}{m-1} \quad (13)$$

The  $\mathbf{p}_i$  vectors are eigenvectors of the covariance matrix; for each  $\mathbf{p}_i$ :

$$\mathbf{cov}(\mathbf{X}) \mathbf{p}_i = \lambda_i \mathbf{p}_i \quad (14)$$

Where  $\lambda_i$  is the eigenvalue associated with the eigenvector  $\mathbf{p}_i$ . The  $\mathbf{p}_i$  are orthonormal columns. Whereas  $\mathbf{t}_i$  form an orthogonal set. Another way to look at it is that  $\mathbf{t}_i$  are the projections of  $\mathbf{X}$  onto the  $\mathbf{p}_i$ .

From a geometrical point of view the first principal component (PC1) is calculated as the line in the the  $K$ -dimensional space that best approximate the data in the least square sense, and represent the maximum variation of the data set. Usually the one component is not sufficient, thus a second component (PC2) is calculated orthogonally to the first line (PC1). PC1 and PC2 define a plane (Figure 20), and the observations/samples are projected in this new defined space. The scores are now defined as the co-ordinate values of each observation on this plane.



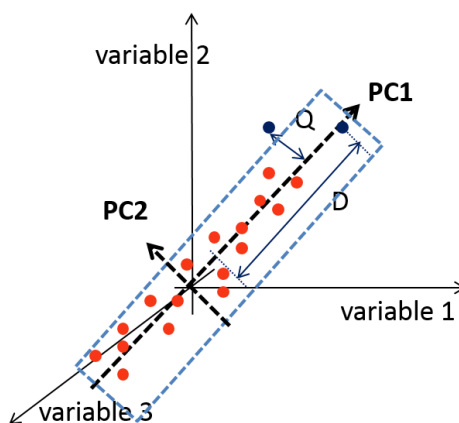


**Figure 20.** Geometric interpretation of PCA

$Q$  and  $D$  are two figures of merit important for PCA models evaluation. The  $Q$ -statistic for one object its distance from the model;  $T^2$ -statistic its distance from the centre of the model. In Figure 20 are reported two extremes observations: a sample with high  $Q$  value and a sample with high  $T^2$  value in order to understand graphically the meaning of the two figures of merit. This is a good demonstration of the possible use of PCA as a screening for outliers' presence in the dataset.

### 3.3 Multivariate Curve Resolution

Multivariate curve resolution, MCR, is a technique commonly used in complex kinetic systems. Indeed it aims to resolve multi-component mixtures into a simple model consisting of the weighted sum of the signal of the pure components involved (Tauler & Barcelò, 1993; Tauler et al. 2005). In detail a given  $\mathbf{D}$  data matrix is resolved in into the product of column wise matrix  $\mathbf{C}$  ( $\mathbf{M} \times \mathbf{F}$ ) associated with concentration profiles and a row-wise matrix  $\mathbf{S}$  ( $\mathbf{F} \times \mathbf{N}$ ) describing spectra profile. The residuals are in the  $\mathbf{E}$  matrix. A schematic overview is reported in Figure 21.

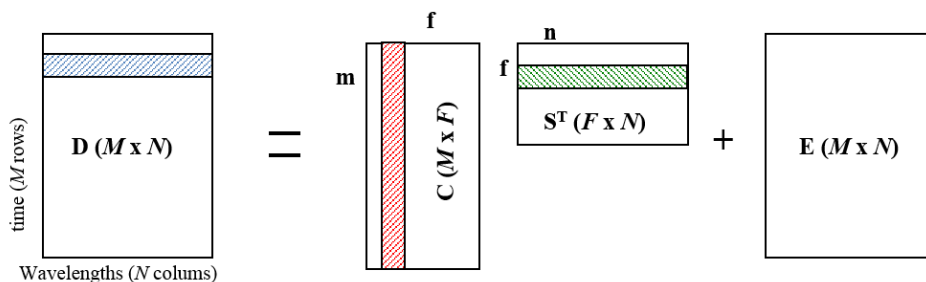


**Figure 21.** Schematic overview of dataset decomposition performed by MCR

As described previously  $\mathbf{M}$  is a scalar of the total number of observation or time points in the dataset, whereas  $\mathbf{N}$  represents the variables, i.e. the wavenumbers. For what concern  $\mathbf{F}$  it is the number of components in the system to be resolved.

Decomposition of  $\mathbf{D}$  is achieved by iterative least-squares minimization of  $\|\mathbf{E}\|$  under suitable constraining conditions (i.e. non-negativity in spectral profiles, unimodality and non-negativity in concentration profiles), and also closure relations between reagents and products of a given reaction.

A powerful extension of MCR used in the technique use in the PAPER II and VII is multi- experiment MCR. When more than one experiment is considered is possible to augment in a column-wise manner the  $\mathbf{D}$  data matrix. The main advantage will be that  $\mathbf{S}^T$  is still a single matrix with the shape of the pure species, describing all the experiments present in the  $\mathbf{D}$  augmented matrix. Whereas the  $\mathbf{C}$  profile will be composed by submatrices,  $\mathbf{C}_i$ , of the individual experiments. In this way the concentration profiles of the chemical species are free to change in independent manner from one experiment to the other.

### 3.3.1 MCR-ALS

The optimization of MCR with ALS was presented by Tauler, Smilde and Kowalski (1995), and has been used in numerous papers, especially in kinetic processes (Amigo et al. 2006a; Amigo et al. 2006b; de Juan et al. 2006; Rodriguez-Rodriguez et al. 2007; Garrido et al. 2008; Pindstrup et al. 2013). The main steps are presented in Figure 22.

Before applying MCR method, the number of component should be selected through PCA, in our case with Single Value Decomposition (SVD) method. Then is necessary to select initial estimates in the concentration and/or spectral profiles. There are different way for choosing initial estimates in spectral profiles.

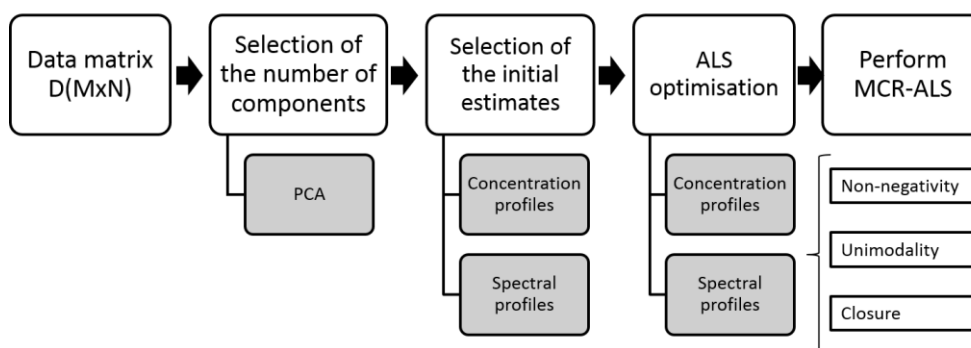


**Figure 22.** Steps characterizing the MCR-ALS optimisation

In the PAPER II the initial estimates were chosen in the most straightforward way, i.e. within a representative batch three spectra recorded at the beginning, in the middle and at the end of the fermentation. In PAPER VII the estimates used were spectra of pure components (ethanol and dextrans) present in the fermenting wort. In that case another commonly strategy was used: in the column-wise augmentation of the  $\mathbf{D}$  matrix were added also the spectra of other pure compounds present in the wort (maltose, maltotriose, sucrose and fructose). This is an additional way to initialize the system parameters and improve the MCR-ALS model results. At this point the ALS optimization starts the interactions. To achieve the final results a stopping criterion must be imposed. The one presented in this thesis is percentage of Lack of Fit (%LOF) and it is generally set to 0.1%, that means that the algorithm stops when the relative difference between two consecutive interactions is below 0.1% LOF. The Equation of %LOF is:

$$\% LOF = 100 \times \sqrt{\frac{\sum_i^I \sum_j^J e_{mn}^2}{\sum_i^I \sum_j^J d_{mn}^2}} \quad (15)$$

where  $e_{mn}$  is each  $mn$ th element of the residual matrix  $\mathbf{E}$ , and  $d_{mn}$  is each  $mn$ th element of the  $\mathbf{D}$  matrix.

As said earlier is necessary to impose some constraints to the MCR-ALS solutions, because the product  $\mathbf{CS}^T$  is subjected to rotational and intensity ambiguities. The constraints used are chosen according to the available information about the target system. The most commonly used are non-negativity, unimodality and closure, and can be applied both on spectral and concentration profiles.

The effect of non-negativity and unimodality are here presented in Figure 23 and 24 as they were applied in PAPER II and VII. Non negativity is applied on spectral profile when is known that the technique used does not allowed negative values, is the case of IR spectroscopy, and as well in concentration profile in case we are talking about concentration that inherently cannot have negative value.

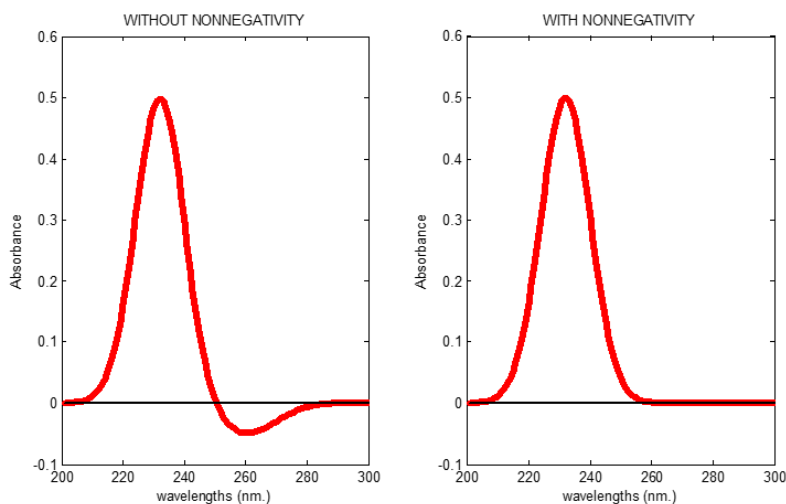


**Figure 23.** Comparison of spectral profile non optimised and with non-negativity constraint

Unimodality constraint was applied in the concentration profiles because it impose the presence of only one maximum in each profile, as it is expected to be in a biotransformation process.

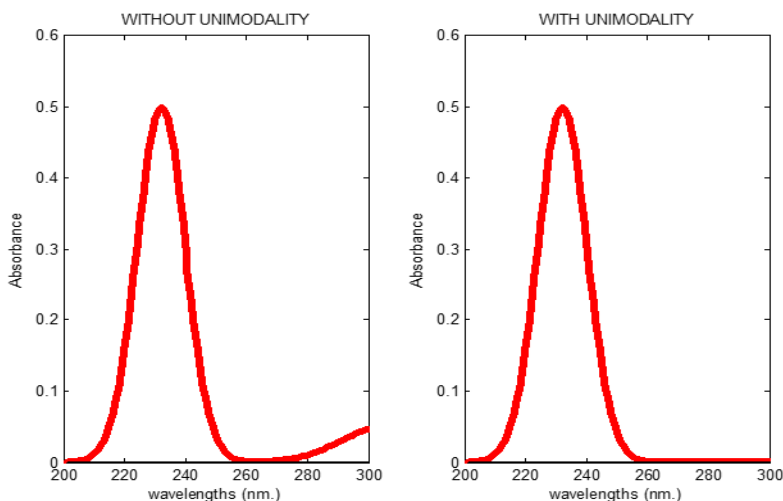


**Figure 24.** Comparison of spectral profile non optimised and with unimodality constraint

As seen the choice of the constraints always depends on previous knowledge of the system and the measure technique employed. Constrains could strongly influence the models obtained so is important to used them as less as possible and, when necessary, to use them properly.

### 3.4 Multivariate regression

This section is not an exhaustive discussion of all the regression techniques applied in Chemometrics, it want just to go in detail into the two techniques applied in this PhD project: Partial Least Square (PLS) regression and Locally weighted regression (LWR).

The multivariate regression methods are regression instruments coming from the necessity of overcome the problems related to OLS Regression (*Ordinary Least Squares*) in treating with predicting variables highly correlated, like spectroscopy data, and influence by noise.

#### 3.4.1 Partial Least Square (Wold et al., 1983; Geladi & Kowalski, 1986)

PLS is one of the chemometric strategy more used with PCA, actually both methods are based on latent variables concept.

PLS is a regression method which constructs a linear regression equation between the scores of the predictor variables and the scores of the dependent variables. Similarly to the PCA method, the PLS decomposes both the X matrix of the predictor variables and simultaneously the Y matrix of the dependent variables, creating principal directions that describe the maximum variability of X and, at the same time, taking into account the maximum covariance between the scores of X and Y.

The PLS model can be considered as consisting of outer relations between X and Y according to the two equations:

$$\mathbf{X} = \mathbf{TP}^T + \mathbf{E} \quad (16)$$

$$\mathbf{Y} = \mathbf{UQ}^T + \mathbf{F} \quad (17)$$

By using the score of X as predictive variables e Y scores as new dependent variables, is possible to obtain their inner relation:

$$\mathbf{U} = \mathbf{T}\mathbf{b}_{PLS} + \mathbf{F}^* \quad \hat{\mathbf{U}} = \mathbf{T}\mathbf{b}_{PLS} \quad (18)$$

Where  $\mathbf{b}_{PLS}$  is the regression coefficients vector of the latent variables,  $\mathbf{F}^*$  is the inner relation residual matrix, and  $\hat{\mathbf{U}}$  is the Y scores matrix.  $\mathbf{b}_{PLS}$  is calculated with least square regression between the single scores of X and Y.

The loading weight, W, can be calculated from the estimation of the scores, T, in the X matrix:

$$\mathbf{W} = \mathbf{T}^T \mathbf{X} \quad (19)$$

In addition to the PCA model, in PLS there is also a relation linking X and Y matrices (Eq.20):

$$Y = TQ^T + F^* = XW^T + F^* = Xb + F^* \quad (20)$$

The properties of scores and loadings are the same as described for PCA, in addition is important to say that the weights are orthonormal.

The regression conducted with PLS method is linear. The choice of a linear model often require a data pre-treatment (mean centring, normalisation and so on) in order to get rid of dynamic character of the trajectories.

### 3.4.2 *Locally weighted regression*

Locally weighted regression (LWR) is a method applied when the correlation between the spectral signal and the reference measure has a non-linear nature. Cleveland and Devlin (1988) LWR as methodology to fulfil this goal and Næs and Isaksson (1992) and Naes, Isaksson and Kowalski (1990) applied the strategy to infrared spectroscopy. In most of the cases the non-linear nature of the correlation between spectra and reference measure is approached correcting the spectral signal with pre-processing methods to eliminate or reduce unwanted contribution to the signal, such as light scattering. Mainly the idea of spectra correction is to make the signal of IR analysis more similar to Beer's law spectroscopy.

In some cases is not enough correcting the spectra to get rid of non-linearities. Is the examples of dataset characterised by high influence of the experimental design or the time trajectory.

The main principal of LWR is to select a set of samples (local points) close to the prediction spectrum to construct a calibration dataset and base the regression surface on these samples. Thus, for each new predicted sample a weighted regression calibration is made. From the first approach investigated until now different closeness techniques have been investigated (Aastveit & Marum, 1993; Wang, Isaksson & Kowalski, 1994; Shen, Berzaghi & Westerhaus, 1997). In the experiments presented in paper VI, as previously reported by Dahlbacka and Lillhonga (2013), the Euclidean distance was applied to determine the closeness to the dependent variable, the auto-scaled distance in PC space to determine the closeness to the spectrum, and enables model regression on PLS.

To summarize the main steps characterizing the analysis are reported (Bevilacqua et al., 2013) as they were applied in the paper VI:

1. Definition of the number of nearest neighbours (local points) close to the prediction spectrum to be used to build local calibration models;
2. Find for every new object the samples closest to it in the local calibration model (nearest neighbours);
3. Build a local calibration model using the nearest neighbours only; assign the weights ( $\alpha$ ) of the neighbours in the local model according to their Euclidean distance to determine the closeness to the dependent variable and the auto-scaled distance in the principal components space;
4. Prediction (by PLS regression) of the new sample by applying the local calibration model developed.

As demonstrated in the works mentioned from the literature and in Paper VI, LWR is a good method to be used to correct nonlinearities in IR relationships. LWR is only one of the possible nonlinear regression approach, other example is nonlinear PLS. However is important to preliminary investigate the data and to try also if the nonlinearities could just be solved by pre-treatment for then performing a linear regression analysis.

### 3.5 References

- Amigo, J. M., de Juan, A., Coello, J. & MasPOCH, S. (2006a). A mixed hard- and soft-modelling approach for the quantitative determination of oxipurines and uric acid in human urine. *Analytica Chimica Acta*, 567(2), 236-244.
- Amigo, J.M., de Juan, A., Coello, J. & MasPOCH, S. (2006b). A mixed hard- and soft-modelling approach to study and monitor enzymatic systems in biological fluids. *Analytica Chimica Acta*, 567(2), 245-254.
- Aastveit, A. H., & Marum, P. (1993). Near-infrared reflectance spectroscopy: different strategies for local calibrations in analyses of forage quality. *Applied spectroscopy*, 47(4), 463-469.
- Bevilacqua, M., Bucci, R., Materazzi, S., Marini, F. (2013). Application of near infrared (NIR) spectroscopy coupled to chemometrics for dried egg-pasta characterization and egg content quantification. *Food Chemistry*, 140, 726-734
- Cleveland, W.S., Devil, S.J. (1988). Locally Weighted Regression: An Approach to Regression Analysis by Local Fitting. *Journal of the American Statistical Association*, 83 (403), 596-610.
- Dhanoa, M.S., Lister, S.J., Sanderson, R. and Barnes, R.J. (1994). The Link Between Multiplicative Scatter Correction (MSC) and Standard Normal Variate (SNV) Transformations of NIR Spectra, *J. Near Infrared Spectrosc.* 2:43–47.

- Dahlbacka, J., Lillhonga, T. (2013). Quantitative measurements of anaerobic digestion process parameters using near infrared spectroscopy and local calibration models. *Journal of Near Infrared Spectroscopy*, 21 (1), pp. 23-33.
- Gorry, P.A. (1990). General least-squares smoothing and differentiation by the convolution (Savitzky-Golay) method. *Analytical Chemistry*, 62 (6),570-573.
- Geladi, P., & Kowalski, B. R. (1986). Partial least-squares regression: a tutorial. *Analytica chimica acta*, 185, 1-17.
- Jackson, J.E. (1981). Principal component and factor analysis: Part 1 – Principal Component. *J. Qual. Tech.*, 13(1): 46-58.
- Jolliffe, I. T. (1986). Principal component analysis. *Spring-verlag, New York*.
- Rinnan, Å., Berg, F. V. D., & Engelsen, S. B. (2009). Review of the most common pre-processing techniques for near-infrared spectra. *TrAC Trends in Analytical Chemistry*, 28(10), 1201-1222.
- Naes, T., Isaksson, T., Kowalski, B. (1990). Locally weighted regression and scatter correction for near-infrared reflectance data. *Analytical Chemistry*, 62(7), 664-673.
- Naes, T., Isaksson, T. (1992). Locally weighted regression in diffuse Near-infrared transmittance spectroscopy. *Applied Spectroscopy*, 46(1), 34-43.
- Savitzky, A., & Golay, M. J. (1964). Smoothing and differentiation of data by simplified least squares procedures. *Analytical chemistry*, 36(8), 1627-1639.
- Shenk, JS, Westerhaus, MO, and Berzaghi, P. (1997). Investigation of a local calibration procedure for near infrared instruments. *J. Near Infrared Spectrosc.*, 5:223-232.
- Tauler, R. & Barceló, D. (1993). Multivariate curve resolution and calibration applied to liquid chromatography diode array detection. *Trends in Analytical Chemistry*, 12(8), 319-327.
- Tauler, R. (1995). Multivariate curve resolution applied to second order data. *Chemometrics and Intelligent Laboratory Systems*, 30, 133-146.
- Tauler, R., Smilde, A. and Kowalski, B.R. (1995) Selectivity, Local Rank, Three-Way Data Analysis and Ambiguity in Multivariate Curve Resolution. *Journal of Chemometrics*, 9, 31 – 58.
- de Juan, A. & Tauler, R. (2006). Multivariate Curve Resolution (MCR) from 2000: Progress in concepts and applications. *Critical Review in Analytical Chemistry*, 36(3-4), 163-176.
- de Juan, A., Casassas, E. & Tauler, R. (2000). Soft-modelling of analytical data. In *Encyclopedia of analytical chemistry instrumentation and applications*. New York: Wiley.
- Rodríguez-Rodríguez, C., Amigo, J. M., Coello, J. & Maspocho, S. (2007). An introduction to multivariate curve resolution-alternating least squares: Spectrophotometric study of the acid–base equilibria of 8-hydroxyquinoline-5-sulfonic acid. *Journal of Chemical Education*, 84(7), 1190-1195.



- Garrido, M., Rius, F. X. & Larrechi, M. S. (2008). Multivariate curve resolution-alternating least squares (MCR-ALS) applied to spectroscopic data from monitoring chemical reactions processes. *Analytical and Bioanalytical Chemistry*, 390(8), 2059-2066.
- Pindstrup, H., Fernández, C., Amigo, J. M. & Skibsted, L. H. (2013). Multivariate curve resolution of spectral data for the pH-dependent reduction of ferrylmyoglobin by cysteine. *Chemometrics and Intelligent Laboratory Systems*, 122, 78-83.
- Wold, S., Martens, H., & Wold, H. (1983). The multivariate calibration problem in chemistry solved by the PLS method. In *Matrix Pencils* (pp. 286-293). Springer Berlin Heidelberg.
- Wang, Z., Isaksson, T., & Kowalski, B. R. (1994). New approach for distance measurement in locally weighted regression. *Analytical Chemistry*, 66(2), 249-260.



## **4. Food fermentation monitoring**



In this chapter the experimental part of the PhD research is reported as scientific papers overview about the four matrices investigated: yoghurt, wine, beer and sourdough.

In the introduction of each paper a comprehensive idea of the state-of-the-art of the traditional techniques used for monitoring each fermentation process is given, together with the recent progresses in infrared spectroscopy implementation for the different kind of fermentation monitoring.

Here a summary, in table format (Table 3), is reported as general overview of FT-NIR and FT-IR implementation for quantitative and qualitative analyses of food fermentation processes and the final products obtained.

**Table 3.** Some applications of FT-IR and FT-NIR for fermented food analysis

<b>Food category</b>	<b>Food product</b>	<b>References</b>
Alcoholic beverage	Wine	Cozzolino & Curtin, 2012; Buratti et al., 2011; Pizarro et al., 2011; Fernández-Navales et al., 2008
	Beer	Engel et al., 2012; McLeod et al., 2009; Inon et al., 2005; Duarte et al., 2004
	Others	Lachenmeier, 2007
Acetic acid product	Vinegar	Bao et al., 2013; Duran et al., 2010; Garrido-Vidal et al., 2004; Sáiz-Abajo et al., 2006
Dairy products	Fermented milks	Ntsame Affane et al, 2011; Navratil et al., 2004; Cimander et al., 2002
	Cheese	González-Martín et al., 2014; Kraggerud et al., 2014; Holroyd, 2013
Fermented meat products	Sausages	Collell et al., 2012
	Ham	Prevolnik et al., 2014; García-Rey et al., 2005
Fermented cereal food	Dough	Li Vigni & Cocchi, 2013; Sinelli et al., 2008; AiT Kaddour et al., 2007

The references reported are not an exhaustive revision of all the bibliography in the literature but the most relevant and recent papers for giving a general idea of infrared application in each of the food category presented.

In all the cited works (Table 1) is well explored how FT-NIR and FT-IR, combined with chemometric techniques, in recent years have proven to be a successful tool for quantitative and qualitative modelling of a wide variety of fermented food products and their production processes. Clearly emerge the advantages of infrared spectroscopy implementation due to its non-destructive nature, no sample preparations and quite low running costs.

## References

- AiT Kaddour, A., Morel, M.-H., Barron, C., & Cuq, B. (2007). Dynamic monitoring of dough mixing using near-infrared spectroscopy: physical and chemical outcomes. *Cereal Chemistry*, 84, 70–79
- Bao, Y., Liu, F., Kong, W., Sun, D.-W., He, Y., Qiu, Z. (2013). Measurement of Soluble Solid Contents and pH of White Vinegars Using VIS/NIR Spectroscopy and Least Squares Support Vector Machine. *Food and Bioprocess Technology*, Article in Press.
- Buratti, S., Ballabio, D., Giovanelli, G., Zuluanga Dominguez, C.M., Moles, A. Benedetti, S., Sinelli, N. (2011). Monitoring of alcoholic fermentation using near infrared and mid infrared spectroscopies combined with electronic nose and electronic tongue. *Analytica Chimica Acta*, 697 (1–2), 67-74.
- Cimander, C., Carlsson, M., Mandenius, C.-F. (2002). Sensor fusion for on-line monitoring of yoghurt fermentation. *Journal of Biotechnology*, 99 (3), pp. 237-248.
- Collell, C., Gou, P., Arnau, J., Muñoz, I., Comaposada, J. (2012). NIR technology for on-line determination of superficial aw and moisture content during the drying process of fermented sausages. *Food Chemistry*, 135 (3), 1750-1755.
- Cozzolino, D., Curtin, C. (2012). The use of attenuated total reflectance as tool to monitor the time course of fermentation in wild ferments. *Food Control*, 26 (2), 241-246.
- Duarte, I.F., Barros, A., Almeida, C., Spraul, M., Gil, A.M. (2004). Multivariate analysis of NMR and FTIR data as a potential tool for the quality control of beer. *Journal of Agricultural and Food Chemistry*, 52, 1031-1038.
- Durán, E., Palma, M., Natera, R., Castro, R., Barroso, C.G. (2010). New FT-IR method to control the evolution of the volatile constituents of vinegar during the acetic fermentation process. *Food Chemistry*, 121 (2), 575-579.
- Engel J., Blanchet L., Buydens L.M.C., Downey G. (2012). Confirmation of brand identity of a Trappist beer by mid-infrared spectroscopy coupled with multivariate data analysis. *Talanta*, 99, 426–432
- Fernández-Navales, J., López, M.-I., Sánchez, M.-T., García, J.-A., Morales, J. (2008). A feasibility study on the use of a miniature fiber optic NIR spectrometer

- for the prediction of volumic mass and reducing sugars in white wine fermentations. *Journal of Food Engineering*, 89, 325–329.
- García-Rey, R.M., García-Olmo, J., De Pedro, E., Quiles-Zafra, R., Luque De Castro, M.D. (2005). Prediction of texture and colour of dry-cured ham by visible and near infrared spectroscopy using a fiber optic probe. *Meat Science*, 70 (2), 357-363.
- Garrido-Vidal, D., Esteban-Díez, I., Pérez-Del-Notario, N., González-Sáiz, J.-M., Pizarro, C. (2004). On-line monitoring of kinetic and sensory parameters in acetic fermentation by near infrared spectroscopy. *Journal of Near Infrared Spectroscopy*, 12 (1), 15-27.
- González-Martín, I., Hernández-Hierro, J.M., González-Pérez, C., Revilla, I., Vivar-Quintana, A., Lobos Ortega, I. (2014). Potential of near infrared spectroscopy for the analysis of volatile components in cheeses. *LWT - Food Science and Technology*, 55 (2), 666-673.
- Holroyd, S.E. (2013). The use of near infrared spectroscopy on milk and milk products. *Journal of Near Infrared Spectroscopy*, 21 (5), 311-322.
- Inon, F. A., Llarío, R., Garrigues, S., de la Guardia, M. (2005). Development of a PLS based method for determination of the quality of beers by use of NIR spectral ranges and sample-introduction considerations. *Analytical and Bioanalytical Chemistry*, 382, 1549–1561.
- Kraggerud, H., Næs, T., Abrahamsen, R.K. (2014). Prediction of sensory quality of cheese during ripening from chemical and spectroscopy measurements. *International Dairy Journal*, 34 (1), 6-18.
- Lachenmeier, D. W. (2007). Rapid quality control of spirit drinks and beer using multivariate data analysis of Fourier transform infrared spectra. *Food Chemistry*, 101, 825–832.
- Li Vigni, M., & Cocchi, M. (2013). Near infrared spectroscopy and multivariate analysis to evaluate wheat flour doughs leavening and bread properties. *Analytica Chimica Acta*, 764, 17– 23.
- McLeod, G., Clelland, K., Tapp, H., Kemsley E.K., Wilson, R.H., Poulter, G., Coombs D., Hewitt, C.J. (2009). A comparison of variate pre-selection methods for use in partial least squares regression: A case study on NIR spectroscopy applied to monitoring beer fermentation. *Journal of Food Engineering*, 90, 300-307.
- Navratil, M., Cimander C., and Mandenius, C.F. (2004). On-line multisensor monitoring of yogurt and filjolk fermentations on production scale. *J. Agric. Food Chem.* **52**, 415.
- Ntsame Affane, A.L., Fox, G.P., Sigge, S.O., Manley M. and Britz, T.J. (2011). Simultaneous prediction of acidity parameters (pH and titratable acidity) in Kefir using near infrared reflectance spectroscopy, *International Dairy Journal*, 21, 896.

- Pizarro, C., González-Sáiz, J.M., Esteban-Díez, I., Orio, P. (2011). Prediction of total and volatile acidity in red wines by Fourier-transform mid-infrared spectroscopy and iterative predictor weighting. *Analytical and Bioanalytical Chemistry*, 399, 2061–2072.
- Prevolnik, M., Andronikov, D., Žlender, B., Font-i-Furnols, M., Novič, M., Škorjanc, D., Čandek-Potokar, M. (2014). Classification of dry-cured hams according to the maturation time using near infrared spectra and artificial neural networks. *Meat Science*, 96 (1), 14-20.
- Sáiz-Abajo, M.J., González-Sáiz, J.M., Pizarro, C. (2006). Prediction of organic acids and other quality parameters of wine vinegar by near-infrared spectroscopy. A feasibility study. *Food Chemistry*, 99 (3), 615-621.
- Sinelli, N., Casiraghi, E., Downey, G. (2008). Studies on proofing of yeasted bread dough using near- and mid-infrared spectroscopy. *Journal of agricultural and food chemistry*, 56, 922-31.



# PAPER I



## Monitoring of lactic acid fermentation process using Fourier transform near infrared spectroscopy

---

**Silvia Grassi, Cristina Alamprese,<sup>\*</sup> Veronica Bono, Claudia Picozzi, Roberto Foschino and Ernestina Casiraghi**

Department of Food, Environmental and Nutritional Sciences (DeFENS), Università degli Studi di Milano, Via Celoria 2, 20133 Milano, Italy.  
E-mail: [cristina.alamprese@unimi.it](mailto:cristina.alamprese@unimi.it)

**Abstract**

The aim of this paper was to evaluate the suitability of Fourier Transform-Near Infrared (FT-NIR) spectroscopy, combined with multivariate data analysis, to monitor milk lactic acid fermentation as an indication of possible deviations in quality parameters. Fermentation trials performed with different inocula (*Streptococcus thermophilus* and *Lactobacillus delbrueckii* subsp. *bulgaricus* as single or in mixed cultures) at three incubation temperatures (37, 41, and 45 °C) were monitored by FT-NIR spectroscopy. Rheology and conventional quality parameters (microbial counts, pH, titratable acidity, lactose, galactose and lactic acid concentrations) were used as reference values to assess the findings with FT-NIR spectroscopy. Principal component analysis was applied to spectra to uncover molecular modifications. PC1 scores, rheological data, and conventional quality parameter values were modelled as a function of fermentation time to designate critical points all along the process. Results showed that FT-NIR spectroscopy is a useful tool for real-time assessment of curd development during fermentation, offering crucial information in agreement with rheology and conventional quality parameters.

**Keywords:** FT-NIR; lactic acid fermentation; modelling; rheology.

## Introduction

Fermentation is one of the earliest methods adopted to obtain value-added milk products with an extended shelf life. Although about 400 different names have been found all over the world for traditional and industrial fermented milks, these products are quite similar, including only a few variations.<sup>1</sup> Three broad categories of fermented milk products have been identified (i.e., lactic fermented, yeast-lactic fermented and mould-lactic fermented milks) depending on the kind of milk used in the production process, the predominant microbial species in the inoculum and their metabolic products.<sup>2</sup> Fermentations carried out by lactic acid bacteria are the most widespread in the dairy industry for milk acidification and flavour development,<sup>3</sup> of which yoghurt is the most common. The Codex Alimentarius Commission defines yoghurt as a symbiotic culture of *Streptococcus thermophilus* and *Lactobacillus delbrueckii* subsp. *bulgaricus* which should be viable, active and abundant in the product to the date of minimum durability.<sup>4</sup> The sour taste characterising lactic acid fermented dairy products originated from the conversion of lactose into lactic acid and the consequent milk pH reduction from around 6.7 to values lower than 4.5.

An at-line control of the fermentation processes usually involves pH measurement and titratable acidity determination. Other key indicators of fermentation progress are lactic acid, carbohydrates (i.e. lactose and galactose), and bacterial concentrations, but they are not routinely measured, being expensive and time-consuming. The final quality of fermented milk products is strictly related to the exact determination of the optimal incubation time. Milk composition variations, an anomalous behaviour of starter microorganisms, an incorrect control of the incubation temperature, as well as a number of other process variables, can yield end products with low overall quality. The risk of product failure can be reduced only by a complete understanding and an accurate monitoring of the process.<sup>5</sup> An effective control at all stages of the fermentation process requires fast methods, providing real-time information. An easy, fairly innovative, cheap and non-destructive technique is near-infrared (NIR) spectroscopy, which has been proposed as an alternative to conventional analyses for in-time monitoring of various products and processes. Absorptions in the spectral range between 14,000 and 4,000  $\text{cm}^{-1}$  are associated to the main chemical components of foodstuff, such as water, proteins, carbohydrates, and fats. In particular, NIR vibration and combination overtones of the fundamental C–H, N–H, O–H and C=O bonds are the main recordable phenomena.<sup>6</sup> The use of NIR spectroscopy for dairy product analysis is well documented.<sup>7-10</sup> In particular, during the last years the interest in dairy fermentation monitoring by means of NIR spectroscopy had increased. Navratil *et al.* described how the fusion of NIR spectroscopy and electronic nose data can be applied to the on-line monitoring of industrial fermented milk production.<sup>11</sup> Moreover, Ntsame Affane *et al.* developed models to predict acidity parameters in Kefir by using NIR

reflectance spectroscopy, demonstrating its adequacy for screening purposes.<sup>10</sup> One of the main features of NIR radiation is that it is composed of broad and mostly overlapped bands, which hinder the direct extraction of information from the raw spectra, making necessary the use of multivariate data analysis.<sup>10,12-13</sup> One of the most widespread chemometric tools for qualitative data analysis is principal component analysis (PCA). It employs an orthogonal transformation to convert the original dataset into a subset of linearly uncorrelated highest-variance components (principal component - PC). The PCs are linear combinations of the original variables and each component explains a part of the total variance of data; in particular, the first significant component accounts for the largest source of total variance, while the further PCs explain the residual variation.<sup>9,14</sup> The aim of this paper was the evaluation of the suitability of NIR spectroscopy, joined with multivariate data analysis (i.e. PCA), for the monitoring of lactic acid fermentation in milk. In particular, the possibility to develop an easy and fast protocol able to promptly detect possible defects in product quality parameters (e.g. acidity and texture) due to deviations from the regular processing trend was investigated. The availability of this protocol could be useful in the assessment of the best strategy for the management of nonconformities. In order to identify the main changes occurring during fermentation, conventional quality parameters and rheological characteristics were analysed and modelled as a function of fermentation time for the identification of the kinetic critical points.

## Materials and methods

### *Materials*

Skim milk powder (Merck, Darmstadt, Germany) was reconstituted to 10% w/v with distilled water, distributed in 1 L bottles, and subjected to heat treatment at 112 °C for 15 min and then stored at 4 °C until use. Bacterial strains were isolated from the commercial yoghurt culture YO-MIX™ 305 (Danisco A/S, Copenhagen, Denmark) and identified, by sequencing the amplified 16S rDNA region, as *Streptococcus salivarius* spp. *thermophilus* and *Lactobacillus delbrueckii* spp. *bulgaricus*. Pure cultures of the two strains were stored at -20 °C in appropriate media (see below) with added glycerol (20% v/v).

### *Fermentation trials*

Frozen stocks of *S. thermophilus* and *L. bulgaricus* were activated by incubation at 37 °C overnight in M17 broth (Merck, Darmstadt, Germany) and de Man, Rogosa, Sharpe (MRS) broth (BD, Franklin Lakes, NJ, USA) respectively, both modified by adding 10% w/v lactose. After centrifugation for 15 min at 3,000 g, cells were harvested and resuspended in sterilized skim milk. For each fermentation trial, 800 mL of skim milk was inoculated with a single culture or with a mixed culture containing both

microorganisms (1:1). A calibration curve obtained through the correlation between cell number and optical density measured at 600 nm with a spectrophotometer (Jasco V650, Jasco Europe, Cremella, Italy) was used to set the inoculum size at approximately  $10^6$  CFU mL<sup>-1</sup>. Aliquots of about 60 mL of the inoculated skim milk were then aseptically distributed into sterile glass bottles and placed in a circulating water bath at the specific fermentation temperature (37 °C, 41 °C or 45 °C), for 7.5 h. Every 45 min, a bottle was taken to analyse the fermented milk, while spectroscopic and rheological evaluations were carried out continuously. A total of 9 different fermentation trials, twice replicated, were performed (18 experimental trials). Analytical results are reported as the average of the two technological replicates for each fermentation condition.

#### *Microbiological analysis*

From the incubated bottles, aliquots of about 10 g of sample were aseptically collected and resuspended in a 2% sodium citrate solution to obtain the first decimal dilution. After homogenization, appropriated serial dilutions (1:10) were made in duplicate, plated on modified (0.5% sucrose, 0.5% lactose) HHD agar (Biolife, Milano, Italy) and incubated at 37 °C for 48 h. The modified medium is able to differentiate the two strains on the basis of their acidifying abilities. Results are expressed as number of colony forming unit per gram of fermented milk (CFU g<sup>-1</sup>).

#### *pH and titratable acidity*

pH values were potentiometrically measured using a pH meter 3510 (Jenway, Dunmow, UK) equipped with a glass electrode. Titratable acidity was determined according to the IDF/ISO Standard n° 150 and expressed as percentage of lactic acid.<sup>15</sup> Both the analyses were performed in duplicate.

#### *Sugars and organic acids*

Lactose, galactose and lactic acid were determined by high-performance liquid chromatography (HPLC), using an equipment (ThermoFinnigan, Milano, Italy) fitted with a Carbo H4 pre-column (3.0 mm ID, Phenomenex, Castel Maggiore, Italy) followed by an Aminex HPX-87H cation exclusion column (300 x 7.8 mm, BioRad Laboratories, Richmond, CA, USA). Elution was performed isocratically at 65 °C with 5 mM H<sub>2</sub>SO<sub>4</sub> (Merck, Darmstadt, Germany) as mobile phase, at a flow rate of 0.8 mL min<sup>-1</sup>. Peaks were detected using a refractive index detector RI-71 (Showa Denko Europe GmbH, Munich, Germany) and registered by the Empower 2™ chromatography data software (Waters Corporation, Milford, MA, USA). For peak identification and quantification, calibration curves of each component were calculated by analyzing standard solutions in mobile phase as follows: lactose monohydrate (Merck, Darmstadt, Germany), ranging from 0.1 to 10 g L<sup>-1</sup>; galactose (Sigma-Aldrich,

St. Louis, MO, USA), ranging from 0.02 to 10 g L<sup>-1</sup>; L(+)-lactic acid (Merck, Darmstadt, Germany), ranging from 0.02 to 3 g L<sup>-1</sup>.

Five grams of sample was added to 10 mL of acetonitrile (Merck, Darmstadt, Germany) and centrifuged at 5,000 g for 12 min at 4 °C (Rotina 380R, Hettich Zentrifugen, Andreas Hettich GmbH & Co. KG, Tuttlingen, Germany). The supernatant was filtered through a 0.45 µm PDVF-filter (Alltech, Milan, Italy) and injected in the 20 µL loop of the HPLC system. Sample preparation and injection were performed in duplicate.

#### *Rheological measurements*

Curd development was monitored at regular intervals on the same sample using a Physica MCR 300 rheometer (Anton Paar GmbH, Graz, Austria), supported by the software Rheoplus/32 (v. 3.00, Physica Messtechnik GmbH, Ostfildern, Germany). A dynamic oscillatory test was performed, using concentric cylinders (CC27) and applying a constant 1% strain at a fixed 1 Hz frequency. The inoculated skim milk (19 mL) was inserted in the measurement element pre-heated at the desired fermentation temperature. Sample evaporation during the test was prevented mounting the proper solvent trap filled with deionised water. Storage ( $G'$ ) and loss ( $G''$ ) moduli were measured in 2 min intervals throughout the whole fermentation process.

#### *FT-NIR spectroscopy*

Near infrared spectra of the inoculated skim milk during the fermentation process were collected at regular intervals from the same sample in transreflectance mode, using a Fourier Transform (FT)-NIR spectrometer equipped with a fibre-optic probe with a 1 mm pathlength (MPA, Bruker Optics, Milan, Italy). The probe was inserted directly into the inoculated skim milk contained in a glass bottle placed in a water bath to maintain the defined fermentation temperature. Spectral data were collected every 15 min over the 12,500-4,000 cm<sup>-1</sup> range, with a resolution of 16 cm<sup>-1</sup>, 64 scans for both background and samples, and a scanner velocity of 10 kHz. Instrument control and data acquisition were performed by the OPUS software (v. 6.5 Bruker Optics, Milan, Italy).

#### *Data processing*

After smoothing (moving average method, segment size = 11 data points), FT-NIR data were transformed into first derivative (Savitzky–Golay method, polynomial order = 2, gap size = 11 data points) to minimize the effect of baseline shifts, and reduced in the range 8,900-5,555 cm<sup>-1</sup> in order to eliminate useless or saturated variables from spectra. PCA was applied to the averaged spectral data obtained by the two technological replicates of each fermentation condition, by using The Unscrambler

v9.8 software (Camo Software AS, Oslo, Norway). All spectral data sets were mean-centred before performing PCA calculations.

The scores of PC1 were modelled as a function of fermentation time, using the sigmoid Eq. (1) implemented in Table Curve software (v. 4.0, Jandel Scientific, San Rafael, CA, USA):

$$y = a + b \cdot \exp\left(-\exp\left(-\left(\frac{(x - d \ln(\ln(2)) - c)}{d}\right)\right)\right) \quad (1)$$

Also the average data obtained by conventional analyses and rheological evaluations were modelled as a function of fermentation time, applying the same sigmoid function, in agreement with the microbial nature of the transformation studied.<sup>16-17</sup>

In order to identify kinetic critical points during fermentation – i.e. time related to the maximum rate and acceleration (or deceleration) of the phenomena - the first and second derivatives of the sigmoid functions were calculated.

## Results and discussion

### *Microbiological analysis*

The use of modified HHD, which provides a morphological differentiation of colonies and recovery close to those obtained by separated specific media (MRS pH 5.4 and M17), permitted the enumeration of the single species on a unique plate.<sup>18</sup>

The change in viable counts of *S. thermophilus* and *L. bulgaricus* during fermentation trials are presented in Figure 1.

The initial mean counts of *L. bulgaricus* for the three different fermentation trials (Figure 1a) ranged from 1.33 to 2.97 x 10<sup>6</sup> CFU g<sup>-1</sup>, increasing then to 2.00-3.07 x 10<sup>8</sup> CFU g<sup>-1</sup> after 5 h of fermentation without significant changes till the end of the experiment (2.52-2.98 x 10<sup>8</sup> CFU g<sup>-1</sup>). As regard to *S. thermophilus* (Figure 1b), the initial concentrations ranged from 2.67 to 4.23 x 10<sup>6</sup> CFU g<sup>-1</sup>, reaching a plateau at about 2.81-3.00 x 10<sup>8</sup> CFU g<sup>-1</sup> after 5 h. In the trials performed with mixed cultures (Figure 1c), *L. bulgaricus* grew faster than *S. thermophilus*, but after 5 h both microorganisms reached their plateau, at about 2.17-4.43 x 10<sup>8</sup> CFU g<sup>-1</sup>.

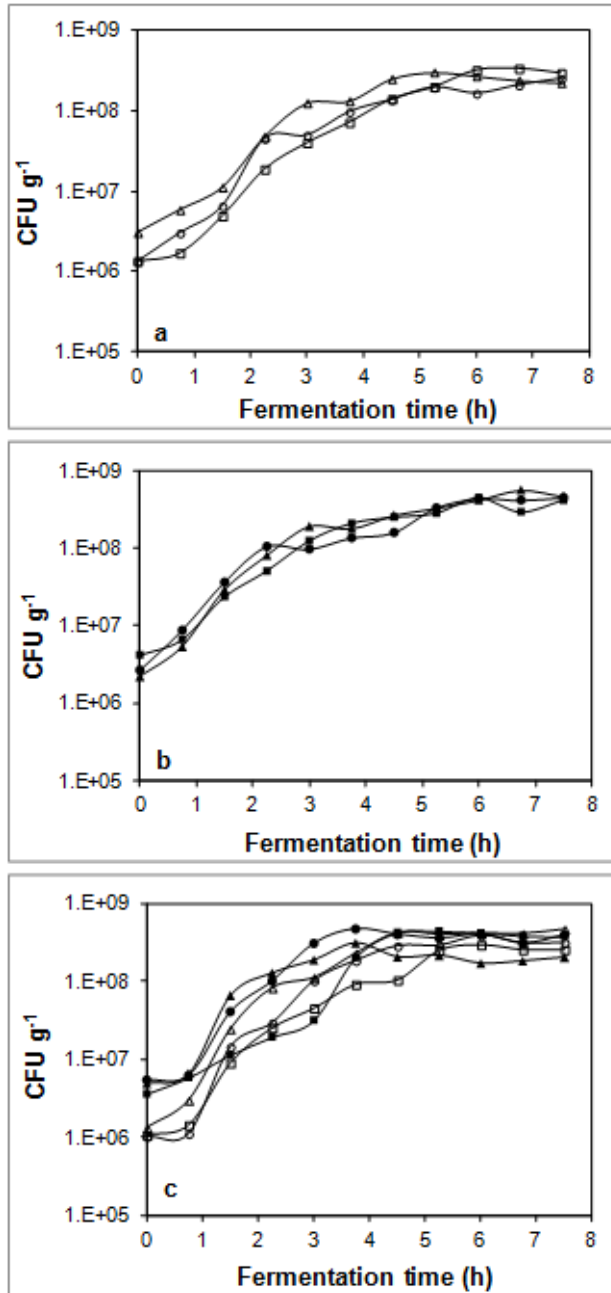


**Figure 1.** Growth of *L. bulgaricus* (a), *S. thermophilus* (b), and the mixed culture (c) during lactic acid fermentations carried out at different temperatures. *L. bulgaricus*, 37 °C (□), 41 °C (○), 45 °C (Δ); *S. thermophilus*, 37 °C (■), 41 °C (●), 45 °C (▲).



*pH and titratable acidity measurements*

Results concerning pH values of fermented milks produced by single and mixed cultures are shown in Figure 2. The mixed culture was the most efficient in lowering pH values, followed by single cultures of *L. bulgaricus* and then *S. thermophilus*.

The mixed culture (Fig. 2c) lowered the pH from 6.5 to 3.8, within 7.5 h at 41 °C, which is the common temperature used for milk lactic acid fermentation; whereas the single cultures of *L. bulgaricus* (Fig. 2a) and *S. thermophilus* (Fig. 2b) lowered the pH value to 3.9 and 4.9, respectively, due to the higher acidification activity of lactobacilli.<sup>19</sup>

The change in titratable acidity, expressed as percentage lactic acid, are illustrated in Table 1. The titratable acidity of reconstituted skim milk (0.13-0.16%) increased till a maximum of 1.18% in milk fermented at 45 °C with the mixed culture. The lowest value was reached when inoculating *S. thermophilus* at 37 °C (0.38%). Our results are in accordance with those reported by Rasic and Kurmann,<sup>19</sup> showing that *S. thermophilus* produces a maximum lactic acid concentration of 0.7-0.8%, while *L. bulgaricus* is a homo-fermenting lactic bacteria producing up to 1.7% of lactic acid. The titratable acidity developed by *S. thermophilus* and *L. bulgaricus* increased with the rise of incubation temperature, as reported by Tamime and Robinson.<sup>5</sup>

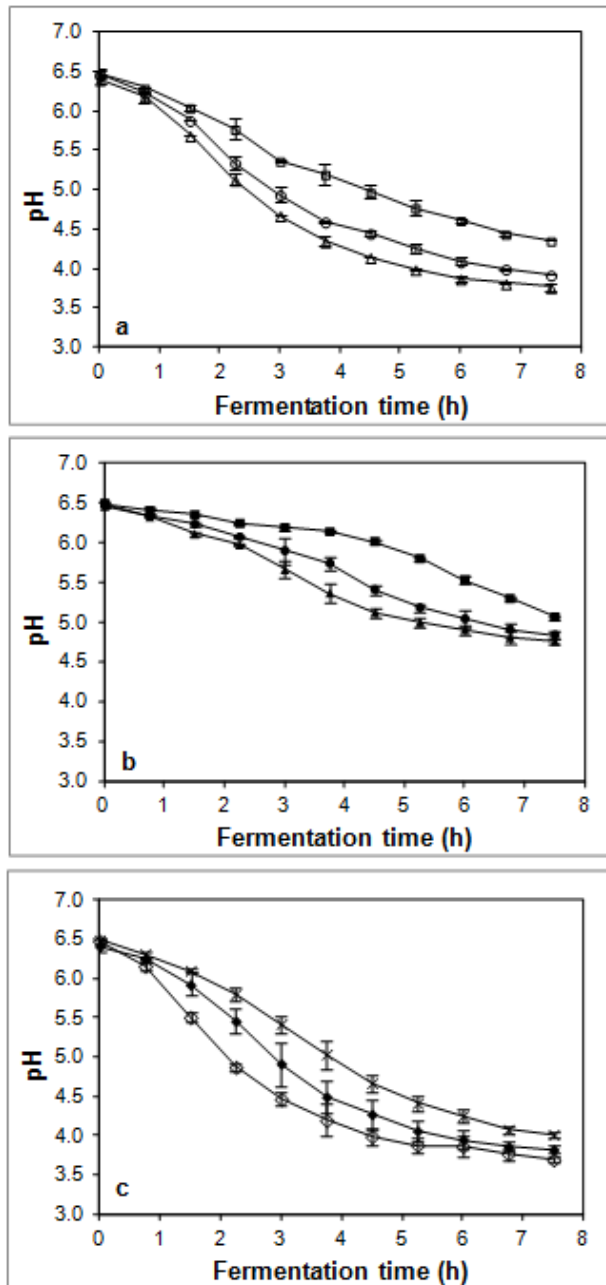


**Figure 2.** Evolution of pH values during lactic acid fermentations carried out at different temperatures with *L. bulgaricus* (a), *S. thermophilus* (b), and the mixed culture (c). □ *Lactobacillus bulgaricus*, 37 °C; ○ *Lactobacillus bulgaricus*, 41 °C; △ *Lactobacillus bulgaricus*, 45 °C; ■ *Streptococcus thermophilus*, 37 °C; ● *Streptococcus thermophilus*, 41 °C; ▲ *Streptococcus thermophilus*, 45 °C; × Mixed culture, 37 °C; ◆ Mixed culture, 41 °C; ◇ Mixed culture, 45 °C.

**Table 1** Changes in titratable acidity (TA), lactose, galactose, and lactic acid concentrations during lactic acid fermentations carried out under different processing conditions.

Inoculum <sup>a</sup>	Temperature (°C)	TA increase		Lactose	Galactose	Lactic acid
		(% acid)	lactic	consumption (g 100g <sup>-1</sup> )	increase (g 100g <sup>-1</sup> )	production (g 100g <sup>-1</sup> )
I1	37	0.62		1.22	0.33	0.30
	41	0.81		0.71	0.51	0.50
	45	0.87		1.25	0.50	0.60
I2	37	0.24		0.66	0.15	0.19
	41	0.34		0.60	0.15	0.20
	45	0.40		0.40	0.16	0.28
I3	37	0.81		1.38	0.34	0.48
	41	0.88		1.51	0.40	0.50
	45	1.02		0.90	0.47	0.65

<sup>a</sup>I1, *L. bulgaricus*; I2, *S. thermophilus*; I3, *S. thermophilus* and *L. bulgaricus* (1:1)

#### *Sugars and organic acids*

Table 1 shows, for each fermentation trial, the changes in the main chemical constituents involved in lactic fermentation (lactose, galactose and lactic acid). Both *L. bulgaricus* and *S. thermophilus* ferment lactose: during the homolactic fermentation the disaccharide is transported into the bacterial cell and transformed by a lactase into glucose and galactose. Glucose is then catabolised to lactic acid, while galactose is thrown out the cell. For this reason a galactose accumulation in the medium is expected, as observed in this work.

Within the 7.5 h of fermentation with *L. bulgaricus*, lactose consumption ranged from 0.71 to 1.25 g 100 g<sup>-1</sup>, while with *S. thermophilus* the decrease was only 0.40-0.66 g 100 g<sup>-1</sup>, due to its lower acidification capacity. As regards the mixed culture, a maximum lactose concentration reduction of 1.51 g 100 g<sup>-1</sup> was registered. At the end of the fermentation process the highest increase of galactose content was observed with the *L. bulgaricus* inoculum, whereas the highest lactic acid production was noticed when the mixed culture was tested. Similar results of lactic acid production were

reported also by Dave and Shah for yoghurt made from commercial starter cultures.<sup>20</sup> The lowest values of lactic acid in the final product were obtained inoculating single culture of *S. thermophilus*, being this species less acid tolerant than the other one.

#### *Rheological behaviour*

Rheological behaviour was studied to monitor the curd development during fermentation as the textural characteristics of fermented milk gel are of paramount importance for the quality of the final product. A small amplitude oscillatory test was used in this research, in order to follow the development of the curd structure without system perturbation. Average storage modulus ( $G'$ ) and loss modulus ( $G''$ ) values over fermentation time in the different trials are illustrated in Figure 3.

The  $G'$  value defines the degree of solid-like character of the gel, whereas the  $G''$  value indicates the degree of the liquid-like behaviour. Thus, at the beginning of fermentation, when milk was still liquid,  $G''$  values were always higher than  $G'$  values. When the gel began to form,  $G'$  and  $G''$  values rapidly increased, with a higher rate for  $G'$ . Usually, the time required for  $G'$  to cross-over  $G''$  is considered as the onset of gelation.<sup>21,22</sup>

As it can be noticed from Figure 3, when the mixed culture (Fig. 3c) or the *L. bulgaricus* (Fig. 3a) inoculum were used, time needed for curd development was shorter than in trials carried out with *S. thermophilus* (Fig. 3b). At the optimum temperature of 41 °C, the onset of gelation occurred after 2, 2.5, and 5.3 h of fermentation for the associative, *L. bulgaricus* and *S. thermophilus* inoculum, respectively.

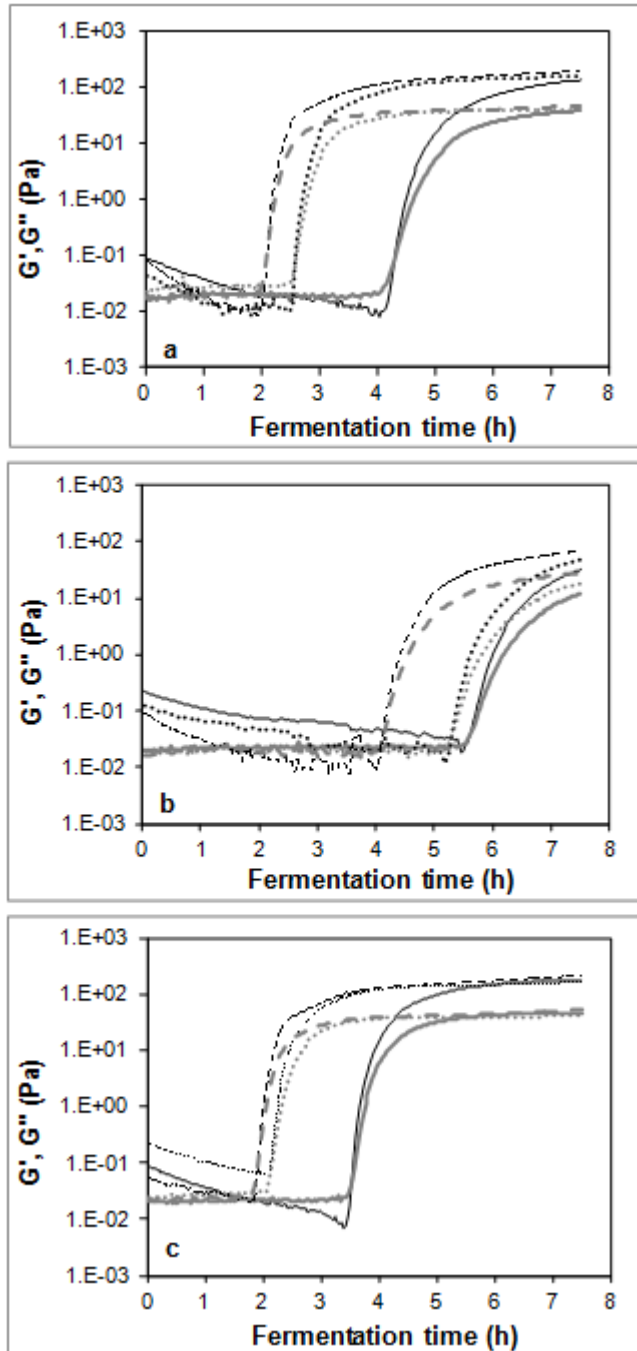


**Figure 3.** Evolution of storage ( $G'$ ) and loss ( $G''$ ) modulus during the lactic acid fermentations carried out at different temperatures with *L. bulgaricus* (a), *S. thermophilus* (b), and the mixed culture (c). —  $G'$ ,  $37^\circ\text{C}$ ; - -  $G''$ ,  $37^\circ\text{C}$ ; .....  $G'$ ,  $41^\circ\text{C}$ ; - · - ·  $G''$ ,  $41^\circ\text{C}$ ; - - -  $G'$ ,  $45^\circ\text{C}$ ; - - -  $G''$ ,  $45^\circ\text{C}$ .

Moreover, trials carried out with *S. thermophilus* resulted in a gel weaker than those developed in the other runs, as can be noticed by the lower final values of  $G'$  and  $G''$ . These results are in agreement with those reported for pH, titratable acidity, and lactic acid development, which showed a better performance of the mixed and the *L. bulgaricus* cultures in comparison with the *S. thermophilus* inoculum.

#### FT-NIR spectroscopy

In this study spectra were acquired in transreflectance mode, which combines transmission and reflectance principles, because during milk fermentation the physical and chemical properties of the matrix evolve. The use of transmitted light is necessary at the beginning of the fermentation when the viscosity of milk is low, whereas a reflectance measurement is required with the progress of the bioprocess leading to a weak gel behaviour of the system.<sup>12</sup>

Figure 4 shows an example of the reduced (8,900-5,555  $\text{cm}^{-1}$ ) FT-NIR spectra collected during the fermentation process carried out with the mixed culture, at 45 °C, and the corresponding signals transformed into first derivative.

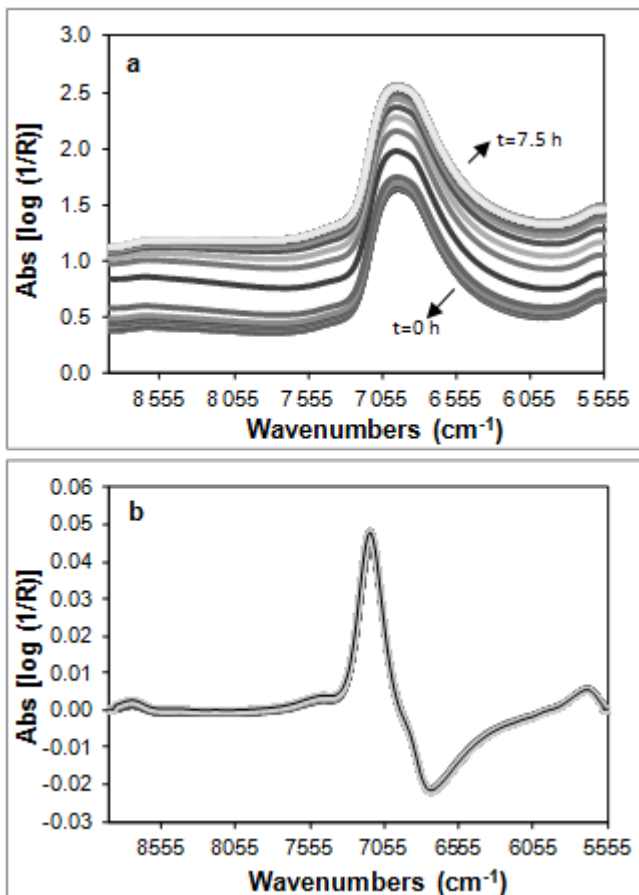


**Figure 4.** Reduced FT-NIR spectra collected during the lactic acid fermentation carried out at 45 °C with the mixed culture of *L. bulgaricus* and *S. thermophilus*: a) raw spectra ( $t$  = fermentation time); b) spectra after transformation with first derivative.

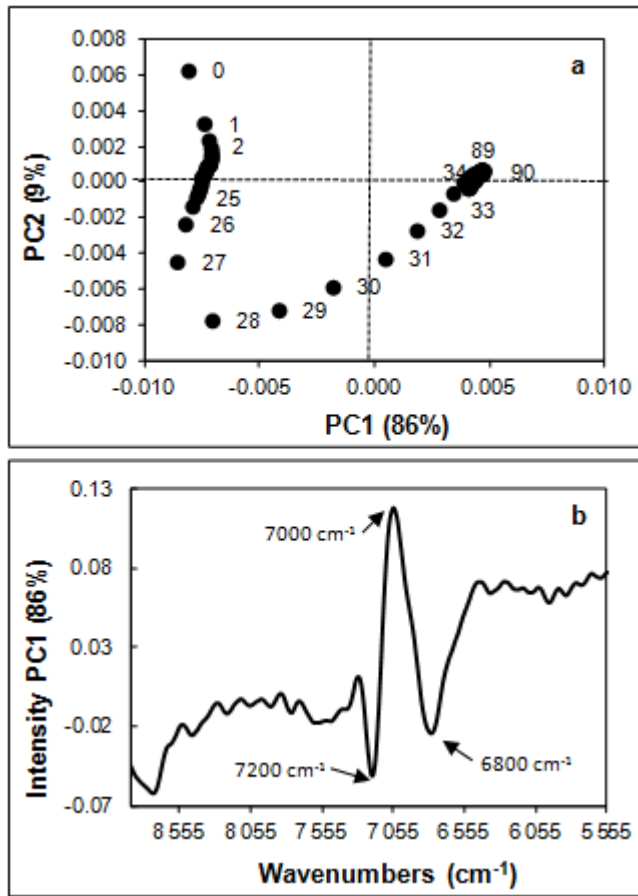


**Figure 5.** Plots obtained from PCA applied to FT-NIR spectra collected during the lactic acid fermentation carried out at 41°C with the mixed culture of *L. bulgaricus* and *S. thermophilus*: a) PC1 vs PC2 score plot; b) loading line plot for PC1. In the score plot, point label numbers increase with fermentation time.

Similar results were obtained for all the fermentation trials (results not shown). The dominant peak at about 6,900  $\text{cm}^{-1}$  in the FT-NIR spectra is related to the O-H first overtone. Qualitative evaluation of the spectra showed a remarkable trend in the FT-NIR spectra during the fermentation time: spectra collected from milk at the beginning of the bioprocess were characterised by absorbance values lower than those of the spectra acquired at the end of fermentation from coagulated milk. This change could be due to physical effects, such as casein micelle size, which heavily influences NIR spectrum.<sup>23</sup> Although the absorption increased with fermentation time, it was difficult to extract information regardless of scattering effects causing the baseline drift. For this reason, a first derivative transformation was applied to the spectral signals.

In order to uncover changes related to the time occurring during milk fermentation, reduced and pre-treated FT-NIR data were processed by PCA. Figure 5 shows the score plot and loading line plot obtained for the fermentation trial performed at 41 °C with the mixed culture.

Similar results were obtained for the other fermentation trials (results not shown). In the score plot, a suited distribution of the samples in the area defined by the first two principal components according to the fermentation time was noticed. The intensity of loadings highlighted that the main wavenumbers responsible for the sample separation were mainly associated with the O-H bands of water.<sup>24</sup>

### *Kinetic models*

In order to evaluate the ability of NIR spectroscopy to follow the milk fermentation process kinetic, PC1 scores obtained from spectra elaboration by PCA, as well as chemical and rheological data, were modelled as a function of the fermentation time, fitting the sigmoid function shown in Eq. (1). PC1 scores were previously normalized from 0 to 1, in order to compare the results obtained in different trials. Figure 6 shows an example of the PC1 scores fitted by Eq. (1) and the first and second derivatives of the curve.

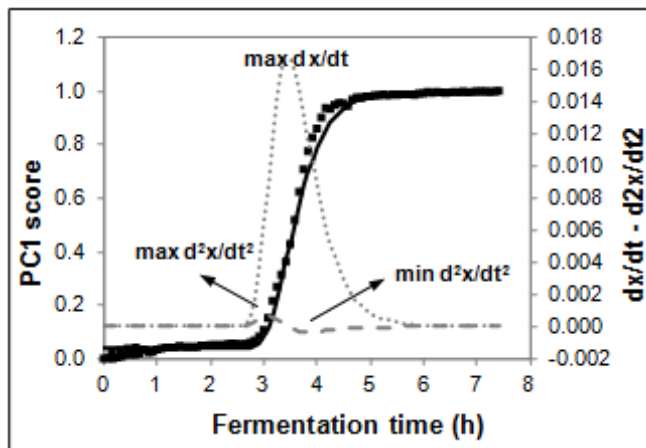


**Figure 6.** Example of PC1 scores modelling as a function of fermentation time.

Derivatives were used to calculate the critical points related to the maximum rate (maximum value of first derivative), acceleration (maximum value of second derivative), and deceleration (minimum value of second derivative) of the phenomena. Scores obtained in all the fermentation trials were well fitted by Eq. (1), giving  $r^2$  values always higher than 0.99. The sigmoid model was reliable also for  $G'$ , pH, titratable acidity and lactic acid data ( $r^2 > 0.94$ ).



The curves obtained by NIR-PCA and rheological data showed a very similar trend, meaning that both techniques detected the evolution of parameters strictly related to the curd development. The phenomenon described could be related to the casein micelles becoming bigger as a consequence of their aggregation, occurring at pH values of 5.5 - 5.2.<sup>25</sup> In fact, also the times corresponding to the critical points of the fermentation were practically the same for these two analytical techniques (Table 2) and corresponded to the development of pH values ranging from 5.5 to 5.2 (Figure 2). A good agreement was also observed with the critical points calculated considering the other analytical parameters. Only the times related to the maximum acceleration of the process, i.e. to the beginning of the fermentation, were lower if calculated on the basis of pH, titratable acidity (Table 2), and lactic acid values (data not shown). These results could be ascribed to the different phenomena associated with the evaluated parameters: pH, acidity and lactic acid concentration are related to the acidification operated by the microorganisms, which generally precedes the curd development described by rheological and spectral data.

**Table 2** Times corresponding to maximum acceleration (max  $d^2x/dt^2$  or min  $d^2x/dt^2$ ), maximum rate (max  $dx/dt$ ) and maximum deceleration (min  $d^2x/dt^2$  or max  $d^2x/dt^2$ ) of the lactic acid fermentation processes.

Inoculum <sup>a</sup>	Temperature (°C)	FT-NIR (PC1)			Rheometer (log G')			pH			Titratable Acidity (% lactic acid)			FT-NIR (ABS at 7,100 cm <sup>-1</sup> )		
		Max $d^2x/dt^2$	Max $dx/dt$	Min $d^2x/dt^2$	Max $d^2x/dt^2$	Max $dx/dt$	Min $d^2x/dt^2$	Min $d^2x/dt^2$	Max $dx/dt$	Max $d^2x/dt^2$	Max $d^2x/dt^2$	Max $dx/dt$	Min $d^2x/dt^2$	Max $d^2x/dt^2$	Max $dx/dt$	Min $d^2x/dt^2$
		(min)	(min)	(min)	(min)	(min)	(min)	(min)	(min)	(min)	(min)	(min)	(min)	(min)	(min)	(min)
I1	37	184	202	225	251	269	287	0	132	277	105	423	450	175	202	225
	41	135	148	157	147	160	174	18	114	209	36	186	314	121	130	144
	45	108	108	117	120	133	142	23	100	186	82	173	264	94	103	112
I2	37	306	337	364	341	359	373	95	263	427	168	314	450	292	328	360
	41	283	306	328	314	337	355	64	209	350	150	255	368	265	297	324
	45	233	265	296	241	260	278	50	155	255	105	223	345	234	279	324
I3	37	184	198	207	206	219	233	59	168	282	118	227	341	180	193	202
	41	130	144	153	124	128	151	50	123	241	114	209	309	112	126	144
	45	103	112	121	111	120	133	23	100	186	64	155	245	90	99	108

<sup>a</sup> I1, *L. bulgaricus*; I2, *S. thermophilus*; I3, *S. thermophilus* and *L. bulgaricus* (1:1).

Times related to the critical points confirmed that a lactic fermentation carried out by *L. bulgaricus* alone or in association with *S. thermophilus* is more efficient than the process performed only by *S. thermophilus*, showing earlier starting point and maximum rate points. As expected, maximum deceleration times, corresponding to the end of the fermentation, showed a wide range, depending on the inoculum and incubation temperature considered.

In order to verify the possibility to simplify the NIR instrumentation, the evolution of the processes at a fixed wavenumber was also tested. In particular, absorbance values of the spectra at  $7,100\text{ cm}^{-1}$ , corresponding to the OH combination band, were plotted against fermentation time and modelled applying Eq. (1). Also in this case,  $r^2$  values higher than 0.99 were obtained for all the fermentation conditions considered and the times corresponding to the critical points were practically the same obtained from the PC1 score modelling (Table 2).

## Conclusion

The obtained results demonstrated that FT-NIR spectroscopy combined with PCA is a valid, simple, cheap and robust tool for the on-line monitoring of milk lactic acid fermentation. FT-NIR spectroscopy gave crucial real-time information in agreement with rheology and conventional quality parameters. In particular, spectroscopic kinetic models were able to describe the curd development during lactic acid fermentation, giving thus the opportunity to easily follow in-line an important quality parameter of fermented milks such as texture.

These models may be used to effectively monitor and control lactic acid fermentation, in order to detect if the process is moving out of control and to establish the best strategy for its management, before operating costs and quality deterioration of the product make the process unprofitable.

Moreover, the good results obtained using only spectral data at a fixed wavenumber ( $7,100\text{ cm}^{-1}$ ) suggest that a simplified and cheaper NIR device could be developed for the industrial monitoring of the lactic acid fermentation process.

## References

1. J.A. Kurmann, J.Lj. Rasic and M. Kroger, *Encyclopedia of Fermented Fresh Milk Products: An International Inventory of Fermented Milk, Cream, Buttermilk, Whey, and Related Products*. Van Nostrand Reinhold, New York, USA (1992).
2. R.K. Robinson, A.Y. Tamime and M. Wszolek, "Microbiology of fermented milks", in *Dairy Microbiology Handbook: The Microbiology of Milk and Milk*

- Products*, Ed by R.K. Robinson. John Wiley & Sons Inc., Hoboken, USA, p. 468 (2005).
3. P. Courtin and F. Rul, "Interactions between microorganisms in a simple ecosystem: Yogurt bacteria as a study model", *Lait*, **84**, 125 (2004).
  4. Codex Alimentarius Commission, "Codex standard for fermented milks. Codex Stan 243-2003", retrieved August, 2012 from [http://www.codexalimentarius.net/download/standards/400/CXS\\_243e.pdf](http://www.codexalimentarius.net/download/standards/400/CXS_243e.pdf)
  5. A.Y. Tamime and R.K. Robinson, *Yoghurt. Science and Technology* 3<sup>rd</sup> Edn. CRC Press LLC, Boca Raton, USA (2007).
  6. C.E. Miller, "Chemical principles of near-infrared technology", in *Near-Infrared Technology in the Agricultural and Food Industries* 2<sup>nd</sup> Edn, Ed by P. Williams and K. Norris. American Association of Cereal Chemists, St. Paul, USA, p. 19 (2004).
  7. J.L. Rodriguez-Otero, M. Hermida and J. Centeno, "Analysis of dairy products by near-infrared spectroscopy: A review", *J. Agric. Food Chem.* **45**, 2815 (1997).
  8. M. Kawasaki, S. Kawamura, M. Tsukahara, S. Morita, M. Komiya and M. Natsuga, "Near-infrared spectroscopic sensing system for on-line milk quality assessment in a milking robot", *Comput. Electron. Agr.* **63**, 22 (2008).
  9. T. Woodcock, G. Downey and C.P. O'Donnell, "Better quality food and beverages: the role of near infrared spectroscopy", *J. Near Infrared Spectrosc.* **16**, 1 (2008).
  10. A.L. Ntsame Affane, G.P. Fox, S.O. Sigge, M. Manley and T.J. Britz, "Simultaneous prediction of acidity parameters (pH and titratable acidity) in Kefir using near infrared reflectance spectroscopy", *Int. Dairy J.* **21**, 896 (2011).
  11. M. Navratil, C. Cimander and C.F. Mandenius, "On-line multisensor monitoring of yogurt and filjolk fermentations on production scale". *J. Agric. Food Chem.* **52**, 415 (2004).
  12. A.E. Cervera, N. Petersen, A.E. Lantz, A. Larsen and K.V. Gernaey, "Application of near-infrared spectroscopy for monitoring and control of cell culture and fermentation", *Biotechnol. Progr.* **25**, 1561 (2009).
  13. D. Landgrebe, C. Haake, T. Höpfner, S. Beutel, B. Hitzmann, T. Scheper, M. Rhiel and F. Reardon, "On-line infrared spectroscopy for bioprocess monitoring", *Appl. Microbiol. Biot.* **88**, 11 (2010).
  14. C.C. Fagan and C.P. O'Donnell, "Application of infrared spectroscopy to food processing systems", in *Nondestructive Testing of Food Quality*, Ed by J. Irudayaraj and C. Reh. Blackwell Publishing Ltd., Oxford, UK, p. 119 (2008).
  15. IDF/ISO Standard 150:1991, "Yogurt. Determination of titratable acidity", International Dairy Federation (1991).

16. S. Benedetti, N. Sinelli, S. Buratti and M. Riva, "Shelf life of Crescenza cheese as measured by electronic nose", *J. Dairy Sci.* **88**, 3044 (2005).
17. N. Sinelli, S. Limbo, L. Torri, V. Di Egidio and E. Casiraghi, "Evaluation of freshness decay of minced beef stored in high-oxygen modified atmosphere packaged at different temperature using NIR and MIR spectroscopy", *Meat Sci.* **86**, 748 (2010).
18. P. Camaschella, O. Mignot, F. Pirovano and T. Sozzi, "Method for differentiated enumeration of mixed cultures of thermophilic lactic acid bacteria and bifidobacteria by using only one culture medium", *Lait* **78**, 461 (1998).
19. J.Lj. Rasic and J.A. Kurmann, *Yogurt. Scientific Grounds, Technology, Manufacture and Preparations*. Technical Dairy Publishing House, Copenhagen, DK (1978).
20. R.I. Dave and N.P. Shah, "Viability of yoghurt and probiotic bacteria in yoghurts made from commercial starter cultures", *Int. Dairy J.* **7**, 31 (1997).
21. E. Kristo, C.G. Biliaderis and N. Tzanetakis, "Modelling of the acidification process and rheological properties of milk fermented with yogurt starter culture using response surface methodology", *Food Chem.* **83**, 437 (2003).
22. S. Ngarize, A. Adams and N. K. Howell, "Studies on egg albumen and whey protein interactions by FT-Raman spectroscopy and rheology", *Food Hydrocolloid.* **18**, 49 (2004).
23. P. Frake, C.N. Luscombe, D.R. Rudd, I. Gill, J. Waterhouse, P. Frake and U.A. Jayasooriya, "Near-infrared mass median particle size determination of lactose monohydrate, evaluating several chemometric approaches", *Analyst* **123**, 2043 (1998).
24. P. Williams and K. Norris, *Near-Infrared Technology in the Agricultural and Food Industries*, 2<sup>nd</sup> Edn. American Association of Cereal Chemists, St. Paul, USA, (2004).
25. T. Andersen, N. Brems, M.M. Borglum, S. Kold-Christensen, E. Hansen, J.H. Jorsen and L. Nygaard, "Casein", in *Modern Dairy Technology*, Ed by R.K. Robinson. Elsevier Applied Science, London, UK, p. 381 (1993).

#### 4.1. Overview on milk lactic acid fermentation

# PAPER II

Food Bioprocess Technol  
DOI 10.1007/s11947-013-1189-2

ORIGINAL PAPER

## **Modelling Milk Lactic Acid Fermentation Using Multivariate Curve Resolution-Alternating Least Squares (MCR-ALS)**

Silvia Grassi • Cristina Alamprese • Veronica Bono •  
Ernestina Casiraghi • José Manuel Amigo

<sup>a</sup> *Department of Food, Environmental and Nutritional Sciences (DeFENS),  
Università degli Studi di Milano, via Celoria 2, 20133 Milano, Italy*

<sup>b</sup> *Department of Food, Quality and Technology, Faculty of Sciences, University of  
Copenhagen, Rolighedsvej 30, DK-1958 Frederiksberg C, Denmark*

**Abstract**

The purpose of the current work was to investigate the capability of multivariate curve resolution-alternating least squares (MCR-ALS) to extract relevant information from Fourier-Transform Near-Infrared (FT-NIR) spectra acquired on-line with a fiber probe during milk lactic acid fermentation. The fermentation trials were conducted replicating twice a factorial design with three different starter cultures (*Streptococcus thermophilus* and *Lactobacillus bulgaricus* alone or as 1:1 mixed culture) and three different incubation temperatures (37 °C, 41 °C and 45 °C), for a total of 18 experiments. The runs were monitored for 7.5 h through pH measurement, dynamic oscillatory test for rheological properties evaluation and FT-NIR spectra acquisition. The obtained MCR-ALS models successfully described the experimental FT-NIR spectra recorded (99.9% of explained variance, 0.63665% lack of fit, and standard deviation of the residuals lower than 0.0072). The three spectral profiles obtained by MCR-ALS pointed to the characteristic coagulation phases of milk lactic acid fermentation. The concentration profiles defined as a function of time for each run were strongly dependent on starter and temperature tested, in agreement with pH and rheological results. MCR-ALS applied to FT-NIR spectroscopy provides to the dairy industry a control system which could be implemented in-line as reliable management method for monitoring fermentation processes and to define the coagulation profile no matter the operative conditions adopted for the process.

**Keywords:** FT-NIR, multivariate curve resolution-alternating least squares, milk fermentation, lactic acid bacteria, rheological properties.



## Introduction

Fermentation processes are complex systems where several and closely related reactions driven by microorganisms take place simultaneously. Due to this complexity, high uniformity and reproducibility standards are hard to be accomplished. In fact, modest changes in different process variables can alter the batch-to-batch reproducibility and, therefore, promote unwanted variations and loss in the final product quality. This is one of the main problems for the food industries working with fermentation processes, because they aim at a reduction of manufacturing costs and, at the same time, consumers require a high standardized final product (Navrátil et al. 2004; Soukoulis et al. 2007).

As a matter of fact, prediction of the most suitable incubation time for every batch is difficult, leading to a forced empirical control of the process (Soukoulis et al. 2007). However, in order to identify possible non-standard behaviour (deviation from the normal operating conditions) and to rapidly assess the end point, the biotransformation progress must be throughout monitored and controlled. Nowadays, only few fast and robust monitoring techniques are applicable in-line under industrial conditions. For instance, lactic acid fermentation is commonly monitored by pH measurements (Chandan & O'Rell 2006), which give just a rough outline of the phenomena. Further information about the process trend could be obtained by means of separate laboratory measurements of different parameters, such as lactic acid and sugar concentration, microbial count, titratable acidity and viscoelastic properties. Nevertheless, they are not routinely measured, because elaborate and time-consuming analyses are required.

In order to overcome all these drawbacks, companies look for methods providing in-time information in order to assure an effective control at all stages of the process. Among the most promising techniques, near-infrared (NIR) spectroscopy represents a fast and non-destructive alternative, able to simultaneously detect, after calibration, the main compounds involved in the fermentation process and to describe the trend of the process (Bock & Connelly 2008). The development of NIR optic probes, which can be directly inserted in the fermenter, increased the interest in the use of in-line monitoring (Huang et al. 2008), in particular for dairy fermentations (Navrátil et al. 2004; Ntsame Affane et al. 2011). They offer detailed information of the on-going of the process in real time, allowing the assurance of the quality parameters of the final product.

NIR spectra can be mathematically modelled by using hard-modelling or soft-modelling methods (de Juan et al. 2000). Hard-modelling methodologies usually provide reliable description for systems where a defined kinetic model can be postulated (Garrido et al. 2008), assuming that no species other than those involved in the process contribute to the measured spectroscopic signal (Amigo et al. 2006b). Applying hard-modelling methodologies in a complex system, such as lactic acid fermentation of milk, could be extremely challenging due to the high amount of closely

related reactions taking place at the same time, being the establishment of an empirical model which controls all the reactions in the system a cumbersome task. Some of the problems of the hard-modelling analysis can be overcome by using soft-modelling methods (de Juan & Tauler 2006), such as the multivariate curve resolution optimized by alternating least squares (MCR-ALS). This is one of the most powerful methods to describe the phenomena occurring in any kinetic reaction (Amigo et al. 2006a; Amigo et al. 2006b; de Juan & Tauler 2006; Rodriguez-Rodriguez et al. 2007; Garrido et al. 2008; Pindstrup et al. 2013). MCR-ALS is a method able to decompose data matrices characterized by overlapped spectral bands recorded from complex systems into the contributions of each single component involved in the system studied. The main advantage is that little information about the nature of the food system and the transformation occurring is necessary. This makes MCR-ALS a perfect tool to fully understand the behaviour of processes in every moment and, therefore, to establish decision parameters that help to monitor and control the final quality of the fermentation product. MCR-ALS has been successfully applied in enzymatic process analysis as reported in the review by Garrido et al. (2008). However, only González-Sàiz et al. (2008) applied the soft-modelling technique to NIR spectra for monitoring alcoholic fermentation, where chemical transformations were related to microorganism growth.

The purpose of the current work is to investigate the capability of MCR-ALS applied to FT-NIR spectra to extract in-line relevant information about milk lactic acid fermentation dynamics. This approach will provide the dairy industry with a suitable methodology for monitoring in real time the kinetic of the whole process, maximizing and standardizing the productivity of the fermenter, while detecting failure in the biotransformation caused by any uncontrolled variable.

## Materials and Methods

### *Fermentation Trials*

For each fermentation trial, sterilized skim milk (10% w/v in distilled water) was inoculated with single or mixed cultures (1:1) of *S. thermophilus* and *L. bulgaricus*, isolated from the commercial yoghurt culture YO-MIX™ 305 (Danisco A/S, Copenhagen, Denmark) and identified by sequencing the amplified 16S rDNA region. The inoculum size was set to approximately  $10^6$  CFU mL<sup>-1</sup>, using a calibration curve obtained by correlating cell number and optical density measured at 600 nm. The inoculated skim milk was then placed in a circulating water bath at the specific fermentation temperature (37 °C, 41 °C or 45 °C) for 7.5 h. Every 45 min, pH analysis was performed, while spectroscopic and rheological evaluations were carried out at regular intervals (every 15 and 2 minutes, respectively) without changing the sample. A total of 9 different fermentation trials were performed, all replicated twice.

*pH*

pH was measured using a pH-meter 3510 (Jenway, Dunmow, England) equipped with a glass electrode.

*Rheological Measurements*

The rheological behaviour of the inoculated skim milk was monitored on the same sample at regular intervals using a Physica MCR 300 rheometer (Anton Paar GmbH, Graz, Austria), supported by the software Rheoplus/32 (v. 3.00, Physica Messtechnik GmbH, Ostfildern, Germany). The inoculated skim milk (19 mL) was inserted in the concentric cylinders (CC27) pre-heated at the desired fermentation temperature (37 °C, 41 °C, or 45 °C). A dynamic oscillatory test was performed, applying a constant 1% strain at a fixed 1 Hz frequency. The solvent trap filled with deionized water was used to prevent sample evaporation during the test. Storage ( $G'$ ) and loss ( $G''$ ) moduli were measured in 2 min intervals throughout the whole fermentation process (7.5 h).

*FT-NIR Spectroscopy*

The inoculated skim milk, placed in a water bath at the desired temperature (37 °C, 41 °C, or 45 °C) was monitored at regular intervals by means of FT-NIR spectroscopy. Spectra were collected in transmittance mode, inserting the fiber optic probe (1 mm pathlength) of a MPA spectrometer (Bruker Optics, Milan, Italy) directly in the sample. Spectral data were collected every 15 min over the 12,500-4,000  $\text{cm}^{-1}$  range, with a resolution of 16  $\text{cm}^{-1}$  and 64 scans for both background and samples. Instrument control and data acquisition were performed by the OPUS software (v. 6.5 Bruker Optics, Milan, Italy).

*Multivariate Curve Resolution-Alternating Least Squares (MCR-ALS)*

Spectral dataset were arranged in a matrix  $\mathbf{D}$  ( $M \times N$ ) where the  $M$  rows corresponded to the spectra obtained at different fermentation times and the  $N$  columns related to the  $n$ th different wavenumbers monitored (Fig. 1a).

MCR-ALS aims at describing the evolution of the obtained profiles through their pure components contributions individually, without the assumption of any previous empirical model. The FT-NIR spectra collected on-line during the process, as spectroscopic data, follow the Beer–Lambert's law bilinear model. MCR-ALS decomposes the  $\mathbf{D}$  matrix into two sub-matrices,  $\mathbf{C}$  ( $M \times F$ ) and  $\mathbf{S}^T$  ( $F \times N$ ), named concentration and spectra profiles respectively.  $\mathbf{C}$  describes the modification of the  $F$  chemical components affecting the signal in the  $M$  different observations during time; whereas  $\mathbf{S}^T$  contains the variation of the response with respect to the different wavenumbers.  $\mathbf{E}$  ( $M \times N$ ) is the residual matrix (Eq. 1):

$$\mathbf{D} = \mathbf{C}\mathbf{S}^T + \mathbf{E} \quad (1)$$

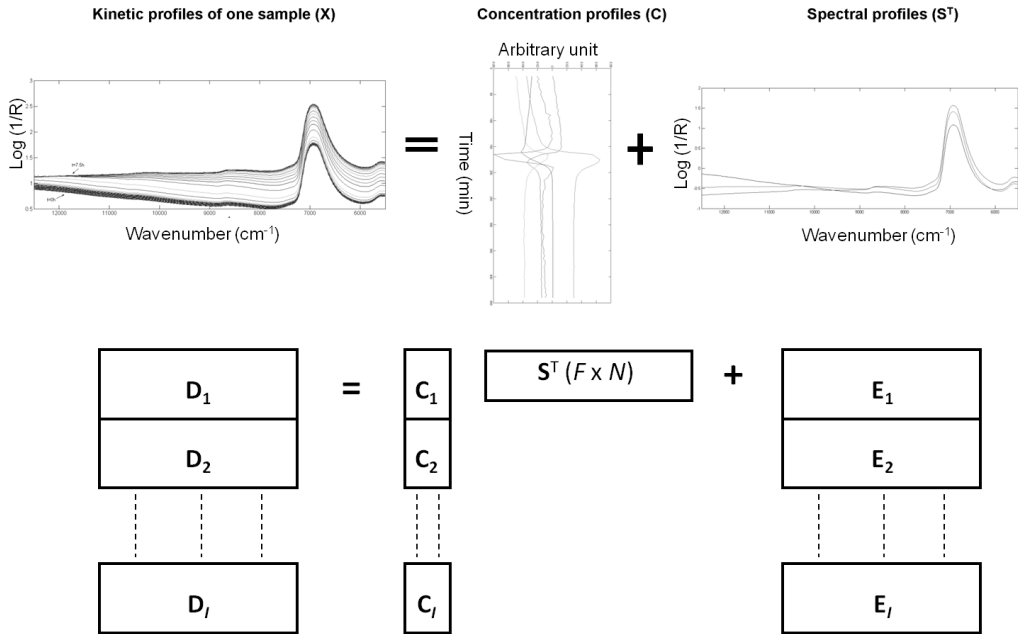


**Fig. 1a)** Graphical and mathematical depiction of MCR-ALS decomposition of a FT-NIR spectra dataset ( $\mathbf{D}_1$ ) to obtain the pure concentration ( $\mathbf{C}_1$ ) and spectral profiles ( $\mathbf{S}^T$ ).  $\mathbf{E}$  denotes the residual matrix. **b)** Column-wise augmentation strategy of the experiments [ $\mathbf{D}_1; \mathbf{D}_2; \dots; \mathbf{D}_I$ ] to obtain individual concentration profiles [ $\mathbf{C}_1; \mathbf{C}_2; \dots; \mathbf{C}_I$ ] and a common spectral profile matrix ( $\mathbf{S}^T$ ). The residual matrices are denoted as [ $\mathbf{E}_1; \mathbf{E}_2; \dots; \mathbf{E}_I$ ].

Before applying MCR method, the number of components of the target system ( $F$ ) should be defined. Then, the ALS optimization will start the iterations by using a previously stated initial estimation of the concentration or spectral profiles (Rodriguez-Rodriguez et al. 2007). The general steps of MCR-ALS are the following:

1. Determination of the number of components in  $\mathbf{D}$ .
2. Generation of non-random initial estimates of either the  $\mathbf{C}$  or the  $\mathbf{S}^T$ .
3. Given  $\mathbf{D}$  and  $\mathbf{S}^T$ , least-squares calculation of  $\mathbf{C}$  under constraints.
4. Given  $\mathbf{D}$  and  $\mathbf{C}$ , least-squares calculation of  $\mathbf{S}^T$  under constraints.
5. Reproduction of  $\mathbf{D}$  as  $\mathbf{CS}^T$ .

Go to 3 till the quality in the data reproduction is satisfactory and convergence in the iterative optimisation is achieved (Amigo et al. 2006b).

To achieve the proper final concentration and spectral profiles, a stopping criterion has to be imposed. The most common is the percentage of Lack of Fit (%LOF) that indicates the difference between the input data  $\mathbf{D}$  and the data reproduced from the  $\mathbf{CS}^T$  product (Eq. 2). The algorithm stops when the relative difference in %LOF values between two consecutive iterations is below a threshold value (commonly 0.1%; Jaumot et al. 2005).

$$\% LOF = 100 \times \sqrt{\frac{\sum_{i=1}^I \sum_{j=1}^J e_{mn}^2}{\sum_{i=1}^I \sum_{j=1}^J d_{mn}^2}} \quad (2)$$

In this equation,  $e_{mn}$  is each  $mn$ th element of the residual matrix  $\mathbf{E}$ , and  $d_{mn}$  is each  $mn$ th element of the  $\mathbf{D}$  matrix.

The main drawback of MCR-ALS is that there are not unique solutions as the product  $\mathbf{CS}^T$  is subjected to ambiguities: rotational and scale (intensity). The ambiguities associated to the resolved profiles can drastically affect the quality of the derived information. Nevertheless, they can be highly minimized by adding soft-modelling constraints. The constraints used are chosen according to the available information about the target system, being non-negativity, unimodality and closure the most commonly used (Tauler 1995). One of the most appreciated benefits of MCR-ALS is the possibility of applying it simultaneously to an individual experiment or to a series of them (Tauler & Barceló 1993; Amigo et al. 2006b), thus minimizing the above mentioned ambiguities. When more than one experiment is considered, the model in Eq. (1) extends to the model shown in Fig. 1b, where now  $\mathbf{D}$  and  $\mathbf{C}$  are column-wise augmented data matrices, with the submatrices of the individual experiments,  $\mathbf{D}_i$  and  $\mathbf{C}_i$ , one on top of the other (column-wise augmentation). The main advantage of this working strategy is that  $\mathbf{S}^T$  is a single data matrix with the shape of the pure spectra of the chemical species, common and valid for all experiments (de Juan & Tauler 2006). The data arrangement in Fig. 1b implies that the shape of the concentration profile of a particular species can change in a completely free manner from experiment to experiment.

### Data Processing

The whole wavenumber range (12,500-4,000  $\text{cm}^{-1}$ ) was reduced to 12,500-5,555  $\text{cm}^{-1}$  in order to eliminate useless or saturated variables from spectra. Chemometrics analysis was performed by means of MCR-ALS (Jaumot et al. 2005) software implemented in MatLab v. 7.4 (MathWorks, Natick, MA). The  $\mathbf{D}$  dataset was

composed of 18 independent sub-matrices, referring to the replicates of the 9 trials different for fermentation conditions. Principal component analysis (PCA) was performed on MCR-ALS concentration profiles obtained for each batch to fully understand the complex mechanisms involved in the fermentation processes. PCA models were developed by using the PLS-Toolbox (Eigenvector Research Inc., Wenatchee, WA) implemented in MatLab.

## Results and Discussion

### *pH*

Fig. 2 shows the changes in pH values of milk during the different fermentation processes carried out; results are expressed as the average of the two replicates. All the fermentation trials started with a milk pH value of  $6.46 \pm 0.44$ ; during the 7.5 h of fermentation this value varied in a different way according to the inoculum and the temperature tested, as already reported also in the scientific literature (Beal et al. 1999; Kristo et al. 2003; Soukoulis et al. 2007). The decreasing of pH was first of all influenced by the microorganisms used as starter.

When only *S. thermophilus* was inoculated, the pH decreased slowly and when incubated at 41 °C after 7.5 h the final pH was still  $4.84 \pm 0.04$  (Fig. 2b). This can be explained by the low acidification capability of the cocci. Indeed, they normally produce less than 1% of lactic acid (Tamime & Robinson 2007). In the same conditions, the fermented milk inoculated with *L. bulgaricus* reached pH values of  $3.92 \pm 0.01$ . The mixed culture was the most efficient in lowering pH values, above all at the lowest temperature (Fig. 2a). As the temperature increased, pH values decreased faster, no matter which inoculum was used.

Generally, dairy industries producing yoghurt consider a pH value of 4.4 - 4.6 as the end point of the fermentation (Chandan & O'Rell 2006). This value was never reached inoculating *S.thermophilus* alone, at any of the temperature tested. When the milk was inoculated with *L. bulgaricus*, it reached a pH value of approximately 4.6 after 360, 225 and 180 min for 37, 41 and 45 °C incubation temperatures, respectively. As mentioned before, the inocula with mixed culture showed a faster decrement of pH for the three temperatures tested (37, 41 and 45 °C) and values lower than 4.6 were reached after 315, 225 and 180 min of fermentation.

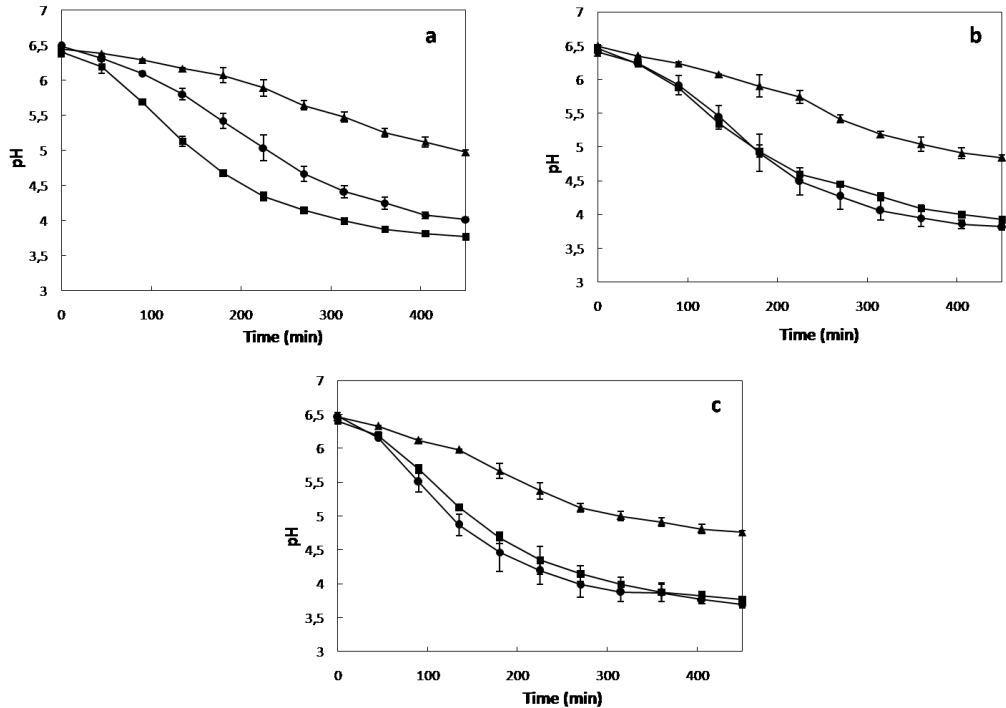


**Fig. 2** pH values for the nine fermentation trials carried out with *L. bulgaricus* (■); *S. thermophilus* (▲) and the mixture culture (●). Trials conducted at a) 37 °C, b) 41 °C and c) 45 °C. The error bars represent the standard deviation of the two technological replicates.

### Rheological measurements

During fermentation, pH decrease causes the coagulation of milk caseins that can be studied by means of rheological measurements. In particular, applying a small amplitude test, it is possible to register the storage ( $G'$ ) and the loss ( $G''$ ) moduli of the media and to observe when  $G'$  crosses over  $G''$ . The cross point is usually considered as the gel point (Kristo et al. 2003; Ngarize et al. 2004).

Fig. 3 shows the typical changes in viscoelastic moduli  $G'$  and  $G''$  of coagulating milks, obtained by the on-line rheological measurements. As already reported in the literature (Trachoo 2002), it is possible to notice that the gel point depends on the temperature and inoculum tested, in agreement with the pH results. When the mixed culture or the *L. bulgaricus* inocula were used, the time needed for curd development was shorter than in trials carried out with *S. thermophilus*. At the optimum temperature of 41 °C, the onset of gelation occurred after 120, 150, and 318 min of fermentation for the associative, the *L. bulgaricus* and the *S. thermophilus* inoculum, respectively.

It is also remarkable the  $G'$  maximum that the gel reached in its plateau: the higher the value, the firmer the gel. Fermentation processes with *S. thermophilus* resulted in a

weaker gel than those developed in the other runs: the highest  $G'$  value for *S. thermophilus* inoculum was 67.1 Pa, one order lower than the values obtained with *L. bulgaricus* and the mixture culture (186 and 244 Pa, respectively).

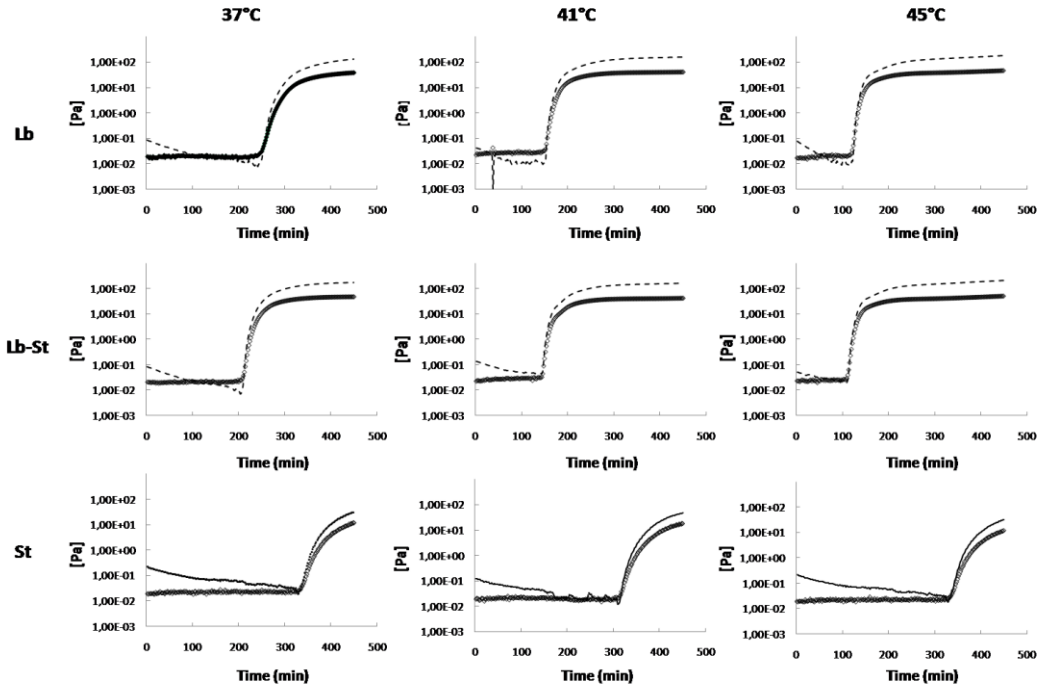


**Fig. 3** Rheological behaviours for one representative fermentation trial for each combination temperature-inoculum (Lb: *L. bulgaricus*; St: *S. thermophilus*; Lb-St: the mixture culture). Dash thin lines (--) represent the  $G'$  modulus and solid thick lines (—) the  $G''$  modulus.

It should be taken into account that the development of the elastic gel structure with a solid-like behaviour starts at pH around 5.6, causing changes in the micelle structure due to solubilisation of colloidal calcium phosphate (Lee & Lucey 2004). Further pH decrease causes a more complex and extensive interconnection of casein particles, leading to the formation of a continuous protein 3D-network and thus governing the structure of yoghurt. In particular, the casein micelles become larger when pH values range between 5.5 and 5.3, indicating the beginning of the aggregation (Andersen et al. 1993). Comparing the rheological curves with the pH results it can be noticed that the gel point in each experiment was close to 5.2 pH value. This behaviour could be considered against the normal value of casein aggregation expected at their isoelectric point (4.6). However, the higher value of the pH at the gel point could be ascribed to the heat treatment of the milk used (Donato et al. 2007). In fact, the isoelectric point of



denatured beta-lactoglobulin associated to the casein micelles is equal to 5.2 (Tamine & Robinson 2007).

### *FT-NIR Spectra*

The FT-NIR spectra recorded during the fermentation trials showed a clear trend: the absorbance increased with the fermentation time, due to a baseline drift caused by scattering effects (Fig. 4a). To minimize these effects the spectra were pre-treated using the Standard Normal Variate (SNV) algorithm (Fig. 4b).

After applying SNV to the raw spectra, three main regions were identified: 5,000-7,000  $\text{cm}^{-1}$  and 10,000-12,500  $\text{cm}^{-1}$  where the spectral absorbance decreased during the biotransformation; 7,000-10,000  $\text{cm}^{-1}$  that showed an increase in absorbance. Characteristic peaks at 6,900, 8,600 and 10,800  $\text{cm}^{-1}$  could be ascribed to the O-H combination band of symmetric and asymmetric stretching of water, the C=O fourth overtone of fundamental stretching band, and the C-H third overtone of fundamental stretching band, respectively (Workman & Weyer 2007). These peaks changed during the bio-transformation due to the conversion of simple carbohydrates into lactic acid and to the modification in the protein structure (casein aggregation to form a 3D network).

In order to uncover spectral time-related changes occurring during milk fermentation, the absorbance values at fixed wavenumbers (11,500, 9,500, 7,500 and 5,500  $\text{cm}^{-1}$ ) were plotted against fermentation time (Fig. 4c). In all cases, it is straightforward to recognize a sigmoidal-like behaviour, typical of a system in which the main changes are due to microorganism growth (Benedetti et al. 2005, Sinelli et al. 2010).

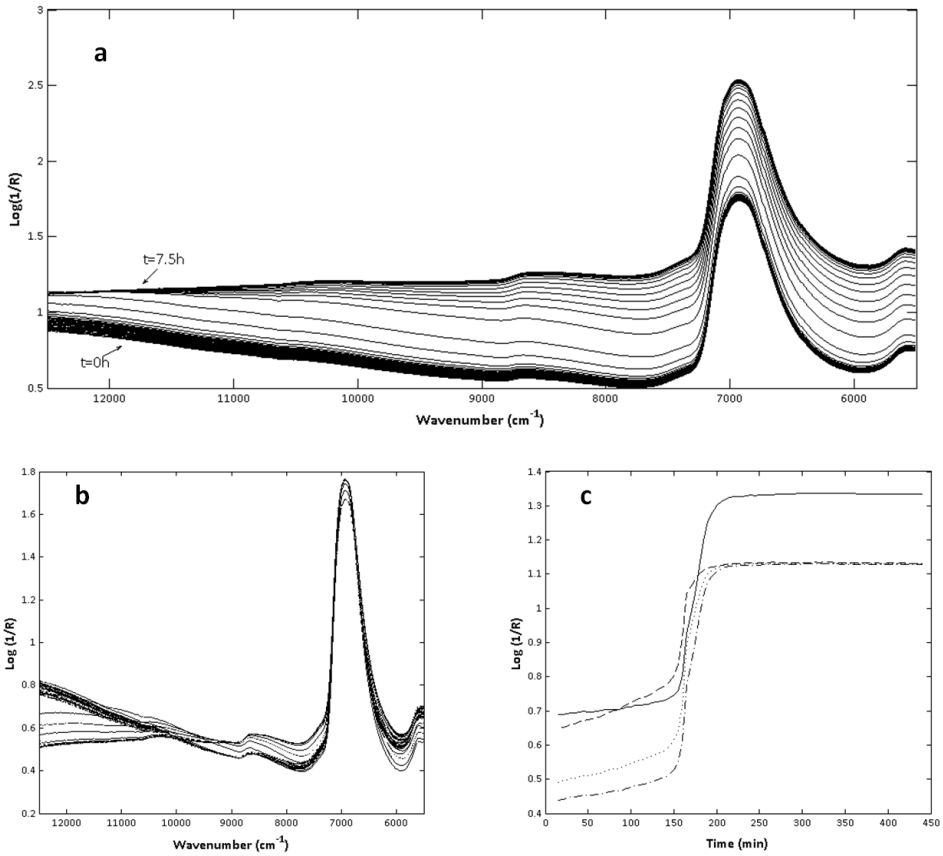


**Fig. 4** a) FT-NIR spectra ( $12,500\text{--}5,555\text{ cm}^{-1}$ ) collected during one of the fermentation trials performed at  $41^\circ\text{C}$  with the mixed starter culture (1:1); b) pre-treated spectra (SNV); c) absorption of single wavenumbers plotted vs. fermentation time: dash line (---),  $11,500\text{ cm}^{-1}$ ; dash-dot line (-.-),  $9,500\text{ cm}^{-1}$ ; solid line (—),  $7,500\text{ cm}^{-1}$ ; dot line (⋯),  $5,500\text{ cm}^{-1}$ .

### *MCR-ALS Results*

MCR-ALS was applied to reduced and pre-treated FT-NIR spectra in order to investigate if there was a general trend describing the development of the biotransformation, taking into account the variability of the production factors affecting the fermentation progress. As the dataset was composed of 18 experiments, MCR-ALS models were built in series with the same constraints, but considering them as individual experiments (Amigo et al. 2006a; Amigo et al. 2006b).

### *Number of Significant Components, Initial Estimates and ALS Constraints*

The number of significant components of the target system was investigated by inspecting the scores, loadings and variance obtained by a PCA model of the reduced

and pre-treated FT-NIR spectra. The first three principal components explained a total of 99.97% of variance and described the kinetic changes occurring in the process.

After determining the number of significant components, it was necessary to choose the initial estimates for starting the MCR-ALS analysis. These values were selected in the most straightforward way, within a representative fermentation batch (mixed culture incubated at 41°C, i.e. the conventional condition for yogurt production), choosing the three spectra recorded at the beginning, in the middle and at the end of the fermentation process.

The MCR algorithm was applied to the **D** spectral matrix under the same constraints to all the column-wise sub-matrices: non-negativity to spectral and concentration profiles and unimodality to concentration profiles. The convergence criterion was set at 0.1.

### Resolution Results

The application of ALS procedure to the milk fermentation runs permitted the resolution of both pure spectra (Fig. 5) and concentration profiles (Fig. 6). MCR-ALS models obtained successfully described experimental FT-NIR spectra recorded. The product  $CS^T$  explained 99.9% of the variance of the data, the percentage of LOF was 0.63665% and the standard deviation of the residuals was lower than 0.0072.

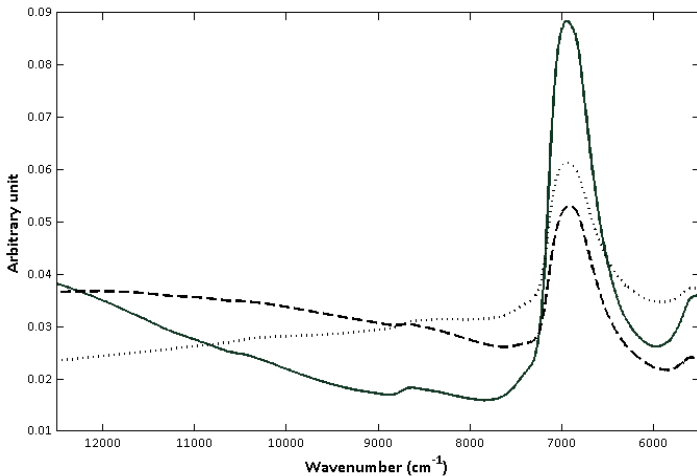


**Fig. 5** MCR-ALS pure component spectra: solid-line profile (—) describes the liquid-like behaviour of milk, dotted profile (···) reflects the solid-like behaviour of coagulated milk and the dashed profile (--) represents the middle passage in the biotransformation.

The three pure spectra profiles obtained (Fig. 5) can be ascribed to the coagulation phases. The solid-line profile represents the typical spectrum recorded at the beginning of the fermentation runs, i.e. when the milk still had a liquid-like behaviour; it shows a visible slope in the base line at slower wavenumbers and a higher peak at 6,900  $cm^{-1}$

due to O-H combination band of symmetric and asymmetric stretching of water. The characteristic spectrum of coagulated milk, influenced by the continuous protein 3D-network of the matrix, is the dotted profile. The last profile stands for the transition phase, during which the first changes in the casein micelle structure due to solubilisation of colloidal calcium phosphate took place.

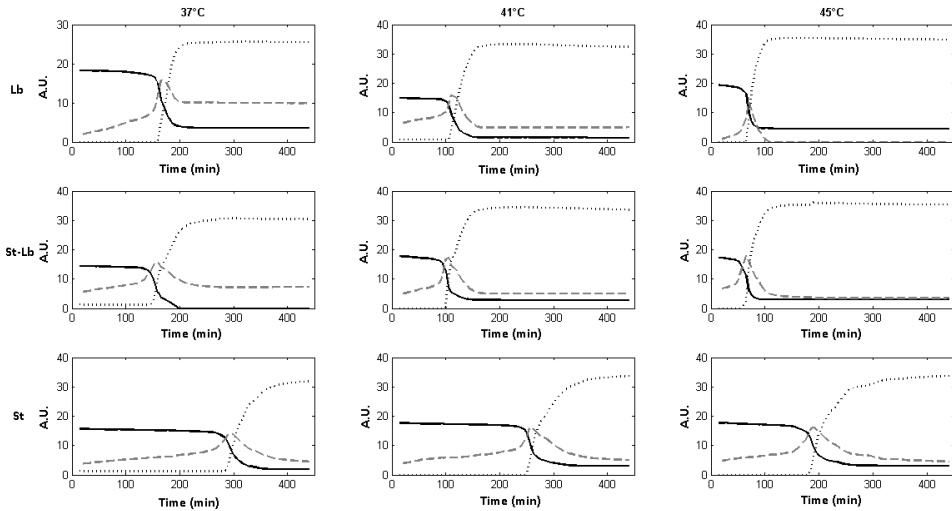


**Fig. 6** MCR-ALS concentration profiles of one representative fermentation trial for each combination temperature-inoculum (Lb: *L. bulgaricus*; St: *S. thermophilus*; Lb-St: the mixture culture). Solid-line profile (—) describes the liquid-like behaviour of milk, dotted profile (···) reflects the solid-like behaviour of coagulated milk and the dashed profile (--) represents the transition phase of the biotransformation. A.U., arbitrary unit.

Fig. 6 reports an example of concentration profile for each experimental condition. The obtained profiles contained information about the main changes occurring in the food matrix. The first MCR-ALS concentration profile (solid line) has an inverse sigmoid shape in all the runs performed: it describes the first stage of the acid coagulation of milk, where rheological data showed low and constant  $G'$  and  $G''$  values (Fig. 3). This profile reaches its minimum when the first aggregation caused a steep increase in visco-elasticity, corresponding to the fast rise of both  $G'$  and  $G''$  (Fig. 3). The concentration profile describing the milk solid-like behaviour (dotted line) has a sigmoid shape which confirms the evolution of the lactic acid fermentation from milk to a more strength visco-elastic structure. As the liquid- and solid-like behaviours were inversely correlated, the maximum rate of decrease of the first profile corresponded to the maximum rate of increase of the latter profile. All the MCR-ALS profiles reached a plateau at the time in which  $G'$  crossed  $G''$  (gelation point), due to the formation of a

continuous protein structure in the fermented milks. The difference in time required to reach the plateau was strictly related to the starter and the temperature tested, in agreement with the rheological results already discussed (Fig. 3) and previous considerations reported in literature (Kristo et al. 2003; Lee & Lucey 2004). Observing the batches inoculated with the same culture but incubated at different temperature, it was possible to notice how increasing the temperature the concentration profiles moved up, pointing out that the coagulation occurred in shorter time. From the profiles referring to milk incubated at the same temperature, it was possible to see that with *L. bulgaricus* and mixed inoculum the kinetics observed had very similar behaviours, while all the trials conducted with *S. thermophilus* showed the same profile shape but always delayed in comparison with the other tested starters. The relationship between casein coagulation and MCR-ALS profiles obtained by FT-NIR spectra analysis could be mainly ascribed to the spectra difference in baseline slope, caused by physical effects (Frake et al. 1998) such as the changes in number and size of casein micelles during acid milk coagulation (Horne & Davidson 1993). Furthermore, during fermentation time, the significant reduction in absorbance at  $6,900\text{ cm}^{-1}$ , due to O-H of water, revealed the syneresis effect characteristic of the acid coagulation process.

#### *PCA of MCR Profiles*

Since the gel firmness at the end of the fermentation process is extremely relevant for the final product quality and customers' acceptance, a PCA model of MCR-ALS profiles was developed in order to investigate if it was possible to visualize the different characteristics of the final gel obtained with different inoculum-incubation temperature conditions. The concentration profiles of the eighteen experiments obtained by MCR-ALS were normalised and mean centred and a data matrix was constructed as shown in Fig. 7.

The PCA model with four components explained 98.15% of the total variance. Fig. 8 shows the score plot and the loading plot obtained. In the score plot PC1 vs. PC2 (Fig. 8a), a satisfactory distribution of the batches in the area defined by the first two principal components according to the temperature and the inoculum can be observed. The first principal component (PC1) (69.43% of variance) divided batches according to the inoculum: the trials performed with *S. thermophilus* inoculated alone (negative PC1 values) were well distinguished from the fermented milks obtained with *L. bulgaricus* and mixed cultures (positive PC1 values).

PC2 (16.92% of variance) separated batches of the same inoculum according to the different fermentation temperatures. Moreover, it was possible to observe a trend of batches distribution (---) which can be ascribed to the coagulum strength, increasing from the left to the right and from the low to the high part of the space defined by the two components. The distribution agreed with the final coagulum strength data

obtained from rheological analysis, thus demonstrating the ability of the MCR-ALS technique to separate the curd obtained as a function of their strength.

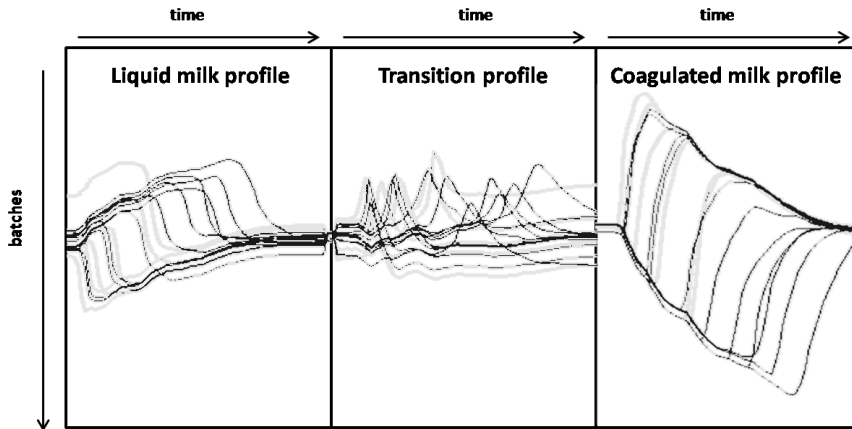


**Fig. 7** Structure of the MCR-profiles dataset for the PCA.

Within the space defined by the first and fourth PCs (Fig. 8b) it was possible to observe a sample distribution according to the fermentation temperature (37, 41, 45 °C) along the PC4. The only two samples not well separated referred to batches inoculated with *S. thermophilus* at 45°C. This distribution could be explained by the fact that even increasing the incubation temperature the curd obtained by *S. thermophilus* was weaker than the others, and thus wrongly grouped.

The three loading plots associated with PC1, PC2 and PC4 gave the whole picture of the final visco-elastic properties of each fermentation condition tested. The comparison of the loadings and the concentration profile shapes makes possible to identify which loadings mainly describe each profile. PC1 loadings were mainly related to the coagulated milk profile; PC2 loadings to the liquid profile and PC4 loadings to the transition profile.

The interaction between all of them are unavoidable because the steps that they are describing are interrelated phases of the same phenomenon, i.e. the lactic acid coagulation in milk. The PCA thus confirmed that the MCR-ALS analysis is a valid investigation technique for physical properties of milk fermented products.

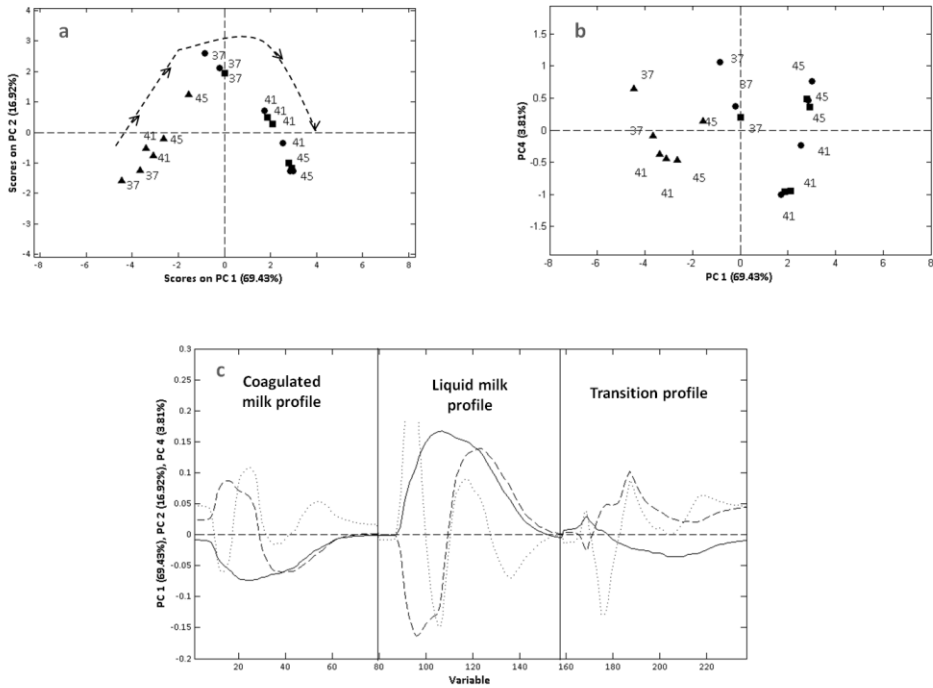


**Fig. 8** PCA of MCR-ALS concentration profiles: a) PC1 vs. PC2 score plot; b) PC1 vs. PC4 score plot; c) loading plot for PC1(—), PC2 (--) and PC4 (···). *L. bulgaricus* (■), *S. thermophilus* (▲) and the mixture culture (●). Numbers in the score plots refer to fermentation temperatures.

## Conclusions

In this paper we demonstrated that MCR-ALS applied to FT-NIR spectra for monitoring milk fermentation provided a comprehensive description of the curd formation. Real-time information on the pH and the different rheological modifications (regardless the original characteristics of the milk and the heat treatment before starter inoculation) have been obtained. As a consequence, the definition of the end point of the fermentation was assessed in a robust and reliable manner.

The results obtained herein can lead to think of the implementation of non-invasive FT-NIR and MCR-ALS in industrial productions for milk coagulation monitoring and controlling. This will give much richer information about the ongoing of the process than the one obtained by only measuring the pH of the process, and avoiding problems of, for instance, the drifting of pH measures due to protein deposits on the electrode.

PCA applied to the profiles obtained by MCR-ALS confirmed that this technique is a valid tool to investigate the viscoelastic properties of curds obtained with different operative conditions. Actually gel formation is the main physical change characterizing

the biotransformation and its control is extremely relevant for final product quality and customers' acceptance.

## References

- Amigo, J. M., de Juan, A., Coello, J. & MasPOCH, S. (2006a). A mixed hard- and soft-modelling approach for the quantitative determination of oxipurines and uric acid in human urine. *Analytica Chimica Acta*, 567(2), 236-244.
- Amigo, J.M., de Juan, A., Coello, J. & MasPOCH, S. (2006b). A mixed hard- and soft-modelling approach to study and monitor enzymatic systems in biological fluids. *Analytica Chimica Acta*, 567(2), 245-254.
- Andersen, T., Brems, N., Borglum, M.M., Kold-Christensen, S., Hansen, E., Jorsen, J. H. & Nygaard, L. (1993). Casein. In R.K. Robinson (Ed.), *Modern dairy technology* (pp. 381-416). London: Elsevier Applied Science.
- Beal, C., Skokanova, J., Latriille, E., Martin, N. & Corrieu, G. (1999). Combined effects of culture conditions and storage time on acidification and viscosity of stirred yogurt. *Journal of Dairy Science*, 82(4), 673-681.
- Benedetti, S., Sinelli, N., Buratti, S. & Riva, M. (2005). Shelf life of crescenza cheese as measured by electronic nose. *Journal of Dairy Science*, 88(9), 3044-3051.
- Bock, J.E. & Connelly, R.K. (2008). Innovative uses of Near-Infrared in food processing. *Journal of Food Science*, 73(7), R91-R98.
- Chandan, R. C. & O'Rell, K.R. (2006). Yogurt Plant: Quality Assurance. In *Manufacturing Yogurt and Fermented Milks*. Oxford: Blackwell Publishing.
- de Juan, A. & Tauler, R. (2006). Multivariate Curve Resolution (MCR) from 2000: Progress in concepts and applications. *Critical Review in Analytical Chemistry*, 36(3-4), 163-176.
- de Juan, A., Casassas, E. & Tauler, R. (2000). Soft-modelling of analytical data. In *Encyclopedia of analytical chemistry instrumentation and applications*. New York: Wiley.
- Donato, L., Alexander, M. & Dalgleish, D. G. (2007). Acid gelation in heated and unheated milks: Interactions between serum protein complexes and the surfaces of casein micelles. *Journal of Agricultural and Food Chemistry*, 55(10), 4160-4168.
- Frake, P., Luscombe, C. N., Rudd, D. R., Gill, I., Waterhouse, J., Frake, P. & Jayasooriya, U. A. (1998). Near-infrared mass median particle size determination of lactose monohydrate, evaluating several chemometric approaches. *Analyst*, 123, 2043-2046. <http://dx.doi.org/10.1039/A802532K>
- Garrido, M., Rius, F. X. & Larrechi, M. S. (2008). Multivariate curve resolution-alternating least squares (MCR-ALS) applied to spectroscopic data from monitoring chemical reactions processes. *Analytical and Bioanalytical Chemistry*, 390(8), 2059-2066.



- González-Sàiz, J.-M., Isabel, E.D., Rodríguez-Tecedor, S. & Pizarro C. (2008). Valorization of onion waste and by-products: MCR-ALS applied to reveal the compositional profiles of alcoholic fermentation of onion juice monitored by Near-Infrared Spectroscopy. *Biotechnology and Bioengineering*, 101(4), 776-787.
- Horne, D.S. & Davidson, C.M. (1993). Direct observation of decrease in size of casein micelles during the initial stages of renneting of skim milk. *International Dairy Journal*, 3(1), 61-71.
- Huang, H., Yu, H., Xu, H. & Ying, Y. (2008). Near infrared spectroscopy for on/in-line monitoring of quality in foods and beverages: A review. *Journal of Food Engineering*, 87, 303-313.
- Jaumot, J., Gargallo, R., de Juan, A. & Tauler, R. (2005). A graphical user-friendly interface for MCR-ALS: a new tool for multivariate curve resolution in MATLAB. *Chemometrics and Intelligent Laboratory Systems*, 76(1), 101-110.
- Kristo, E., Biliaderis, C. G. & Tzanetakis, N. (2003). Modelling of the acidification process and rheological properties of milk fermented with a yogurt starter culture using response surface methodology. *Food Chemistry*, 83(3), 437-446.
- Lee, W.J. & Lucey, J.A. (2004). Structure and physical properties of yogurt gels: Effect of inoculation rate and incubation temperature. *Journal of Dairy Science*, 87(10), 3153-3164.
- Navrátil, M., Cimander, C. & Mandenius, C-F. (2004). On-line multisensor monitoring of yogurt and filmjolk. *Journal of Agricultural and Food Chemistry*, 52(3), 415-420.
- Ngarize, S., Adams, A. & Howell, N. K. (2004). Studies on egg albumen and whey protein interactions by FT-Raman spectroscopy and rheology. *Food Hydrocolloids*, 18, 49-59.
- Ntsame Affane, A. L., Fox, G. P., Sigge, S. O., Manley, M. & Britz, T. J. (2011). Simultaneous prediction of acidity parameters (pH and titratable acidity) in Kefir using near infrared reflectance spectroscopy. *International Dairy Journal*, 21(11), 896-900.
- Pindstrup, H., Fernández, C., Amigo, J. M. & Skibsted, L. H. (2013). Multivariate curve resolution of spectral data for the pH-dependent reduction of ferrylmyoglobin by cysteine. *Chemometrics and Intelligent Laboratory Systems*, 122, 78-83.
- Rodríguez-Rodríguez, C., Amigo, J. M., Coello, J. & Maspocho, S. (2007). An introduction to multivariate curve resolution-alternating least squares: Spectrophotometric study of the acid-base equilibria of 8-hydroxyquinoline-5-sulfonic acid. *Journal of Chemical Education*, 84(7), 1190-1195.
- Sinelli, N., Limbo, S., Torri, L., Di Egidio, V. & Casiraghi, E. (2010). Evaluation of freshness decay of minced beef stored in high-oxygen modified atmosphere

- packaged at different temperature using NIR and MIR spectroscopy. *Meat Science*, 86(3), 748-752.
- Soukoulis, C., Panagiotidis, P., Koureli, R. & Tzia, C. (2007). Industrial yogurt manufacture: Monitoring of fermentation process and improvement of final product quality. *Journal of Dairy Science*, 90(6), 2641-2654.
- Tamime, A. Y. & Robinson, R. K. (2007). *Yoghurt. Science and technology*. (3<sup>rd</sup> edition). Boca Raton: CRC Press LLC.
- Tauler, R. & Barceló, D. (1993). Multivariate curve resolution and calibration applied to liquid chromatography diode array detection. *Trends in Analytical Chemistry*, 12(8), 319-327.
- Tauler, R. (1995). Multivariate curve resolution applied to second order data. *Chemometrics and Intelligent Laboratory Systems*, 30, 133-146.
- Trachoo, N. (2002). Yogurt: The fermented milk. *Songklanakarin Journal of Science and Technology*, 24 (4), 727-737.
- Workman, J. & Weyer, L. (2007). *Practical guide to interpretive Near-Infrared Spectroscopy*. Boca Raton: CRC Press LLC.

# PAPER III

## **Applicazione di tecniche spettroscopiche IR al monitoraggio della produzione di lattici fermentati**

Cristina Alamprese, Silvia Grassi, Claudia Picozzi, Veronica Bono,  
Ernestina Casiraghi

*Dipartimento di Scienze per gli Alimenti, la Nutrizione e l'Ambiente (DeFENS),  
Università degli Studi di Milano, Via G. Celoria 2 - 20133 Milano*

Proceeding in: 5° Simposio Italiano di Spettroscopia NIR,  
AGROPOLIS, Legnaro (PD)

ISBN 97888904064XX

## Riassunto

I lattici fermentati sono prodotti diffusi ed apprezzati in tutto il mondo grazie alle loro caratteristiche sensoriali e salutistiche. Una delle maggiori esigenze dell'industria alimentare è quella di avere a disposizione un metodo rapido e non distruttivo che permetta il controllo *on-line* della fermentazione. L'obiettivo di questo lavoro è stato quindi quello di indagare la possibilità di utilizzo della spettroscopia IR per determinare con un'unica e rapida misura numerosi indici di fermentazione. Allo scopo sono state allestite in doppio prove di fermentazione lattica protratte per 7.5 h e condotte a 37°C, 41°C e 45°C utilizzando *S. thermophilus* e *L. delbrueckii* subsp. *bulgaricus* sia in associazione (1:1) che singolarmente. Le fermentazioni sono state monitorate in continuo mediante acquisizione degli spettri FT-NIR (12500-4500 cm<sup>-1</sup>; risoluzione 16 cm<sup>-1</sup>) in trasflettanza diffusa, utilizzando uno spettrometro MPA (Bruker Optics) dotato di fibra ottica. Ogni 45 minuti sono stati raccolti gli spettri FT-IR (4000-700 cm<sup>-1</sup>; risoluzione 4 cm<sup>-1</sup>) mediante uno spettrometro Vertex 70 (Bruker Optics) dotato di cella a multipla riflessione ATR in cristallo di germanio e sono stati inoltre valutati il pH, l'acidità titolabile, le conte microbiche e la concentrazione dei metaboliti (galattosio, acido lattico e lattosio). Gli spettri FT-NIR e FT-IR, trasformati in derivata prima, sono stati utilizzati per la costruzione di modelli di regressione PLS (*Partial Least Square*), validati mediante *cross-validation*. Tutti i modelli PLS calcolati hanno mostrato coefficienti di correlazione elevati in calibrazione ( $R^2 \geq 0.83$ ), associati a bassi errori standard. Anche in validazione si sono ottenuti risultati soddisfacenti, con l'esclusione di alcune variabili che hanno mostrato problematiche di *overfitting* soprattutto nel medio infrarosso. Il lavoro ha quindi permesso di dimostrare che la spettroscopia IR potrebbe essere utile per il monitoraggio *on-line* della fermentazione lattica, previa costruzione di modelli più robusti e calibrati sulle produzioni industriali.

## Introduzione

Tra i prodotti fermentati, lo yogurt è il latte fermentato tradizionalmente più diffuso ed apprezzato nel mondo. Questo prodotto si ottiene mediante fermentazione del latte, senza successiva sottrazione di siero, operata da due microrganismi specifici in associazione: *Streptococcus thermophilus* e *Lactobacillus delbrueckii* subsp. *bulgaricus*.

Il monitoraggio della fermentazione avviene comunemente mediante la determinazione del pH e dell'acidità titolabile. In aggiunta possono essere valutati anche la carica batterica e la concentrazione di metaboliti tipici del bioprocesso, come lattosio, acido lattico e galattosio. Il controllo di questi parametri avviene mediante metodiche analitiche convenzionali, come ad esempio conta su piastra, kit enzimatici e HPLC, che, nella maggior parte dei casi, richiedono lunghi tempi di analisi e preparazione del campione, rendendo così difficoltose eventuali azioni correttive sul processo. Per questa ragione sarebbe utile sviluppare metodiche analitiche rapide, poco costose, attendibili ed integrabili nel processo produttivo. In questo contesto, la spettroscopia NIR e MIR, grazie anche allo sviluppo di tecniche chemiometriche avanzate, si sta dimostrando uno strumento valido, in quanto consente di ottenere in pochi minuti e contemporaneamente molte informazioni qualitative e quantitative del prodotto in analisi. Negli anni le applicazioni della spettroscopia IR sono notevolmente aumentate, coprendo una vasta categoria di alimenti (Takuo, 2007) e diffondendosi in studi di monitoraggio di processi alimentari *in-line* ed *on-line* (Huang et al., 2008).

Lo scopo di questo lavoro è stato quindi quello di indagare la possibilità di utilizzo della spettroscopia IR, unitamente all'analisi chemiometrica dei dati, per la determinazione di numerosi indici di fermentazione con un'unica e rapida misura.

## Materiali e Metodi

Le prove di fermentazione sono state condotte utilizzando latte scremato in polvere (Merck, Darmstadt, Germania) ricostituito al 10% p/v in acqua distillata e trattato termicamente a 112°C per 15 min. L'inoculo è stato preparato a partire da ceppi batterici isolati da una coltura commerciale, YO-MIX™ 305 (Danisco A/S, Copenhagen, Danimarca), e identificati, attraverso sequenziamento dell'amplificazione della regione 16S rDNA, come *Streptococcus salivarius* subsp. *thermophilus* and *Lactobacillus delbrueckii* subsp. *bulgaricus*.

Sono state effettuate in doppio 9 prove di fermentazione lattica a 37°C, 41°C e 45°C, inoculando il latte con *S. thermophilus* e *L. bulgaricus* sia in associazione (1:1) che singolarmente (ca. 10<sup>6</sup> UFC/g). Le fermentazioni sono state protratte per 7.5 h, effettuando un prelievo ogni 45 min per determinare, in doppio, la conta batterica, il

pH, l'acidità titolabile, la concentrazione di zuccheri e acido lattico e per acquisire gli spettri FT-IR. Gli spettri FT-NIR sono stati invece acquisiti in continuo.

La concentrazione microbica è stata determinata per conta in piastra su terreno HHD modificato (Biolife, Milano, Italia), dopo omogeneizzazione e opportune diluizioni decimali del campione. L'incubazione è avvenuta a 37 °C per 48 h. I valori di pH sono stati misurati potenziometricamente mediante pHmetro 3510 (Jenway, Dunmow, UK). L'acidità titolabile è stata determinata secondo lo standard IDF/ISO n° 150 (IDF/ISO, 1991) ed espressa in percentuale di acido lattico. Le concentrazioni di lattosio, galattosio e acido lattico sono state determinate mediante HPLC, utilizzando una colonna Aminex HPX-87H (BioRad Laboratories, Richmond, CA, USA) e un detector a indice di rifrazione (RI-71, Showa Denko Europe GmbH, Monaco, Germania). Dopo allontanamento delle proteine dal campione mediante precipitazione con acetonitrile e successiva centrifugazione, il surnatante filtrato è stato eluito isocraticamente a 65°C con una soluzione 5 mM di H<sub>2</sub>SO<sub>4</sub>, ad un flusso operativo di 0.8 mL/min. L'identificazione dei picchi e le curve di calibrazione sono state ottenute analizzando soluzioni standard di ciascun composto.

Gli spettri FT-IR sono stati acquisiti ogni 45 min in un *range* spettrale di 4000-700 cm<sup>-1</sup> (risoluzione 4 cm<sup>-1</sup>, 16 scan), mediante uno spettrometro Vertex 70 (Bruker Optics, Milano, Italia) dotato di cella a multipla riflessione attenuata (ATR) in cristallo di germanio. Gli spettri FT-NIR sono stati raccolti in continuo utilizzando una fibra ottica a trasflettanza (passo ottico 1 mm) collegata ad uno spettrometro MPA (Bruker Optics) ed inserita direttamente nel campione durante la fermentazione. I dati spettrali sono stati acquisiti ogni 5 min in un *range* spettrale di 12500-4000 cm<sup>-1</sup> (risoluzione 16 cm<sup>-1</sup>, 64 scan). Il controllo degli strumenti IR e l'acquisizione dei dati sono stati effettuati con il *software* OPUS (v. 6.5, Bruker Optics).

L'elaborazione degli spettri è stata condotta tramite il *software* The Unscrambler (v 9.8, Camo Software AS, Oslo, Norvegia), previa selezione delle zone spettrali più informative: 8900-5555 cm<sup>-1</sup> per i dati FT-NIR e la zona del *fingerprint* (1800-970 cm<sup>-1</sup>) per i dati FT-IR. Per minimizzare l'effetto dello slittamento della linea di base dovuto a fenomeni di *scattering*, gli spettri sono stati trasformati in derivata prima (metodo Savitzky-Golay). I modelli di regressione sono stati calcolati mediante l'applicazione dell'algoritmo PLS (*Partial Least Square*) e sono stati validati internamente utilizzando 10 gruppi di cancellazione (*cross-validation*).

## Risultati e Discussione

Il monitoraggio mediante metodiche tradizionali (conte in piastra, pH, acidità titolabile e concentrazione di metaboliti) delle diverse prove fermentative allestite ha prodotto i

risultati attesi, evidenziando l'influenza della temperatura e del tipo di inoculo sull'andamento cinetico e sulle concentrazioni dei diversi parametri investigati.

Le Figure 1 e 2 mostrano, a titolo di esempio, gli spettri IR ottenuti da una delle prove fermentative monitorate, dopo riduzione del *range* spettrale e trasformazione in derivata prima. Gli spettri FT-NIR (Fig. 1) sono caratterizzati da due picchi di assorbimento intorno a 7150 e 6800  $\text{cm}^{-1}$ , associati, rispettivamente, alla banda di combinazione del legame O-H dell'acqua e al primo *overtone* dell'O-H dell'acqua (Williams e Norris, 2001).

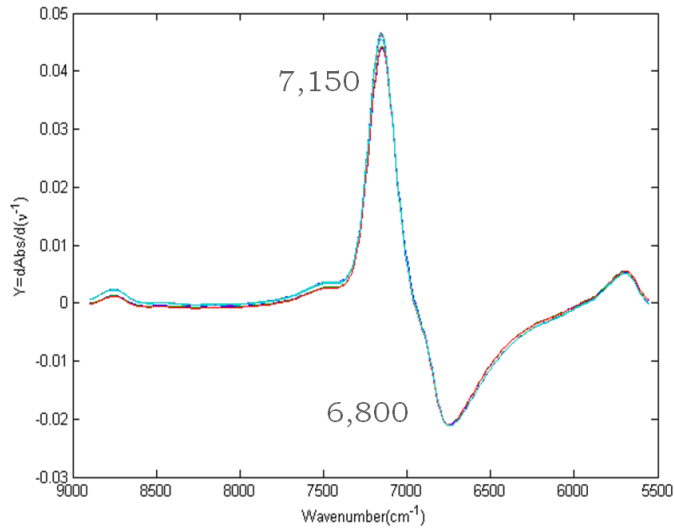


**Figura 1.** Spettri FT-NIR dopo riduzione del *range* spettrale e trasformazione in derivata prima.

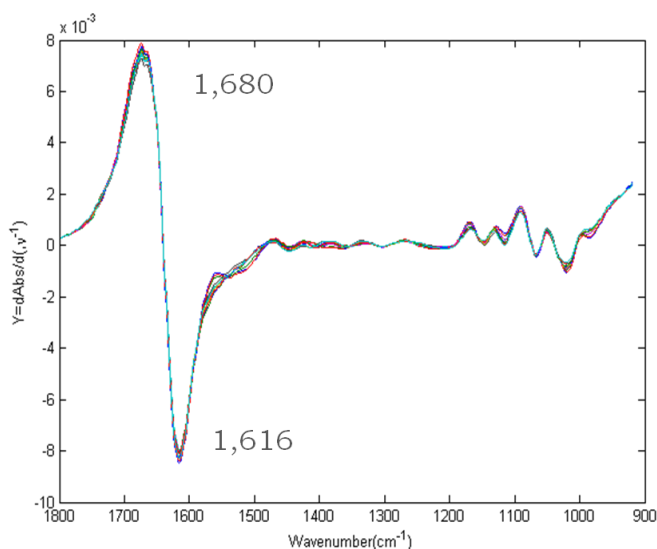


**Figura 2.** Spettri FT-IR dopo riduzione del *range* spettrale e trasformazione in derivata prima.

La regione *fingerpint* degli spettri FT-IR (1800-970  $\text{cm}^{-1}$ ; Fig. 2) presenta due picchi caratteristici, associati all'acqua (1680  $\text{cm}^{-1}$ ) (De Marchi et al., 2009) e al legame N-H delle proteine (1616  $\text{cm}^{-1}$ ) (Sivakesava et al., 2001).

Tramite algoritmo PLS sono stati calcolati modelli di regressione tra i dati spettrali (FT-NIR e FT-IR) e i valori ottenuti dalle analisi di riferimento (conta in piastra, pH, acidità titolabile e metaboliti), validati internamente applicando un metodo di cross-validazione a blocchi *random*. Le Tabelle 1 e 2 mostrano i parametri statistici relativi ai modelli calcolati. In alcuni casi i modelli sono stati costruiti utilizzando insieme tutti i dati provenienti dalle prove di fermentazione effettuate; in altri casi si sono ottenuti risultati migliori utilizzando *dataset* parziali, relativi ai differenti inoculi testati.



**Tabella 1.** Parametri statistici dei modelli PLS costruiti con i dati FT-NIR per la predizione durante la fermentazione lattica di pH, acidità titolabile, metaboliti (lattosio, galattosio, acido lattico) e conta batterica.

Parametri	Calibrazione			Cross-validation		
	VL	Min – Max	R <sup>2</sup>	RMSE	R <sup>2</sup>	RMSE
pH	13	6.51 - 3.67	0.9639	0.1701	0.9327	0.2345
Ac. titolabile Lb (% ac. lattico)	9	0.13 - 1.18	0.9485	0.0203	0.8358	0.0364
Ac. titolabile St (% ac. lattico)	7	0.13 - 1.18	0.9451	0.0014	0.9100	0.0180
Lattosio St+Lb (g/100g)	16	3.02 - 8.05	0.9671	0.7263	0.8221	1.7155
Galattosio (g/100g)	13	0.02 - 3.45	0.8525	0.6435	0.8243	0.7601
Acido Lattico (g/100g)	15	n.r. - 2.48	0.9307	0.5444	0.8556	0.7887
Conte Lb (log UFC/g)	15	6 - 8.65	0.9457	0.2024	0.8566	0.3315
Conte St (log UFC/g)	13	6.35 - 8.65	0.8342	0.2886	0.6755	0.4067

Le regressioni ottenute modellando i dati FT-NIR risultano affidabili soprattutto per i principali indici valutati industrialmente (pH, acidità titolabile) e per la concentrazione di acido lattico, avendo valori di  $R^2$  superiori a 0.93 in calibrazione e 0.85 in cross-validazione, associati ad errori standard contenuti.

**Tabella 2.** Parametri statistici dei modelli PLS costruiti con i dati FT-IR per la predizione durante la fermentazione lattica di pH, acidità titolabile, metaboliti (lattosio, galattosio, acido lattico) e conta batterica.

Parametri	VL	Min – Max	Calibrazione		Cross-validation	
			$R^2$	RMSE	$R^2$	RMSE
pH	11	6.51 - 3.67	0.9762	0.1374	0.9542	0.1901
Ac. Titolabile Lb (% ac. lattico)	9	0.13 - 1.18	0.9915	0.0081	0.9514	0.0020
Ac. Titolabile St (% ac. lattico)	10	0.13 - 1.18	0.9743	0.0095	0.8548	0.0032
Lattosio St+Lb (g/L)	20	3.02 - 8.05	0.9969	0.2240	0.7006	2.2269
Galattosio (g/L)	13	0.02 - 3.45	0.8936	0.5401	0.7755	0.7879
Acido Lattico (g/L)	11	n.r. - 2.48	0.9632	0.3885	0.9233	0.5635
Conte Lb (log UFC/mL)	11	6 - 8.65	0.9247	0.2378	0.8204	0.3662
Conte St (log UFC/mL)	9	6.35 - 8.65	0.9613	0.1385	0.7914	0.3296

Nel caso delle regressioni costruite con i dati spettrali FT-IR, i risultati ottenuti in calibrazione sono buoni per tutti i modelli riportati, mostrando valori di  $R^2$  superiori a 0.89 e valori contenuti di RMSE; è da sottolineare, però, che alcune variabili (lattosio e galattosio in particolare) hanno mostrato problematiche di *overfitting*, ottenendo elevati valori di  $R^2$  in calibrazione, non confermati poi in validazione. Anche in questo caso i modelli costruiti per pH, acidità titolabile e acido lattico correlano in modo più che soddisfacente i dati spettrali con i valori ottenuti dalle analisi di riferimento.

Sono da considerarsi molto promettenti i risultati ottenuti per la determinazione della conta di *L. bulgaricus* e *S. thermophilus* ( $R^2$  in calibrazione pari a 0.9247 e 0.9613,

rispettivamente), che potrebbero incoraggiare l'utilizzo della spettroscopia IR al posto della conta in piastra, tecnica che richiede lunghi tempi di preparazione del campione e di analisi.

## Conclusioni

In conclusione, il lavoro ha permesso di dimostrare che la spettroscopia IR, in combinazione con appropriate tecniche chemiometriche, può considerarsi utile nel monitoraggio delle fermentazioni lattiche, permettendo di predire simultaneamente diversi parametri chiave della fermentazione. Tuttavia, i modelli ottenuti in questo lavoro devono essere considerati preliminari in quanto il numero di campioni utilizzati per la loro costruzione non è sempre molto elevato (min 66; max 198) e non fa riferimento a dati provenienti da produzioni industriali.

## Bibliografia

- M. De Marchi, C.C. Fagan, C.P. O'Donnell, A. Cecchinato, R. Dal Zotto, M. Cassandro, M. Penasa and G. Bittante, *J. Dairy Sci.* **92**, 423 (2009).
- H. Huang, H. Yu, H. Xu and Y. Ying, *J. Food Eng.* **87(3)**, 303 (2008).
- IDF/ISO Standard n° 150. International Dairy Federation (1991).
- S. Sivakesava, J. Irudayaraj and D. Ali, *Process Biochem.* **37**, 371 (2001).
- Y. Takuo (2007) In Y. Ozaki, W. F. McClure, A. A. Christy, *Near-Infrared Spectroscopy Food Science and Technology*, John Wiley & sons, Inc., Hoboken, New Jersey.
- J. Workman and L. Weyer (2007) *Practical Guide to Interpretive Near-Infrared Spectroscopy*, CRC – Taylor and Francis, Boca Raton, FL.

#### 4.1. Overview on milk lactic acid fermentation

# Paper IV

articles

doi: 10.1255/nirn.12xx

## **Near infrared and mid infrared spectroscopy in oenology: determination of main components involved in malolactic transformation**

---

Silvia Grassi, Ileana Vigentini, Nicoletta Sinelli, Roberto Foschino and Ernestina Casiraghi\*

Università degli Studi di Milano, Dipartimento di Scienze e Tecnologie Alimentari e Microbiologiche (DISTAM), via Celoria 2, 20133 Milano, Italy. E-mail: [ernestina.casiraghi@unimi.it](mailto:ernestina.casiraghi@unimi.it)

---

## 4.2. Wine malolactic biotransformation monitoring

## Introduction

There are two main fermentations associated with the winemaking process. Alcoholic fermentation conducted by yeast followed by a secondary fermentation, called malolactic fermentation (MLF) performed by lactic acid bacteria (LAB) specifically from the genera *Oenococcus*, *Lactobacillus* and *Pediococcus*.<sup>1</sup>

MLF is a complex biotransformation, usually defined as the conversion of malic acid to lactic acid and CO<sub>2</sub>, that contributes to deacidification, microbial stability and modification of the aroma profile.

Winemakers usually trust to spontaneous MLF conducted by indigenous LAB occurring on grape surfaces, grape must, cellar environment, including barrels and winery equipment. For this reason spontaneous MLF is often unpredictable. Commonly it occurs after completion of alcoholic fermentation, when the wine conditions are favourable for the growth of lactic acid bacteria, but it may start after long delays.<sup>1</sup> Even with the use of commercial starter cultures, complete and successful MLF is not always guaranteed, especially under difficult wine conditions (i.e. low pH, high ethanol and SO<sub>2</sub> concentrations).<sup>1</sup>

Nowadays winemakers don't carry out a real monitoring of the bioprocess, instead they rely upon oenologists' experience who assess the beginning and the end of the MLF according to sensory evaluations.

Thus, it is desirable to supply winemakers with new simple and rapid analytical systems to monitor MLF and to establish the best strategy for its management. Attempts have been made by other authors to use either near (NIR) or mid infrared (MIR) spectroscopy to predict chemical compounds or fermentation products<sup>2-4</sup> during wine fermentation, however, no references are available in literature concerning MLF monitoring.

In this work we use IR analysis to develop specific calibrations models for malic, lactic acids and total acidity in order to provide a useful tool for MLF monitoring during large scale wine fermentations.

## Materials and methods

### *Sampling and reference analyses*

Samples were collected from different large scale fermentation tanks of Nebbiolo grapes in wineries located in Northern Italy. The samples used in this study were of the same vintage and had not been blended with any other variety or wine from other regions. Each one was characterized by different pH values, SO<sub>2</sub> and alcoholic degree, in order to create an extensive case study. A total of 112 samples were collected taking care to ensure that the set covered the compositional range generally expected in wine. Because FT-NIR and FT-MIR spectroscopy are a secondary analytical method, it was

first necessary to calibrate the instruments against the chemical reference methods for the different components.

Each sample was centrifuged to remove the lactic acid bacteria, and assayed for the consumption of L-malic acid and the production of L-lactic acids by spectrophotometric analysis with enzymatic kits (SCIL diagnostics, GMBH).

Total acidity (expressed as g L<sup>-1</sup> of tartaric acid, endpoint pH 7.0) was carried out by automatic titrator (Titromatic, 2S Crison, Spain).

#### *FT-NIR and FT-IR spectroscopy*

Acquisition of the samples spectra was performed in transmission mode using a glass cuvettes with an optical path of 0.2 mm path length with a Fourier transform (FT-NIR spectrometer, MPA, Bruker Optics, Milano) at different times during the fermentation process. The spectral data were collected over the range 12,500–3,800 cm<sup>-1</sup> (resolution, 16 cm<sup>-1</sup>; background, 32 scans; sample, 32 scans) at controlled temperature (23 ± 1 °C). In addition FT-IR measurements were performed with a spectrometer (Vertex70, Bruker Optics, Milano) equipped with a deuterated triglycine sulphate (DTGS) detector. The spectral data were collected over the range 4,000–700 cm<sup>-1</sup> (resolution, 8 cm<sup>-1</sup>; background, 16 scans; sample, 16 scans) at controlled temperature (23 ± 1 °C). The samples were positioned on a germanium crystal ATR (Attenuated Total Reflectance) with multiple reflection. Instrument control and initial data processing were performed using OPUS software (v. 6.5, Bruker Optics, Ettlingen, Germany).

#### *NIR and MIR data processing*

The Unscrambler software (v. 9.7, Camo, Inondhchim, Norway) was used for spectral data elaboration.

The spectral data collected during the process, raw or pre-treated with first derivative transformation, were correlated with chemical parameters by partial least squares (PLS) regression algorithm. The PLS calibration was preferred because it compensates the interferences from uninteresting compounds. This method has been successfully applied in many bioprocesses monitoring with this intent and has shown strong predictive capacity for unknown samples.<sup>5</sup>

Internal cross validation (leave-one-out) was used to assess the predictive ability of calibration model; the coefficients of determination (R<sup>2</sup>), the root mean square error in calibration (RMSEC) and in cross-validation (RMSECV) were computed. The R<sup>2</sup> gives the percentage of variance present in the component values, which is reproduce in the prediction; the higher the coefficient, the better the correlation between the concentration data and spectral data. The RMSECV is the prediction error of a calibration model and it is defined as the standard deviation of differences between spectral data and reference values in the cross-validation sample set.<sup>6</sup>



## Results and discussion

### *Chemical analysis*

Table 1 shows changes of chemical parameters involved in the biotransformation (malic acid, lactic acid and total acidity) for the 112 samples collected. Average values and the corresponding standard deviation for these parameters, are reported.

During the MLF, L-malic acid is converted into L-lactic acid and CO<sub>2</sub>; the transformation from a diacid (malic acid) to a monoacid (lactic acid) causes a slight decrease of total acidity. The concentration of malic acid ranged from a maximum of 4.01 g L<sup>-1</sup> to a minimum of 0.01 g L<sup>-1</sup>, on the other hand, lactic acid content ranged from 0.05 g L<sup>-1</sup> to 2.63 g L<sup>-1</sup> (Table 1). Samples characterized by malic acid values close to zero and high concentration of lactic acid could be considered as wine at the end of the MLF. Concerning total acidity, collected samples ranged from 8.52 to 5.28 g L<sup>-1</sup> (Table 1). Samples having high total acidity values are referring to wine where the L-malic acid is still present, while lower values are characteristic of wine which have already undergone to the biotransformation. The precise monitoring of total acidity during MLF provides relevant information for global control and optimization of the process.<sup>16</sup>

**Table 1.** Minimum, maximum and mean values for malic acid, lactic acid and total acidity measured for the 112 samples collected at different fermentation stages and from different winery.

Parameter	N	Mean	Minimum	Maximum	S.D.
Malic acid (g L <sup>-1</sup> )	112	2.41	0.01	4.0	1.26
Lactic acid (g L <sup>-1</sup> )	112	0.68	0.05	2.63	0.77
Total acidity (g L <sup>-1</sup> )	112	7.25	5.28	8.52	1.01

S.D.= standard deviation

### *FT-NIR and FT-IR spectroscopy*

NIR row spectra of the samples collected are characterized by some peaks at 6,873, 5,176 and 3,950 cm<sup>-1</sup> (Figure 1). Small peaks are also evident at the region between 4,550 and 4,300 cm<sup>-1</sup>.

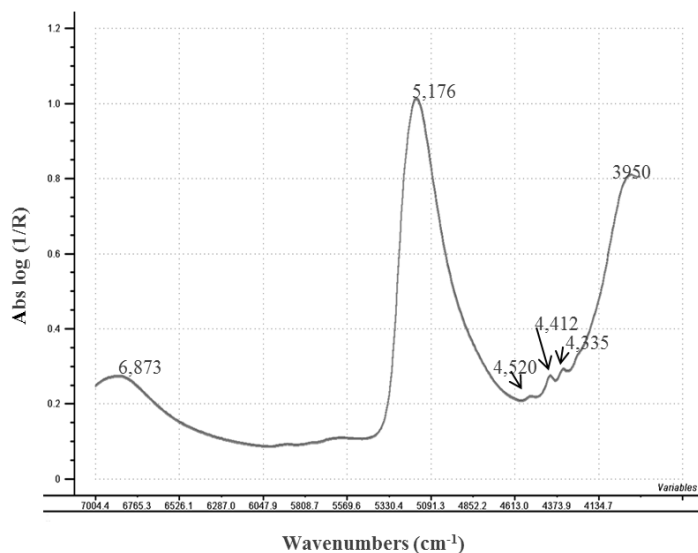


**Figure 1.** Example of aFT- NIR row spectra of a wine sample.

Three peaks are the more significant and correspond to the absorption of C–H and C=O stretching combination band ( $4,520\text{ cm}^{-1}$ ), the absorption of C–H stretching and bending combination band ( $4,412\text{ cm}^{-1}$ ) and O–H and C–O from glucose ( $4,335\text{ cm}^{-1}$ )<sup>6</sup>. The most commonly used chemometric techniques in the bioprocessing context is partial least squares (PLS)<sup>3,4</sup>, in particular is widely applied to complex fluids such as wine.

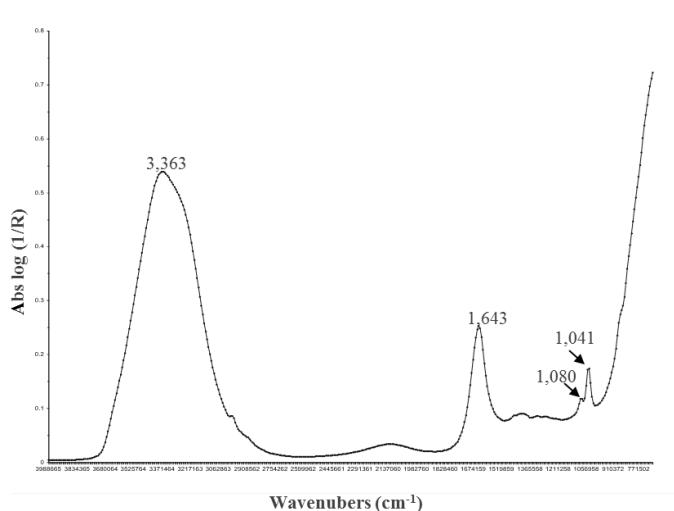


**Figure 2.** Example of PLS models. FT- NIR-predicted data *versus* reference data for the calibration and cross-validation sets for malic acid content in must samples.

NIR spectral data collected from the 112 samples and transformed in first derivative were correlated with the main MLF compounds (L-malic acid and of L-lactic acids) and total acidity values using partial least squares (PLS) regression algorithm.

The results obtained show the ability of FT-NIR spectroscopy in quantifying the main changes in chemical composition occurring during the biotransformation. In Figure 2 is reported an example of regression model for malic acid.

The models developed in the NIR region performed well in the prediction of malic and lactic acids, indeed they are characterized by  $R^2$  in calibration above 0.95, while in validation it reach values of 0.92 for malic acid prediction (Table 2). The models constructed are also characterized by low prediction error for both the chemical indexes (RMSECV = 0.37 g L<sup>-1</sup> for malic acid and RMSECV = 0.27 g L<sup>-1</sup> for lactic acid) (Table 2).

**Table 2.** Statistical parameters for the prediction of malic acid, lactic acid and total acidity in samples collected at different stages of fermentation using FT-NIR spectroscopy

Dependent Variable	Data pre- processing	LV	Calibration		Cross-validation	
			R <sup>2</sup>	RMSEC	R <sup>2</sup>	RMSECV
Malic acid (g L <sup>-1</sup> )	d <sup>1</sup>	10	0.962	0.249	0.918	0.374
Lactic acid (g L <sup>-1</sup> )	d <sup>1</sup>	11	0.958	0.159	0.884	0.269
Total acidity (g L <sup>-1</sup> )	d <sup>1</sup>	10	0.956	0.208	0.879	0.348

**D1**= first derivative, **LV**= number of latent variables, **R<sup>2</sup>**= coefficient of determination, **RMSEC**= root mean square error of calibration, **RMSECV**=root mean square error of cross-validation.

Good predictive model was also achieved for total acidity; in the NIR region correlation coefficient in calibration were 0.96 and RMSEC values were 0.21 g L<sup>-1</sup> (Table 2).

As described for NIR spectroscopy, also FT-IR spectra, evaluated on the same samples, were elaborated using PLS algorithm to build regression models for the main chemical indexes of wine.

An example of FT-IR spectrum collected is shown in Figure 3; the main peaks observable are at 3,363 cm<sup>-1</sup> and 1,643 cm<sup>-1</sup>, related to O–H group stretching in water and the C=O bond stretching of carboxylic acids. It is possible to notice the characteristic bands associated with sugars in the MIR region (C–O stretch for fructose at 1,080 cm<sup>-1</sup> and glucose at 1,041cm<sup>-1</sup>)<sup>4</sup>.

Regression models were developed from spectral ranges between  $3,826\text{ cm}^{-1}$  to  $2,870\text{ cm}^{-1}$  and  $1,905\text{ cm}^{-1}$  to  $694\text{ cm}^{-1}$ , associated with the absorption of O-H group, C-O and C-C bonds of principal molecules present in wine <sup>6,7</sup>.

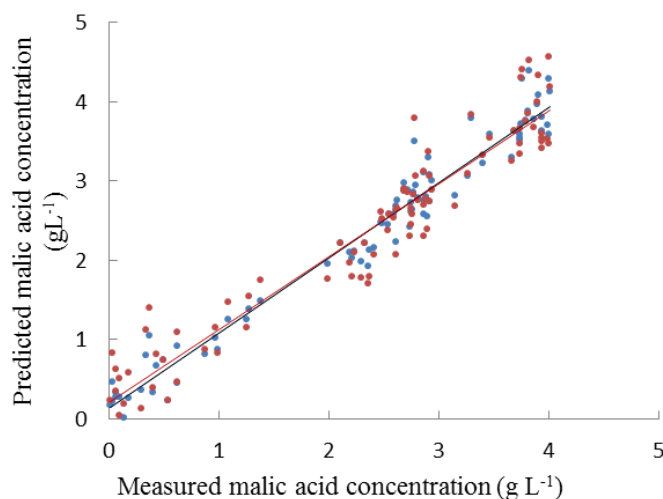


**Figure 3.** Example of aFT- IR row spectra of a wine sample.

An example of model developed in the MIR region for malic acid prediction is shown in Figure 4.

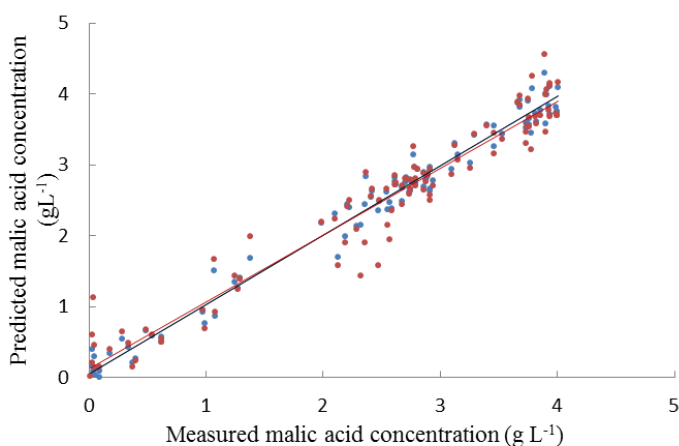


**Figure 4.** Example of PLS models. FT- IR-predicted data *versus* reference data for the calibration and cross-validation sets for malic acid content in must samples.

Fagan and O'Donnell<sup>6</sup> suggest that an  $R^2$  value greater than 0.9 indicates excellent quantitative information. The MIR models obtained were characterized by  $R^2$  values in

cross-validation  $\geq 0.94$ , thus indicating that the correlation equations will provide excellent quantitative information.

**Table 3.** Statistical parameters for the prediction of malic acid, lactic acid and total acidity in samples collected at different stages of fermentation using FT-IR spectroscopy

Dependent Variable	Data pre-processing	LV	Calibration		Cross-validation	
			R <sup>2</sup>	RMSEC	R <sup>2</sup>	RMSECV
Malic acid (g L <sup>-1</sup> )	Abs	9	0.979	0.186	0.943	0.307
Lactic acid (g L <sup>-1</sup> )	Abs	9	0.970	0.020	0.944	0.026
Total acidity (g L <sup>-1</sup> )	Abs	6	0.973	0.166	0.946	0.237

**Abs**= row data with any pre-processing, **LV**= number of latent variables, **R<sup>2</sup>**= coefficient of determination, **RMSEC**= root mean square error of calibration, **RMSECV**= root mean square error of cross-validation.

All the models developed are characterized by low prediction error, indeed RMSECV are 0.31, 0.03, and 0.24 g L<sup>-1</sup> for malic acid, lactic acid and total acidity, respectively (Table 3). Although for many years FT-IR spectroscopy has found generally a more limited application than FT-NIR these results demonstrate great potential for rapid determination of multiple wine components. The regression models in MIR region obtained in this study, if compared with PLS models in NIR region, used a limited number of latent variables, are characterized by greater R<sup>2</sup> values and lower values of root mean square error (both in calibration and cross-validation).

## Conclusions

These results suggest the succeeding in the challenge of meeting the winery's need. The developed calibration models in both NIR and MIR regions provided good estimations for malic acid, lactic acid and total acidity in samples collected from Nebbiolo musts. Within a short time, much of the relevant information can be simultaneously procured. Additionally, a good overview of the sample can be obtained. The FT-MIR method is very user friendly and fast method.

The small estimation errors achieved for the components in this study allowed distinction between samples before MLF and after malic acid transformation. The sampling design, planned using samples from Nebbiolo must fermented in different wineries, performed according different wine-making procedures and wine cellars temperatures, allow to construct global calibration models with a better robustness.

## References

1. E. Lerm, L. Engelbrecht and M. du Toit, “Malolactic fermentation: The ABC’s of MLF”, *S. Afr. J. Enol. Vitic.* 31, 186–212 (2010). <http://www.sasev.org/journal-sajev/sajev-articles/volume-31-2/Lerm%20et%20al%20pp%20186%20to%20212.pdf/view>
2. D. Cozzolino, M. Parker, R.G. Damberg, M. Herderich and M. Gishen “Chemometrics and visible-near infrared spectroscopic monitoring of red wine fermentation in a pilot scale”, *Biotech. Bioeng.* 95, 1102–1107 (2006). doi: 10.1002/bit.21067
3. S. Frago, L. Aceña, J. Guasch, M. Mestres and O. Busto, *J. Agric. Food Chem.* 59, 10795–10802 (2011). doi: 10.1021/jf201973e
4. V. Di Egidio, N. Sinelli, G. Giovanelli, A. Moles and E. Casiraghi, *Eur. Food Res. Technol.* 230, 947–955 (2010). doi: 10.1007/s00217-010-1227-5
5. A.E. Cervera, N. Petersen, A.E. Lantz, A. Larsen and K.V. Gernaey, *Biotechnol. Progr.* 25, 1561–1581 (2009). doi: 10.1002/btpr.280
6. P. Williams and K. Norris, *Near-Infrared Technology in the Agricultural and Food Industries*. American Association of Cereal Chemists Inc., St Paul, USA (2002).
7. C.C. Fagan and C.P. O’Donnell, in *Nondestructive Testing of Food Quality*, Ed by Joseph Irudayaraj and Christoph Reh. Blackwell Publishing, Oxford, UK (2008).

# Paper V

## **Near and Mid Infrared Spectroscopy to detect malolactic biotransformation of *Oenococcus oeni* in a wine-model**

Vigentini I.‡, Grassi S. ‡, Sinelli N., Di Egidio V., Picozzi C.,  
Foschino R., Casiraghi E.

‡ Both the authors contributed to the work at the same extent

*Università degli Studi di Milano, DeFENS, via Celoria 2, 20133 Milano, Italy. E-mail:  
ernestina.casiraghi@unimi.it*

Accepted in: Journal of Agricultural Science and Technology

**JAST-E13110601**

## **Abstract**

The aim of this work was to verify the potential of Infrared (IR) spectroscopy in near and mid regions to detect the beginning of the malolactic fermentation (MLF) occurring in a model-wine. MLF in wine is a secondary biotransformation due to Lactic Acid Bacteria that usually occurs spontaneously or after starter inoculation at the end of alcoholic fermentation. Nowadays, it is desirable to supply winemakers with a new rapid and non-destructive approach to monitor MLF progress and IR spectroscopy technology appears to be suitable for this purpose. The transformation of L-malic acid into L-lactic acid was carried out by inoculating a synthetic wine with an *Oenococcus oeni* culture and it was monitored through microbiological and chemical methods. At the same time FT-NIR spectral data, in diffusive transfection mode using an optic probe, and FT-IR spectra, using a ATR cell, were collected. Principal Component Analysis of the spectra was able to identify absorption bands related to the key molecular modifications that took place during the L-malic acid transformation. Thus, to discriminate samples according to the fermentation phase. Although this study is a preliminary approach, results confirm that NIR and MIR spectroscopy could be successfully applied to detect the start of MLF.

**Keywords** malolactic fermentation, wine, FT-IR, FT-NIR, *Oenococcus oeni*



## Introduction

In some wines characterised by a high total acidity the L-malic acid conversion into L-lactic acid is advisable to increase the quality of the end product. This biotransformation, called malolactic fermentation (MLF), is carried out by lactic acid bacteria (LAB) belonging to *Lactobacillus*, *Oenococcus* and *Pediococcus* genera; among them a key role is played by *Oenococcus oeni*, recognized as the species most tolerant to the wine environment, which is characterised by low pH, high SO<sub>2</sub> and alcohol content [1]. From a technological point of view, the MLF influences quality and taste of the end product as result of the transformation of a diacid (malic acid) into a monoacid (lactic acid), resulting in wine deacidification, flavour complexity enhancement and microbiological stability [2,1]. Small and medium enterprises usually rely on a spontaneous MLF, conducted by indigenous LAB occurring on grape, must and cellar environment, including barrels and winery equipment [3-5]. In particular, the climate can differently trigger MLF; in cold areas spontaneous MLF may take place many months after alcoholic fermentation conclusion [6, 7], whereas warm climates can favour the bacterial growth which activate the MLF throughout or afterwards the alcoholic fermentation. Depending on the wine type and on its required sensorial profile, the biotransformations should be either avoided, controlled or even encouraged, especially in aged Italian red wines, such as Amarone, Barbaresco, Barolo, Brunello di Montalcino, Valtellina Superiore and Sforzato. For this reason both substrate and product concentrations (e.g. sugars, ethanol, L-malic and/or L-lactic acids) must be assayed during the whole process. The monitoring of MLF is usually carried out by traditional methods such as measuring of total and volatile acidity of wine, microbial counts, determination of malic and lactic acids by chromatography techniques or enzymatic assays. These protocols require sample preparation, specific analytical equipment and are time-consuming. The modern oenology needs instead fast and reliable quality control methods that provide real time information. Near (NIR) and mid infrared (MIR) spectroscopy represent fast and non-destructive methods, alternative to conventional analyses. The absorption in these spectral ranges can be related to the main chemical components of food, such as carbohydrates, fats, proteins and water. In particular, in the NIR region (between 750 and 2,500 nm), vibration and combination overtones of the fundamental O–H, C–H and N–H bounds are the main recordable phenomena [8]; while the MIR measurements provide information on fundamental frequencies of chemical bonds in functional groups such as C–C, C–H, O–H, C–O and N–H [9].

IR spectroscopy has already been used in wine composition studies [10-13] and to control microbial fermentations [14-18]; however, as far as concern wine fermentation control, few references are available in literature on the application of NIR and MIR techniques [19-21], and the interest in MLF as proof the works by Cozzolino *et al.* [22]

and Grassi *et al.* [23]. However these approaches are mainly for screening differences of malolactic bacterial strains for metabolic activity in red and white wines and for metabolites quantification. Another interesting approach is to evaluate the kinetics of the biotransformation to describe the dynamics of the process. For this purpose in this work Principal Component Analysis (PCA) and kinetic modelling were applied to spectral data to test out the potential of IR spectroscopy in monitoring time related changes in a malolactic biotransformation in a wine-model.

## Materials and methods

### *Biotransformation medium and conditions*

Tests were performed using a synthetic medium, similar in composition to a wine, prepared modifying Verduyn broth [24] by adding fructose (7.0 g L<sup>-1</sup>), L- malic acid (2.5 g L<sup>-1</sup>), casaminoacids (0.5%), KH<sub>2</sub>PO<sub>4</sub> (3.0 g L<sup>-1</sup>), MgSO<sub>4</sub> (0.5 g L<sup>-1</sup>), ethanol (10% v/v) and adjusting to pH 5.5. The biocatalysis of L-malic acid into L-lactic acid was triggered inoculating 16Z05 *O. oeni* strain [25] which was isolated from an Italian red wine (Valtellina district, SO, Lombardy). To carry on the process, 500 mL of modified Verduyn broth (mVB) was transferred to flasks and inoculated at approximately 10<sup>7</sup> CFU mL<sup>-1</sup>. Cells were incubated at 30°C. To obtain the best survival condition for *O. oeni*, an anaerobic environment was obtained adding 25 mL of sterile liquid paraffin on the surface. The experimental design consisted in two replicates per trial.

### *Microbiological and chemical analyses*

Fifty millilitres of cell culture were collected at 0, 3 and 7 days from the inoculum. Afterwards a regular sampling was performed every 7 days up to 24 days period. A sample aliquot was immediately submitted to the microbiological analysis; after the serial dilution in sterile water plus peptone 10% w/v, 100 µL of cell suspension was plated on MRS (Merck, Darmstadt, Germany), agar 1.5% (w/v) supplemented with 20% v/v apple juice and incubated in anaerobiosis (Anaerocult<sup>®</sup> A; Merck, Darmstadt, Germany) at 30°C for 7 days to obtain the viable cell count. The rest of the sample was filtered 0.22 µm and conserved at -20°C for the following chemical assays.. Fructose, L-malic and L-lactic acids and acetic acid production were measured by spectrophotometric analyses (DU 650, Beckman, Fullerton, CA) using enzymatic kits according to the supplier's recommendations (SCIL diagnostics GMBH). The pH determination was carried out by a pH-meter (3510, JENWAY).

### *FT-NIR and FT-IR spectroscopy*

NIR spectral data were collected using a Fourier transform (FT)-NIR spectrometer (MPA, Bruker Optics, Milano) equipped with an optic probe working in diffusive

transflection mode (path length =1 mm). The data were collected over the 12,500 – 3,800  $\text{cm}^{-1}$  range (resolution, 64  $\text{cm}^{-1}$ ; background, 128 scans; sample, 128 scans) at controlled temperature ( $23 \pm 1^\circ\text{C}$ ).

In addition, the same samples were also analysed by a FT-IR spectrometer (Vertex70, Bruker Optics, Milano) equipped with a deuterated triglycine sulphate (DTGS) detector. Spectral data were collected over the 4,000 – 700  $\text{cm}^{-1}$  range (resolution, 8  $\text{cm}^{-1}$ ; background, 16 scans; sample, 16 scans) at controlled temperature ( $23 \pm 1^\circ\text{C}$ ) placing the samples on a germanium crystal ATR (Attenuated Total Reflectance) with multiple reflection (Pike Technologies, Inc., Madison, USA). Instrument control and initial data processing were performed using OPUS v. 6.5 software (Bruker Optics, Ettlingen, Germany).

The NIR and MIR spectra were acquired up to 24 days of fermentation. In particular, the spectra were collected daily for the firsts eight days, twice a day between 9th and 17th day, and then again daily up to the 24th day.

#### *NIR and MIR data processing*

Both NIR and MIR spectral datasets were analysed using “The Unscrambler v. 9.7” software (Camo, Trondheim, Norway). Before performing the PCA analysis, the NIR and MIR spectral data were pre-treated using a second derivative transform calculation (Savitzky-Golay method, gap size = 15 data points) and mean-centred. To uncover spectral trends occurring during the biotransformation PCA was applied to data. This analysis permits to highlight the similarities among samples and the relationships among variables.

For NIR and MIR data, PCA was performed over the 5,600 – 4,160  $\text{cm}^{-1}$  and 1,535 – 868  $\text{cm}^{-1}$  ranges, respectively. These spectral ranges are characterized by the principal absorption bands of the compounds involved in the biotransformation.

The values of the PC1 scores were modelled as a function of time, using a sigmoid function (1) implemented in Table Curve software (v. 4.0, Jandel Scientific, San Rafael, CA, USA):

$$(1) \quad y = a + b \cdot \exp\left(-\exp\left(-\left(\frac{(x - d \ln(\ln(2)) - c)}{d}\right)\right)\right)$$

with the aim of better describing the spectral changes undergone during process [26-28]. In order to identify critical points during fermentation and therefore to determine the time related to the maximum acceleration and deceleration of the phenomenon, the second derivatives of sigmoid functions were calculated.

## Results and discussion

### *ML biotransformation: microbiological and chemical analyses*

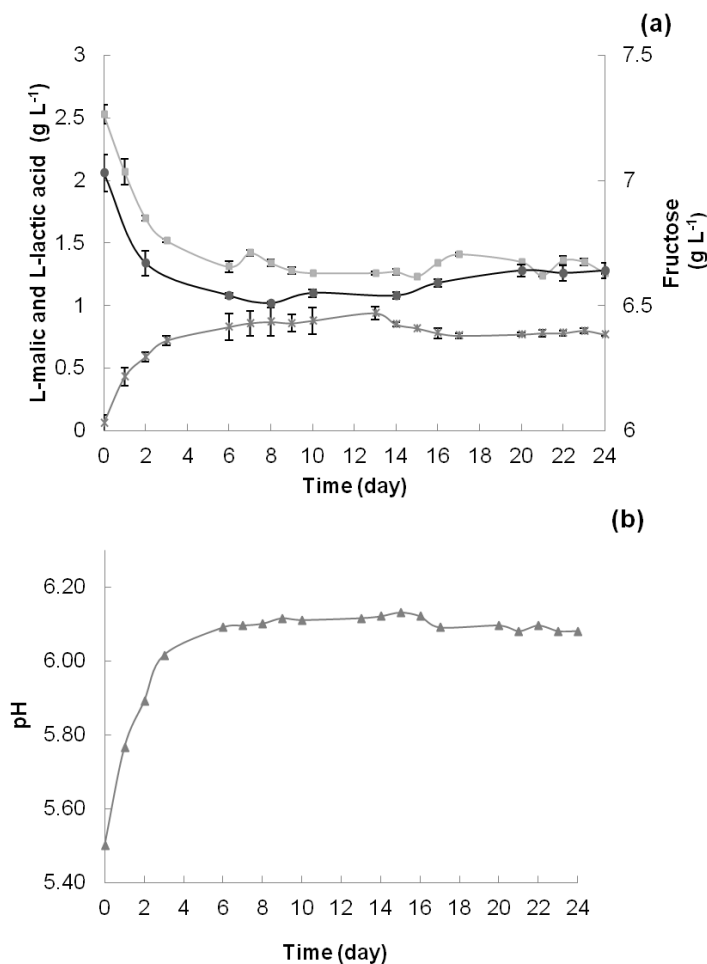
All the results discussed in this section refer to the average values of the data collected by two replicates of the experimental trial. The initial microbial concentration of the inoculum (day 0) was confirmed to be approximately  $10^7$  CFU mL<sup>-1</sup>; after three days, the population was at the same level as expected [29]. After the tenth day, no viable count was detected anymore (data not shown). The fructose evolution shows that the cellular metabolism has been active up to 6-8 days and the higher fructose consumption has occurred in the three days after the inoculum, changing from a start value of 7.0 g L<sup>-1</sup> to 6.6 g L<sup>-1</sup> (Fig. 1a). From the eighth day on the fructose concentration detected remains stable (6.5 g L<sup>-1</sup>). *O. oeni* has numerous nutritional requirements for growth [30]; Terrade & Mira de Orduña [31] underlined that LAB nutritional requirements are genus, species and strain specific. On the other hand, our synthetic medium, prepared to be similar in composition to a wine, may have a limited content of nutrients despite the implementation in casaminoacids, leading to a microbial starvation.

Fig. 1 shows changes of chemical parameters involved in MLF (fructose, L-malic, L-lactic acids and pH): average values and the corresponding standard deviations for these parameters, measured at defined time intervals are reported. No acetic acid production was detected at any time, although it is a potential metabolite of *O. oeni* metabolism [32].

During the first days after the inoculum, L-malic acid was converted into L-lactic acid; in particular, L-malic acid was quickly consumed, decreasing from 2.53 g L<sup>-1</sup> to 1.34 g L<sup>-1</sup> at the eighth day; afterwards, the concentration hold steady. As a consequence, L-lactic acid amount increased from 0 g L<sup>-1</sup> to 0.87 g L<sup>-1</sup> (Fig. 1a).

However, The pH values fast increased during the first three days, growing from 5.50 to 6.02; from the sixth day, all along the trial the pH was stable at 6.10 (Fig. 1b).

The lack in viable counts and the static behaviour of chemical compounds investigated could be ascribable to cell lysis phenomenon, which can occur at the end of MLF in wine production.



**Figure 1.** Evolution of malolactic transformation parameters (a): fructose (●), L- malic acid (■) and L-lactic (x) and pH (b). The results are reported as average values of two replicates and standard deviation.

### ***FT-NIR and FT-IR spectroscopy***

NIR raw spectra of the samples collected at different times during the fermentation process (from initial time to the twenty-fourth day) are characterized by two absorption bands at 6,896 cm<sup>-1</sup> and 5,183 cm<sup>-1</sup> (spectra not shown). These wavenumbers are associated with the first overtone and the combination band of O-H in water, respectively. In order to minimize the background noise and to highlight the main dominant features, data are converted into the 2nd derivative (Fig. 2).

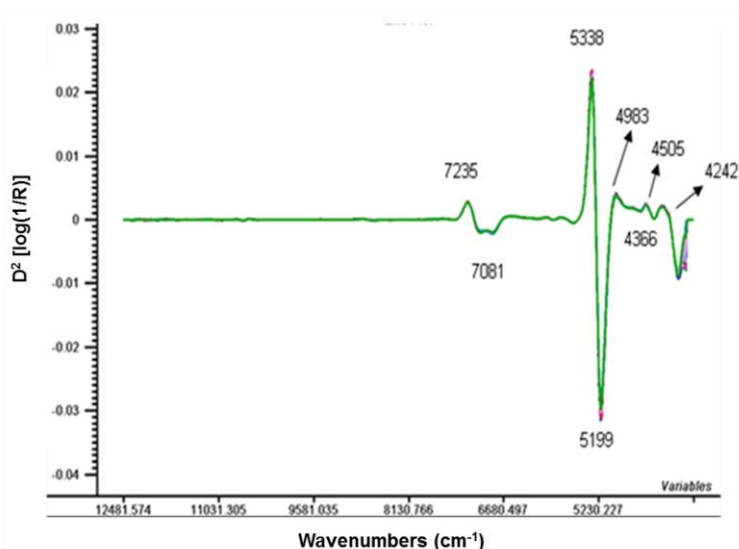


**Figure 2.** Second derivative of NIR spectra of the samples collected at different time during the biotransformation process in mVB (from initial time to the twenty-fourth day).

The main dominant features observed in the transformed spectra are absorption in the range of 7,235 – 7,081  $\text{cm}^{-1}$  and 5,338 – 5,199  $\text{cm}^{-1}$  which are related to the first overtone of the O-H of water and to the combination of stretching and deformation of the O-H group in water, respectively [15]. The second derivative of spectra shows a peak at 4,983  $\text{cm}^{-1}$  related to -NH combination band of amino acidic fraction; small peaks are also evident in the region between 4,505 - 4,242  $\text{cm}^{-1}$ , which correspond to O-H bending and C-O stretching combination and the absorption of C-H stretching and  $\text{CH}_2$  deformation combination band of carbohydrates, respectively [33].

A preliminary examination of the spectra was performed by PCA applied to the second derivative of the spectra in the range 5,600 - 4,170  $\text{cm}^{-1}$ . The results are reported in Fig. 3 and 4.

Through the analysis of the score plot (Fig. 3), obtained by applying PCA to FT-NIR, a samples distribution in the area defined by the first two principal components was obtained according to the fermentation stages. On the score plot the number beside each point represents the fermentation time in days. The samples are distributed along PC1, which accounts for 55% of the variance in the spectral collection, from right to left mainly on the basis of increasing fermentation time. This distribution is clear up to 8 days of fermentation but becomes less distinct thereafter. This sample separation is in good accordance with the time indicated by the microbiological and chemical analyses. In fact, the main biotransformation, according to chemical analyses, were observed up to the ninth day, time at which the MLF has interrupted. At this point the biotransformation occurs no longer in accordance with the microbiological data.

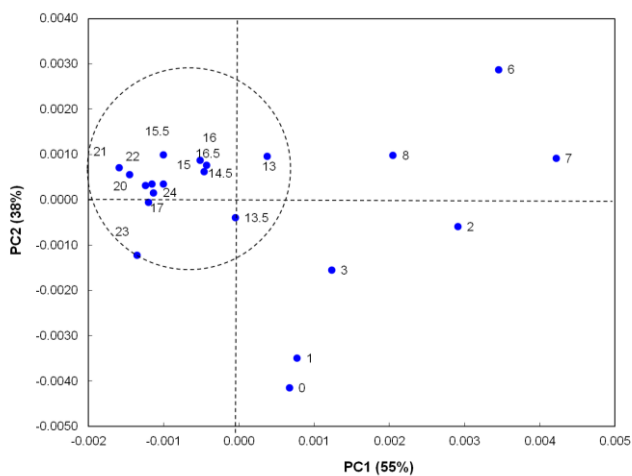


**Figure 3.** Score plot, obtained by applying PCA to FT-NIR data, in the area defined by the first two principal components.

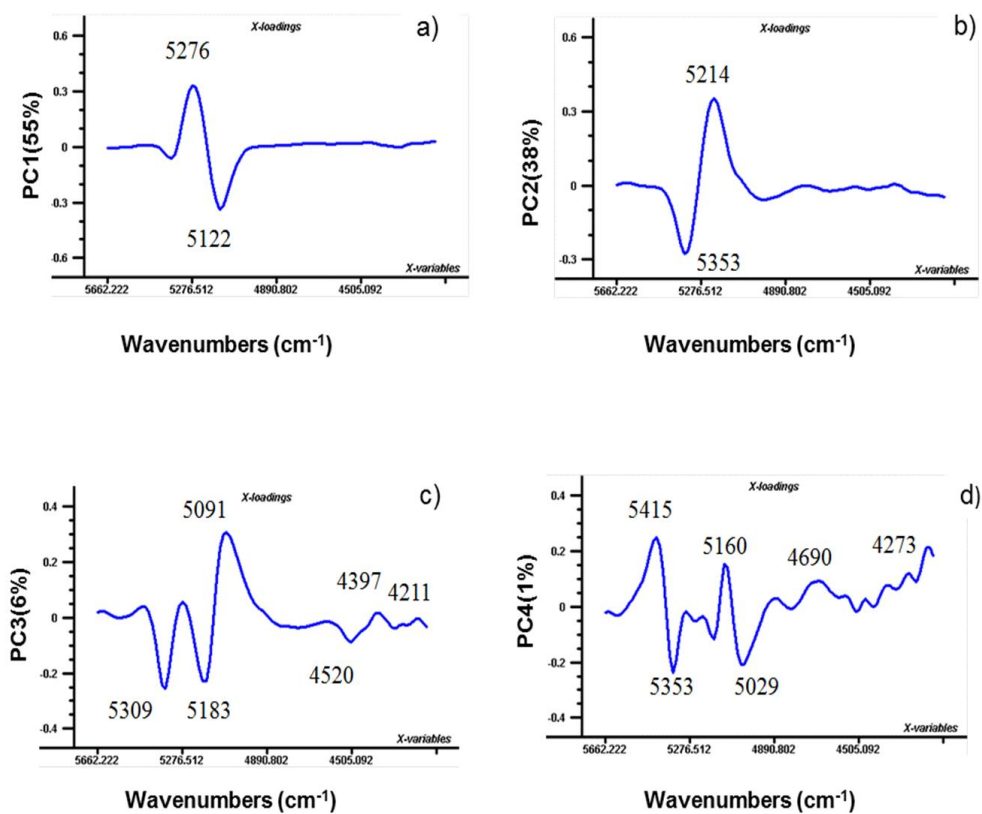


**Figure 4.** Loading plot PC1(a), PC2 (b), PC3 (c) and PC4 (d); NIR spectra.

In attempt to uncover the causes of these score patterns, the loading plots of the first four principal components, which accounts for the 100% of the variance in the spectral collection, were studied (Fig. 4).

The main wavenumbers of the loadings plot on PC1 (Fig. 4a) and PC2 (Fig. 4b) responsible for sample separation during the fermentation process are related to O-H band associated with the water absorption ( $5,353 - 5,122 \text{ cm}^{-1}$ : stretching and deformation of the O-H). The loadings plot on PC2 (Fig. 4b) show also small peaks in the range of  $4,500 - 4,200 \text{ cm}^{-1}$ . These peaks become more evident on PC3 loadings plot (Fig. 4c), and are related to the absorption of C-H stretching and C=O combination band of carbohydrates and O-H and C-O associated with ethanol, sugars and other organic compounds produced during the biotransformation. On PC4 loadings plot (Fig. 4d) the main wavenumbers are related to -NH combination band of peptides ( $5,415 \text{ cm}^{-1}$ ) which are in the broth or are released after lysis of the cell membrane.

The same multivariate approach was used to analyse the FT-IR spectra collected during the MLF.

The main dominant features observed in the second derivative spectra are in the range  $1,477 - 1,326 \text{ cm}^{-1}$ , which is associated with compounds characterized by  $-\text{CH}_2$  and  $-\text{CH}_3$  bonds (such as organic acids) and in the range  $1,110 - 1,045 \text{ cm}^{-1}$ , which is related to C-O and C-C stretching, corresponding to fructose, ethanol and organic acids [34] (Fig. 5).

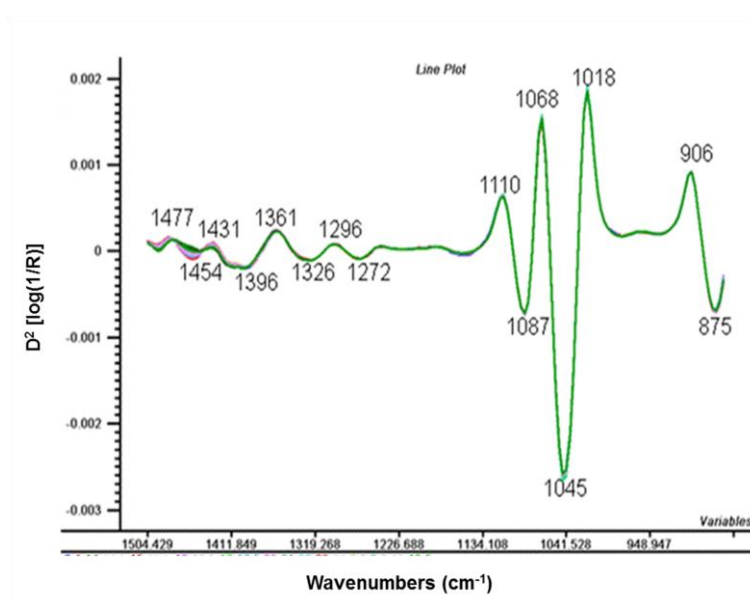


**Figure 5.** Second derivative of FT-IR spectra of samples collected at different time during the biotransformation process in mVB (from initial time to the twenty-fourth day).



The PCA was performed using the second derivative spectra in the spectral range 1,535 - 868  $\text{cm}^{-1}$ .

As in NIR spectroscopy, the PCs score plot (Fig. 6) shows a samples distribution on the basis of the fermentation stage, distinguishing samples collected before the ninth day from the one collected afterwards. This time is in good accordance with those obtained with NIR spectroscopy and with microbiological and chemical analyses.

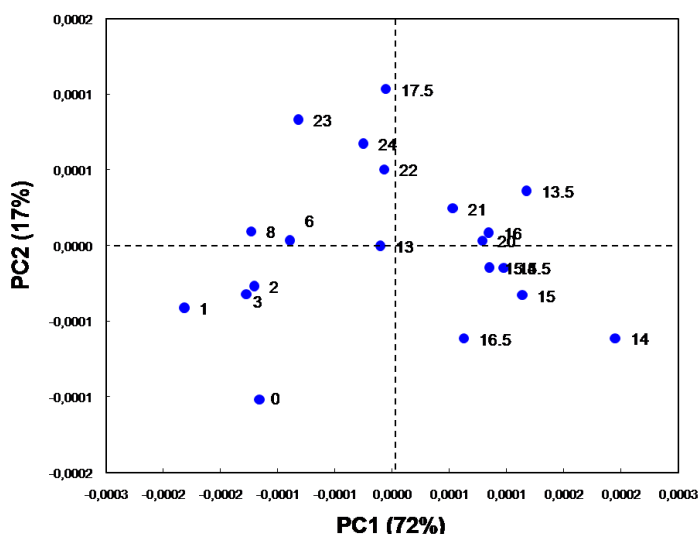


**Figure 6.** Score plot, obtained by applying PCA to FT-IR data, in the area defined by the first two principal components.

The loading intensity on the first four principal components (Fig. 7), which account for the 95% of the total variance, shows that samples distribution could be associated with C-C and C-O bonds vibrations due to proteins and amino acids, and to P=O symmetric stretching mode characteristic of the ribose or deoxyribose nucleic acid (approximately 1,080  $\text{cm}^{-1}$ ) which can be found in the cultural broth following bacterial lysis, as reported for yeast cultures by Filip and Hermann [35], Al-Quadiri *et al.* [36] and Cavagna *et al.* [37]. The main wavenumbers of loadings plot on PC1 (Fig. 7a) and PC2 (Fig. 7b) responsible for sample separation during the fermentation process are related to C-H stretch of  $-\text{CH}_2$  and  $-\text{CH}_3$  groups (1,485 - 1,350  $\text{cm}^{-1}$ ).

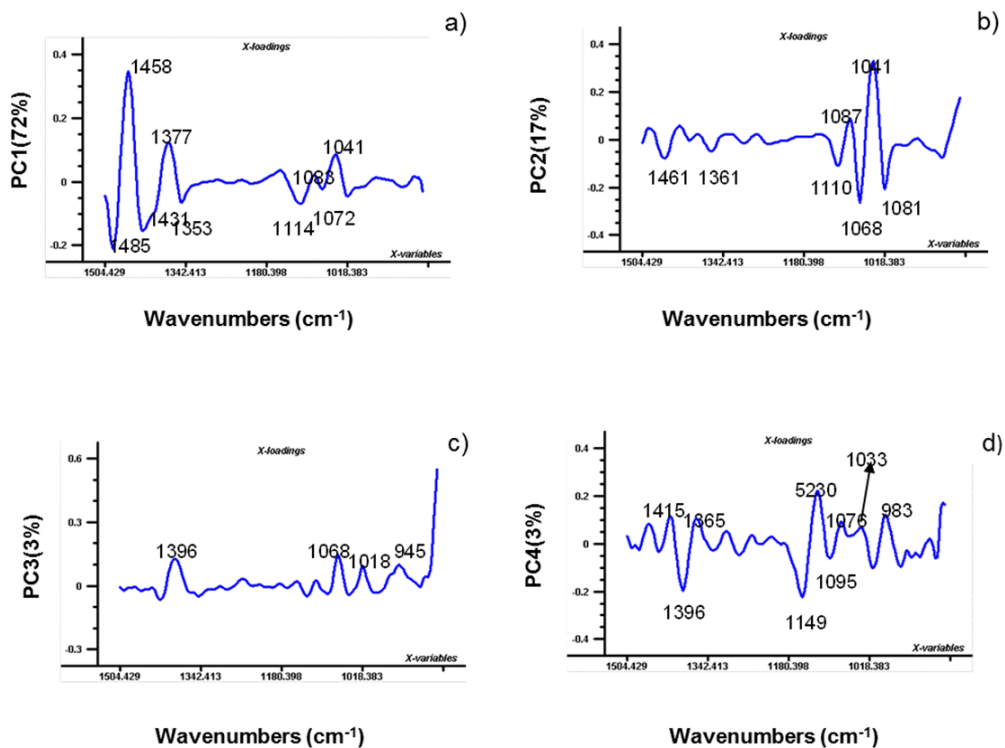


**Figure 7.** Loading plot PC1(a), PC2 (b), PC3 (c) and PC4 (d); MIR spectra.

The loadings plot on PC2 (Fig. 7b) displays also peaks in the range 1,100 - 1,080  $\text{cm}^{-1}$ , due to the absorption band of C-C and C-O. These absorption are also present on the PC3 and PC4 loadings plots (Fig. 7c and 7d).

In order to study the molecular transformations and to better describe the spectral changes during MLF process, the values of PC1 scores obtained by PCA applied to NIR and MIR data, were modelled as a function of time, using a sigmoid function (Table Curve V.4.0, Jandel Scientific, San Rafael, CA, USA). The use of this sigmoid function is related to the nature (enzymatic or microbial-induced) of the biotransformation. In Fig. 8 the modelling of PC1 scores of NIR spectral data is presented: the minimum (6.6 days) and the maximum (14 days) of the second derivative represents the time of the maximum acceleration and deceleration of the bioprocess, respectively.

As for NIR spectroscopy, the PC1 sample scores obtained by MIR spectroscopy, were plotted against time (Fig. 9), and the maximum acceleration and deceleration of the process were calculated in order to define the critical points of MLF revealed by MIR spectroscopy. These times were 7.7 and 13.6 days respectively and they were in good accordance with those obtained by NIR spectroscopy.

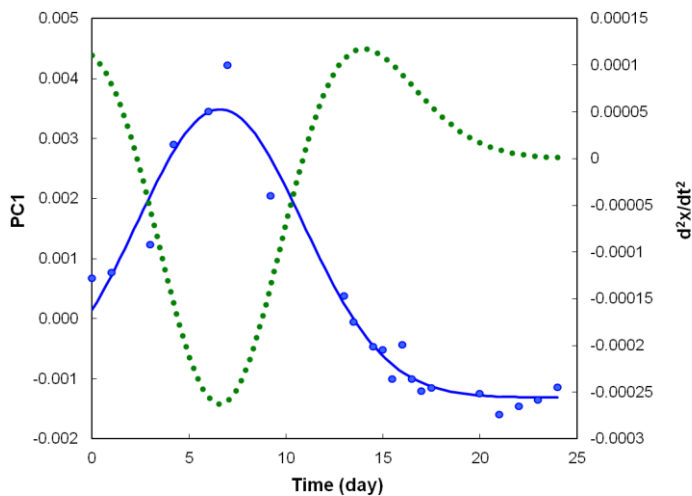


**Figure 8.** PC1 scores versus time for FT-NIR spectral data (●), model obtained fitting the PC1 scores with the sigmoid function (-), second derivative of the model obtained (--).

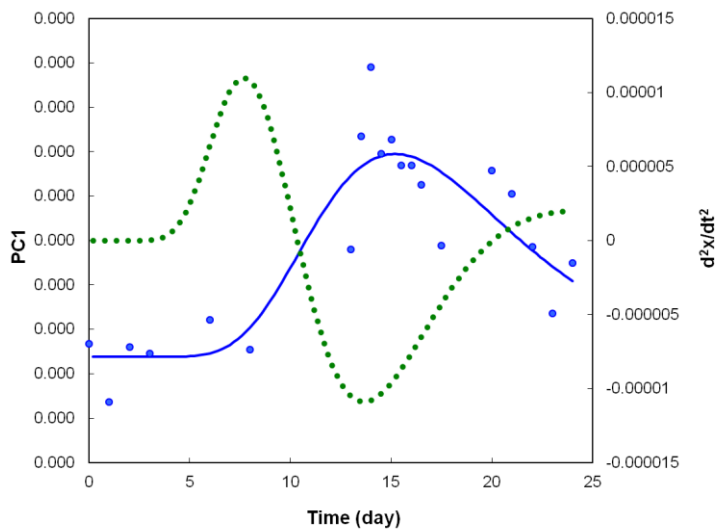


**Figure 9.** PC1 scores versus time for FT-IR spectral data(●), model obtained fitting the PC1 scores with the sigmoid function (-), second derivative of the model obtained (--).

The times, associated with the maximum acceleration of the MLF and revealed by spectroscopic techniques are very similar with those achieved with the chemical analysis: the main biotransformation occurred in the eight day after the inoculum. In particular it agrees in principle with microbiological data: as a consequence of starvation cells stopped growing and they started lysis process after the tenth day. Therefore we can assess that spectroscopic methods, in both near and medium region, are able to monitor the molecular changes that occur during the transformation of L-malic acid into L-lactic acid. Moreover the kinetic approach would permit an evaluation of the performance of the strain rather than just the quantification of the main metabolites. This strategy also allowed to detect the lysis process which could occur in a complex and variable matrix as wine.

### Conclusion

Results obtained in this work revealed that non-destructive methods, such as NIR and MIR spectroscopy, could be employed in studying the evolution of the malolactic transformation, supporting data obtained by conventional techniques (chemical and microbiological analyses).

The modelling of PC scores obtained by NIR and MIR spectroscopy can be used to follow the biotransformation steps giving crucial information on the process. In fact the critical points identified by these techniques during fermentation are in agreement with the times revealed by chemical and microbiological analyses. Therefore, these spectroscopic techniques can be regarded as valid and simple tools able to provide real time information throughout the biotransformation. Although in this study the measurements were carried out during a biotransformation in a model-wine in off-line mode, sensors or probes could be implemented. Future works could be performed during a MLF in wine throughout an on-line monitoring, giving real time signals related to the development of the process.

### References

1. A. Versari, G.P. Parpinello, M. Cattaneo, " *Leuconostoc oeni* and malolactic fermentation in wine: a review", *J. Ind. Microbiol. Biot.*, **23**, 447–455 (1999).
2. G. Chongxiao, G.H. Fleet, "The degradation of malic acid by high density cell suspensions of *Leuconostoc*", *J. Appl. Microbiol.* **76**, 632-637 (1994).
3. R.B. Boulton, V.L. Singleton, L.F. Bisson, R.E. Kunkee, Principles and Practices of Winemaking, International Thomson Publishing, Chapman and Hall, New York, USA (1996).

- 4.C.F. Delfini, J.V. Formica, "Biological degradation of malic acid", in *Wine microbiology Science and Technology*, Ed by Marcel Dekker Inc., New York , USA, pp. 357-378 (2001).
5. R.S. Jackson, *Wine Science: Principles and applications*, Academic Press, California, USA (2008).
6. C.R. Davis, "Practical implications of malolactic fermentation: a review", *Am. J. Enol. Viticult.* **36**, 290–301 (1985).
7. P. A. Henschke, „An overview of malolactic fermentation research”, *Aust. NZ. Wine Ind. J.* **2**, 69–79 (1993).
8. C.E. Miller, “ Chemical Principles of Near-Infrared Technology”, in *Near-Infrared Technology in the Agricultural and Food Industry*, Ed by American Association of Cereal Chemists, St. Paul, Minnesota, USA, pp.19-38 (2001).
9. B.H. Stuart, *Infrared Spectroscopy: fundamentals and Applications*, John Wiley & Sons Ltd., Chichester, UK (2004).
10. J. Fernández-Navales, M.-I. López, M.-T. Sánchez, J.-A. García, J. Morales, "A feasibility study on the use of a miniature fiber optic NIR spectrometer for the prediction of volumic mass and reducing sugars in white wine fermentations", *J. Food Eng.*, **89**, 325–329 (2008).
11. T. Garde-Cerdán, C. Lorenzo, G.L. Alonso, M. Rosario Salinas, "Employment of near infrared spectroscopy to determine oak volatile compounds and ethylphenols in aged red wines". *Food Chem.*, **119**, 823-828 (2010).
12. Á.L. Gallego, A.R. Guesalaga, E. Bordeu, Á.S. González, "Rapid Measurement of Phenolics Compounds in Red Wine Using Raman Spectroscopy", *IEEE T. Instrum. Meas.*, **60**, 507-512 (2011).
13. C. Pizarro, J.M. González-Sáiz, I. Esteban-Díez, P. Orio, "Prediction of total and volatile acidity in red wines by Fourier-transform mid-infrared spectroscopy and iterative predictor weighting", *Anal. Bioanal. Chem.*, 399, 2061–2072 (2011).
14. P. Roychoudhury, R. O’Kennedy, B. McNeil, L.M. Harvey, "Multiplexing fibre optic near infrared (NIR) spectroscopy as an emerging technology to monitor industrial bioprocesses" *Anal. Chim. Acta*, **590**, 110–117 (2007).
15. A. Nordon, D. Littlejohn, A.S. Dann, P.A. Jeffkins, M.D. Richardson, S.L. Stampson, " *In situ* monitoring of the seed stage of a fermentation process using non-invasive NIR spectrometry" *Analyst*, **133**, 660–666 (2008).
16. A.E. Cervera, N. Petersen, A.E. Lantz, A. Larsen, K.V. Gernaey, "Application of Near-Infrared Spectroscopy for Monitoring and Control of Cell Culture and Fermentation", *Biotechnol. Progr.*, **25**, 1561-1581 (2009).
17. D. Landgrebe, C. Haake, T. Höpfer, S. Beutel, B. Hitzmann, T. Scheper, M. Rhiel, K.F. Readon, “ On-line spectroscopy for bioprocess monitoring”, *Appl. Microbiol. Biotech.*, **88**, 11-22 (2010).

18. J. Dahlbacka, T. Lillhonga, “Quantitative measurements of anaerobic digestion process parameters using near infrared spectroscopy and local calibration models”, *J. Near Infrared Spectrosc.* **21**, 23–33 (2013).
19. A. Urtubia, J.R. Pérez-Correa, F. Pizarro, E. Agosin, “Exploring the applicability of MIR spectroscopy to detect early indications of wine fermentation problems”, *Food Control* **19**, 382–388 (2008).
20. D. Cozzolino, R. Dambergs, L. Janik, W. Cynkar, M. Gishen, “Review: Analysis of grapes and wine by near infrared spectroscopy”, *J. Near Infrared Spectrosc.* **14**, 279–289. (2006).
21. V. Di Egidio, N. Sinelli, G. Giovanelli, A. Moles, E. Casiraghi, “NIR and MIR spectroscopy as rapid methods to monitor red wine fermentation”, *Eur. Food Res. Technol.* **230**, 947–955 (2010).
22. D. Cozzolino, J. McCarthy, E. Bartowsky, “Comparison of near infrared and mid infrared spectroscopy to discriminate between wines produced by different *Oenococcus Oeni* strains after malolactic fermentation: A feasibility study”, *Food Control* **26**, 81 – 87 (2012).
23. S. Grassi, I. Vigentini, N. Sinelli, R. Foschino, E. Casiraghi, “Near infrared and mid infrared spectroscopy in oenology: determination of main components involved in malolactic transformation”, *NIR news* **23**, 11–14 (2012).
24. C. Verduyn, E. Postma, W.A. Scheffers, J.P. Van Dijken, “Effect of benzoic acid on metabolic fluxes in yeasts: A continuous-culture study on the regulation of respiration and alcoholic fermentation”, *Yeast* **8**, 501–517 (1992).
25. I. Vigentini, C. Picozzi, A. Tirelli, A. Giugni, R. Foschino “Survey on indigenous *Oenococcus oeni* strains isolated from red wines of Valtellina, a cold climate wine-growing Italian area”, *Int. J. Food Microbiol.* **136**, 123–128 (2009).
26. N. Sinelli, E. Casiraghi, E. G. Downey, “Studies on proofing of yeasted bread dough using near- and mid-infrared spectroscopy” *J. Agr. Food Chem.* **56**, 922-31 (2008).
27. V. Di Egidio, N. Sinelli, S. Limbo, L. Torri, L. Franzetti, E. Casiraghi, “Evaluation of shelf life of fresh-cut pineapple by using FT-NIR and FT-IR spectroscopy”, *Postharvest Biol. Tec.* **54**, 87–92 (2009).
28. S. Limbo, L. Torri, N. Sinelli, L. Franzetti, E. Casiraghi, “Evaluation and predictive modelling of shelf life of minced beef stored in high-oxygen modified atmosphere packaging at different temperatures”, *Meat Sci.* **84**, 129-136 (2010).
29. G. Zapparoli, M. Moser, F. Dellaglio, R. Tourdot-Maréchal, J. Guzzo, “ Typical metabolic traits of two *Oenococcus oeni* strains isolated from Valpolicella wines”, *Letters Appl. Microbiol.* **39**, 48-54 (2004).

30. P.A. Aredes Fernández, F.M. Saguir, C.M. Manca de Nadra, “Effect of Dipeptides on the Growth of *Oenococcus oeni* in Synthetic Medium Deprived of Amino Acids”. *Curr. Microbiol.* **49**, 361–365 (2004).
31. N. Terrade, R. Mira de Ordina, “Determination of essential nutrient requirements of wine-related bacteria from the genera *Oenococcus* and *Lactobacillus*”, *Int. J. Food Microbiol.* **133**, 8-13 (2009).
32. M. Vincenzini, P. Romano, G.A. Farris, *Microbiologia del vino*. Casa editrice Ambrosiana, Milan, Italy (2005).
33. J. Workman, L. Weyer, *Practical guide to interpretative near infrared spectroscopy*. CRC Press, Taylor and Francis Group, Boca Raton, USA (2008).
34. D. Cozzolino, W. Cynkar, N. Shah, P. Smith, “Feasibility study on the use of attenuated total reflectance mid-infrared for analysis of compositional parameters in wine”. *Food Res. Int.* **44**, 181–186 (2011).
35. Z. Filip, S. Hermann, “An attempt to differentiate *Pseudomonas* spp. and other soil bacteria by FT-IR spectroscopy”, *Eur. J. Soil Biol.* **37**,137–43 (2001).
36. H.M. Al-Qadiri, M. Lin, M.A. Al-Holy, A.G. Cavinato, B.A. Rabasco, “Detection of Sublethal Thermal Injury in *Salmonella enterica* Serotype Typhimurium and *Listeria monocytogenes* Using Fourier Transform Infrared (FT-IR) Spectroscopy (4000 to 600  $\text{cm}^{-1}$ )”, *J. Food Sci.* **73**, 54-61 (2008).
37. M. Cavagna, R. Dell’Anna, F. Monti, F. Rossi, S. Torriani, “Use of ATR-FTIR Microspectroscopy to Monitor Autolysis of *Saccharomyces cerevisiae* Cells in Base Wine”, *J. Agr. Food Chem.* **58**,39-45 (2010).

## 4.2. Wine malolactic biotransformation monitoring



# PAPER VI





Food Chemistry

Available online 27 January 2014

In Press, Accepted Manuscript — Note to users



## Beer fermentation: monitoring of process parameters by FT-NIR and Multivariate data analysis

Silvia Grassi<sup>a</sup>, José Manuel Amigo<sup>b</sup>,  , Christian Bøge Lyndgaard<sup>b</sup>, Roberto Foschino<sup>a</sup>, Ernestina Casiraghi<sup>a</sup>

<sup>a</sup> Department of Food, Environmental and Nutritional Sciences (DeFENS), Università degli Studi di Milano, via Celoria 2, 20133 Milano, Italy

<sup>b</sup> Department of Food Science, Faculty of Sciences, University of Copenhagen, Rolighedsvej 30, DK -1958 Frederiksberg C, Denmark

**ABSTRACT**

This work investigates the capability of Fourier-Transform near infrared (FT-NIR) spectroscopy to monitor and assess process parameters in beer fermentation at different operative conditions. For this purpose, the fermentation of wort with two different yeast strains and at different temperatures was monitored for nine days by FT-NIR. To correlate the collected spectra with °Brix, pH and biomass, different multivariate data methodologies were applied. Principal component analysis (PCA), partial least squares (PLS) and locally weighted regression (LWR) were used to assess the relationship between FT-NIR spectra and the abovementioned process parameters that define the beer fermentation. The accuracy and robustness of the obtained results clearly show the suitability of FT-NIR spectroscopy, combined with multivariate data analysis, to be used as a quality control tool in the beer fermentation process. FT-NIR spectroscopy, when combined with LWR, demonstrates to be a perfectly suitable quantitative method to be implemented in the production of beer.

**Keywords:** Beer fermentation; quality control; NIR; FT-NIR; PCA; PLS; LWR

## 1. Introduction

Beer is, arguably, the most widespread alcoholic beverage in the world and its success is related, among other factors, to its suitability for large scale production. Beer production was originally handcrafted and the control of the fermentation was exerted by skilled brew masters able to evaluate the progress of the process with empirical sensory evaluations (Bolton & Quain, 2006). In the past decades, thanks to the rise of industrial beer production, the subjective evaluation of the process has been outdated by initial control parameters, being the regulation of wort composition and yeast strain the main ones (Bamforth, 2006). Despite the precise assessment of the previous mentioned parameters the brewing industry still has to face different variation in the cycle of the fermentation that might hamper the quality of the final product. Therefore, large scale production of beer leads to the necessity of quality assurance systems to guarantee the fulfilment of the required quality consistency of the final product, forcing the breweries to define and control one or several parameters during the process to meet the proper standards. Although each company defines its own specifications, some are required by law. In particular, for what regards the final product, alcohol content or Plato degree per hectolitre are the legal parameters upon which beer is taxed (Directive 92/84/EEC, 1992). For this motive, an unavoidable parameter to be controlled during the first fermentation of beer is specific gravity (SG), correlated with sugar concentration in the wort and, therefore, alcohol content in the final product. The industrial trend is to monitor the fulfilment of SG to the defined specification through the use of Quality Control Charts, which allow a fast visual check of the trend of the system being controlled through mean and control limits statistically defined. However, with this univariate quality assurance strategy is difficult to date back to the source of the no standard behaviour leading to the abnormality in the batch (Kourti, 2005). The main problem is that a failure in a parameter evaluated might be originated from several correlated variables, often non-measured, governing such a complex bioprocess as it is beer first fermentation (Kourti, 2006).

Recently, companies started to look for methods providing comprehensive information of the on-going process in order to assure an effective control at all stages. The implementation of Fourier-Transform near-infrared (FT-NIR) probes has been proved to offer detailed information in real-time in several food processes, allowing the assurance of meeting the quality parameters to the defined specifications (Huang, Yu, Xu & Ying, 2008). Despite being a promising technique, FT-NIR has several drawbacks to be considered as well. For instance, the spectral signal generally obtained in the fermentation of beer is strongly characterized by the overlapping of the bands due to the heterogeneous and complex composition of the medium. In fact, the wort is

mainly composed by fermentable sugars (i.e. maltose, maltotriose, glucose, sucrose, and fructose), non-fermentable sugars (i.e. dextrins) and nitrogen sources in the form of proteins, peptides and aminoacids (Lewis & Young, 2002). All the mentioned compounds absorb in the NIR region (12,000-4,000  $\text{cm}^{-1}$ ), as they contain C–H, N–H, O–H and C=O bonds, giving an overlapped signal. Moreover, water is the major constituent of the wort (ca. 92% ) and it strongly characterises NIR spectral information with its peaks around 6,900  $\text{cm}^{-1}$  (O-H first overtone) and around 5,300  $\text{cm}^{-1}$  (combination of the asymmetric stretch and bending of the water molecule) (Workman & Weyer, 2008).

Chemometrics has been applied in the last 30 years to overcome the mentioned drawbacks and to extract relevant information from FT-NIR data (Bock & Connelly, 2008). Principal component analysis (PCA) and Partial Least Square (PLS) regression became of interest, as they are able to take advantage of the structures in highly overlapping and co-linear data (Martens & Næs, 1989). Both methods are linear. Nevertheless, in some cases, the correlation between the spectral signal and the reference measure has a non-linear nature. In these cases, methods for linear modelling of nonlinear surfaces are needed. Cleveland and Devlin (1988) proposed locally weighted regression (LWR) as methodology to fulfil this goal and Næs and Isaksson (1992) and Naes, Isaksson and Kowalski (1990) applied the strategy to infrared spectroscopy.

To what brewing monitoring concerns, FT-NIR spectroscopy combined with Chemometrics has been applied to simultaneous determination of compounds in brewing final product (Duarte, Barros, Almeida, Spraul & Gil, 2004; Inon, Llario, Garrigues, de la Guardia, 2005; Lachenmeier, 2007; Ghasemi-Varnamkhasia Rodriguez-Mendoza, Gomes, Ugulino Araújo and Galvão, 2012) and for beer authentication (Di Egidio, Olivieri, Woodcock, Downey, 2011; Engel, Blanchet, Buydens, Downey, 2012). Nevertheless, little research exists on the use of FT-NIR for monitoring and assessment of changes in relevant physico-chemical parameters in the beer fermentation process (McLeod et al. 2009).

Therefore, much more intensive work is needed to really assess the usefulness and power of FT-NIR and Chemometrics in modelling, controlling the beer fermentation process. This work investigates the capability of FT-NIR spectroscopy to monitor wort fermentation conducted at different operative conditions (temperature and yeast type), deepening into the robust correlation between NIR spectra collected during fermentation and different key factors in beer manufacturing. For this purpose, PCA was applied to the FT-NIR spectra of a set of six different beer fermentation conditions, to ascertain whether beer spectral changes may be correlated with the biotransformation progress, both biomass increase and chemical modifications. Furthermore, PLS and LWR models were calculated to correlate sugar content ( $^{\circ}\text{Brix}$ ),

pH and biomass to the spectral information in order to develop a rapid method to detect the changes of these parameters in real-time during the fermentation process.

## 2. Materials and methods

### 2.1. Materials

Standard commercial wort “Highland heavy Ale wort” was purchased (Muntons plc©, Suffolk, UK) and reconstituted according to instructions of the manufacturers in 2 L of heat treated water for each trial, agitated at 200 rpm for 2 h to saturated level. Two different *Saccharomyces cerevisiae* strains, one for British Ale (WLP005) and the other for Belgian Ale (WLP570) (WhiteLab Inc., San Diego, CA, USA), were separately inoculated into the wort, reaching approximately the concentration of  $7 \times 10^6$  CFU mL<sup>-1</sup>. The preparation of the inoculum was performed as follow: one fresh colony for each strain was aerobically propagated in 10 mL YEPD broth (Yeast Extract 10 g L<sup>-1</sup>, Peptone 20 g L<sup>-1</sup>, Dextrose 20 g L<sup>-1</sup>, pH 6.4) at 20°C for 24 h; afterwards, the suspension was transferred in 100 mL of fresh broth with a magnetic stirrer (200 rpm) for 24 h at 20°C, then transferred in 400 mL YEPD and incubated for 24 h at 20°C. The harvested cells were pitched in the wort and gently agitated to create a homogeneous distribution before sharing out about 300 mL into sterile glass bottles, one for each sampling point, closed with airlock caps. The cell concentration for each strain was determined using a calibration curve obtained by correlating plate counts on YEPD agar and optical density values measured at 620 nm.

### 2.2. Fermentation trials

The experiments were performed according to a factorial design with the two different *S. cerevisiae* strains (WLP005 and WLP570) and three different fermentation temperatures (19, 21 and 24°C), all replicated twice, giving a total amount of 6 different experiments for each beer type.

Samples were collected in triplicate right after pitching (0 hour, starting time) and then every 22 hours until the 9<sup>th</sup> day of fermentation, using two different sampling methods: directly from supernatant and after centrifugation for 15 min at 3,000 g.

### 2.4. pH, °Brix and biomass determination

pH was measured at each sampling point by a Portamess® 911 pH-meter (Knick Elektronische Messgeräte GmbH & Co. KG, Berlin, Germany).

Total sugar content was measured by a refractometer (Bellingham and Stanley RMF 340, Kent, UK).

The changes in biomass were determined by optical density measured at 620 nm with a UV-visible spectrometer (Hemlett Packard 8453, Agilet Technologies, Waldbronn, Germany).

### 2.7. FT-NIR spectroscopy

FT-NIR spectra were collected in transmission mode, with a Bomem QFA Flex FT-NIR spectrometer (Q-Interline A/S, Roskilde, Denmark) equipped with a 1 mm path length cuvette. The data were collected in the range 12,000–4,000  $\text{cm}^{-1}$ , with a resolution of 16  $\text{cm}^{-1}$  and 128 scans for both background and samples.

### 2.8. Data processing

The whole wavenumber range (12,000–4,000  $\text{cm}^{-1}$ ) was reduced in order to eliminate useless or saturated variables from spectra. For PCA and regressions of chemical indexes the final two spectral ranges selected were from 7,500 to 5,500  $\text{cm}^{-1}$  and from 4,700 to 4,350  $\text{cm}^{-1}$ . They are characterized by the principal absorption bands of the compounds involved in the biotransformation. Only for the regression models for biomass prediction the spectra range used was 10,500 to 5,500  $\text{cm}^{-1}$  and from 4,700 to 4,350  $\text{cm}^{-1}$ , in order to keep the information about baseline changes which are correlated to the yeast growth in the media.

Except for biomass regression, the spectra were pre-processed to minimize the effect of baseline shifts and noise and to highlight modifications due to the chemical composition. Thus, Standard Normal Variate (SNV), first derivative Savitzky – Golay (7 wavelengths gap size and 2<sup>nd</sup> order polynomial) was performed. Before data analysis with PCA, the final pre-processed spectra were mean centred. In the same way, before regression models, the pre-processed spectra were mean centred and the variable to predict auto-scaled.

All models were developed by the PLS\_Toolbox (Eigenvector Research Inc., Wenatchee, WA) working under MatLab v. 7.4 (The MathWorks, Natick, MA).

PCA and PLS models are quite common in literature, and further information can be found elsewhere (Kramer, 1998; Kramer, Workman & Reeves, 2004).

Briefly, PCA is a suitable tool for simplification, data reduction, outlier detection and pattern recognition (Jolliffe, 1986), highlighting the variance of the spectra. PLS, on the contrary, is a standard method to solve multivariate regression problems, maximizing the correlation between the NIR spectra and the parameters to quantify (Naes, Isaksson, Fearn & Davies, 2002).

LWR, though, is not frequently presented as regression techniques applied to spectroscopy.

Therefore, the main steps characterizing the analysis are reported (Bevilacqua, Bucci, Materazzi, Marini, 2013) as they were applied in this work:

1. cDefinition of the number of nearest neighbours (local points) close to the prediction spectrum to be used to build local calibration models;
2. Find for every new object the samples closest to it in the local calibration model (nearest neighbours);
3. Build a local calibration model using the nearest neighbours only; assign the weights ( $\alpha$ ) of the neighbours in the local model according to their Euclidean distance to determine the closeness to the dependent variable and the auto-scaled distance in the principal components space;
4. Prediction (by PLS regression) of the new sample by applying the local calibration model developed.

### 3. Results and discussion

#### 3.1. pH and Brix degree

pH values obtained at the inoculation time ( $t=0$ ) were very similar for all the samples, having an average value of  $5.64 \pm 0.07$ . This confirms the reproducibility of the wort reconstitution protocol (Figure 1a and 1b). Just after the fermentation started, a fast drop in pH values was observed for all the trials performed within 22 h of fermentation. This decay in the pH, though, was different (as observed in Figure 1a and 1b) depending of the yeast strain inoculated. The trials performed with WLP005 strain showed a minimum pH value at  $24^\circ\text{C}$  after 72 h ( $4.45 \pm 0.02$ ) (Figure 1a), followed by a modest rise up to  $4.52 \pm 0.03$  at the end of the monitoring ( $t=216\text{h}$ ). This behaviour of the pH after the fermentation “mid-point” was previously reported by Berner & Arneborg (2011).

Concerning the trials inoculated with WLP570 strain, the pH decay continued until the last sampling point ( $t=216$  h) (Figure 1b). More precisely, it is possible to observe the temperature effect for the trials incubated at  $19^\circ\text{C}$  (the slope of the pH curve is lower than for the trials performed at higher temperatures in Figure 1a and 1b). Nevertheless, the final pH values were comparable at all the temperature tested ( $4.41 \pm 0.13$ ).

Figure 1 (c and d) shows as well the  $^\circ\text{Brix}$  changes for all the trials performed. As observed for pH, the  $^\circ\text{Brix}$  at starting time were the same for all the trials ( $9.37 \pm 0.07$   $^\circ\text{Bx}$ ) corresponding to a sugar content of approx.  $97.50\text{g/L}$ . The total sugar content showed a fast decrease in all the trials performed within three days of fermentation. The sugar consumption was faster when WLP005 strain was used, reaching  $6.55 \pm 0.05$   $^\circ\text{Bx}$  after 46 h at  $24^\circ\text{C}$  (Figure 1c) and remaining constant after 142 h of fermentation, due to the characteristic high flocculation of the yeast cells and the consequent low sugar consumption. The main difference was observed when wort inoculated with WLP005 was incubated at  $19^\circ\text{C}$ ; in this case the sugar content decreased with a lower speed but reaching at the fermentation end-point the same level of the other trials performed ( $5.19 \pm 0.04$   $^\circ\text{Bx}$ ). The sugar depletion in the fermentations conducted with

WLP570 strain showed a lower and more constant slope than those inoculated with WLP005 (Figure 1d).

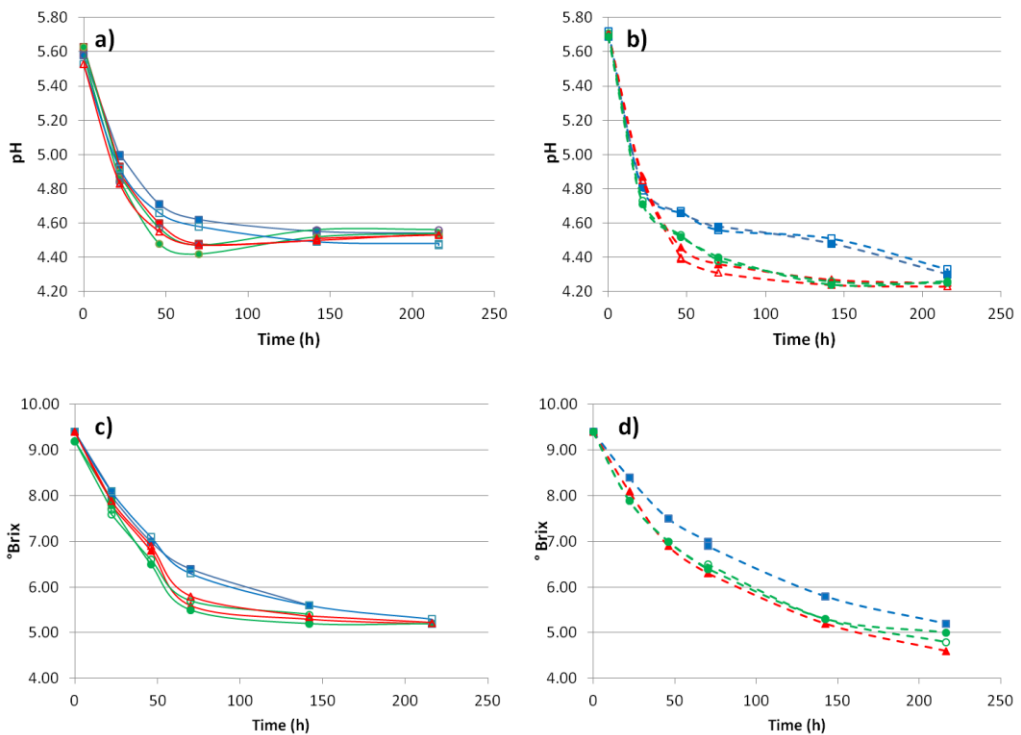


**Figure 1.** pH and °Brix profiles for the three tested temperatures: blue squares for trails performed at 19°C, green circles for the one at 21°C and red triangles for the one at 24°C. pH evolution of trials conducted with WLP005 strain (a), and WLP570 (b). Soluble Solid Content of trials conducted with WLP005 strain (c), and WLP570 (d).

This is probably due to the ability of WLP570 yeast cells to remain in suspension in the wort during the fermentation time. To assess if the end points of the trials performed were significantly different according to the temperature and yeast used the mean of °Brix and pH values at the final points were subjected to a two way analysis of variance (ANOVA). Table 1 reports the results obtained. At 95% of confidence level there were found no significant differences in the end points.



**Table 1.** Two way analysis of variance for °Brix and pH value at the end-points to assess the influence of the three temperatures and the two yeast strains tested ( $\alpha=0.05$ ).

	Source of variation	SS	DF	MS	Effect of Factor
<b>°Brix</b>	Temperature	0.016	2	0.008	0.043 n.s.
	Yeast strain	0.112	1	0.112	0.60 n.s.
<b>pH</b>	Temperature	0.008	2	0.004	0.101 n.s.
	Yeast strain	0.015	1	0.015	0.366 n.s.

SS= Sum of Square; DF= Degree of Freedom; MS=Mean Square

As described beforehand, the trends of the pH and °Brix could be different according to the yeast used, but evaluating their values at end point is not possible to find out differences due to the strain inoculated or the operating temperature. In this regard pH and °Brix measurement alone could not be an exhaustive tool to monitor the overall fermentation performance as is not possible to find out differences in the processes due to failure of temperature control or due to the yeast strain governing the fermentation.

### 3.2 FT-NIR spectroscopy

Figure 2a shows an example of the spectra collected directly from the supernatant for the fermentation conducted at 19°C with WLP570. Here it is possible to observe an increase in absorption and baseline drift due to the scattering effect caused by the yeast growth in the media. The main peak around 6,900  $\text{cm}^{-1}$  is related to O-H first overtone of water (Workman & Weyer, 2008), which is the main compound present in the fermenting wort (around 90%). Other small features are present in the 4,700-4,350  $\text{cm}^{-1}$  region, being related to the sugars consumption and ethanol production (McLoad et al., 2009). Figure 2b shows in detail the second spectral area, being able to observe the characteristic peak of ethanol around 4,420  $\text{cm}^{-1}$  and its evolution with time.

The pre-processed spectra obtained at 19°C with WLP570 are shown in Figure 2c. Main changes are highlighted in the region 7,500-5,500  $\text{cm}^{-1}$ . In particular changes are associated with water O-H absorption (7,000-6,500) and with C-H methyl associated with O-H as R-OHCH<sub>3</sub> (5,925  $\text{cm}^{-1}$ ) (Workman & Weyer, 2008). Moreover in the region 4,700-4,350  $\text{cm}^{-1}$  ethanol and sugars modifications (C-H combination bands, and O-H stretch overtone) are evident.

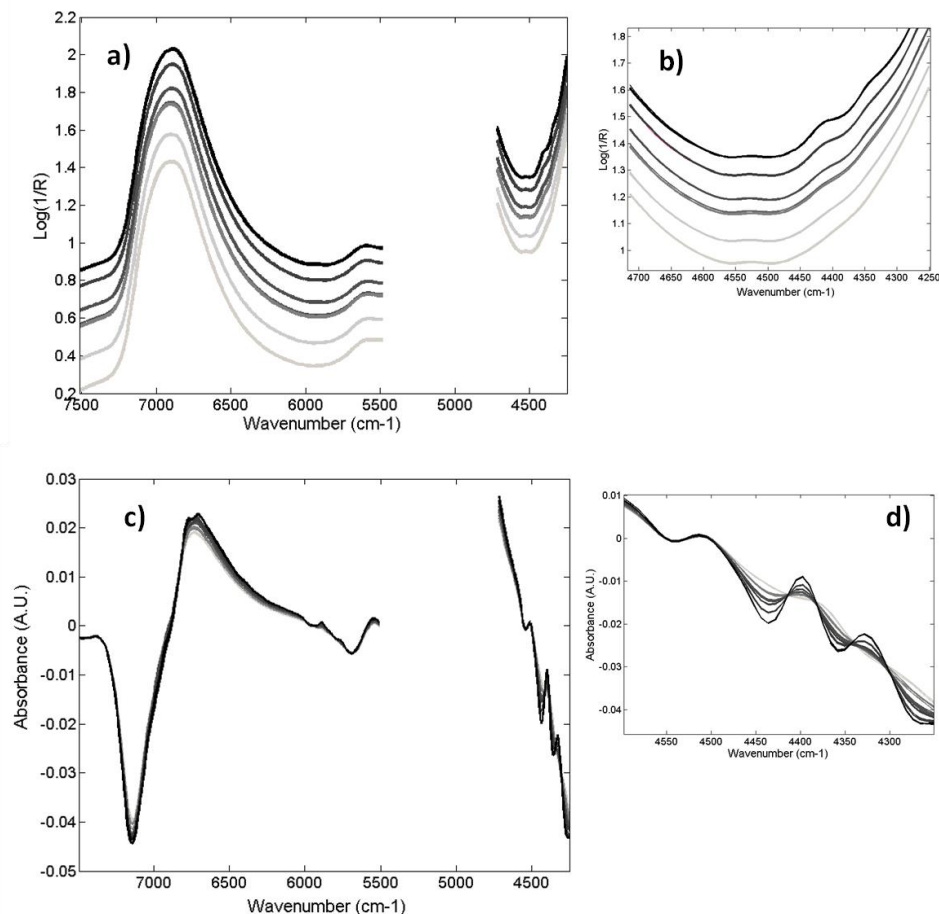


**Figure 2.** FT-NIR spectra collected directly from the supernatant for the fermentation conducted at 19°C with WLP570. Raw spectra in the region 7,500-5,500 and 4,700-4,350  $\text{cm}^{-1}$  (a), detail of the region 4,700-4,350  $\text{cm}^{-1}$  (b). Spectra transformed with SNV and first derivative (7 pt, 2<sup>nd</sup> polynomial order) (c), detail of the region 4,700-4,350  $\text{cm}^{-1}$  after pre-treatments (d).

The increase of ethanol content according to fermentation time is well highlighted in Figure 2d. The highlighted wavelength range (4,700-4,350  $\text{cm}^{-1}$ ) recorded at the beginning of the fermentation (light gray colour) does not have the characteristic ethanol peaks due to the O-H stretching combined with O-H bending (Workman & Weyer, 2008); whereas it is possible to observe the appearance of the peaks and their increment with time.

### 3.3 Principal component analysis

Figure 3a shows the score plot of the first and the second principal components, PC1 and PC2, respectively, with samples coloured according to the fermentation time. PC1 explains 63.21% of the total variance and clearly describes the evolution of the spectra according to the fermentation time. It is noteworthy that this clear definition of the

evolution of fermentation by PC1 is repeated for all the fermentations, no matter the sampling method used, the yeast or the temperature tested, denoting the precision and robustness of FT-NIR spectra in reporting fermentation evolution under different conditions. Samples collected at time = 0 (red triangles) have positive PC1 values and are grouped together, in agreement with the results obtained by pH and °Brix measurements. With the progress of the fermentation time samples have lower PC1 scores, with a good separation between each sampling time.

The main peaks responsible of samples distribution along the PC1 (Fig. 3d) are due to the influence of ethanol (peaks around 6,000-5,500  $\text{cm}^{-1}$  and 4,400  $\text{cm}^{-1}$ ), sugars (first combination region C-H around 4,500  $\text{cm}^{-1}$ ) and the consequently change in water (O-H first overtone at 6,900  $\text{cm}^{-1}$ ).

On the other hand, PC2 clearly separates the samples according to the sampling method used (Figure 3b). All the samples collected after wort centrifugation have negative PC2 values; while most of the samples collected directly from the supernatant have positive values, which generally increase with the time progress.

This outcome can be associated with the physical effect of increasing of the concentration of suspended cells in the medium (Beauvoit, Liu, Kang, Kaplan, Miwa & Chance, 1993). However, there are some of the samples collected from the supernatant which are characterised by low PC2 values. Looking at Figure 3c is possible to find an explanation about the supernatant samples having low PC2 values with the progress of time. The samples collected directly from the supernatant of the wort fermented with WLP005 ( $\square$ ) have PC2 values increasing until  $t=70\text{h}$ , thereafter the values decrease up to reaching the same value of the samples collected just after the starting time.

This phenomenon can be ascribed to the flocculating nature of this strain. Indeed, the loading profile of PC2 (Figure 3d, (---)) is highly influenced by scattering effect in the regions 6,500-5,500  $\text{cm}^{-1}$  and 5,000-4,500  $\text{cm}^{-1}$  which was not completely corrected by SNV pre-treatment. To better understand the different behaviours observed according to the yeast strains inoculated, PCA models on the single strain were performed. Figure 4a reports the scores plot of the PC1 vs PC3 performed by selecting from the dataset only the experiments performed with WLP005.

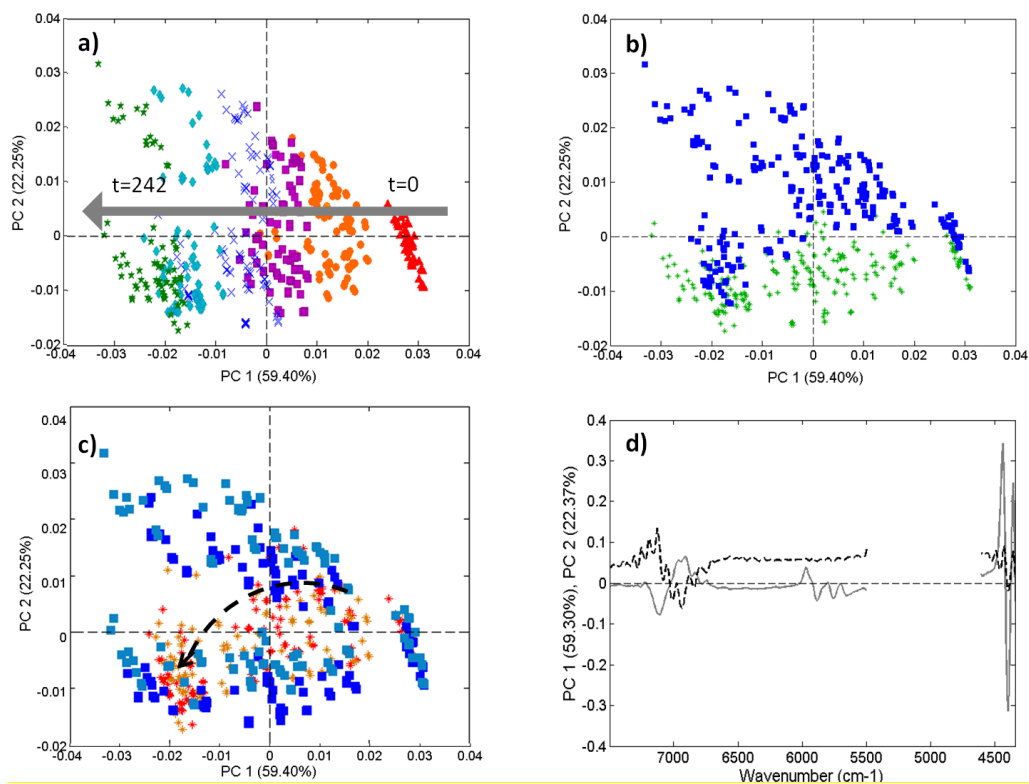


**Figure 3.** Principal component analysis of all the FT-NIR spectra collected. Score plots: (a) PC1 vs PC2 with samples coloured according to fermentation time (red  $\Delta$ =0h, orange  $\circ$ =22h, purple  $\square$ =46h, blue  $\times$ =70h, light blue  $\diamond$ =142h, green  $*$ =216h), (b) samples coloured according the sampling method used (blue  $\square$ =centrifuged and green  $*$ =not centrifuged), (c) samples coloured according to the strain inoculated ( $\square$  for WLP005 and  $*$  for WLP570). Loadings plot: (d) represents the PC1 loading (gray line) and PC2 loading (black-dashed line).

As observed in the global PCA (Fig. 3) this strain is characterised by flocculation behaviour, which causes the precipitation of the cells on the bottom of the flask after 70 hours. In this case the scatter effect and changes in the water peak ( $6,900\text{ cm}^{-1}$ ) is described mainly by the PC3. High values of PC3 correspond to a high number of yeast cells in the media, i.e. high scattering effect. Moreover the third component is influenced by changes in the O-H first overtone ( $6,900\text{ cm}^{-1}$ ), as observed in the corresponding loadings plot (Fig.4c).

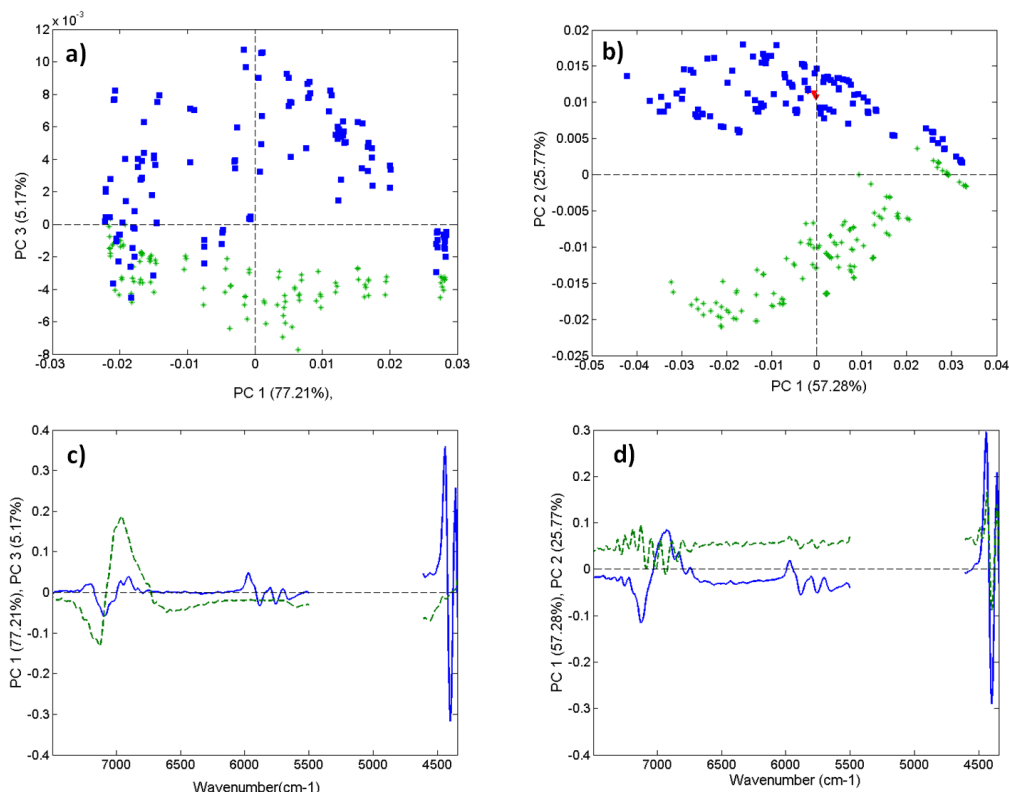


**Figure 4.** Principal component analysis of the FT-NIR spectra collected from the trials performed with WLP005 strain (*a* and *c*) and with WLP570 (*b* and *d*). (a) PC1 vs PC3 of WLP005 with samples coloured according the sampling method used (blue  $\square$ =centrifuged or green  $*$ =not centrifuged). (b) PC1 vs PC2 of WLP570 with samples coloured according the sampling method used (blue  $\square$ =centrifuged or green  $*$ =not centrifuged). (c) PC1 (solid line) and PC3 (dashed line) loadings plot of WLP005 samples. (d) PC1 (solid line) and PC2 (dashed line) loadings plot of WLP570 samples.

Figure 4b shows the scores plot referred to the PCA performed by selecting just the WLP570 strain. In this case the scattering effect is described by the PC2 and two groups are well defined according to the sampling method used (Fig.4b). All the spectra collected from centrifuged samples have negative PC2 values whereas samples collected directly from the supernatant are characterised by positive PC2 values increasing during fermentation time due to the higher concentration of yeast in the media causing scattering effect. In both individual PCA (Fig. 4a and 4b) the PC1 described the time progress related to the main modification occurring during the biotransformation progress no matter the sampling method used. In particular the regions effecting the samples distribution are related to sugars (4,500-4,300 cm<sup>-1</sup>) and ethanol (6,000-5,500 cm<sup>-1</sup> and 4,200 cm<sup>-1</sup>) (Fig. 4c and 4d).

### 3.4 Quantitative determination of Solid Content, pH and biomass

PLS analysis was employed as initial method to estimate °Brix , pH and biomass for all the spectra collected. PLS calibration models were constructed using the whole dataset comprising 6 experiments run at different temperatures (19, 21, 24 °C) and with different inoculated strains (WLP005 and WLP570), replicated twice and collected with two different sampling methods (centrifuge and from the supernatant) with a total of 497 spectra. Before regression analyses different spectral regions were selected following the suggestions made by McLeod et al. (McLeod et al. 2009). From 7,500 to 5,500  $\text{cm}^{-1}$  and from 4,700 to 4,350  $\text{cm}^{-1}$  for °Brix and pH and from 10,500 to 5,500 and from 4,700 to 4,000  $\text{cm}^{-1}$  for biomass. Different pre-treatments were tested (SNV and first derivative) always followed by mean centering. a double cross-validation in both PLS and LWR models. A double cross-validation procedure was performed following these steps:

- 1) Select one of the batches (whole fermentation) as external test set.
- 2) The remaining batches conformed the training/calibration set.
- 3) Perform the calibration model using leave – one batch out – cross validation methodology.
- 4) Predict the test set batch with the calibration model.
- 5) Select another batch to be considered as external test set and come back to step 2.

This flow-chart was repeated as many times as batches comprise the full dataset. In our case, twelve times. The figures of merit reported are the mean value of the figures of merit calculated in every iteration. In this way, more robust and reliable models can be constructed compared to a single cross-validation procedure, especially in the cases where there are not many samples available. The figures of merit of the PLS models are reported in Table 2.

**Table 2. Figures of merit of the PLS and LWR models obtained for total solid content (°Brix), pH and biomass.**

Model	Parameter	Range	pre-treat	variable selection	LV	Global PC	Local points	Local LV	$\alpha$	Iteration	Calibration		Cross-validation		Prediction	
											R <sup>2</sup>	RMSEC	R <sup>2</sup>	RMSECV	R <sup>2</sup>	RMSEP
PLS	°Brix	4.9-9.4	SNV	none	4	-	-	-	-	-	0.969	0.255	0.964	0.275	0.964	0.249
			SNV	4500-4000 cm <sup>-1</sup>	4	-	-	-	-	-	0.975	0.227	0.971	0.250	0.970	0.230
			SNV+d1	none	5	-	-	-	-	-	0.977	0.220	0.970	0.253	0.970	0.237
			SNV+d1	4500-4000 cm <sup>-1</sup>	3	-	-	-	-	-	0.968	0.256	0.964	0.272	0.964	0.253
	pH	5.71-4.27	SNV	none	4	-	-	-	-	-	0.773	0.201	0.752	0.208	0.743	0.205
			SNV	4500-4000 cm <sup>-1</sup>	4	-	-	-	-	-	0.872	0.105	0.839	0.168	0.827	0.166
			SNV+d1	none	5	-	-	-	-	-	0.865	0.153	0.818	0.179	0.811	0.175
			SNV+d1	4500-4000 cm <sup>-1</sup>	4	-	-	-	-	-	0.796	0.190	0.756	0.207	0.746	0.203
	Biomass*	0.14-3.19	none	none	5	-	-	-	-	-	0.911	0.267	0.894	0.291	0.829	0.262
			none	10,500-5,500 cm <sup>-1</sup>	5	-	-	-	-	-	0.922	0.249	0.908	0.271	0.848	0.240

			-	-	3	50	4	0.00	5	0.987	0.128	0.960	0.291	0.962	0.266	
	°Brix	4.9-9.4	SNV+d1	-	-	3	50	4	0.50	5	0.987	0.126	0.960	0.294	0.960	0.269
				-	-	<b>3</b>	<b>50</b>	<b>4</b>	<b>0.75</b>	<b>5</b>	<b>0.988</b>	<b>0.141</b>	<b>0.906</b>	<b>0.289</b>	<b>0.961</b>	<b>0.259</b>
LWR				-	-	3	50	4	0.00	5	0.987	0.055	0.917	0.122	0.913	0.117
	pH	5.71-4.27	SNV+d1	-	-	<b>3</b>	<b>50</b>	<b>4</b>	<b>0.50</b>	<b>5</b>	<b>0.987</b>	<b>0.046</b>	<b>0.923</b>	<b>0.116</b>	<b>0.921</b>	<b>0.112</b>
				-	-	3	50	4	0.75	5	0.974	0.063	0.915	0.123	0.910	0.119
			none	-	-	3	50	3	0.00	5	0.956	0.184	0.910	0.271	0.851	0.216
	Biomass*	0.14-3.19	none	-	-	<b>3</b>	<b>50</b>	<b>3</b>	<b>0.50</b>	<b>5</b>	<b>0.951</b>	<b>0.166</b>	<b>0.910</b>	<b>0.270</b>	<b>0.852</b>	<b>0.211</b>
			none	-	-	3	50	3	0.75	5	0.953	0.170	0.905	0.273	0.852	0.212

**SNV**= standard normal variate, **d1**= first derivative (window size 7, second polynomial order), **Global PC**= number of principal components in the global model, **local LV**= number of latent variables in the local model,  **$\alpha$**  = weighting of y-distances in selection of local points, **iteration**= iterations in determining local points,  **$R^2$** = coefficient of determination, **RMSEC**= root mean square error of calibration, **RMSECV**=root mean square error of cross-validation, **RMSEP**=root mean square error of prediction.

\*O.D. (optical density) for biomass at 620 nm.



The number of latent variables (LVs) was selected by inspecting root mean square error of calibration (RMSEC) and cross-validation (RMSECV), selecting the number of LVs that led to a minimum of both RMSEC and RMSECV and, most important, containing information about the chemical features of the samples. Moreover, the root mean square error of prediction (RMSEP) and the coefficient of determination ( $R^2$ ) were also reported for all the models.

Inspecting the regression vectors of the models for °Brix and pH it was noticed that the variables in the region 4,500 to 4,000  $\text{cm}^{-1}$  were the one explaining most of the variance of the model, no matter the pre-treatment used. This finding confirmed what have been stated by McLoad et al. (2009). This region, related to sugar and ethanol content, was selected for further PLS analysis (Table 2). For what concern the model for biomass no pre-treatment was used because the main idea was to describe the dispersion of the cells in the fermenting beer. The region from 10,500 to 5,500  $\text{cm}^{-1}$  was the one remarkable in the corresponding regression vectors, mainly describing the slope changes in this region, i.e. the scattering effect of the yeast in the media. With regard to the Total Solid content (°Brix) excellent models were obtained for all the pre-treatments and the variable selected tested. In particular, the PLS model obtained with the spectra pre-treated with SNV and using the selected spectral region presented coefficient of determination ( $R^2$ ) in calibration, cross-validation and prediction of 0.975, 0.971 and 0.970, respectively and a small error (RMSE) in calibration, cross validation and prediction (0.227, 0.250 and 0.230, respectively). This highlights the extreme importance that data exploration step has when dealing with FT-NIR, showing that the small spectral area between 4,500-4,000  $\text{cm}^{-1}$  is, indeed, the most informative one. The use of first derivative in addition to the SNV caused a general slight reduction of the figures of merit, assessing that the best models were those with minimum pre-processing.

For what concerns the models obtained for pH, the results were of lower quality. The best performance was obtained by calculating the model with spectra transformed with SNV, with variable selection, using 5 LVs. This lack of good performance for pH and its logarithmic behaviour suggested that there might be a nonlinear relationship between the spectra and the pH.

With reference to biomass the models obtained were good, especially when the region 10,500-5,500  $\text{cm}^{-1}$  was selected (in prediction the  $R^2$  was 0.848 and the RMSEP=0.240). However, the samples grouping in the score of LV1 against LV2 revealed the influence of the different experimental conditions (strain inoculated) which can effect in the models results in the same extent as a nonlinear relationship.

LWR-PLS regression results are summarised in Table 2. For all the models reported the number of local point (neighbours) was set to 50; the number of global component set to 3; the number of local latent variables set to 3 or 4; and the interactions set to 5. The alpha parameter, the relative weight of the Euclidian distance to prediction in the

selection of the subset of calibration spectra, was tested at different level (0, 0.5 and 0.75). For pH and biomass, the best models were achieved with  $\alpha=0.50$ , indeed the coefficients of determination were higher than 0.95 in calibration, 0.91 in cross-validation and 0.85 in prediction. For what concern Total Solid Content ( $^{\circ}$ Brix) the best model was obtained with  $\alpha=0.75$  with  $R^2$  in prediction of 0.961. The LWR root mean errors in prediction were lower than 0.054 in the case of pH and 0.029 for biomass if compared with the ones obtained with PLS methodology. For what concern  $^{\circ}$ Brix the LWR did not improved the quality of the figure of merit obtained with PLS modelling.

#### 4. Conclusions

In this study the application of FT-NIR spectroscopy as a method to monitor beer manufacturing parameters, i.e. soluble solid content ( $^{\circ}$ Brix), pH and biomass, with a simple centrifugation and without any sample preparation was investigated.

Different multivariate data techniques were applied on the spectroscopic data. PCA results demonstrated that is possible to follow biomass evolution, i.e. concentration of suspended cells in the medium, and the evolution of fermentation from a chemical point of view, no matter the sampling method adopted.

The use of PLS provided acceptable models for  $^{\circ}$ Brix, pH and biomass determination, even though the results suggested a possible nonlinear relationship between the spectra and the parameter investigated. The better results obtained with LWR-PLS technique instead of the linear PLS confirmed the nonlinearity relationship and permitted to achieve precision and robustness models to determine  $^{\circ}$ Brix, pH and biomass, no matter the sampling method used.

The results obtained in this research suggest the robust and reliable possibility that the implementation of NIR instruments, with the proper configuration, provides for on-line industrial brewing systems to monitor  $^{\circ}$ Brix, pH and biomass evolution during the beer fermentation. Supplying industries with a system giving information in real-time would allow the assurance of meeting the main parameters to the defined specifications and the action in case of non standard trends detection.

#### Acknowledgements

The authors thank Michael Crafac, University of Copenhagen, Department of Food Science - Food Microbiology for providing the yeast strains used and the material for the performance of the microbiological analysis.

#### References

Bamforth, C.W. (2006). *Brewing, new technology*. Cambridge: Woodhead Publishing, (Chapter 11).

- Beauvoit, B., Liu, H., Kang, K., Kaplan, P. D., Miwa, M., Chance, B. (1993). Characterization of absorption and scattering properties for various yeast strains by time-resolved spectroscopy. *Cell Biophysics*, 23, 91-109.
- Berner, T.S. and Arneborg, N. (2001). The role of lager beer yeast in oxidative stability of model beer. *Letters in Applied Microbiology*, 54, 225–232.
- Bevilacqua, M., Bucci, R., Materazzi, S., Marini, F. (2013). Application of near infrared (NIR) spectroscopy coupled to chemometrics for dried egg-pasta characterization and egg content quantification. *Food Chemistry*, 140, 726-734.
- Bock, J.E., Connelly, R.K. (2008). Innovative uses of Near-Infrared spectroscopy in food processing. *Journal of food science*, 73(7), R91-R98.
- Boulton, C. & Quain, D. (2006). *Brewing Yeast and Fermentation*. Oxford: Blackwell Science, (Chapter 6).
- Cleveland, W.S., Devil, S.J. (1988). Locally Weighted Regression: An Approach to Regression Analysis by Local Fitting. *Journal of the American Statistical Association*, 83 (403), 596-610.
- Di Egidio, V., Olivieri, P., Woodcock, T., Downey, G. (2011). Confirmation of brand identity in foods by near infrared transreflectance spectroscopy using classification and class-modelling chemometric techniques — The example of a Belgian beer. *Food Research International*, 44, 544–549.
- Directive 92/84/EEC: OJ L 316, 1992. 31.10.1992 Bull. 10-1992.
- Duarte, I.F., Barros, A., Almeida, C., Spraul, M., Gil, A.M. (2004). Multivariate analysis of NMR and FTIR data as a potential tool for the quality control of beer. *Journal of Agricultural and Food Chemistry*, 52, 1031-1038.
- Engel, J., Blanchet, L., Buydens, L.M.C., Downey, G. (2012). Confirmation of brand identity of a Trappist beer by mid-infrared spectroscopy coupled with multivariate data analysis. *Talanta*, 99, 426–432.
- Ghasemi-Varnamkhashtia, M., Mohtasebi, S.S., Rodriguez-Mendoza M.L., Gomes, A. A., Ugulino Araújo, M.C., Galvão R.K.H. (2012). Screening analysis of beer ageing using near infrared spectroscopy and the Successive Projections Algorithm for variable selection. *Talanta*, 89: 286– 291.
- Huang, H., Yu, H., Xu, H., & Ying, Y. (2008). Near infrared spectroscopy for on/in-line monitoring of quality in foods and beverages: A review. *Journal of Food Engineering*, 87(3), 303-313.
- Inon, F. A., Llario, R., Garrigues, S., de la Guardia, M. (2005). Development of a PLS based method for determination of the quality of beers by use of NIR spectral ranges and sample-introduction considerations. *Analytical and Bioanalytical Chemistry*, 382, 1549–1561.
- Jolliffe, I. T. (1986). Principal Component Analysis. Springer-Verlag. *Journal of Food Science*, 73 (7), R92-R98.

- Kourti, T. (2005). Application of latent variable methods to process control and multivariate statistical process control in industry. *International Journal of Adaptive Control and Signal Processing*, 19 (4), 213–246.
- Kourti, T. (2006). The process analytical technology initiative and multivariate process analysis, monitoring and control. *Analytical and bioanalytical chemistry*, 384: 1043-1048.
- Kramer, R. (1998). *Chemometric techniques for quantitative analysis*. New York: Marcel Dekker Inc.
- Kramer, R., Workman, J. Jr., Reeves, J.B. III. (2004). Qualitative analysis. In: Roberts, C.A., Workman, J. Jr., Reeves, J.B. III, editors. *Near-infrared spectroscopy in agriculture*. Madison, Wis.: American Society of Agronomy Inc.; Crop Science Society of America Inc.; and Soil Science Society of America Inc. Publishers.
- Lachenmeier, D. W. (2007). Rapid quality control of spirit drinks and beer using multivariate data analysis of Fourier transform infrared spectra. *Food Chemistry*, 101, 825–832.
- Lewis, M.J., Young, T.W. (2002). *Brewing* (second edition). Chapter 2. New York: Klumer Academic/Plenum Publishers.
- Martens, H. & Næs, T. (1989). *Multivariate calibration*. Chichester: Wiley.
- McLeod, G., Clelland, K., Tapp, H., Kemsley E.K., Wilson, R.H., Poulter, G., Coombs D., Hewitt, C.J. (2009). A comparison of variate pre-selection methods for use in partial least squares regression: A case study on NIR spectroscopy applied to monitoring beer fermentation. *Journal of Food Engineering*, 90, 300-307.
- Naes, T., Isaksson, T., Kowalski, B. (1990). Locally weighted regression and scatter correction for near-infrared reflectance data. *Analytical Chemistry*, 62(7), 664-673.
- Naes, T., Isaksson, T. (1992). Locally weighted regression in diffuse Near-infrared transmittance spectroscopy. *Applied Spectroscopy*, 46(1), 34-43.
- Naes T., Isaksson T., Fearn T., Davies T. (2002). *A User-friendly Guide to Multivariate Calibration and Classification*. Chichester: NIR Publications.
- Workman, J., Weyer, L. (2008). *Practical guide to interpretative Near-Infrared spectroscopy*. Chapter 6. Boca Raton: CRC Press.

# PAPER VII

## Assessment of the sugars and ethanol development in beer fermentation with FT-IR and multivariate curve resolution models

Silvia Grassi<sup>a</sup>, José Manuel Amigo<sup>b\*</sup>, Christian Bøge Lyndgaard<sup>b</sup>,  
Roberto Foschino<sup>a</sup>, Ernestina Casiraghi<sup>a</sup>

<sup>a</sup> *Department of Food, Environmental and Nutritional Sciences (DeFENS),  
Università degli Studi di Milano, via Celoria 2, 20133 Milano, Italy*

<sup>b</sup> *Department of Food, Quality and Technology, Faculty of Sciences, University of  
Copenhagen, Rolighedsvej 30, DK-1958 Frederiksberg C, Denmark*

**Submitted to: FOOD RESEARCH INTERNATIONAL**

**FOODRES-D-14-00269**

**Abstract:**

The progress of the fermentation process is a key point in defining the conformance of the final beer to its defined specification. In this work six beer fermentation trails were performed according to a factorial design with the two different *S. cerevisiae* strains (WLP005 and WLP570) and three different fermentation temperatures (19, 21 and 24°C), all replicated twice. Samples were collected directly from the supernatant every 22 h until day nine and analyzed through a Fourier-transform infrared attenuated total reflectance (FT-IR ATR) spectroscopy and a refractometer. Multivariate curve resolution – alternating least square (MCR-ALS) models were successfully developed to follow the fermentation progress (99.9% of explained variance, 0.63665% lack of fit, and standard deviation of the residuals lower than 0.0072). The spectral changes occurring during the fermentation of beer were described with six components correlated to the spectra of the main components of wort (maltose, maltotriose, fructose, sucrose, dextrans and ethanol) attributing the main changes governing the processes to maltose, maltotriose and ethanol evolutions.

**Highlights**

- MCR-ALS decomposed the overlapped FT-IR signal into single constituents of beer
- MCR models describe the fermentation progress of maltose conversion to ethanol
- The results show a suitable methodology for monitoring and understanding the kinetics of the whole process
- FT-IR fingerprint region revealed the evolution of sugars and ethanol

**Keywords:** Fermentable sugars; Ethanol; Beer fermentation; Modelling; MCR-ALS; FT-IR;

## Introduction

Beer fermentation is characterized by a large number of biochemical transformations leading to a final product highly different from the raw materials in the context of sugar, alcohol and aroma profile.

The main changes produced in beer fermentation are related to the activity of the yeast. In presence of oxygen, sugars and free amino nitrogen are consumed to obtain energy and lead to the production of ethanol, CO<sub>2</sub> and secondary metabolites contributing to the final flavors (Ingledew, 1999). The progress and the outcome of the fermentation relied mainly on wort composition and yeast physiological state, two composite variables. The wort composition depends on the malting and mashing processes. Both processes influence protein composition and the sugars content. Proteins are degraded into low-molecular weight nitrogenous compounds by proteases and peptidases; whereas sugars derivate from the breakdown of the starch from barley due to amylases activities (Kunze, 2004). Not all the starch present in the malt is attacked by wort amylases. Therefore, a non-fermentable sugar fraction (at least 20% of the total extract) is present and is mainly represented by dextrans. The main part of wort carbohydrates (75-78%) is represented by fermentable sugars: maltose, maltotriose, glucose, fructose and sucrose (Stewart, 2009). Due to the complexity of the raw materials, it is clear that the setup of the initial parameters for the beer fermentation is essential, but not enough for the process control. Measurements of changes in chemical composition, especially different sugars and ethanol, are thus needed to monitor the development of the whole process and to maintain the consistency of the final product under control in order to keep the process economics and to meet the expectations of the consumers.

A number of scientific organizations (e.g. American Society of Brewing Chemistry and European Brewery Convention) published their own series of reference brewing analytical methods. Few analytical measurements can be carried out directly in the fermenting tanks; they are mainly physical and physicochemical measurements (specific gravity, refractive index, turbidity and viscosity) and pH measure among the chemical ones. The official methods, defined by the Analysis Committee of the European Brewery Convention (Hagen & Schwarz, 2000), for the determination of fermentable sugars in wort are based on high performance liquid chromatography (HPLC) analysis; the ones for ethanol in beer are based on Gas Chromatography, pycnometry or enzymatic reaction. The application of traditional analytical techniques becomes problematic when following the progress of a whole fermentation; mainly because they require sampling from the tanks, sample preparation, specific instruments, highly qualified person and they are time consuming.

The application of the gravity sensing devices has been proposed and it could be implemented in small-scale productions for determination of extract and alcohol content approximation. The advantage is that is not necessary the sampling from the

fermenter, but this approach does not allow the differentiation between sugars and must be fitted in to each single fermenter (Boulton, 2006).

The implementation of Fourier-Transformed mid-infrared (FT-IR) probes has been proved to offer detailed information in real-time in several food processes (van de Voort, 1992), allowing the assurance of meeting the quality parameters to the defined specifications (Karoui et al., 2010). To what brewing monitoring concerns, FT-IR spectroscopy has been applied to simultaneous determination of compounds in brewing final product and for brand identity (Duarte et al., 2004; Llarío et al., 2006; Inon et al., 2006; Lachenmeier, 2007; Castrius et al., 2012; Engel et al., 2012).

Despite being a promising technique, FT-IR has drawbacks to be considered and handled as well. For instance, the spectral signals of the different sugars generally obtained in the fermentation of beer are characterized by the strong overlap of the bands due to the high similarity of their structure. Moreover, some sugars do not change during the fermentation, or evolve between them making the direct monitoring with FT-IR more difficult, since the changes related to the signal cannot be directly associated to any sugar. The beer being fermented also contains other compounds absorbing in IR region. Above all, the absorption of ethanol and water (Inon et al., 2006) are crucial and highly overlapped with the signal of the sugars. Therefore, if fast monitoring of sugar development and behavior wants to be performed in a fast, easy and non-destructive manner, a powerful data analysis methodology is definitively required in combination with FT-IR spectroscopy.

It is many years now that multivariate curve resolution (MCR) methods are demonstrating their usefulness in modeling and monitoring different biochemical systems that evolve with time by using different spectroscopic data (Amigo et al., 2006a; Amigo et al., 2006b; de Juan & Tauler, 2006; Rodríguez-Rodríguez et al., 2007; Garrido et al., 2008; Pindstrup et al., 2013). The ability of unravel the real physico-chemical behavior of the evolving species makes MCR a perfect method to obtain useful qualitative and quantitative information from the spectra collected during any process. MCR is especially useful in complex systems where the evolving species are highly overlapped or in presence of interferences that hamper the perfect elucidation of the analytes being transformed (Amigo et al., 2006a; Pindstrup et al., 2013).

The purpose of the current work is, therefore, to investigate the capability of MCR applied to FT-IR spectra to extract relevant information about beer fermentation dynamics in six different experimental conditions. This approach showed the possibility of following the changes in ethanol and different sugars, thanks to the ability of MCR to resolve the highly overlapped signal of the sugars. The results provide the brewing industry with a suitable methodology for monitoring and understanding the kinetics of the whole process, maximizing and standardizing the productivity of the batches.



## 2. Material and Methods

### 2.1. Materials

Standard commercial wort “Highland heavy Ale wort” was purchased (Munttons plc©, Suffolk, UK) and reconstituted according to instructions of the manufacturers in 2 L of heat treated water for each trial, agitated at 200 rpm for 2 h to saturated level. Two different *Saccharomyces cerevisiae* strains, one for British Ale (WLP005) and the other for Belgian Ale (WLP570) (WhiteLab Inc., San Diego, CA, USA), were separately inoculated into the wort, reaching approximately the concentration of  $7 \times 10^6$  CFU mL<sup>-1</sup>. The preparation of the inoculum was performed as follow: one fresh colony for each strain was aerobically propagated in 10 mL YEPD broth (Yeast Extract 10 g L<sup>-1</sup>, Peptone 20 g L<sup>-1</sup>, Dextrose 20 g L<sup>-1</sup>, pH 6.4) at 20°C for 24 h; afterwards, the suspension was transferred in 100 mL of fresh broth with a magnetic stirrer (200 rpm) for 24 h at 20°C, then transferred in 400 mL YEPD and incubated for 24 h at 20°C. The harvested cells were pitched in the wort and gently agitated to create a homogeneous distribution before sharing out about 300 mL into sterile glass bottles, one for each sampling point, closed with airlock caps. The cell concentration for each strain was determined using a calibration curve obtained by correlating plate counts on YEPD agar and optical density values measured at 620 nm.

Fermentable sugars (maltose, maltotriose, maltose, maltotriose, glucose, fructose and sucrose) and dextrin were purchased from Sigma-Aldrich Co. and diluted in distilled water to a final concentration of 50gL<sup>-1</sup>. Ethanol (Sigma-Aldrich Co.) solution at 5% (v/v) was also prepared as reference for ethanol.

### 2.2. Fermentation trials

The experiments were performed according to a factorial design with the two different *S. cerevisiae* strains (WLP005 and WLP570) and three different fermentation temperatures (19, 21 and 24°C), all replicated twice, giving a total amount of 6 different experiments for each beer type.

Samples were collected in triplicate right after pitching (0 hour, starting time) and then every 22 hours until the 9<sup>th</sup> day of fermentation directly from supernatant.

### 2.3. °Brix determination

Total sugar content was measured by a refractometer (Bellingham and Stanley RMF 340, Kent, UK).

### 2.4. FT-NIR spectroscopy

FT-NIR spectra of fermenting beer were collected in transmission mode, with a Bomen MB-series FT-IR spectrometer equipped with an ATR cell. The spectra were collected

in the range 6,000–600  $\text{cm}^{-1}$ , with a resolution of 8  $\text{cm}^{-1}$  and 16 scans for both background and samples. The same approach was followed for pure compounds spectra acquisitions.

### 2.5. Data processing

The whole wavenumber range (6,000-600  $\text{cm}^{-1}$ ) was reduced to the fingerprint region (1,200-950  $\text{cm}^{-1}$ ).

Standard Normal Variate (SNV) was performed in order to correct scattering effects. All models were developed by using the PLS\_Toolbox (Eigenvector Research Inc., Wenatchee, WA) working under MatLab v. 7.4 (The MathWorks, Natick, MA).

As mentioned before, MCR has been used for several years now. Therefore, a brief summary of the main theoretical background and specific features to the analysis performed will be exposed herein. More detailed information can be found elsewhere (Tauler, 1995; Rodriguez-Rodriguez et al., 2007).

The IR spectra collected for one fermentation process can be arranged in a data matrix  $\mathbf{D}$  ( $M \times N$ ) where  $M$  is the number of spectra recorded for each time and  $N$  is the number of wavelengths for each spectrum. The aim of MCR is then to decompose  $\mathbf{D}$  into the product of two sub-matrices (Eq. 1):

$$\mathbf{D} = \mathbf{C}\mathbf{S}^T + \mathbf{E} \quad (\text{Eq. 1})$$

The main feature of MCR is that  $\mathbf{C}$  ( $M \times P$ ) and  $\mathbf{S}^T$  ( $P \times N$ ) matrices correspond to the concentration evolution and the spectral profiles, respectively, of the  $P$  pure components that are evolving in the fermentation process  $\mathbf{D}$ ; being  $\mathbf{E}$  ( $M \times N$ ) the residuals of the model (see Figure 1).

## a) Graphical representation of MCR model

$$\boxed{\mathbf{D}_1} = \boxed{c_1} \boxed{\mathbf{S}} + \boxed{\mathbf{E}_1}$$

## b) Graphical representation of column-wise MCR model

$$\begin{array}{c} \boxed{\mathbf{D}_1} \\ \boxed{\mathbf{D}_2} \\ \boxed{\mathbf{D}_3} \\ \boxed{\mathbf{D}_4} \\ \vdots \\ \boxed{\mathbf{D}_{\text{exp}}} \end{array} = \begin{array}{c} \boxed{c_1} \\ \boxed{c_2} \\ \boxed{c_3} \\ \boxed{c_4} \\ \vdots \\ \boxed{c_{\text{exp}}} \end{array} \boxed{\mathbf{S}} + \begin{array}{c} \boxed{\mathbf{E}_1} \\ \boxed{\mathbf{E}_2} \\ \boxed{\mathbf{E}_3} \\ \boxed{\mathbf{E}_4} \\ \vdots \\ \boxed{\mathbf{E}_{\text{exp}}} \end{array}$$

**Figure 1. a)** Graphical representation of MCR decomposition of a FT-NIR spectra dataset ( $\mathbf{D}_1$ ) to obtain the pure concentration ( $\mathbf{C}_1$ ) and spectral profiles ( $\mathbf{S}^T$ ).  $\mathbf{E}$  denotes the residual matrix. **b)**

Column-wise augmentation strategy of the experiments [ $\mathbf{D}_1; \mathbf{D}_2; \dots; \mathbf{D}_i$ ] to obtain individual concentration profiles [ $\mathbf{C}_1; \mathbf{C}_2; \dots; \mathbf{C}_i$ ] and a common spectral profile matrix ( $\mathbf{S}^T$ ). The residual matrices are denoted as [ $\mathbf{E}_1; \mathbf{E}_2; \dots; \mathbf{E}_{\text{exp}}$ ].

This decomposition can be done by using alternating least squares (ALS) algorithm. ALS decomposes  $\mathbf{D}$  by performing the following four steps in an iterative manner (Rodriguez-Rodriguez et al., 2007):

1. Generation of initial estimates of either  $\mathbf{C}$  or  $\mathbf{S}^T$ . In our case, the initial estimations used were the pure spectra of the sugars and ethanol (more detail below).
2. Given  $\mathbf{D}$  and  $\mathbf{S}^T$ , least-squares calculation of  $\mathbf{C}$  under the suitable constraints.

3. Given  $\mathbf{D}$  and the new calculated  $\mathbf{C}$ , least-squares calculation of  $\mathbf{S}^T$  under the suitable constraints.

4. Calculation of  $\hat{\mathbf{D}}$  as the product of the new calculated  $\mathbf{C}\mathbf{S}^T$ . If the convergence criterion is fulfilled (that is, the difference between the residuals in consecutive iterations is below a certain threshold) the process is finished. Otherwise, go back to step 2 by using the  $\mathbf{S}^T$  calculated in step 3.

MCR-ALS works under two important assumptions. The first one is that the exact number of compounds evolving in the fermentation (i.e. the chemical rank) must be perfectly known. For this purpose, methods like principal component analysis (PCA) or evolving factor analysis (EFA) (Keller & Massart, 1992) might be used, together with the previous knowledge of the chemical composition of the fermentation. The second important assumption is that the spectra collected with time follow a linear model analogous to the Lambert Beer's Law.

As said before, the main advantages of MCR-ALS is the ability of recovering analytical responses (concentration and pure spectral profiles) which are chemically interpretable without the assumption of any previous empirical model. Nevertheless, the mathematical resolution of the product of two unknown variables ( $\mathbf{C}$  and  $\mathbf{S}^T$ ) has not a unique solution. This is translated into plausible ambiguities in the final solution (Tauler, 1995). Nevertheless, these ambiguities can be minimized by using two strategies.

The first strategy is to apply several constraints in the iteration of the algorithm. The most common constraints are non-negativity (the concentration and/or spectral profiles can be constrained to have only positive values), unimodality (the shape of the profiles only have one maximum), closure (the total concentration of the components is constant throughout the fermentation), or selectivity (applied if a pure spectrum of one compound is known or in a certain area of the experiment where it known that the change in the signal is due only to one specific component).

The second strategy for minimizing ambiguities and also handle rank deficiency problems is that MCR-ALS can be applied to an individual experiment or to a series of experiments simultaneously (Figure 1b). This is what is called matrix augmentation, being possible to augment a matrix in a column-wise (same spectral information, different fermentation trials), row-wise (same fermentation measured with different spectroscopic techniques), or column-row-wise (different fermentation processes measured with different spectroscopic techniques). In our case, the column-wise augmentation manner was performed, since different fermentation trials were measured with the same spectroscopic technique. Equation 2 shows the performance of MCR-ALS in a column-wise augmented matrix:

$$\begin{bmatrix} D_1 \\ D_2 \\ \dots \\ D_{ex} \end{bmatrix} = \begin{bmatrix} C_1 \\ C_2 \\ \dots \\ C_{ex} \end{bmatrix} S^T \quad (\text{Eq. 2})$$

where **D** and **C** are column-wise augmented data matrices that contain the sub-matrices of the individual experiments and the individual concentration profiles, respectively, one on top of each other; **S<sup>T</sup>** is a single data matrix containing the pure spectra of the chemical species, common and valid for all experiments. The main advantage of this configuration is that specific spectral information that can be hidden in one fermentation process can be taken into account by another fermentation process with different experimental conditions.

The ALS optimization stops when the difference between the differences between the residuals of consecutive iterations (a.k.a. percentage of lack of fit %LOF) is below a certain threshold. %LOF is defined as in equation 3:

$$\%LOF = 100 \times \sqrt{\frac{\sum_m^M \sum_n^N e_{mn}^2}{\sum_m^M \sum_n^N d_{mn}^2}} \quad (\text{Eq. 3})$$

where *e* is each *m*n<sup>th</sup> element of the residual matrix **E**, and *d* is each *m*n<sup>th</sup> element of the **D** matrix. The threshold value of LOF should be selected according to the noise in the spectra. A very used criterion is to stop the iterations when the difference between two consecutive LOF values is below 0.1% (Jaumot et al., 2005).

### 3. Results and discussion

#### 3.1 Total Solid Content determination

Figure 2a and 2b shows the Total solid content changes (expressed in °Brix ) for all the trials performed. The °Brix at starting time were the same for all the trials (9.37±0.07 °Bx) corresponding to a sugar content of approx. 97.50g/L and confirming the reproducibility of the wort reconstitution protocol. The total sugar content showed a fast decrease in all the trials performed within three days of fermentation.

The sugars consumption was faster when WLP005 strain was used, reaching 6.55±0.05 °Bx after 46 h at 24°C (Figure 2a) and remaining constant after 142 h of fermentation, due to the characteristic high flocculation of the yeast cells and the consequent low sugar consumption. The main difference was observed when wort inoculated with WLP005 was incubated at 19°C; in this case, the sugar content decreased with a lower speed but reaching at the fermentation end-point the same level of the other trials

performed ( $5.19 \pm 0.04$  °Bx). The sugar depletion in the fermentations conducted with WLP570 strain showed a lower and more constant slope than those inoculated with WLP005 (Figure 2b). This is probably due to the ability of WLP570 yeast cells to remain in suspension in the wort during the fermentation time.

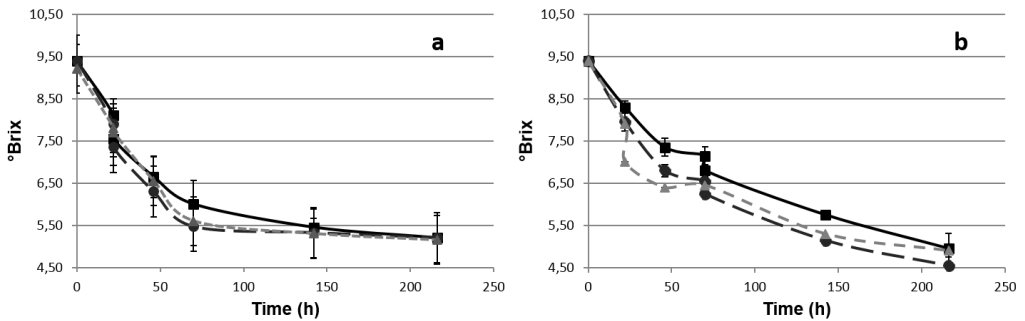


**Figure 2.** °Brix profiles for the yeast tested (WLP005 strain (a), and WLP570 (b)) at three different temperatures: squares for trials performed at 19°C, circles for the one at 21°C and triangles for the one at 24°C.

#### 4.2. Raw FT-IR data observation

The FT-IR spectra recorded during the fermentation trials showed a clear trend: the absorbance increased with the fermentation time, due to a baseline drift due to the yeast present in the sampled beer. Fig. 3a shows an example of the spectra recorded during one fermentation process conducted at 21°C with WLP005. Herein, the spectra are colored according to the fermentation time: black at the beginning to light dotted gray at 216 h.

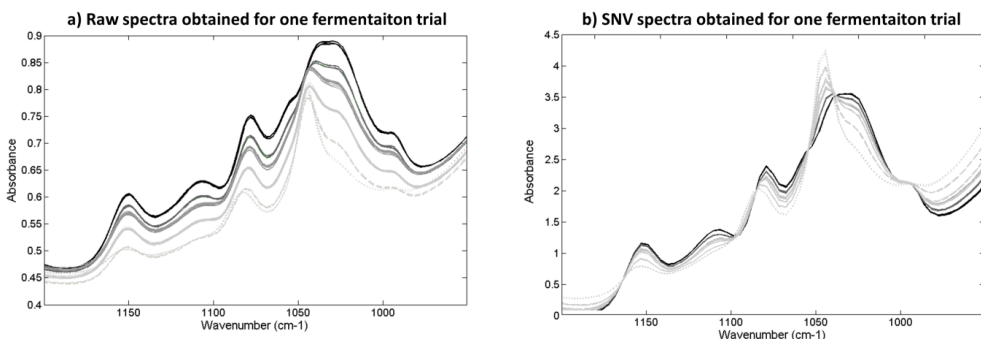


**Figure 3.** Spectra collected during a fermentation trial conducted at 21°C with WLP005 strain, cut in the fingerprint area ( $1,200\text{--}950\text{ cm}^{-1}$ ). a) Raw spectra colored according to fermentation time in gray scale; b) spectra after SNV pre-treatment colored in gray scale according to the fermentation time.

To minimize this effect the spectra were pre-treated using Standard Normal Variate (SNV) algorithm (Fig. 3b). After applying SNV to the raw spectra, the main peaks characterizing the spectra are clearer and it is possible to distinguish a clear change in the profile during time. Spectra collected at the beginning of the fermentation are characterized by typical maltose peaks: 1,151, 1,111, and 1,078  $\text{cm}^{-1}$  (Duarte, 2004). This is justified as maltose is the main sugar present in wort: 50-60% of the fermentable sugars (Stewart, 2009). Moreover, all the sugars present in beer are characterized by similar absorption bands in the finger print region and is almost impossible to distinguish by visual observation the contribution of each of them. For instance, the broad peak around 1,040-1,020  $\text{cm}^{-1}$  is probably due to the overlapping of a maltotriose-maltose band (1,041  $\text{cm}^{-1}$ ) with the dextrin band (1,024  $\text{cm}^{-1}$ ). Also the small shoulder visible at 1,055  $\text{cm}^{-1}$  could be due to presence of fructose, which as a characteristic peak at 1,060  $\text{cm}^{-1}$  (Schndler et al., 1999).

With the evolution of the fermentation, the absorption at those peaks decreases. In particular, the peak at 1,111  $\text{cm}^{-1}$  almost disappears; the peak at 1,078  $\text{cm}^{-1}$  shifts to 1,085  $\text{cm}^{-1}$ ; the blunt peak at 1,041  $\text{cm}^{-1}$  changes shape and decreases whereas a peak at 1,045  $\text{cm}^{-1}$  grows. The peaks rising at 1,085, 1,045  $\text{cm}^{-1}$  and clearly defined at the end of the fermentation trials are related to ethanol absorption (Duarte, 2004).

#### 4.3. MCR-ALS results

With the obtained spectral evolutions in the fermentation processes, it is not possible to find out how the different wort fermentable sugars contribute individually to the changes in the signal, as their signals are highly overlapped. Moreover, there are compounds present in the beer not evolving with time, i.e. dextrans, which anyway contributes to the recorded spectral signal. To face these problems MCR-ALS was applied to the reduced and pre-treated FT-IR dataset, taking into account the variability of the production factors affecting the fermentation progress, i.e. different yeast and temperatures. As the dataset was composed of 12 experiments, MCR-ALS models were built in series with the same constraints, but considering them as individual experiments (Amigo et al. 2006a; Amigo et al. 2006b). The **D** data matrix of the fermentation trials was augmented with the spectra recorded for the pure components.

The initial estimates for starting the MCR-ALS analysis were defined by choosing the spectra of pure dextrans and ethanol among the pure compounds spectra recorded.

MCR-ALS was applied to the different **D** spectral matrix under the same constraints to all the column-wise sub-matrices: non-negativity to concentration profiles. It was necessary to fix dextrin and ethanol as initial guesses due to the high spectral overlapping. The convergence criterion was set at 0.1.

The results obtained for the spectral and the concentration profiles obtained can be seen in Figure 4 and Figure 6, respectively. MCR-ALS models obtained described

successfully the experimental FT-IR spectra recorded. The model explained 99.87% of the total variance and standard deviation of the residuals lower than 0.0230; and a %LOF of 3.5%.

In Figure 4 the obtained spectral profiles are compared with the pure spectra for all the compounds. Here, it is possible to see a high similarity between the six spectral profiles obtained by MCR-ALS analysis and the pure components spectra.

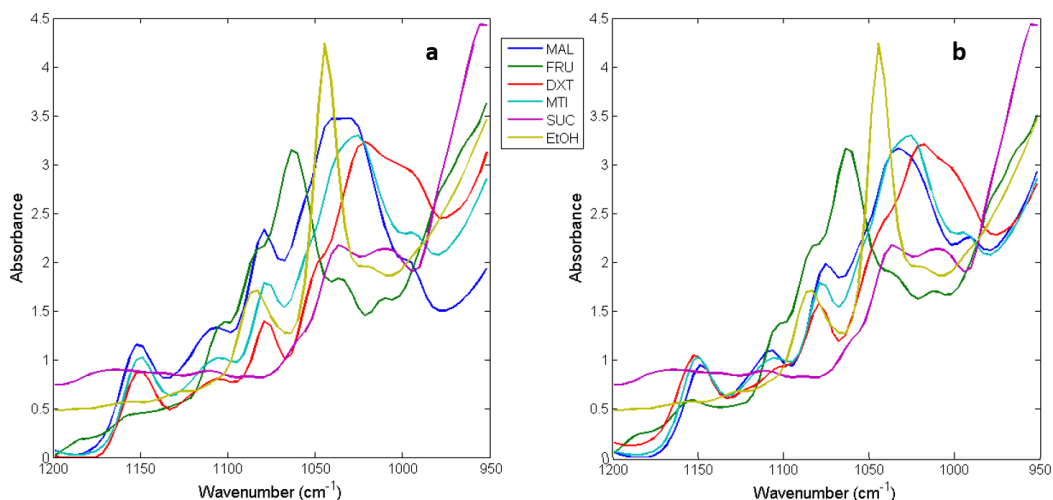


**Figure 4.** Comparison of the MCR-ALS spectral profiles (a) and the pure spectra components (b) measured for each compound expected in wort and final beer. Blue profile corresponds to maltose (MAL), green to fructose (FRU), red to dextrins (DXT), cyan to maltotriose (MTI), purple to sucrose (SUC) and yellow to ethanol (EtOH).

The first profile obtained (Fig. 4a in blue) has two peaks at 1,150 and 1,110  $\text{cm}^{-1}$  which perfectly match with the ones belonging to maltose; the other peaks of the first profile shift a little from the pure ones and are at 1,070, 1,040 - 1,020  $\text{cm}^{-1}$  and a small peak (995  $\text{cm}^{-1}$ ) in the shoulder of the previous one. The second profile (green) matches with the pure spectra of fructose: it has a main peak at 1,060  $\text{cm}^{-1}$  with in its shoulder small peaks at 1,105, 1,085 and 1,035  $\text{cm}^{-1}$ . The other profiles (red and cyan) are similar to pure spectra obtained from dextrins and maltotriose pure compounds, respectively. The cyan profile, attributed to maltotriose absorption, has the same peaks as the maltose; this is expected as maltotriose is a trisaccharide containing three glucoses and maltose is a disaccharide (glucose-glucose). The profile obtained for dextrins differs from the maltose profile just for a broad peak at 1,050-980  $\text{cm}^{-1}$ . The purple profile matches with the pure sucrose profile as a broad band at 1,040-1,000  $\text{cm}^{-1}$  characterizes it. The yellow profile corresponds to the ethanol spectra as it has two main peaks at 1,085, 1,045  $\text{cm}^{-1}$ .



In order to verify the goodness of the obtained profiles a cross-correlation between them and the pure components was estimated and the results are reported in Figure 5. The results reported in Figure 5 confirm what have been discussed previously by preliminary comparison of the peaks of the MCR-ALS profiles and the pure components. Complete correspondence ( $R=1$ ) was observed for the profiles associated with ethanol, sucrose and maltotriose, and for dextrins and fructose ( $R>0.99$ ). The correspondence between the profile associated with maltose and the pure spectra was also high,  $R$  of 0.91, and its lower value is mainly due to the small shift of the peak at  $1,040 - 1,020 \text{ cm}^{-1}$ . The only case of missed-correspondence is observable for the attribution of maltose and maltotriose. In that case the cross-correlations failed to assign the MCR-ALS profile to the two pure sugars because the correlation coefficients found between MCR-ALS profile attributed to maltose has high  $R$  value also with the spectra obtained for the pure maltotriose. The reason is related to the chemical composition of the two sugars, which are both composed only by glucose monosaccharaides. Is remarkable the fact that all the other cross-correlation coefficients were below 0.75.

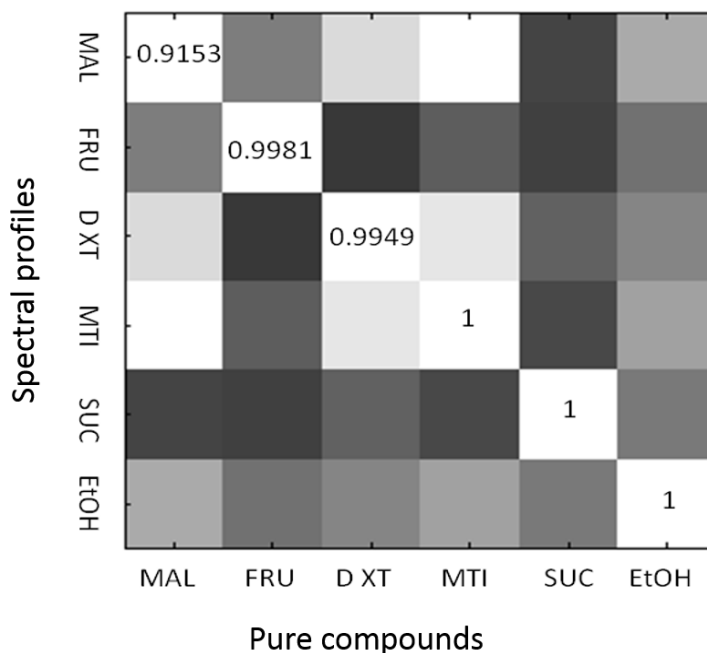


**Figure 5.** Visual representation of the cross-correlation coefficients calculated between the MCR-ALS profiles and the pure components spectra. The representation in grey scale represents the values of  $R$ : dark grey cells stands for low correlations up to white cells were  $R$  values are higher than 0.90.

The other main information obtained with MCR-ALS analysis concerns the evolution of each single spectral profile during the fermentation processes. Figure 6 reports the concentration profiles against time for each experimental condition, for each combination yeast-temperature, both technological replicates are reported with the same color and different marker (circle or star).

The concentration profiles resolved by MCR-ALS method are not true concentration but rather profile changes in their concentrations. As the idea is to evaluate the changes occurring in the fermenting wort, the concentrations are expressed as relative changes. The concentration profiles related with the content of dextrans, fructose and sucrose appear to be zero. The meaning of that is arguable with the fact that the concentration of fructose and sucrose in the wort are generally 1-2% of the total sugar content in wort and the relative change is too small to be seen in a so complex matrix (Stewart, 2009). For what concern dextrans, as they are not fermentable saccharides no change in their concentration is expected during fermentation time. The main remarkable evolutions are the ones of maltose (blue in Figure 6) and ethanol (yellow in Figure 6). The starting points of the profile associated with maltose were similar for all the trials with the exception of one replicate of the experiment conducted with WLP 570 at 19°C (Figure 6, bottom left). In that case, the high similarity of the maltose and maltotriose profiles seems to affect the results obtained. Indeed, the initial relative concentration of maltotriose is higher than the levels observed in the other trials to the detriment of the maltose concentration at time 0.

As general trend is possible to see how the higher consumption of maltose occurred in the first 70 hours (Figure 6).

This situation is particularly characteristic for the trial conducted with WLP005: at 19 and 21°C the relative concentration of maltose (blue profile) decreases of the 37% in the first 70 hours, whereas the total maltose consumption estimated from the model after 216 hours of fermentation is around 47%. In the trials conducted with WLP 050 at 24°C the maltose consumption was estimated to be faster in the first hours if compare with the lower temperatures trials, but after 70 hours the content remained constant. These results are in accordance with the °Brix values obtained at the end of the fermentations conducted with WLP005. Indeed the °Brix value at the end of the fermentation register a total sugars consumption up to 46% (Figure 2), no matter the incubation temperature tested.

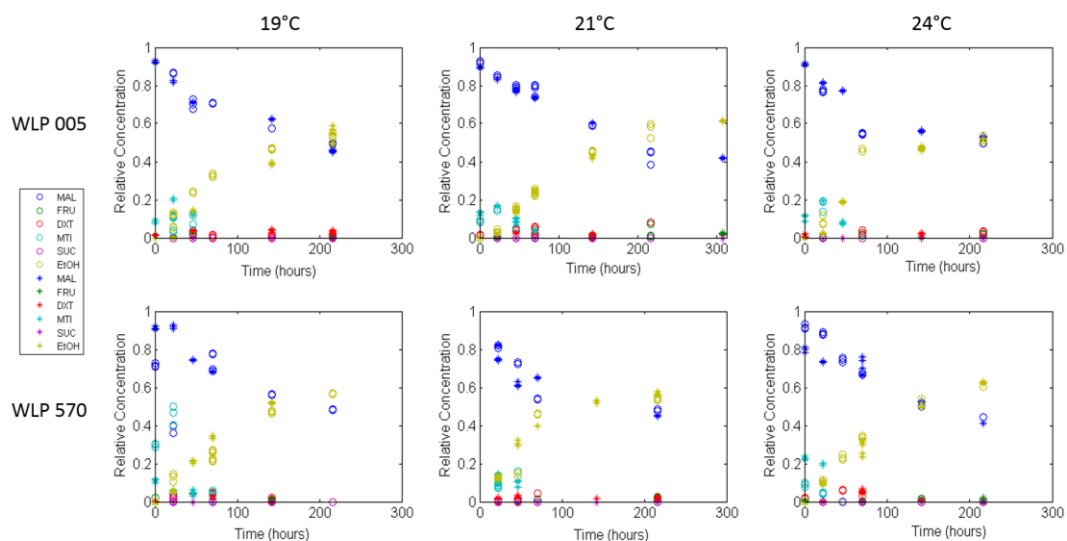


**Figure 6.** Concentration profiles obtained by MSC-ALS analysis. The results are expressed as relative concentrations against time (h). For each strain tested (WLP 005 and WLP 570) and each temperature (19, 21 and 24°C) the technological replicates are reported in the same subplot with different marker (circle or star). Blue profile corresponds to maltose (MAL), green to fructose (FRU), red to dextrins (DXT), cyan to maltotriose (MTI), purple to sucrose (SUC) and yellow to ethanol (EtOH).

Regarding WLP570 trials (Figure 6 bottom), the maltose profiles describe a slower but more constant consumption of the sugar by the yeast, which is characterised by low flocculation capability. The MCR-ALS models find at the end of the trials a reduction of the initial maltose up to the 53%.

The other major compound involved in the fermentation is the ethanol. The profile associated with ethanol (yellow profile) started in all trials with a value of zero, which is reasonable, as it is not expected to have ethanol in wort before the fermentation starts. After 216 hours of fermentation, the relative concentration rises over 0.6 in the trial conducted with WLP570 at 24°C.

Small changes can be notice in the cyan profile, which was associated with maltotriose. Mainly the initial relative concentration is 0.1-0.2 and the depletion of the trisaccharide occurs in the first 70 hours as has been previously reported by other authors (Stewart, 2009).

## 5. Conclusions

This research work showed the potential effectiveness of FT-IR spectroscopy, joint with MCR-ALS, for beer fermentation monitoring and fully understanding of the evolution of sugars during the fermentation.

The FT-IR fingerprint region ( $1,200\text{-}950\text{ cm}^{-1}$ ) revealed the main changes occurring throughout the fermentation at expense of wort sugars and leading to ethanol rising. With MCR-ALS was possible to decompose the influence of each single constituent involved in the biotransformation. The proposed MCR-ALS model was applied to fermentation runs conducted under different conditions (yeast inoculated and temperature) and the results were found to well describe the bioprocess no matter the environmental condition.

The six spectral profiles obtained were validated by comparison with the spectra recorded for the pure compounds (i.e. maltose, maltotriose, fructose, sucrose, dextrans and ethanol), obtaining high cross-correlation coefficients. The concentration profiles resolved by MCR-ALS method expressed relative changes of each of the six components. The main evolutions were related to maltose and maltotriose depletion and ethanol production by the yeast activity.

This approach will give much richer information about the ongoing of the process than the one obtained by only measuring total sugar content by refractometer. As shown in this work, the combined use of FT-IR spectroscopy and MCR-ALS technique facilitates the study of a complex beverage bioprocesses, as it is the beer brewing.

## Acknowledgements

The authors thank Michael Crafock, University of Copenhagen, Department of Food Science - Food Microbiology for providing the yeast strains used and the material for the performance of the microbiological analysis.

## 6. References

- Amigo, J. M., de Juan, A., Coello, J., MasPOCH, S. (2006a). A mixed hard- and soft-modelling approach for the quantitative determination of oxipurines and uric acid in human urine. *Analytica Chimica Acta*, 567(2), 236-244.
- Amigo, J.M., de Juan, A., Coello, J., MasPOCH, S. (2006b). A mixed hard- and soft-modelling approach to study and monitor enzymatic systems in biological fluids. *Analytica Chimica Acta*, 567(2), 245-254.
- Boulton, C., Quain, D. (2006). *Brewing Yeast and Fermentation*. Oxford: Blackwell Science, (Chapter 6).
- Castritius, S., Geier, M., Jochims, G., Stahl, U., Harms, D. (2012). Rapid Determination of the Attenuation Limit of Beer Using Middle-Infrared (MIR) Spectroscopy and a Multivariate Model. *Journal of agricultural and food chemistry* 60(25), 6341 -6348.

- de Juan, A., Tauler, R. (2006). Multivariate Curve Resolution (MCR) from 2000: Progress in concepts and applications. *Critical Review in Analytical Chemistry*, 36(3-4), 163-176.
- Duarte, I.F., Barros, A., Almeida, C., Spraul, M., Gil, A.M. (2004). Multivariate analysis of NMR and FTIR data as a potential tool for the quality control of beer. *Journal of Agricultural and Food Chemistry*, 52, 1031-1038.
- Engel, J., Blanchet, L., Buydens, L.M.C., Downey, G. (2012). Confirmation of brand identity of a Trappist beer by mid-infrared spectroscopy coupled with multivariate data analysis. *Talanta*, 99, 426-432.
- Garrido, M., Rius, F. X., Larrechi, M. S. (2008). Multivariate curve resolution-alternating least squares (MCR-ALS) applied to spectroscopic data from monitoring chemical reactions processes. *Analytical and Bioanalytical Chemistry*, 390(8), 2059-2066.
- Hagen, W., Schwarz, H. (2000). Analytica-EBC – Precision values of wort analysis. *Journal of the Institute of Brewing*, 106 (3), 139-146.
- Ingledeu, W. M. (1999). Alcohol production by *Saccharomyces cerevisiae*: a yeast primer. *The alcohol textbook*, 3, 49-87.
- Inon, F. A., Garrigues, S., de la Guardia, M. (2006). Combination of mid and near-infrared spectroscopy for the determination of the quality properties of beers. *Analytica Chimica Acta*, 571, 167-174.
- Jaumot, J., Gargallo, R., de Juan, A., Tauler, R. (2005). A graphical user-friendly interface for MCR-ALS: a new tool for multivariate curve resolution in MATLAB. *Chemometrics and Intelligent Laboratory Systems*, 76(1),101-110.
- Karoui, R., Downey, G., Blecker, C. (2010). Mid-Infrared Spectroscopy Coupled with Chemometrics: A Tool for the Analysis of Intact Food Systems and the Exploration of Their Molecular Structure– Quality Relationships– A Review. *Chemical reviews*, 110(10), 6144-6168.
- Keller, H.R., Massart, D.L. (1992). Evolving factor analysis. *Chemometrics and Intelligent Laboratory Systems*, 12, 209-224.
- Kunze, W. (2004). *Technology Brewing and Malting*. VLB, Berlin, pp. 32-49.
- Lachenmeier, D. W. (2007). Rapid quality control of spirit drinks and beer using multivariate data analysis of Fourier transform infrared spectra. *Food Chemistry*, 101, 825-832.

- Llario, R., Inon, F. A., Garrigues, S., de la Guardia, M. (2006). Determination of quality parameters of beers by the use of attenuated total reflectance FT-MIR. *Talanta*, 69, 469–480.
- Pindstrup, H., Fernández, C., Amigo, J. M., Skibsted, L. H. (2013). Multivariate curve resolution of spectral data for the pH-dependent reduction of ferrylmyoglobin by cysteine. *Chemometrics and Intelligent Laboratory Systems*, 122, 78-83.
- Rodríguez-Rodríguez, C., Amigo, J. M., Coello, J. & Maspoch, S. (2007). An introduction to multivariate curve resolution-alternating least squares: Spectrophotometric study of the acid–base equilibria of 8-hydroxyquinoline-5-sulfonic acid. *Journal of Chemical Education*, 84(7), 1190-1195.
- Schindeler, R., Lendi, B. (1999). Simultaneous determination of enzyme activities by FTIR-spectroscopy in an one-step assay. *Analytica chimica Acta*, 391, 19-28.
- Stewart, G.G. (2009). The horace brown medal lecture: forty years of brewing research. *Journal of the Institute of Brewing*, 115 (1), 3-29
- Tauler, R. (1995). Multivariate curve resolution applied to second order data. *Chemometrics and Intelligent Laboratory Systems*, 30, 133-146.
- van de Voort, F.R. (1992). Fourier transform infrared spectroscopy applied to food analysis. *Food Research International*, 25 (5), 397-403.

## Near Infrared Spectroscopy to monitor sourdough fermentation

### 4.4.1 State-of-the-art

Sourdough technology is widespread in Europe. It is traditionally used for a variety of baked products, such as rye and wheat bread, crackers, brioches, Italian panettone and similar cakes (De Vuyst & Neysens, 2005).

The Panettone is one of the most well-known leavened product in Italy and also in the European market. It is characterized by a light texture with irregular elongated alveoli and the typical aroma conferred by the micorbiota. The production process is long and complex, and is characterized by three kneading followed by as many risings.

In particular, the first fermentation of the dough (first dough), produced by mixing sourdough, flour, sugar, butter and water, is the most important phase of the interior process. To avoid non-compliance, it is therefore important to have a rapid method of monitoring of the fermentation, which allows a timely corrective action when necessary.

A specific need of baking industry is the controlled management of the process in order to obtain an optimization of production (Li Vigni & Cocchi, 2013). Nowadays leavening process is monitored by physico-chemical parameters like pH and temperature, and by personal valuation of the operator that “taste” the dough structure on the basis of subjective criteria. The traditional methods performed for sourdough analyses are metabolites dosage through HPLC (Lefebvre et al., 2002), rheological profiles (Clarke et al., 2004) and microorganisms count (Picozzi et al., 2005). The performance of these analysis could improve knowledge and control of the fermentative process, but they need long timing (samples preparation, analysis execution and data elaboration) and are very expensive, so that their application is not practicable and they are not useful for corrective actions on the process.

So there is a need to have available analytical methods that are rapid, inexpensive, and reliable and integrated within the production process. The near-infrared spectroscopy, supported by chemometric techniques, is proving to be a valuable tool, as it allows you to get in a few minutes, and at the same time a lot of information on the progress of fermentation processes. In last years few stadies have been performed concerning near-infrared spectrospy use for dough monitoring (Ait Kaddour et al., 2008; Sinelli et al., 2008; Li Vigni & Cocchi, 2013). All the mentions studies are about dough fermented

with the unique usage of beer yeast; however there are no investigation about sourdough fermentation.

The purpose of this work was to experimentally verify the potential of NIR spectroscopy for monitoring in -line of the changes that occur during the fermentation of the first mixture for the production of panettone.

#### 4.4.2 Materials and methods

2 Kg of first dough were sampled from a large-scale production and incubated in a thermostat at constant temperature (26°C). Five technological replicates were performed from six different productions. The preparation of the sourdough was performed according the production protocol and they main ingredients were: sourdough, drawn butter, sugar and different kind of flour.

##### *Chemical analyses*

Every 45 minutes a sample of about 50 g was withdrawn from the sourdough in fermentation to be analysed for the pH and titratable acidity.

##### *pH*

About 10g of sample were weighed (Scale "ALC-3100.2," Acculab), carried to 100g with distilled water in a stomacher bag and homogenized for 5 minutes ("Stomacher 400", Colworth). The pH was measured with a pH meter "3510 Meter" (Jenaway) previously calibrated, with the sample maintained under stirring with stirrer "MR Hei-Standard" (Heidolph).

##### *Titratable acidity*

The same sample homogenized was titrated with 0.1 N sodium hydroxide (Sigma-Aldrich, USA) until reaching pH 8.4 (IDF method 50:1991). The titratable acidity was expressed in Sauer grade (° S) that correspond to the milliliters of 0.1 N NaOH used for titration. The acidity in ° S is expressed by the formula (Equation 1):

$$\text{Acidity} = (A * N * 100) / P \text{ (Eq. 1)}$$

where A are hte mL of 0.1 N NaOH used for titration, N the normality of the NaOH solution and P the weight in grams of the product.



### ***FT-NIR spectroscopy***

NIR spectral data were collected using a Fourier transform (FT)-NIR spectrometer (MPA, Bruker Optics, Milano) equipped with an optic probe directly inserted in the sourdough. The data were collected over the 12,500 – 3,800 cm<sup>-1</sup> range (resolution, 16 cm<sup>-1</sup>; background, 128 scans; sample, 128 scans)

The NIR spectra were acquired starting from 1 h after the mixing up to 7 h 30 min of fermentation every 15 min.

### ***NIR data processing***

NIR spectral datasets were analysed using Matlab version R2007a, The MathWorks, Inc, Cambridge, UK. Before performing the PCA analysis, spectra were transformed (Savitzky – Golay first derivative, 11 data points) and mean centred.

The spectral data were also correlated with the chemical results through the PLS regression method (PLS Toolbox, Eigenvector Research, Inc., Wenatchee, WA). Before performing the regression different pre-treatments and a variable selection method were tested (Interval PLS) in order to improve the models obtained.

### **4.4.3 Preliminary results**

In this section are presented only preliminary results, since the experimental part has been finished during the PhD research period but the complexity of the matrix under study requires more detailed investigation in order to extract all the main information to fully describe the sourdough leaving process.

### ***Chemical analysis***

The initial pH values are in agreement with the values obtained with this type of dough by other authors (4.70 to 5.40) (Collar et al., 1994). All the results of the determinations of pH, titratable acidity and temperature detection for the six trial are reported in Table 1. The trials have shown trends of pH during the leavening similar, with a starting pH between 5.30 and 5.39 and a final value between 5.23 and 4.91. Two exceptions were observed for trial Y and Z, in this case the final pH decrease up to 4.38. These values indicate acidification is not very high but still within the acceptable range and the company also found in other studies of similar mixtures (Lefebvre et al., 2002).

#### 4.4 Overview of dough fermentation for Panettone production

**Table 1.** Average values of pH and titratable acidity (TTA, °S) for the six trials performed. Also the temperature values are reported as an average of every hour.

Trial	Time(h)	pH		TTA (°S)		Temperature (°C)
		average	S.D.	average	S.D.	average
<b>A</b>	1	5,34	0,04	2,5	0,2	26,8
	2	5,28	0,05	2,8	0,3	26,8
	3	5,22	0,10	3,0	0,1	26,8
	4	5,24	0,01	2,9	0,1	27,0
	5	5,18	0,02	2,8	0,1	27,2
	6	5,09	0,08	2,9	0,1	27,2
	7	4,98	0,02	3,3	0,1	27,0
	7,5	<b>4,97</b>	0,02	3,4	0,0	26,8
<b>B</b>	1	5,30	0,03	2,8	0,0	26,3
	2	5,16	0,06	2,8	0,0	26,3
	3	5,21	0,02	2,9	0,2	26,5
	4	5,17	0,02	2,9	0,1	26,7
	5	5,09	0,01	3,0	0,1	26,5
	6	5,03	0,00	3,3	0,1	26,5
	7	4,99	0,04	3,6	0,1	26,5
	7,5	<b>4,96</b>	0,10	3,9	0,4	26,7
<b>C</b>	1	5,39	0,02	2,6	0,1	25,7
	2	5,42	0,00	2,5	0,1	26,2
	3	5,29	0,08	3,0	0,3	26,5
	4	5,36	0,01	2,8	0,1	26,7
	5	5,30	0,03	2,7	0,2	26,8
	6	5,30	0,00	2,9	0,1	27,2
	7	5,26	0,08	3,2	0,1	27,2
	7,5	<b>5,23</b>	0,14	3,2	0,4	27,2
<b>X</b>	1	5,39	0,00	2,8	0,1	26,5
	2	5,39	0,13	3,1	0,2	26
	3	5,32	0,06	3,4	0,1	26
	4	5,22	0,02	3,2	0,3	26
	5	5,21	0,02	3,2	0,1	26
	6	5,00	0,03	3,5	0,0	26
	7	5,04	0,00	3,8	0,1	26

#### 4.4 Overview of dough fermentation for Panettone production

Trial	Time(h)	pH		TTA (°S)		Temperature (°C)
		average	S.D.	average	S.D.	average
	7,5	<b>4,91</b>	0,03	3,8	0,1	26
Y	1	5,31	0,04	2,5	0,1	26,5
	2	5,24	0,09	2,8	0,1	26
	3	5,14	0,01	3,3	0,0	26
	4	4,99	0,02	3,5	0,0	26
	5	4,93	0,02	3,7	0,1	26,5
	6	4,91	0,06	3,8	0,1	26,5
	7	4,84	0,00	4,3	0,2	26
	7,5	<b>4,63</b>	0,03	4,5	0,1	26
Z	1	5,39	0,06	2,9	0,0	26
	2	5,15	0,01	3,3	0,2	26
	3	5,03	nd	3,1	nd	26,5
	4	5,02	0,04	3,7	0,2	26
	5	4,86	0,00	4,0	0,5	27
	6	4,83	0,04	3,6	nd	27
	7	4,64	0,05	4,5	0,5	26,5
	7,5	<b>4,38</b>	0,06	4,8	0,2	25

The results obtained from titrable acidity analysis revealed the same trends. All the trials were characterised by a similar starting point (2.5-2.8°S), the final values were similar (3.2-3.9°S), with exception of trials Y and X, in which the acidification reached 4.8 °S.

#### ***FT-NIR spectroscopy***

The FT-NIR spectra were acquired continuously every 15 minutes after one hour from the mixing process for a total of 7.5 hours of fermentation. In Figure 1 are shown the FT-NIR spectra collected during the trial B as an example (12,500-3,800 cm<sup>-1</sup>).

As can be observed in Fig 1 we highlight two main absorption peaks around about 6,900 and 5,200 cm<sup>-1</sup>, associated respectively to the first overtone and combination band of the-OH group of the water (Williams & Norris, 2001). Other characteristic peaks can be observed at 8,840 cm<sup>-1</sup>, which seems to be linked to the stretch of the bond C = O (Siriex & Downey, 1993) and 5,600-5,650 cm<sup>-1</sup>, probably due to the absorption of the peptide bond, in particular to gluten (Osborne, 1996).

#### 4.4 Overview of dough fermentation for Panettone production

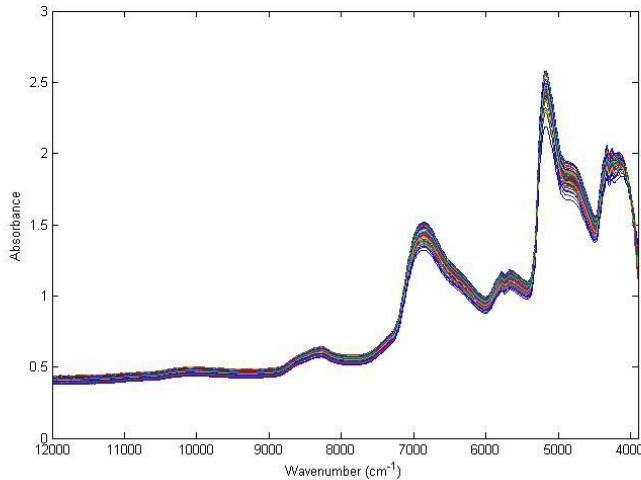


**Figure 1.** Spectra collected in one fermentation trial (A).

In correspondence with the region situated around  $4,700\text{ cm}^{-1}$  could be associated absorptions related to the structures amylaceous (Pram Nielsen et al., 2001).

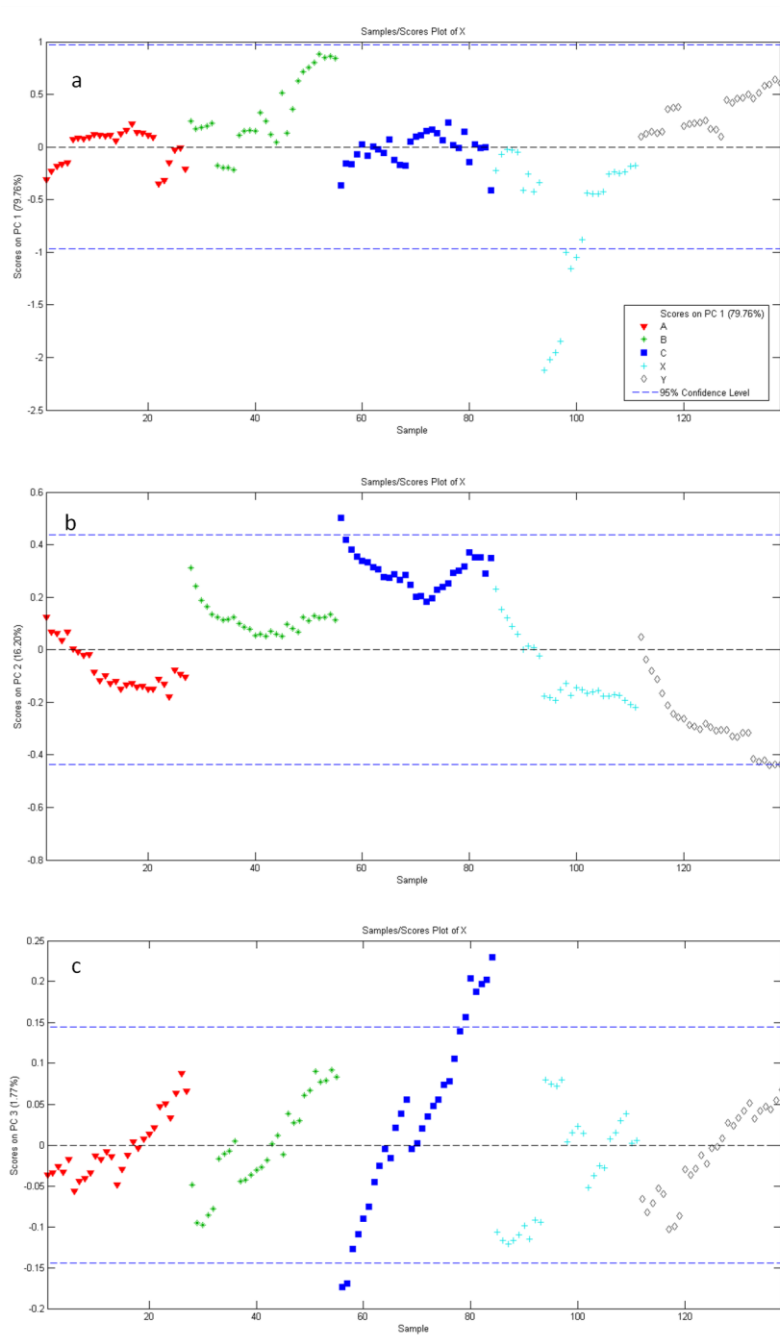
The whole spectral region was reduced in the range between  $9,700$  and  $4,500\text{ cm}^{-1}$  in order to eliminate not informative regions.

##### ***Principal component analysis***

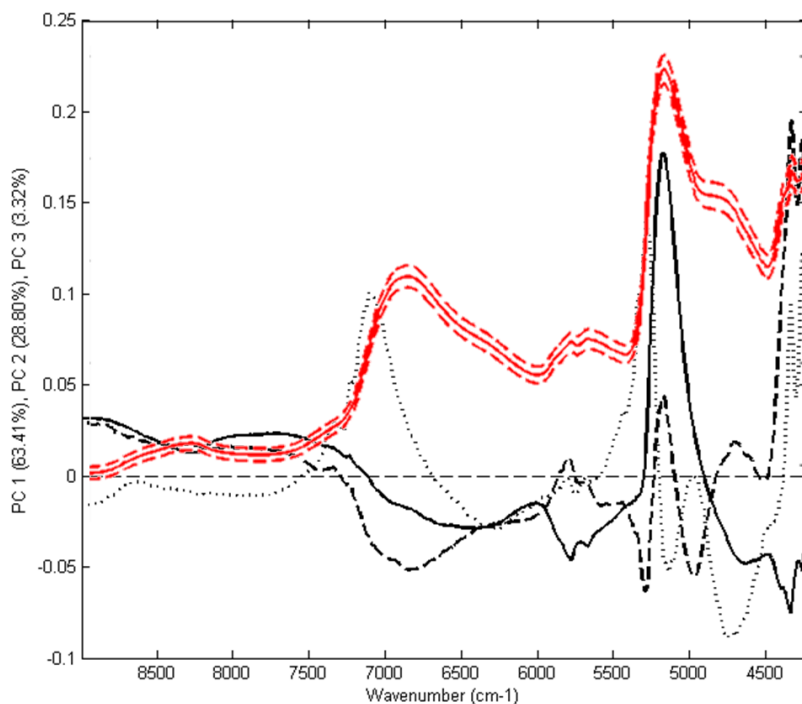
Before performing PCA the whole spectral dataset was pretreated by Standard normal variate (SNV) in order to remove scattering effect and mean centered.

Figure 2 shows the three principal components plotted against time progress and coloured according to the trial.

## 4.4 Overview of dough fermentation for Panettone production



**Figure 2.** Scores of PC1 (a), PC2 (b) and PC3(c) for the five trials performed.



**Figure 3.** Loadings of PC1 (continued line), PC2 (dashed line), PC3 (dotted line). In red the mean spectra (continued line) and the standard deviation (dashed lines) among all the dataset.

The loadings of the PC1 are related to the absorption at 5,777 and 5,654  $\text{cm}^{-1}$ , 5,168  $\text{cm}^{-1}$ , and the region of 4,500-4,200  $\text{cm}^{-1}$ . The loadings of PC2 are also related to the absorbances at 5,777 and 5,654  $\text{cm}^{-1}$ , 5,168  $\text{cm}^{-1}$  and strongly influenced by changes in the region of water absorption (7,000-6,800  $\text{cm}^{-1}$ ) and the region of 4,500-4,200  $\text{cm}^{-1}$ . Another peak characterizing the loadings of PC2 is at 4,700  $\text{cm}^{-1}$ . Mainly the same peaks characterised the PC3 loadings.

Osborne (1996) associated the changes in the region 7,000 – 6,800  $\text{cm}^{-1}$  to modification of hydrogen bonds due to the interaction of water and flour constituents. This was also confirmed by studied by Wesley et al (1998), they said that the water first overtone is influence also by the combination of NH first overtone with CH first overtone.

Is clear how this spectral region influences the loadings of the three PCs; in particular the shift of the peak in the third component could be ascribed to the influence of flour constituents on water absorption. Moreover Osborne (1996) related the region 4,500-4,200  $\text{cm}^{-1}$  to absorption bands associated with proteins.

Workman and Meyer (2007) referred to the area 3,950-4,400  $\text{cm}^{-1}$  as the one characteristic for C-H stretching combined with CH deformation for peptide groups.

**Partial least square regression**

It was investigated the possibility of using NIR spectroscopy to predict with a single and rapid measurement values of pH and titratable acidity. For this purpose regression models using the PLS algorithm (Partial Least Square regression) have been developed.

Table 2 reports the figure of merit for the models developed using different pre-processing methods and different spectral range according to the variable selected through the iPLS method.

**Table 2.** Figure of merits of the PLS models calculated for pH and total titratable acidity (TTA)

	Preprocessing	LV	Variable range selected	CALIBRATION		CV	
				R <sup>2</sup>	RMSE	R <sup>2</sup>	RMS E
pH	Absorbance	5	100-200; 250-300; 400-500; 550-600; 750-800	0.972	0.022	0.941	0.032
	SNV	5	0-200; 250-300; 350-500	0.969	0.023	0.924	0.033
	First derivative	6	150-250; 300-350; 400-500; 700-750	0.996	0.113	0.927	0.158
TTA (°S)	Absorbance	6	75-125; 150-200; 250-300; 400-500	0.964	0.06	0.861	0.125
	SNV	5	0-250; 300-450	0.880	0.113	0.768	0.158
	First derivative	5	0-50; 150-250; 275-350; 400-475	0.983	0.042	0.848	0.128

As is possible to observe in Table 2 high correlation coefficients were obtained for the models calculated for pH prediction. In particular, the model obtained without any spectral pre-treatment is characterized by high R<sup>2</sup> in both calibration and in cross-validation (R<sup>2</sup><sub>Cal</sub> = 0.9722, = 0.9417 R<sup>2</sup><sub>CV</sub>), by very low errors (RMSEC and RMSECV), the absence of overfitting and, finally, a small number of latent variables (LV 5).

Also for the results obtained for TTA correlation the model calculated with the raw spectra seems to have the best performance (R<sup>2</sup><sub>Cal</sub>=0,9642; R<sup>2</sup><sub>CV</sub>=0,8610). However the models calculated for the prediction of total acidity are characterised by overfitting phenomenon, which can be notice from the high difference between the correlation coefficients in calibration and cross-validation. As future prospective non-linear regression models could be investigated to improve the results obtained.

This behaviour, partially true also for the pH regression models, could be ascribed to a non-linear behaviour of the spectral data.

One of the main problems in studying sourdough with infrared spectroscopy is related to the solid nature of the matrix itself.

In the future, this approach at an industrial scale would allow the monitoring of the first dough in fermentation in quick and non-destructive approach, allowing fast corrective action to be taken in case of non-conformity.

#### 4.4.4 References

- Ait Kaddour, A., Barron, C., Robert, P., & Cuq, B. (2008). Physico-chemical description of bread dough mixing using two-dimensional near-infrared correlation spectroscopy and moving-window two-dimensional correlation spectroscopy. *Journal of Cereal Science*, *48*(1), 10-19.
- Clarke, C. I., Schober, T. J., Dockery, P., O'Sullivan, K., & Arendt, E. K. (2004). Wheat sourdough fermentation: effects of time and acidification on fundamental rheological properties. *Cereal chemistry*, *81*(3), 409-417.
- Collar, C., Benedito de Barber, C., & Martinez-Anaya, M. A. (1994). Microbial sourdoughs influence acidification properties and breadmaking potential of wheat dough. *Journal of Food Science*, *59*, 629-633.
- De Vuyst, L., & Neysens, P. (2005). The sourdough microflora: biodiversity and metabolic interactions. *Trends in Food Science & Technology*, *16*(1), 43-56.
- Di Egidio, V., Sinelli, N., Limbo, S., Torri, L., Franzetti, L., Casiraghi, E. (2009). Evaluation of shelf life of fresh-cut pineapple by using FT-NIR and FT-IR spectroscopy. *Postharvest Biol. Tec.* **54**, 87-92.
- Grassi, S., Vigentini, I., Sinelli, N., Foschino, R., Casiraghi, E. (2012). Near infrared and mid infrared spectroscopy in oenology: determination of main components involved in malolactic transformation. *NIR news* **23**, 11-14.
- Lefebvre, D., Gabriel, V., Vayssier, Y., & Fontagne-Faucher, C. (2002). Simultaneous HPLC determination of sugars, organic acids and ethanol in sourdough process. *LWT-Food Science and Technology*. *35*(5), 407-414.
- Li Vigni, M., & Cocchi, M. (2013). Near infrared spectroscopy and multivariate analysis to evaluate wheat flour doughs leavening and bread properties. *Analytica Chimica Acta*, *764*, 17- 23.
- Limbo, S., Torri, L., Sinelli, N., Franzetti, L., Casiraghi, E. (2010). Evaluation and predictive modelling of shelf life of minced beef stored in high-oxygen modified atmosphere packaging at different temperatures. *Meat Science*, **84**, 129-136.



#### 4.4 Overview of dough fermentation for Panettone production

- Osborne, B. G. (1996). Near Infrared Spectroscopic studies of starch and water in some processed cereal foods. *Near Infrared Spectroscopy*, 4, 195–200.
- Picozzi, C., Gallina, S., Fera, T. D., & Foschino, R. (2005). Comparison of cultural media for the enumeration of sourdough lactic acid bacteria. *Annals of microbiology*, 55(4), 317.
- Pram Nielsen, J., Bertrad, D., Micklander, E., Courcoux, P., & Munk, L. (2001). Study of NIR Spectra, particle size and chemical parameters of wheat flours: a multi-way approach. *Journal of Near Infrared Spectroscopy*, 9, 275–285.
- Sinelli, N., Casiraghi, E., Downey, G. (2008). Studies on proofing of yeasted bread dough using near- and mid-infrared spectroscopy. *Journal of agricultural and food chemistry*, 56, 922-31.
- Siriex, A., & Downey, G. (1993). Commercial wheat flour authentication by discriminant analysis of near infrared reflectance spectra. *Journal of Near Infrared Spectroscopy*, 1(4), 187.
- Williams, P., & Norris, K. (2001). *Near-Infrared Technology: In the Agricultural and Food Industries* (2nd ed.). Amer Assn of Cereal Chemists.

## 4.4 Overview of dough fermentation for Panettone production

## **5. Conclusions and perspectives**

The research presented in this PhD thesis gives an overview of the application of FT-IR and FT-NIR spectroscopy in the monitoring and controlling different food fermentation processes. The two spectroscopic techniques, combined with different chemometric strategies, have proven to be a successful working methodology for quantitative, qualitative and kinetic modelling of different food matrices being fermented, from liquid ones (wine and beer) to semi-solid ones (sourdough) passing by yoghurt with its viscoelastic behaviour.

For what concern the experiments conducted to investigate yoghurt fermentation, it was possible to assess the real-time development of the curd during fermentation, no matter the operative conditions adopted for the process, and to predict the main quality parameters in the milk fermentation (pH, titratable acidity, lactose, galactose and lactic acid). This was possible thanks to the combination of FT-IR spectroscopy with MCR-ALS, and FT-IR with PLS regression technique, respectively. These findings are interesting as they provided not only regression models to predict process parameters, but also real-time strategies for monitoring the rheological modifications occurring in the fermenting milk. As a consequence, the definition of the end point of the fermentation could be assessed in a robust and reliable manner.

The use of FT-NIR and FT-IR spectroscopy combined with PLS technique provided good estimations of malic acid, lactic acid and total acidity content in samples collected from *Nebbiolo* musts coming from large-scale fermentations. The small errors achieved in the estimation of the parameters under study allow the distinction between samples before MLF and after malic acid transformation. These results suggest the success in facing the need of the winery in understanding and controlling the biotransformation.

Furthermore, the combination of FT-NIR and FT-IR spectroscopy with PCA fitted with a sigmoidal function provided real-time information of the evolution of the biotransformation. In particular, critical points identified by spectroscopic techniques during the fermentation were in agreement with the time points revealed by chemical and microbiological analyses.

The experiments conducted with beer fermentation aim to monitor and assess different process parameters in beer fermentation at different operative conditions. The FT-NIR data provided good results describing the general trend of the fermentation (through PCA) and estimating ethanol, °Brix and biomass content (regression models). The fingerprint region ( $1,200-950\text{ cm}^{-1}$ ) extracted from the FT-IR data revealed the main changes occurring throughout the fermentation at expense of wort sugars and leading to ethanol rising. In particular, the results obtained with MCR-ALS accurately describe the bioprocess in term of relative concentration variations of the main sugars presented in wort (maltose, maltotriose, fructose, sucrose and dextrans) and ethanol.

The preliminar results reported about sourdough fermentation confirmed that it is possible to follow the main modifications characterizing dough in fermentation. PCA revealed that the main changes in the samples were due to the effect of flour constituents on water absorption and modifications of the proteins in the gluten fraction. Good models were obtained for pH and titratable acidity correlation. As future prospective non-linear regression models will be investigated to improve the results obtained.

Nowadays, more and more sensors have been implemented in food productions and a huge amount of data needs to be handled in PAT prospective. In perspective, as response to the need of improved understanding of the process and the quality, the implementation of infrared spectroscopy in food industries will be of higher interest. In particular, the use of specific chemometric strategies will be crucial in this approach. As discussed in this PhD thesis the combination of spectroscopy and chemometrics allows the identification of critical process parameters not just one by one but in a multivariate approach. Thus, it provides a better management of the process in an immediate perspective with real-time process control possibilities.





## Microbial food fermentation : innovative approach using NIR and MIR spectroscopy



Silvia Grassi ([silvia.grassi@unimi.it](mailto:silvia.grassi@unimi.it))

Department of Food Science Technology and Microbiology, University of Milan, Italy  
Tutor: Prof.ssa Ernestina Casiraghi; Co-Tutor: Prof. Roberto Foschino

### 1. State-of-the-art

In the last years has been growing the interest on the real-time assessment of food process and on the relationship between its performance and the quality and safety of final products. Currently in industry there is an increasing demand for rapid instruments that could be used for on-line monitoring and food processes analysis (Bock and Connelly, 2008), since process management could be more effective if the products of interest were more closely monitored and the smallest changes could be instantaneously detected.

Many unit operations in food processes, namely milk coagulation in cheese production and dough rising in bakery, as well as must fermentation in wine making are mostly based on microbial fermentation, which entails modifications in the final product. Due to the phenomenon complexity and variability, the process management has traditionally relied on the subjective assessment of craftsmen or highly trained personnel to produce consistent, high-quality products.

Traditional chemical and microbiological methods used for the off-line monitoring of fermentation processes are labour intensive and time consuming, moreover results are obtained too late for any meaningful changes to be made to the process; consequently often the biotransformations are controlled retrospectively, taking action only after the quality of the final product has not met expectations. Whereas a monitoring technique should be rapid, nondestructive, operable in near-real-time, capable of automation.

Among the innovative techniques infrared spectroscopy in both near (NIR) and mid (MIR) regions, combined with multivariate data analysis, has these characteristics and has proven to be a successful analytical method for quantitative and qualitative modelling in industrial applications.

The earliest studies involving foodstuff were of analytical nature and simply sought to correlate infrared spectroscopy (IRS) with standard methods of compositional analyses. In addition, researchers are pursuing dynamic applications of spectroscopic methods in order to monitor a sample *in situ* during processing (Huang *et al.*, 2008), achieving good results thanks to the development of optic fibre probes adapted for on-line measurements and computer science ability to process extensive data in a short time.

In particular, NIR and MIR spectroscopy have been used for the determination of compositional parameters affecting quality and safety of food products (Huang *et al.*, 2008) such as wine, yoghurt, vinegar, vinegar and leavening agents in bread and bakery products. As far as concern complex biotransformations monitoring IRS has been used in fed-batch microbial bioprocess (Landgrebe *et al.*, 2010) and is an emerging technique in food fermentations monitoring (Navrátil *et al.*, 2004; Urtubia *et al.*, 2008).

Thus, this PhD research project is aimed to use IRS for an innovative purpose: a real-time monitoring of whole fermentation process of some food matrix characterized by different food texture (liquid, semi-solid and solid) driven by microbial consortia.

### 2. PhD Thesis Objectives and Milestones

Within the objectives mentioned above, the following activities were planned, as reported on the Gantt diagram given in *Table 1*:



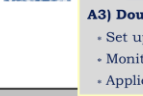
#### A1) Wine fermentation monitoring

- Set up of malolactic fermentation (MLF) micro-vinification with different *Oenococcus oeni* strains
- Monitoring of the whole process by IR spectroscopy and traditional methods
- Correlation of the results achieved by traditional and innovative methods, through the use of regression models
- Building of predictive and classification models



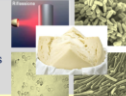
#### A2) Dairy fermentation monitoring

- Selection of different products characterized by lactic fermentation with thermophiles and/or mesophiles strains
- Monitoring of fermentation by using IR spectroscopy and traditional methods
- Regression and classification models will be built to predict quality parameters and to evaluate strains adequacy



#### A3) Dough rising monitoring

- Set up of dough rising using different microbial consortia for typical baked products
- Monitoring of fermentation through IR spectroscopy, traditional microbiological and chemical methods
- Application of a multivariate approach to obtain regression and classification models



#### A4) Writing and editing of the PhD thesis, annually reports, scientific report and oral or poster communications.

**Table 1.** Gantt chart for this PhD thesis project.

Activity	Month																																					
	1	2	3	4	5	6	7	8	9	10	11	12	13	14	15	16	17	18	19	20	21	22	23	24	25	26	27	28	29	30	31	32	33	34	35	36		
A1 Wine MLF monitoring																																						
A2 Dairy fermentation monitoring																																						
A3 Sourdough rising monitoring																																						
A4 Thesis and paper preparation																																						

### 3. Selected References:

Bock JE and Connelly RK (2008) Innovative Uses of Near-Infrared Spectroscopy in Food Processing *J Food Sci* 73: 91-98. Huang H, Yu H, Xu H, Ying Y (2008) Near infrared spectroscopy for on/in-line monitoring of quality in foods and beverages: A review. *J Food Eng* 87: 303-313. Landgrebe D, Haake C, Höpfner T, Beutel S, Hitzmann B, Schepel T, Rhiel M, Reardon KF (2010) On-line infrared spectroscopy for bioprocess monitoring. *Appl Microbiol Biotechnol* 88:11-22. Navrátil M, Cimander C and Mandenius C-F (2004) On-line Multisensor Monitoring of Yogurt and Filmjölk Fermentations on Production Scale. *J Agr Food Chem* 52:415-420. Urtubia A, Pérez-correa JR, Pizarro F, Agosin E (2008) Exploring the applicability of MIR spectroscopy to detect early indications of wine fermentation problems. *Food Control* 19: 382-388

Poster presented at: 16th Workshop on the Developments in the Italian PhD Research on Food Science Technology and Biotechnology, 21-23 September 2011, Lodi



## Lactic acid fermentation: innovative approach using NIR spectroscopy



Silvia Grassi (silvia.grassi@unimi.it)

Department of Food, Environmental and Nutritional Sciences, University of Milan, Italy  
Tutor: Prof.ssa Ernestina Casiraghi; Co-Tutor: Prof. Roberto Foschino

### INTRODUCTION

Monitoring fermentation carried out by lactic acid bacteria (LAB) is highly interesting in the competitive dairy food sector, where product quality reproducibility is decisive in the manufacture.

One of the main requirements of the food industry is the availability of a rapid and non-destructive method for the real-time control of the fermentation process.

Therefore, the aim of this work was to evaluate the suitability of FT-NIR spectroscopy, joined with multivariate data analysis, as an easy and fast method to quickly detect any possible deviation from the regular trend of a lactic acid fermentation in order to establish the best management strategy.

### MATERIAL and METHODS

Skim milk powder was reconstituted to 10% (w/v), heat treated and inoculated with approximately  $10^6$  cfu/mL of single cultures or a mixed culture (1:1) strains of *S. thermophilus* and *L. bulgaricus*, previously isolated from a commercial culture (Danisco A/S). Milk fermentations were carried out in duplicate, for 7.5 h, at 37° C, 41° C and 45° C.

† FT-NIR spectra were collected in diffuse transreflectance (12,500-4,500  $\text{cm}^{-1}$ ; resolution 16  $\text{cm}^{-1}$ ), by using an MPA spectrometer (Bruker Optics) equipped with an optic probe.

† Principal Component Analysis (PCA) was applied to the spectral data transformed in first derivative by using The Unscrambler software [v. 9.8 Camo Software AS].

† The PC1 scores were modelled as a function of time, using a sigmoidal function implemented in Table Curve software (v.4.0, Jandel Scientific).

### RESULTS and DISCUSSION

In Figure 1a is shown an example of the raw FT-NIR spectra of one trial performed at 41° C. It is possible to notice a difference in absorption according to the fermentation time. This change could be due to physical effects, such as casein micelle size, which heavily influences NIR spectrum [1]. Although the absorption increased with fermentation time, it was difficult to extract information due to the scattering.

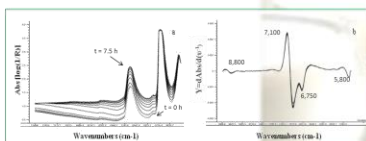


Figure 1. FT-NIR spectra of the trial conducted at 41° C with the mixed culture: raw FT-NIR spectra (a), first derivative of FT-NIR spectra (b).

Reduced FT-NIR spectra (8,900-5,555  $\text{cm}^{-1}$ ) were transformed in first derivative (Figure 1b). Peculiar absorption peaks can be observed around 7,100 and 6,750  $\text{cm}^{-1}$ , corresponding to O-H combination and first overtone bands,

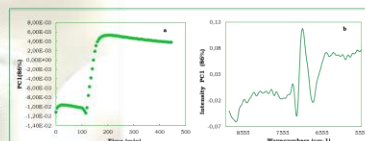


Figure 2. Principal Component Analysis of the trial conducted at 41° C with the mixed culture: (a) PC1 scores vs. time (min) and (b) Loading plot of PC1

PCA was performed on transformed FT-NIR spectra and PC1 scores were plotted as function of time (Figure 2a). A sigmoidal distribution of samples according to the fermentation time could be observed.

The Loading plot associated with PC1 (Figure 2b) permits to define the main wavenumbers responsible for the distribution of the samples.

Table 1. Time (min) corresponding to maximum acceleration ( $\text{max } d2x/dt2$ ), maximum rate ( $\text{max } dx/dt$ ) and maximum deceleration ( $\text{min } d2x/dt2$ ) of the lactic fermentation process by kinetic approach.

Trial	<i>S. thermophilus</i>			<i>L. bulgaricus</i>			<i>S. thermophilus + L. bulgaricus</i>		
	37°c	41°c	45°c	37°c	41°c	45°c	37°c	41°c	45°c
Max $d2x/dt2$ (min)	306	283	233	184	135	108	184	130	103
Max $dx/dt$ (min)	337	306	265	202	148	117	198	144	112
Min $d2x/dt2$ (min)	364	328	297	225	157	126	207	153	121

Normalized PC1 scores obtained were modelled applying a sigmoidal equation. This function offered a good fit with the raw data ( $R^2 > 0.993$ ). First and second derivatives of the models obtained gave the time related to the maximum rate, acceleration and deceleration of the phenomena (Table 1). The time of maximum deceleration could be associated with the formation of the curd.

### CONCLUSION

Results obtained by PCA and kinetic modelling of FT-NIR spectra demonstrated to be reliable techniques for extracting information from lactic acid fermentation. The models could be used to detect deviations from the regular trend of the bioprocess and to establish the best strategy for its management.

In future prospective the results obtained will be compared with other microbiological and chemical data recorded during the trials to draw more information about the biotransformation.

### REFERENCES

- [1] Frake, P., Luscombe, C. N., Rudd, D. R., Gill, I., Waterhouse, J., Frake P. & Jayasooriya, U. A. (1998). Near-infrared mass median particle size determination of lactose monohydrate, evaluating several chemometric approaches. *Analyst*, 123, 2043-2046.
- [2] Sivakesava, S., Irudayaraj, J., Ali D. (2001). Simultaneous determination of multiple components in lactic acid fermentation using FT-MIR, NIR, and FT-Raman spectroscopic techniques. *Process Biochemistry* 37: 371-378.
- [3] Workman J. and Weyer L. (2007). *Practical Guide to Interpretive Near-Infrared Spectroscopy*, Edited by: Workman, J. and Weyer, L. Boca Raton,FL: CRC Press

Poster presented at: 17th Workshop on the Developments in the Italian PhD Research on Food Science Technology and Biotechnology, 19-21 September 2012, Cesena





## IR spectroscopy for monitoring the production of lactic acid fermented milks



Cristina Alamprese, Silvia Grassi, Claudia Picozzi, Veronica Bono, Ernestina Casiraghi

Dipartimento di Scienze per gli Alimenti, la Nutrizione e l'Ambiente (DeFENS)

Università degli Studi di Milano, Via G. Celoria 2 - 20133 Milano



### INTRODUCTION

Lactic acid fermented milks are very popular products, appreciated for their sensory and healthy properties.

Only a thorough understanding and monitoring of the fermentation process can reduce the risk of product failure and assure quality reproducibility. Hence, one of the main requirements of the food industry is the availability of a rapid and non-destructive method providing real time information in order to assure an effective control at all stages of the process.

Therefore, **the aim of this study** was to evaluate the suitability of IR spectroscopy, joined with Partial Least Square Regression, as a tool for the simultaneous determination of the commonest fermentation indexes.

### MATERIALS and METHODS

**Skim milk powder** was reconstituted to 10% (w/v) in distilled water, heat-treated and inoculated with approximately  $10^6$  cfu/mL of single or mixed (1:1) cultures of *S. thermophilus* and *L. bulgaricus*, previously isolated from a commercial culture (Danisco A/S, Denmark). Milk fermentations were carried out in duplicate, for 7.5 h, at 37°C, 41°C and 45°C.

**FT-NIR spectra** were collected in continuous in diffuse transmittance ( $12,000\text{--}4,500\text{ cm}^{-1}$ ; resolution  $16\text{ cm}^{-1}$ ; 64 scan), by using an MPA spectrometer (Bruker Optics, Italy) equipped with a fiber-optic probe.

**FT-IR spectra** were collected ( $4,000\text{--}700\text{ cm}^{-1}$ ; resolution  $4\text{ cm}^{-1}$ ; 16 scan) every 45 min, by a Vertex 70 spectrometer (Bruker Optics, Italy) fitting a multiple reflection ATR cell with a germanium crystal.

Every 45 min, **pH, titratable acidity, microbial counts, and metabolite concentration** (galactose, lactic acid, and lactose) were also evaluated by means of conventional methods.

**PLS (Partial Least Square) regression models** were developed using pre-treated ( $1^{\text{st}}$  derivative, Savitzky-Golay method) FT-NIR and FT-IR spectra. A cross-validation procedure with 10 CV was applied.

### RESULTS and DISCUSSION

Fermentative trials were monitored through IR-spectroscopy and traditional methods: microbial plate counts, pH, titratable acidity and metabolites (galactose, lactic acid and lactose). The obtained results were used to develop PLS regression models.

As regards the FT-NIR spectra, only the region from  $8,900$  to  $5,555\text{ cm}^{-1}$  was selected for PLS models (Fig. 1a). The main absorption peaks ( $7,150\text{ cm}^{-1}$ ;  $6,800\text{ cm}^{-1}$ ) are due to the combination and first overtone bands of O-H bond, respectively [1].

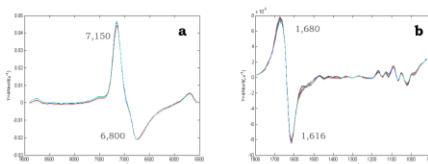


Figure 1. FT-NIR (a) and FT-IR (b) reduced spectra, after transformation in first derivative

The fingerprint region ( $1,800\text{--}970\text{ cm}^{-1}$ ) of FT-IR spectra was used in PLS models (Fig. 1b). Peculiar absorption peaks were observed around  $1,680\text{ cm}^{-1}$  and  $1,616\text{ cm}^{-1}$ , corresponding to the O-H bond of water and N-H bond of proteins, respectively [2-3].

Statistical parameters of calculated PLS models are reported in Table 1. In some cases, data originated from all the fermentation trials were used for regression; in other cases (as specified in the Table), better models were obtained selecting partial datasets on the basis of the tested inoculum.

Table 1. Statistical parameters of the PLS model calculated with FT-NIR and FT-IR data, for the prediction of fermentation monitoring indices.

Parameter	Range (Min-Max)	LV	FT-NIR data			FT-IR data					
			Calibration R <sup>2</sup>	Cross-validation R <sup>2</sup>	RMSE	Calibration R <sup>2</sup>	Cross-validation R <sup>2</sup>	RMSE			
pH	3.67 - 6.51	13	0.9639	0.1701	0.9327	0.2345	11	0.9762	0.1374	0.9542	0.1901
TA Lb (% ac. lattico)	0.13 - 1.18	9	0.9485	0.0203	0.8358	0.0364	9	0.9915	0.0081	0.9514	0.0020
TA St (% ac. lattico)	0.13 - 1.18	9	0.9451	0.0014	0.9100	0.0180	10	0.9743	0.0095	0.8548	0.0032
Lactose Lb+St (g/L)	3.02 - 8.05	16	0.9671	0.7263	0.8221	1.7155	20	0.9969	0.2240	0.7006	2.2269
Galactose (g/L)	0.02 - 3.45	13	0.8525	0.6435	0.8243	0.7601	13	0.8936	0.5401	0.7755	0.7879
Lactic Acid (g/L)	n.d. - 2.48	15	0.9307	0.5444	0.8556	0.7887	11	0.9632	0.3885	0.9233	0.5635
<i>L. bulgaricus</i> (log CFU/mL)	6.90 - 8.65	15	0.9457	0.2024	0.8566	0.3315	11	0.9247	0.2378	0.8204	0.3662
<i>S. thermophilus</i> (log CFU/mL)	6.35 - 8.65	13	0.8342	0.2886	0.6755	0.4067	9	0.9613	0.1385	0.7914	0.3296

LV, latent variables; R<sup>2</sup>, correlation coefficient; RMSE, root mean square error; Lb, *L. bulgaricus* inoculum; St, *S. thermophilus* inoculum; Lb+St, mixed inoculum.

n.d., not detectable

High correlation coefficients and little standard errors were obtained in calibration for all the PLS models. The best results in prediction were obtained for pH, TA and lactic acid, the reference parameters typically required in fermentation monitoring.

### CONCLUSIONS

The study demonstrated that IR spectroscopy, in combination with chemometric techniques, has potential to become a useful tool in monitoring of lactic acid fermentations. The major advantage of the presented approach is the simultaneous prediction of quantitative process variables which otherwise are not available on-line. The development of more robust models, based on industrial productions, is required.



### REFERENCES

- J. Workman and L. Weyer (2001) Practical Guide to Interpretive Near Infrared Spectroscopy, CRC - Taylor and Francis, Boca Raton, FL.
- M. De Marchi, C.C. Fagan, C.P. O'Donnell, A. Cecchinato, R. Dal Zotto, M. Cassandro, M. Penasa and G. Bittante, J. Dairy Sci. 92, 423 (2009).
- S. Sivakesava, J. Irudayaraj and D. Ah, Process Biochem. 37, 371 (2001).

Poster presented at: 5° Simposio Italiano di Spettroscopia NIR. Atti: SISNIR, 2012 ISBN 9788890406454. pp. 131-136



# MCR-ALS applied to milk lactic acid fermentation monitoring



Silvia Grassi<sup>a</sup>, Cristina Alamprese<sup>a</sup>, Veronica Bono<sup>a</sup>,  
Claudia Picozzi<sup>a</sup>, Roberto Foschino<sup>a</sup>, Ernestina Casiraghi<sup>a</sup>, José Manuel Amigo<sup>b</sup>

<sup>a</sup> Department of Food, Environmental and Nutritional Sciences (DeFENS), Università degli Studi di Milano, via Celoria 2, 20133 Milano, Italy  
<sup>b</sup> Department of Food Science, Quality and Technology, Faculty of Life, University of Copenhagen, Rolighedsvej 30, DK -1958 Frederiksberg C, Denmark

## INTRODUCTION

Fermentation is one of the earliest methods adopted to obtain value-added milk products with an extended shelf-life. Despite its old manufacturing tradition, the dairy industry needs continuous improvement of methods providing real time information about the progress of the process. Among the most promising techniques, near-infrared (NIR) spectroscopy represents a fast and non-destructive alternative, able to simultaneously detect, after calibration, the main compounds involved in the fermentation process and to describe the trend of the process (Bock et al., 2008). Soft-modelling methods, such as the multivariate curve resolution optimized by alternating least squares (MCR-ALS), demonstrated to be the most powerful method to describe the phenomena occurring in any kinetic reaction (Garrido et al., 2008) and seems to be suitable to extract information from FT-NIR spectra acquired during fermentation processes (González-Sáiz et al., 2008).

## AIM

The purpose of the current work is to investigate the capability of MCR-ALS applied to FT-NIR spectra to extract in-line relevant information about milk lactic acid fermentation dynamics.

## MATERIALS and METHODS

Skim milk powder was reconstituted to 10% (w/v) in distilled water, heat-treated and inoculated with approximately 10<sup>6</sup> cfu/mL of single or mixed (1:1) cultures of *S. thermophilus* and *L. bulgaricus*, previously isolated from a commercial culture (Danisco A/S, Denmark). Milk fermentations were carried out in duplicate, for 7.5 h, at 37 °C, 41 °C and 45 °C.

FT-NIR spectra were collected in continuous in diffuse transmittance (12,000-4,500 cm<sup>-1</sup>; resolution 16 cm<sup>-1</sup>; 64 scan), by using a MPA spectrometer (Bruker Optics, Italy) equipped with a fiber-optic probe.

Curd development was monitored on-line using a Physica MCR 300 rheometer (Anton Paar GmbH, Graz, Austria) through a dynamic oscillatory test (constant 1% strain, 1 Hz frequency).

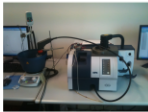
MCR-ALS analyses were performed by means of MCR-ALS software (<http://www.mcrals.info/>) implemented in MatLab v. 7.4 (The Mathworks Inc., Cambridge, UK). The spectra matrix (D) is decomposed by MCR-ALS into two sub-matrices, concentration, C (M × F), and spectra profiles, S<sup>t</sup> (F × N).

ALS optimization:

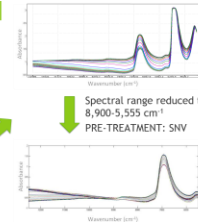
- Convergence criterion: 0.1%;
- Number of significant components: 3;
- The initial estimates: 3 spectra from D recorded at the beginning, middle and end of a representative fermentation batch;
- Constraints: non-negativity to C and S<sup>t</sup>, and unimodality to C.

## RESULTS and DISCUSSION

### FT-NIR SPECTRA

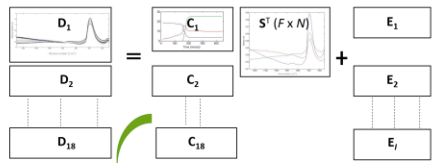


FT-NIR spectra (12,500-4,500 cm<sup>-1</sup>) collected during one of the fermentation processes performed at 41°C with the mixed starter culture (1:1) and reduced spectra (12,500-5,355 cm<sup>-1</sup>) pre-treated by SNV.



### MCR-ALS

#### Depiction of MCR-ALS decomposition



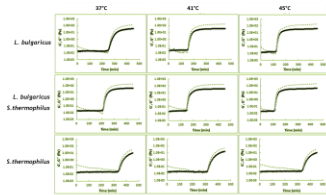
99.9% of explained variance; %LOF: 0.63665; S.D. residuals <0.007

#### Concentration profiles

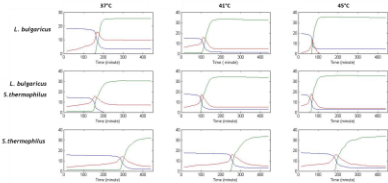
The obtained profiles contained information about the main changes occurring in the food matrix.



### RHEOLOGICAL MEASUREMENTS



Rheological behaviours for one representative fermentation trial for each combination temperature-inoculum. Dash thin lines (---) represent the G' modulus and solid thick lines (—) the G'' modulus.



MCR-ALS pure component spectra: blue profile describes the liquid-like behaviour of milk, green profile reflects the solid-like behaviour of coagulated milk and the red profile represents the middle passage in the biotransformation.

## CONCLUSIONS

MCR-ALS applied to FT-NIR spectra for monitoring milk fermentation provided a possible automated control system, which can be implemented in industrial productions to describe curd formation and, as a consequence, to define the end point of the fermentation. In particular the comparison of MCR concentration profiles with the rheological measurements showed that it is possible to follow the viscoelastic behaviour of curds, no matter the operative conditions used. Actually gel formation is the main physical change characterizing this biotransformation and even if it is extremely relevant in final product quality and customers' acceptance, there are no on-line systems available for its monitoring.

## References

Bock JF & Cerny RK (2008) Innovative uses of Near-Infrared in food processing. *Journal of Food Science*, 73(7), 891-898.  
Garrido A, Ruiz FX & Larruchi R (2008) Multivariate curve resolution-alternating least squares (MCR-ALS) applied to spectroscopic data from monitoring chemical reactions processes. *Analytical and Bioanalytical Chemistry*, 390(8), 2099-2106.  
González-Sáiz J, M. Huelo ED, Rodríguez-Troncoso S & Pizarro C (2008) Valorization of Onion Waste and By-Products: MCR-ALS applied to reveal the compositional profiles of alcoholic fermentation of onion juice monitored by Near-Infrared Spectroscopy. *Biotechnology and Bioengineering*, 101(4): 776-787.

**Acknowledgments**  
Dr. Silvia Grassi and Dr. Veronica Bono acknowledge the "Società Italiana di Spettroscopia NIR - SISNIR" for funding for the conference fees and the travel grant.



Poster presented at: Icnirs2013 - 16th International Conference on Near Infrared Spectroscopy; 01-06/06/2013, Montpellier



# Beer fermentation monitoring by using FT-NIR spectroscopy



Silvia Grassi <sup>a</sup>, José Manuel Amigo <sup>b</sup>, Christian Bøge Lyndgaard <sup>b</sup>, Illeana Vigentini <sup>a</sup>, Ernestina Casiraghi <sup>a</sup>

<sup>a</sup> Department of Food, Environmental and Nutritional Sciences (DeFENS), Università degli Studi di Milano, via Celoria 2, 20133 Milano, Italy  
<sup>b</sup> Department of Food, Quality and Technology, Faculty of Sciences, University of Copenhagen, Rolighedsvej 30, DK -1958 Frederiksberg C, Denmark

## INTRODUCTION

- The legal parameters for beer fermentation control are **specific gravity (SG)** and **alcohol content** (Directive 92/84/EEC, 1992).
- Nowadays SG determination is an easy way for the identification of the **fermentation end-point**.
- However the process is influenced by **multitude of factors** (e.g. temperature, pH, sugar composition, yeast type) which can affect a large number of **quality parameters**, thus brewing industry needs **rapid** and **non-invasive** methods to estimate them.

## AIM

The work investigates the capability of FT-NIR spectroscopy to monitor wort fermentations conducted at different operative conditions.

## MATERIALS & METHODS

Highland heavy Ale wort (Muntons, Suffolk, UK) was reconstituted according to instructions of the manufacturer.

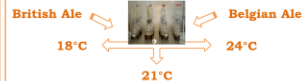
Two *Saccharomyces cerevisiae* strains (WhiteLab Inc., San Diego, CA, USA), with different fermentation characteristics, were pitched in the hopped malt to obtain  $7 \cdot 10^6$  CFU  $\text{mL}^{-1}$  concentration.

**British Ale**  
 High flocculation  
 Attenuation: 70%  
 Optimum: 18-21°C



**Belgian Ale**  
 Low flocculation  
 Attenuation: 78%  
 Optimum: 20-24°C

The fermentation trials were conducted in a factorial design according to the scheme:



Each combination was replicated twice, giving a total amount of 12 different experiments.

Samples were collected in triplicate right after pitching (t=0) and then every **24 hours** until the **9<sup>th</sup> day** using two different techniques:

- Directly from the supernatant
- Centrifugation (15 min at 3,000 g)

NIR spectra were collected in transmission mode, with a QFA Flex FT-NIR spectrometer (Q-Interline A/S, Roskilde, Denmark) equipped with a 1 mm path length cuvette. The data were collected in the range 10,000–4,000  $\text{cm}^{-1}$ , with a resolution of 16  $\text{cm}^{-1}$  and 128 scans for both background and samples.

Principal Component Analysis (PCA) was applied to the spectral data pre-treated by using Matlab (The Mathworks Inc., Cambridge, UK) and the PLS toolbox version 200 6.7.1 (Eigenvector Research, Inc., USA).

## RESULTS



Baseline drift for samples collected directly from the supernatant since yeast growth in the media

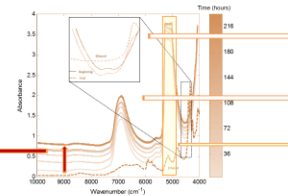


Figure 1. Example of raw spectra collected from the supernatant during one fermentation trial performed at 18°C (Belgian Ale) and ethanol spectrum in dotted line. In detail the region 4,800–4,300  $\text{cm}^{-1}$ .

Changes in the absorption at 4,400  $\text{cm}^{-1}$  were typical for spectra recorded at the end of the fermentation, caused by the rise in ethanol content.

6,900  $\text{cm}^{-1}$ : first overtone of OH stretching.

5,200  $\text{cm}^{-1}$ : combination band of OH stretching and OH bending.  
 Region 5,450–4,800  $\text{cm}^{-1}$ : excluded in the PCA.

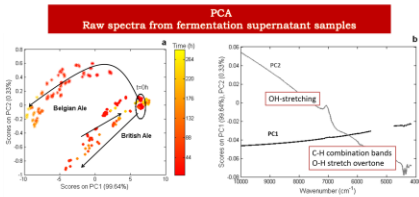


Figure 2. PCA analysis for non-centrifuged samples collected during fermentation: raw spectra were only mean centered before the PCA. (a) Scores plot coloured according to fermentation time where (●) is British Ale strain and (○) is Belgian Ale. (b) Loadings plot for PC1 and PC2.

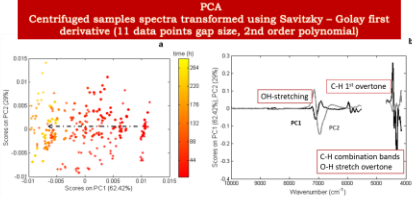


Figure 3. PCA analysis for samples collected after centrifugation. The raw spectra were transformed using Savitzky-Golay first derivative (11 data points gap size, 2<sup>nd</sup> order polynomial). Scores plot (a) coloured according to fermentation time where (●) is British Ale strain and (○) is Belgian Ale. Loadings plot (b) for PC1 and PC2.

## CONCLUSIONS

- The explorative PCA analyses showed that it is possible to follow beer fermentation evolution performed with two different *S. cerevisiae* strains and at three different fermentation temperatures.
- This technique could be suggested to the **brewing industry** as a control system able to give **simultaneous** and **real-time information** about the progression of the bioprocess.

## REFERENCES

Council Directive 92/84/EEC. OJ L 214, 1992, 31.10.1992 Bull. 10-1992.  
 Di Egidio, S., Olivero, P., Benedek, T., Donny, C. (2011). Classification of brand identity in foods by near infrared transmittance spectroscopy using classification and class-including clustering techniques – The example of a Belgian beer. *Food Research International*, 44, 244–249.  
 Rodriguez, G., Oudejans, S., Topp, B., Kowalski, E.K., Wilson, K.E., Pothier, G., Gonzalez, J., Hervey, C.J. (2009). A comparison of noise pre-selection methods for use in partial least squares regression: A case study on NIR spectroscopy applied to assessing beer bitterness. *Journal of Food Engineering*, 90, 300–307.



Poster presented at: **Incirs2013 - 16th International Conference on Near Infrared Spectroscopy;**  
 01-06/06/2013,  
 Montpellier

*They are ill discoverers that think there is no land, when they can see nothing but sea.*

Francis Bacon